AD_____

Award Number: DAMD17-96-1-6161

TITLE: Anticancer Agents Based on a New Class of Transition-State Analog Inhibitors for Serine and Cysteine Proteases

PRINCIPAL INVESTIGATOR: Christopher Seto, Ph.D.

CONTRACTING ORGANIZATION: Brown University
Providence, Rhode Island 02912

REPORT DATE: August 2000

TYPE OF REPORT: Final

PREPARED FOR: U.S. Army Medical Research and Materiel Command
Fort Detrick, Maryland 21702-5012

REPORT DOCUMENTATION PAGE

Form Approved
OMB No. 074-0188

1. AGENCY USE ONLY (Leave blank)	2. REPORT DATE	3. REPORT TYPE AND DATES COVERED
	August 2000	Final (1 Aug 96 - 31 Jul 00)

4. TITLE AND SUBTITLE
Anticancer Agents Based on a New Class of Transition-State Analog Inhibitors for Serine and Cysteine Proteases

5. FUNDING NUMBERS
DAMD17-96-1-6161

6. AUTHOR(S)
Christopher Seto, Ph.D.

7. PERFORMING ORGANIZATION NAME(S) AND ADDRESS(ES)
Brown University
Providence, Rhode Island 02912

E-MAIL:
christopher_seto@brown.edu

8. PERFORMING ORGANIZATION REPORT NUMBER

9. SPONSORING / MONITORING AGENCY NAME(S) AND ADDRESS(ES)
U.S. Army Medical Research and Materiel Command
Fort Detrick, Maryland 21702-5012

10. SPONSORING / MONITORING AGENCY REPORT NUMBER

11. SUPPLEMENTARY NOTES

12a. DISTRIBUTION / AVAILABILITY STATEMENT
Approved for public release; distribution unlimited

12b. DISTRIBUTION CODE

13. ABSTRACT ***(Maximum 200 Words)***

In this Final Report we describe our efforts over the last four years to develop a new class of competitive inhibitors for serine and cysteine proteases. These compounds are potential anticancer agents that would act by inhibiting metastasis and angiogenesis. Our work has shown that the 4-heterocyclohexanone pharmacophore can be used to synthesize effective inhibitors of both serine and cysteine proteases. We have rationally designed an inhibitor of the serine protease plasmin, and shown that it has good activity and specificity for plasmin over other proteases. In addition, we have used the 4-heterocyclohexanone pharmacophore to construct a combinatorial library of 400 different protease inhibitors. These compounds are unique in that they are designed to interact with both the S and S' binding sites of proteases; a feature which will increase both their potency and specificity. The library was screened against a variety of cancer-related proteases, which lead us to identify a second, even more potent inhibitor of plasmin. Finally, our investigations into the mechanism of action of these inhibitors has shown that 4-heterocyclohexanones inhibit the proteases be reacting in a reversible covalent manner with the active site nucleophile of the enzymes.

14. SUBJECT TERMS	15. NUMBER OF PAGES
Breast Cancer	77
	16. PRICE CODE

17. SECURITY CLASSIFICATION OF REPORT	18. SECURITY CLASSIFICATION OF THIS PAGE	19. SECURITY CLASSIFICATION OF ABSTRACT	20. LIMITATION OF ABSTRACT
Unclassified	Unclassified	Unclassified	Unlimited

NSN 7540-01-280-5500

Standard Form 298 (Rev. 2-89)
Prescribed by ANSI Std. Z39-18
298-102

Table of Contents

Introduction. The goal of this research project is to design inhibitors of proteolytic enzymes that promote the processes of angiogenesis and metastasis. Such proteases act by directly degrading components of the basement membrane which surround blood vessels, or in an indirect fashion by activating other proteases that in turn attack the basement membrane. Compounds that inhibit these proteases are potential anticancer chemotherapeutic agents. This Final Report describes our efforts, over the past four years, to attain this goal. We have demonstrated that the 4-heterocyclohexanone pharmacophore is a useful platform for designing potent and specific inhibitors of serine and cysteine proteases. Investigations into the mechanism of inhibition show that 4-heterocyclohexanones inhibit the proteases by forming reversible covalent bonds with the active site nucleophile. We have applied a rational design strategy to synthesize and evaluate several potent inhibitors of the serine protease plasmin. In addition we have constructed a combinatorial library of 400 different protease inhibitors that interact with both the S and S' binding sites of the enzyme. This library of compounds was assayed against a variety of different proteases that are implicated in angiogenesis and metastasis.

Body. During the period from 1996-2000, our work on developing anticancer agents that are based on a new class of protease inhibitors has been supported by an USAMRMC Breast Cancer Career Development award to the P.I., Christopher T. Seto. In this Final Report we will summarize the accomplishments that we have attained during this period. Over the last four years we have published five papers that are related to inhibition of serine and cysteine proteases. These papers are listed below. In addition we have published four other papers on other research topics. Reprints of these articles are provided in the Appendix.

1. "Using the Electrostatic Field Effect to Design a New Class of Inhibitors for Cysteine Proteases" Conroy, J. L; Sanders, T. C.; Seto, C. T. *J. Am. Chem. Soc.* **1997**, *119*, 4285.
2. "^{13}C NMR Studies Demonstrate that Tetrahydropyranone-Based Inhibitors Bind to Cysteine Proteases by Reversible Formation of a Hemithioketal Adduct" Conroy, J. L.; Seto, C. T., *J. Org. Chem.* **1998**, *63*, 2367.
3. "Synthesis of Cyclohexanone-Based Cathepsin B Inhibitors that Interact with Both the S and S' Binding Sites" Conroy, J. L.; Abato, P.; Ghosh, M.; Austermuhle, M. I.; Kiefer, M. R.; Seto, C. T. *Tetrahedron Lett.* **1998**, *39*, 8253 - 8256.
4. "4-Heterocyclohexanone-Based Inhibitors of the Serine Protease Plasmin" Sanders, T. C.; Seto, C. T. *J. Med. Chem.* **1999**, *42*, 2969.
5. "A Combinatorial Library of Serine and Cysteine Protease Inhibitors that Interact with Both the S and S' Binding Sites" Abato, P.; Conroy, J. L.; Seto, C. T. *J. Med. Chem.* **1999**, *42*, 4001.

In order to review our progress over the period of this Career Development Award we have reproduced the Statement of Work from the original proposal and provided a brief description of our accomplishments concerning each task. The Statement of Work contains twelve research goals. We have completed work on Tasks 1, 2, and 4-10. Concerning Task 3, our strategy for

synthesizing the protease inhibitors has changed over the last several years. This change has made Task 3 much less relevant to the overall goals of the project, and we have thus chosen to pass over this Task in order to pursue more interesting and productive avenues of research. A more complete explanation of our rationale is provided below. Although we have not completed Tasks 11 and 12, we are actively pursuing these goals. This research project will continue past the end of this non-renewable grant since we have obtained funding for the project from the NIH (See the Reportable Outcomes section of this report). By way of summary, we have addressed or are currently addressing every Task that was in the Statement of Work in our original proposal.

Statement of Work

Task 1: Months 1 - 4 Finish with preliminary model studies that involve synthesis and evaluation of inhibitors for the enzyme papain. Prepare a manuscript for an initial publication on cysteine protease inhibitors that are based on the 4-heterocyclohexanone nucleus.

Progress: This task has been completed, as indicated in our first Annual Report (1997). The work was published in the *J. Am. Chem. Soc.* **1997**, *119*, 4285. A reprint of this manuscript is provided in the Appendix.

Task 2: Months 4 - 10 Prepare and evaluate inhibitors for the serine protease chymotrypsin. Chymotrypsin inhibitors have been shown to have potential as cancer chemopreventive agents.

Progress: This task has been completed. The work was reported in our second and third Annual Reports (1998 and 1999). A full description of these studies are provided in "4-Heterocyclohexanone-Based Inhibitors of the Serine Protease Plasmin" Sanders, T. C.; Seto, C. T. *J. Med. Chem.* **1999**, *42*, 2969, which is provided in the Appendix. As noted in our second Annual Report, we have elected to study the serine protease plasmin rather than chymotrypsin, since plasmin has a better established role in angiogenesis and metastasis.

Task 3: Months 6 - 12 Develop methodology for the stereoselective synthesis of our protease inhibitors. Use this methodology to synthesize chymotrypsin inhibitors in a stereoselective manner.

Progress: During the course of our research, our view of the utility of this task has changed. At the outset of the project, we believed that developing a method to synthesize our

inhibitors in a stereoselective manner would increase the efficiency of the syntheses. While this is still true, we have found that each time we begin to study a new enzyme, there is rarely enough structural information available about the active site of the enzyme to allow us to accurately predict the absolute stereochemistry of an inhibitor which will bind in the active site. Thus we have found that it is more useful to synthesize the inhibitors as a mixture of two diastereomers, separate the diastereomers by high pressure liquid chromatography, and evaluate the biological activity of each of them separately. This is the strategy that we have used in all of our work, as detailed in our publications: *J. Am. Chem. Soc.* **1997**, *119*, 4285; *J. Org. Chem.* **1998**, *63*, 2367; *J. Med. Chem.* **1999**, *42*, 2969; and *J. Med. Chem.* **1999**, *42*, 4001. A copy of all of these manuscripts is provided in the Appendix. For these reasons we have not pursued this Task any further.

Task 4: Months 13 - 18 Develop methodology for synthesizing the 4-heterocyclohexanone core of extended inhibitors that are able to make contacts with both the S and S' subsites of a target enzyme.

Progress: This task has been completed, as indicated in our second Annual Report (1998). The work was published in *Tetrahedron Lett.* **1998**, *39*, 8253. A reprint of this manuscript is provided in the Appendix.

Task 5: Months 19 - 20 Develop methodology for incorporating the 4-heterocyclohexanone core described in task 4 into a solid phase approach to synthesis of protease inhibitors.

Progress: This task has been completed, as indicated in our second Annual Report (1998). The work was published in *Tetrahedron Lett.* **1998**, *39*, 8253. A reprint of this manuscript is provided in the Appendix.

Task 6: Months 21 - 24 Apply the 4-heterocyclohexanone core described in task 4 to the synthesis of a tight binding inhibitor of cathepsin B. Evaluate this new inhibitor of cathepsin B.

Progress: This task has been completed as indicated in our third Annual Report (1999). We chose to use the 4-heterocyclohexanone core described in task 4 as the basis for constructing a combinatorial library of 400 different inhibitors. We assayed this library of inhibitors against several enzymes including cathepsin B. Using this technique we identified a 4-heterocyclohexanone-based inhibitor that has an inhibition constant against cathepsin B of 1.1 mM. This work is described in detail *J. Med. Chem.* **1999**, *42*, 4001, and a reprint is provided in the Appendix.

Task 7: Months 8 - 24 Use ^{1}H-NMR spectroscopy to investigate the reactivity of the chymotrypsin and cathepsin B inhibitors with nucleophiles in aqueous solution.

Progress: We have completed these experiments using inhibitors of papain as we reported in our first Annual Report (1997), and in the publication *J. Am. Chem. Soc.* **1997**, *119*, 4285. These studies were useful because they provided a physical-organic understanding of the structure-activity relationships among the 4-heterocyclohexanone ring systems, their reactivity with nucleophiles in aqueous solution, and their reactivity with enzyme active site nucleophiles. Based upon these studies we now have a good understanding of what controls the formation of a covalent bond between the inhibitors and active site nucleophiles.

Task 8: Months 25 - 28 Synthesize an inhibitor which incorporates a ^{13}C label at the reactive ketone functionality.

Progress: This task has been completed, as indicated in our first Annual Report (1997). The work was published in *J. Org. Chem.* **1998**, *63*, 2367. A reprint of this manuscript is provided in the Appendix.

Task 9: Months 29 - 31 Use ^{13}C-NMR spectroscopy to investigate the interactions between the ^{13}C-labeled inhibitor and the enzyme active site residues.

Progress: This task has been completed, as indicated in our first Annual Report (1997). The work was published in *J. Org. Chem.* **1998**, *63*, 2367. A reprint of this manuscript is provided in the Appendix.

Task 10: Months 25 - 36 Synthesize and evaluate inhibitors for other serine and cysteine proteases that have been implicated in the initiation and metastasis of cancer such as urokinase type plasminogen activator, plasmin, and cathepsin L.

Progress: This task has been completed as reported in our third Annual Report (1999). We have used the 4-heterocyclohexanone core described in task 4 as the basis for constructing a combinatorial library of 400 different inhibitors. We have assayed this library of inhibitors against several enzymes including cathepsin B, plasmin, urokinase type plasminogen activator, and kallikrein. Using this technique we have identified an inhibitor that has excellent activity and specificity for plasmin. In addition, we have learned a great deal of valuable information concerning the specificities of the binding pockets within the active sites of these enzymes. This work is described in detail in *J. Med. Chem.* **1999**, *42*, 4001, and a reprint is provided in the Appendix.

In addition, the inhibitors that we describe in *J. Med. Chem.* **1999**, *42*, 2969 have been screened against the serine proteases plasmin, trypsin, thrombin, and kallikrein. Again, a reprint of the manuscript is provided in the Appendix.

Task 11: Months 37 - 48 Replace the peptide bonds in the inhibitors with hydrolytically stable peptidomimetic linkages in order to improve the bioavailability of the compounds.

Progress: We are currently working on the synthesis of compound **6** (Figure 1). This compound should be the most potent inhibitor of plasmin that we have synthesized to date. It incorporates three key design elements that we know, from separate studies, to be important for conferring both potency and specificity for the protease. These include an alkylammonium side chain (R group in compound **6**) that is meant to bind in the S1 specificity site of the enzyme, and two tryptophan units that are designed to interact with the S2 and the S2' specificity sites. In addition, the molecule incorporates the cyclohexanone pharmacophore that will react with the active site serine residue to give a reversibly formed hemiketal linkage. We anticipate that this compound will have an inhibition constant against plasmin that is in the mid-nanomolar range.

There are four peptide-type linkages present in compound **6**. However, in three out of the four linkages we have replaced an amide bond with an alternate functionality that may provide better stability to the compound against degradation by biological fluids. Moving from the N-terminal side to the C-terminal side of the inhibitor, we have replaced the amide linkages with: 1) a carbamate functionality; 2) a tertiary amide bond; 3) a standard peptide bond; and 4) a methyl ester. Carbamates are known to be resistant to hydrolysis by many proteases. The tertiary amide bond, though more hydrolytically labile than standard amide bonds, should not bind well to the catalytically active residues in most proteases and thus is likely to be stable in biological media. The ester linkage may be hydrolyzed to the corresponding carboxylic acid by non-specific esterases. However, we know from previous studies that this chemical change does not significantly alter the potency of inhibition against plasmin.

The synthesis of inhibitor **6** begins with compound **1**. We have previously reported the synthesis of compound **1** in *Tetrahedron Lett.* **1998**, *39*, 8253 - 8256. Reduction of the ketone in **1** with $NaBH_4$ followed by protection of the resulting alcohol with TBDMSCl gives alkene ester **2**. Hydrolysis of the ester, treatment of the resulting carboxylic acid with diphenylphosphoryl azide,

then trapping of the isocyanate with the anion of benzyl alcohol gives Cbz alkene **3**. Cleavage of the double bond with permanganate and periodate, coupling of the resulting carboxylic acid to a protected tryptophan derivative, and removal of the Cbz protecting group by catalytic hydrogenation gives amine **4**. Reductive amination of the amine, coupling of the resulting secondary amine with a protected tryptophan, and cleavage of the silyl protecting group with tetrabutylammonium flouride gives alcohol **5**. This is currently where we stand in the synthesis. The remaining two steps are yet to be completed, and are indicated by a dashed arrow in Figure 1. These steps include oxidation of the alcohol to the corresponding ketone with Dess-Martin periodinane, and removal of the Boc protecting groups with trifluoroacetic acid. We do not anticipate any problems with these final two steps of the synthesis.

Figure 1. Synthesis of a plasmin inhibitor with only one natural amide linkage.

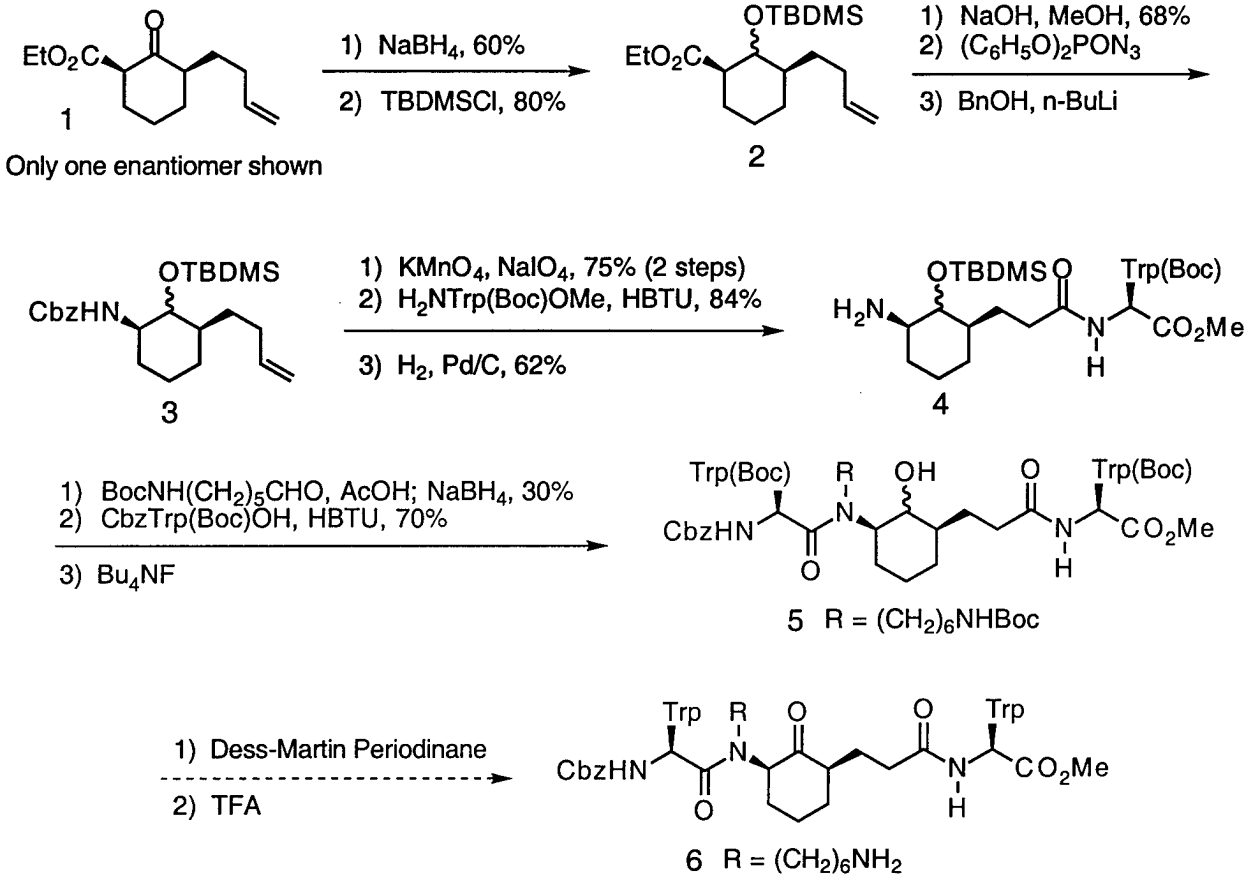

Once the synthesis of the inhibitor is complete, we will assay its activity against plasmin and other serine and cysteine proteases using techniques that we have used previously. In addition we will monitor the stability of compound **6** in biological fluids such as plasma in order to determine if the peptide replacements that we have made to the molecule have been effective in increasing its biocompatability.

Task 12: Months 37 - 48 Initiate collaborations with other researchers in order to evaluate our protease inhibitors for anticancer activity in live cell systems.

Progress: We are in the process of developing a collaboration with Dr. Robert W. Mason, Head of the Clinical Biochemistry Laboratory in the Department of Research at the Alfred I. DuPont Hospital for Children in Wilmington, DE. Through this collaboration we will study the *in vivo* biological activity of the combinatorial library of protease inhibitors that we have already developed (*J. Med. Chem.* **1999**, *42*, 4001), as well as new, larger libraries of inhibitors. Dr. Mason is investigating the role that particular cysteine proteases play in tumor cell invasion and proliferation (Xing, R.; Wu, F.; Mason, R. W. *Cancer Research* **1998**, *58*, 904). He is also interested in discovering new proteases that are important in placental development.

Key Research Accomplishments

- We have demonstrated that the 4-heterocyclohexanone pharmacophore is an excellent platform for the development of potent and specific inhibitors for serine and cysteine proteases.

- We have shown that the potency of inhibition for a variety of 4-heterocyclohexanones is directly correlated with the strength of the through-space electrostatic interaction between the electrophilic ketone functionality and the ring heteroatom. This correlation allows us to make accurate predictions concerning the potency of inhibition across a homologous series of inhibitors.

- We have demonstrated that the mechanism of inhibition involves formation of a reversible covalent bond between the ketone of the inhibitor and the enzyme nucleophile in the active site of the protease.

- We have developed both solution and solid phase methodologies for synthesizing inhibitors that make noncovalent contacts with both the S and S' protease binding sites.

- We have synthesized a variety of inhibitors that are based upon the 4-heterocyclohexanone ring system. These inhibitors were screened against four different serine proteases: plasmin, trypsin, thrombin, and kallikrein. The best of these inhibitors has high selectivity and good affinity for plasmin.

- We have synthesized a 400-membered combinatorial library of protease inhibitors that are designed to interact with both the S and S' enzyme binding sites, and screened the library against a variety of proteases. Using this strategy we have identified a potent inhibitor of plasmin that has an inhibition constant of 5 μM.

Reportable Outcomes

Publications

1. "Using the Electrostatic Field Effect to Design a New Class of Inhibitors for Cysteine Proteases" Conroy, J. L; Sanders, T. C.; Seto*, C. T. *J. Am. Chem. Soc.* **1997**, *119*, 4285.
2. "^{13}C NMR Studies Demonstrate that Tetrahydropyranone-Based Inhibitors Bind to Cysteine Proteases by Reversible Formation of a Hemithioketal Adduct" Conroy, J. L.; Seto*, C. T., *J. Org. Chem.* **1998**, *63*, 2367.
3. "Synthesis of Cyclohexanone-Based Cathepsin B Inhibitors that Interact with Both the S and S' Binding Sites" Conroy, J. L.; Abato, P.; Ghosh, M.; Austermuhle, M. I.; Kiefer, M. R.; Seto*, C. T. *Tetrahedron Lett.* **1998**, *39*, 8253 - 8256.
4. "Hydrolysis of Amides Catalyzed by 4-Heterocyclohexanones: Small Molecule Mimics of Serine Proteases" Ghosh, M.; Conroy, J. L.; Seto*, C. T. *Angew. Chemie. Int. Ed. Engl.* **1999**, *38*, 514 - 516.
5. "4-Heterocyclohexanone-Based Inhibitors of the Serine Protease Plasmin" Sanders, T. C.; Seto*, C. T. *J. Med. Chem.* **1999**, *42*, 2969.
6. "A Combinatorial Library of Serine and Cysteine Protease Inhibitors that Interact with Both the S and S' Binding Sites" Abato, P.; Conroy, J. L.; Seto*, C. T. *J. Med. Chem.* **1999**, *42*, 4001.
7. "Inhibition of Phosphatase Activity by Positively-Charged Cyclodextrins" Ghosh, M.; Sanders, C. T.; Zhang, R.; Seto*, C. T. *Org. Lett.* **1999**, *1*, 1945..
8. "The Effects of Buffers on the Thermodynamics and Kinetics of Binding Between Positively-Charged Cyclodextrins and Phosphate Ester Guests" Ghosh, M.; Zhang, R.; Lawler, R. G.; Seto*, C. T. *J. Org. Chem.* **2000**, *65*, 735.

9. "Biotinylation of Substituted Cysteines in the Nicotinic Acetylcholine Receptor Reveals Distinct Binding Modes for α-Bungarotoxin and Erabutoxin a" Spura, A.; Riel, R. U.; Freedman, N. D.; Agrawal, S.; Seto, C. T.; Hawrot, E.* *J. Biol. Chem.* **2000**, *275*, 22452.

Funded Research Grants

- American Chemical Society - Petroleum Research Fund Type G - Grant 30544-G4
  Title: "Through-Space Electronic Interactions as the Basis for a New Class of Serine and Cysteine Protease Inhibitors"
  Level of Funding: $20,00 Duration: 1996 - 98
- Brown University - Salomon Faculty Research Award
  Title: "Anticancer Agents Based on a New Class of Transition-State Analog Inhibitors for Serine and Cysteine Proteases"
  Level of Funding: $15,000 Duration: 1996 - 98
- National Institutes of Health - R01 - Grant GM57327-01
  Title: "A New Class of Serine and Cysteine Protease Inhibitors"
  Level of Funding: $809,852 Duration: 1998 - 2003

Invited Research Presentations

- Ischia Advanced School of Organic Chemistry VII conference - September 30, Ischia, Italy
- Zeneca Pharmaceuticals Group - December 5, 1996
- Wesleyan University - October 15, 1997
- University of Rhode Island - October 17, 1997
- University of Maryland - November 11, 1997
- Rhode Island College - November 21, 1997
- Rutgers University, Newark - April 17, 1998

- University of Massachusetts, Amherst - April 30, 1998
- National Science Foundation Workshop on Natural Products - July 16 - 20, 1998
- University of Connecticut - November 9, 1998
- University of Missouri at Columbia - February 10, 1999
- University of Wisconsin - February 11, 1999
- Tufts University - March 2, 1999
- Wellesley College - October 29, 1999
- Boston College - November 23, 1999
- Merrimack College – February 2, 2000
- Aventis Pharmaceuticals Inc. – May 24, 2000
- Bioorganic Gordon Research Conference Short Talk – June 20, 2000

Conclusions

This Final Report describes our efforts, over the last four years, to systematically investigate a new class of serine and cysteine protease inhibitors as potential anticancer agents. Cancer cells release a number of serine and cysteine proteases that have been shown to stimulate angiogenesis and to promote the proliferation and migration of tumor cells. These enzymes either act directly by degrading components of the extracellular matrix and basement membrane such as collagen, elastin, fibronectin, laminin, and entactin, or indirectly by activating other proteolytic enzymes. Inhibition of these proteases has been shown to be an effective method for blocking tumor invasion of the extracellular matrix and basement membrane by cancer cells. Thus development of a new class of potent and specific inhibitors for these enzymes should have a direct impact on the treatment of breast cancer by providing chemotherapeutic agents which are designed to inhibit tumor growth and metastasis.

During the past four years we have demonstrated that the 4-heterocyclohexanone pharmacophore is useful for developing a number of potent and specific inhibitors for serine and cysteine proteases that are important in both angiogenesis and metastasis. Our mechanistic investigations have shown that these inhibitors act by forming a reversible covalent bond with the active site nucleophile of the proteases. These studies demonstrate that our initial design process for these inhibitors was successful. We have expanded the structure of the inhibitors to make noncovalent contacts with both the S and S' subsites of the proteases. This modification was expected to further increase their potency and specificity for cancer-related proteases. Using the core pharmacophore that resulted from this synthetic work, we have constructed a 400-membered combinatorial library of protease inhibitors and screened this library against a variety of cancer-related proteases. This process resulted in the discovery of a highly potent inhibitor of the serine protease plasmin. We are currently making rational modifications to this plasmin inhibitor to increase its stability *in vivo*. We are also initiating a collaboration in order to investigate the anticancer activity of the protease inhibitors in live cell systems.

References

1. "Using the Electrostatic Field Effect to Design a New Class of Inhibitors for Cysteine Proteases" Conroy, J. L; Sanders, T. C.; Seto*, C. T. *J. Am. Chem. Soc.* **1997**, *119*, 4285.
2. "^{13}C NMR Studies Demonstrate that Tetrahydropyranone-Based Inhibitors Bind to Cysteine Proteases by Reversible Formation of a Hemithioketal Adduct" Conroy, J. L.; Seto*, C. T., *J. Org. Chem.* **1998**, *63*, 2367.
3. "Synthesis of Cyclohexanone-Based Cathepsin B Inhibitors that Interact with Both the S and S' Binding Sites" Conroy, J. L.; Abato, P.; Ghosh, M.; Austermuhle, M. I.; Kiefer, M. R.; Seto*, C. T. *Tetrahedron Lett.* **1998**, *39*, 8253 - 8256.
4. "Hydrolysis of Amides Catalyzed by 4-Heterocyclohexanones: Small Molecule Mimics of Serine Proteases" Ghosh, M.; Conroy, J. L.; Seto*, C. T. *Angew. Chemie. Int. Ed. Engl.* **1999**, *38*, 514 - 516.
5. "4-Heterocyclohexanone-Based Inhibitors of the Serine Protease Plasmin" Sanders, T. C.; Seto*, C. T. *J. Med. Chem.* **1999**, *42*, 2969.
6. "A Combinatorial Library of Serine and Cysteine Protease Inhibitors that Interact with Both the S and S' Binding Sites" Abato, P.; Conroy, J. L.; Seto*, C. T. *J. Med. Chem.* **1999**, *42*, 4001.
7. "Inhibition of Phosphatase Activity by Positively-Charged Cyclodextrins" Ghosh, M.; Sanders, C. T.; Zhang, R.; Seto*, C. T. *Org. Lett.* **1999**, *1*, 1945..
8. "The Effects of Buffers on the Thermodynamics and Kinetics of Binding Between Positively-Charged Cyclodextrins and Phosphate Ester Guests" Ghosh, M.; Zhang, R.; Lawler, R. G.; Seto*, C. T. *J. Org. Chem.* **2000**, *65*, 735.
9. "Biotinylation of Substituted Cysteines in the Nicotinic Acetylcholine Receptor Reveals Distinct Binding Modes for α-Bungarotoxin and Erabutoxin a" Spura, A.; Riel, R. U.; Freedman, N. D.; Agrawal, S.; Seto, C. T.; Hawrot, E.* *J. Biol. Chem.* **2000**, *275*, 22452.

All other references pertinent to this Annual Report are provided at the end of the manuscripts that are contained in the Appendices.

Appendices

These appendices contain copies of the nine manuscripts listed below:

1. "Using the Electrostatic Field Effect to Design a New Class of Inhibitors for Cysteine Proteases" Conroy, J. L; Sanders, T. C.; Seto*, C. T. *J. Am. Chem. Soc.* **1997**, *119*, 4285.
2. "^{13}C NMR Studies Demonstrate that Tetrahydropyranone-Based Inhibitors Bind to Cysteine Proteases by Reversible Formation of a Hemithioketal Adduct" Conroy, J. L.; Seto*, C. T., *J. Org. Chem.* **1998**, *63*, 2367.
3. "Synthesis of Cyclohexanone-Based Cathepsin B Inhibitors that Interact with Both the S and S' Binding Sites" Conroy, J. L.; Abato, P.; Ghosh, M.; Austermuhle, M. I.; Kiefer, M. R.; Seto*, C. T. *Tetrahedron Lett.* **1998**, *39*, 8253 - 8256.
4. "Hydrolysis of Amides Catalyzed by 4-Heterocyclohexanones: Small Molecule Mimics of Serine Proteases" Ghosh, M.; Conroy, J. L.; Seto*, C. T. *Angew. Chemie. Int. Ed. Engl.* **1999**, *38*, 514 - 516.
5. "4-Heterocyclohexanone-Based Inhibitors of the Serine Protease Plasmin" Sanders, T. C.; Seto*, C. T. *J. Med. Chem.* **1999**, *42*, 2969.
6. "A Combinatorial Library of Serine and Cysteine Protease Inhibitors that Interact with Both the S and S' Binding Sites" Abato, P.; Conroy, J. L.; Seto*, C. T. *J. Med. Chem.* **1999**, *42*, 4001.
7. "Inhibition of Phosphatase Activity by Positively-Charged Cyclodextrins" Ghosh, M.; Sanders, C. T.; Zhang, R.; Seto*, C. T. *Org. Lett.* **1999**, *1*, 1945..
8. "The Effects of Buffers on the Thermodynamics and Kinetics of Binding Between Positively-Charged Cyclodextrins and Phosphate Ester Guests" Ghosh, M.; Zhang, R.; Lawler, R. G.; Seto*, C. T. *J. Org. Chem.* **2000**, *65*, 735.
9. "Biotinylation of Substituted Cysteines in the Nicotinic Acetylcholine Receptor Reveals Distinct Binding Modes for α-Bungarotoxin and Erabutoxin a" Spura, A.; Riel, R. U.; Freedman, N. D.; Agrawal, S.; Seto, C. T.; Hawrot, E.* *J. Biol. Chem.* **2000**, *275*, 22452.

Using the Electrostatic Field Effect to Design a New Class of Inhibitors for Cysteine Proteases

Jeffrey L. Conroy, Tanya C. Sanders, and Christopher T. Seto*

Contribution from the Department of Chemistry, Brown University, Providence, Rhode Island 02912

Received December 4, 1996[⊗]

Abstract: A new class of competitive inhibitors for the cysteine protease papain is described. These inhibitors are based upon a 4-heterocyclohexanone ring and are designed to react with the enzyme active site nucleophile to give a reversibly formed hemithioketal. The electrophilicity of the ketone in these inhibitors is enhanced by ring strain and by through-space electrostatic repulsion with the heteroatom at the 1-position of the ring. Equilibrium constants for addition of water and 3-mercaptopropionic acid to several 4-heterocyclohexanones were measured by ^{1}H NMR spectroscopy. These reactions model addition of the active site nucleophile to the corresponding inhibitors. The equilibrium constants give a linear correlation with the field substituent constant F for the functional group at the 1-position of the heterocyclohexanone. These equilibrium constants also correlate well with the inhibition constants for the 4-heterocyclohexanone-based inhibitors, which range from 11 to 120 μM. Thus, the model system can be used to predict the potency of structurally related enzyme inhibitors.

Introduction

The Field Effect. The physical-organic literature contains many examples of chemical systems that use through-space electronic interactions to control equilibria or regio- and stereospecificity of organic reactions.[1,2] Molecules such as 4-substituted bicyclo[2.2.2]octane-1-carboxylic acid have been developed to investigate the Coulombic interaction between a polar substituent and a carboxylic acid.[3] The through-space electrostatic interaction between these groups perturbs the pK_a of the acid. More recently, Siegel and co-workers examined through-space polar π interactions in *para*-substituted 2,6-diphenylbenzoic acids.[4] In this system, the substituents alter the polarity of the phenyl rings, which in turn influence the acidity and hydrogen-bonding characteristics of the carboxylic acid. These examples demonstrate that through-space electrostatic interactions can exert a powerful influence on chemical reactions. Despite the importance of these studies, we and others[4] have noted that through-space interactions are seldom used as a rational design element in bioorganic and medicinal chemistry.[5] In this paper, we present a physical-organic strategy for designing a new class of inhibitors for cysteine proteases. These inhibitors are based on a 4-heterocyclohexanone nucleus and take advantage of through-space electrostatic repulsion to control the potency of enzyme inhibition.

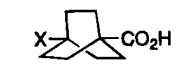

bicyclo[2.2.2]octane-1-carboxylic acids

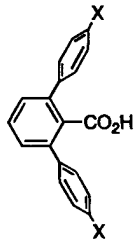

2,6-diphenylbenzoic acids

Other Cysteine Protease Inhibitors. Cysteine proteases are important targets in medicinal chemistry. They have been implicated in diseases such as rheumatoid arthritis,[6] muscular dystrophy,[7] and cancer metastasis.[8] Many types of chemical functionality have served as the central pharmacophore for reversible and irreversible inhibitors of cysteine proteases. Among the reversible inhibitors are aldehydes,[9] nitriles,[10] α-keto carbonyl compounds,[11] and cyclopropenones.[12] Aldehydes and nitriles inhibit proteases by forming a reversible covalent bond between the electrophilic functionality of the inhibitor and the nucleophilic sulfur atom of the active site cysteine residue.[13]

[⊗] Abstract published in *Advance ACS Abstracts,* May 1, 1997.

(1) (a) Winstein, S.; Shatavsky, M.; Norton, C.; Woodward, R. B. *J. Am. Chem. Soc.* **1955**, *77*, 4183. (b) Winstein, S.; Shatavsky, M. *J. Am. Chem. Soc.* **1956**, *78*, 592. (c) For a recent review, see: Bowden, K.; Grubbs, E. J. *Chem. Soc. Rev.* **1996**, *25*, 171.

(2) Lowry, T. H.; Richardson, K. S. *Mechanism and Theory in Organic Chemistry*, 3rd ed.; Harper and Row: New York, 1987.

(3) (a) Roberts, J. D.; Moreland, W. T., Jr. *J. Am. Chem. Soc.* **1953**, *75*, 2167. (b) Holtz, H. D.; Stock, L. M. *J. Am. Chem. Soc.* **1964**, *86*, 5188.

(4) Chen, C.-T.; Siegel, J. S. *J. Am. Chem. Soc.* **1994**, *116*, 5959.

(5) (a) For an example taken from synthetic organic chemistry, see: Boeckman, R. K., Jr.; Connell, B. T. *J. Am. Chem. Soc.* **1995**, *117*, 12368. (b) For a discussion of field and resonance effects in benzoxazinone inhibitors of human leukocyte elastase, see: Krantz, A.; Spencer, R. W.; Tam, T. F.; Liak, T. J.; Copp, L. J.; Thomas, E. M.; Rafferty, S. P. *J. Med. Chem.* **1990**, *33*, 464.

(6) Van Noorden, C. F.; Smith, R. E.; Rasnick, D. *J. Rheumatol.* **1988**, *115*, 1525.

(7) Prous, J. R., Ed. *Drugs Future* **1986**, *11*, 927−943.

(8) (a) Liotta, L. A.; Steeg, P. S.; Stetler-Stevenson, J. G. *Cell* **1991**, *64*, 327. (b) Baricos, W. H.; Zhou, Y.; Mason, R. W.; Barrett, A. J. *Biochem. J.* **1988**, *252*, 301.

(9) (a) Hanzlik, R. P.; Jacober, S. P.; Zygmunt, J. *Biochim. Biophys. Acta* **1991**, *1073*, 33. (b) Cheng, H.; Keitz, P.; Jones, J. B. *J. Org. Chem.* **1994**, *59*, 7671.

(10) Hanzlik, R. P.; Zygmunt, J.; Moon, J. B. *Biochem. Biophys. Acta* **1990**, *1035*, 62.

(11) Hu, L.-Y.; Abeles, R. H. *Arch. Biochem. Biophys.* **1990**, *281*, 271.

(12) Ando, R.; Morinaka, Y.; Tokuyama, H.; Isaka, M.; Nakamura, E. *J. Am. Chem. Soc.* **1993**, *115*, 1174.

(13) (a) Moon, J. B.; Coleman, R. S.; Hanzlik, R. P. *J. Am. Chem. Soc.* **1986**, *108*, 1350. (b) Brisson, J.-R.; Carey, P. R.; Storer, A. C. *J. Biol. Chem.* **1986**, *261*, 9087. (c) Gamcsik, M. P.; Malthous, J. P. G.; Primrose, W. U.; Mackenzie, N. E.; Boyd, A. S. F.; Russell, R. A.; Scott, A. I. *J. Am. Chem. Soc.* **1983**, *105*, 6324. (d) Liang, T.-C.; Abeles, R. H. *Arch. Biochem. Biophys.* **1987**, *252*, 626.

S0002-7863(96)04186-8 CCC: $14.00

Chart 1. Structures of Cysteine Protease Inhibitors

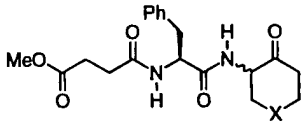

X = CH_2, S, O, NH_2^+

This mechanism is also likely to be operative in the α-keto carbonyl[11] and cyclopropenone inhibitors.

Design of Inhibitors. Chart 1 shows the structures of 4-heterocyclohexanone-based inhibitors for the cysteine protease papain. These inhibitors consist of a 4-heterocyclohexanone core that is appended with an *N*-(methoxysuccinyl)phenylalanine side chain. We have chosen papain for our initial studies because its structure and mechanism have been thoroughly characterized. In addition, it provides a good model for evaluating the design of new inhibitors and for comparing them to previously reported compounds. The inhibitors include a phenylalanine residue because papain has a high specificity for this amino acid at the P2 position.[14] The methoxysuccinyl group was attached in order to increase solubility of the compounds in aqueous solution.

The inhibitors incorporate an electrophilic ketone moiety that is designed to give a reversibly formed hemithioketal with the enzyme active site nucleophile, in analogy with previously reported inhibitors. Compounds based upon unactivated ketones are not electrophilic enough to react with the active site cysteine nucleophile.[15] However, the carbonyl groups in 4-heterocyclohexanones are more electrophilic than standard ketones. Two factors increase their reactivity. First, there is an unfavorable dipole–dipole repulsion between the carbonyl and the heteroatom at the 1-position of the ring.[16–18] This interaction destabilizes the ketone, but is dissipated by addition of nucleophiles. Second, ring strain enhances the reactivity of 4-heterocyclohexanones. The cyclic compounds are more strained than their acyclic counterparts, and this strain is relieved by nucleophilic addition to the carbonyl to give a tetrahedral center.[18,19] Variations in the bond angles and bond lengths associated with the heteroatom will modulate this effect.[20]

An alternate method for increasing the electrophilicity of ketones is to add electron-withdrawing substituents to them. This strategy, which relies on through-bond inductive effects, has been implemented in the synthesis of potent trifluoromethyl ketone inhibitors of serine proteases.[21] However, these compounds have been found to be poor reversible inhibitors of cysteine proteases.[22]

We have synthesized a series of inhibitors that incorporate increasingly electronegative functional groups at the 1-position of the heterocyclohexanone ring. These compounds have allowed us to examine the relationship between the electronic characteristics of the X group (Chart 1) and the potency of the inhibitor. Electronegative X groups are expected to destabilize the ketone via through-space electrostatic repulsion, thereby shifting the ketone–hemithioketal equilibrium in favor of the hemithioketal and resulting in more potent inhibition.

The compounds reported in this paper are first-generation inhibitors that interact only with the S subsites of the enzyme active site. However, the 4-heterocyclohexanone nucleus can be derivatized on both sides of the electrophilic carbonyl to yield inhibitors that make contacts with both the S and S′ subsites. This is in contrast to aldehyde- and nitrile-based inhibitors that are limited to interactions with only half of the active site.

Table 1. Equilibrium Constants for Addition of Water and Thiol to Selected Ketones[a]

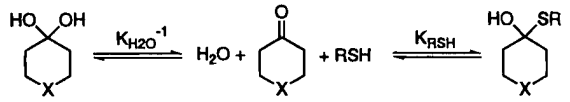

X	K_{H_2O} (M^{-1})	K_{RSH} (M^{-1})	$K_{RSH,app}$ (M^{-1})
CH_2	8.1×10^{-4}	0.22	0.21
S	9.0×10^{-3}	1.5	0.99
O	8.0×10^{-3}	1.8	1.3
NH_2^+	0.18	27.6	2.7
SO	0.068	11.7	2.5
SO_2	0.30	60.2	3.5
	Other Ketones		
CH_3COCH_3[b]	2.3×10^{-5}	0.0052	0.0052
CH_3COCO_2H[b]	0.031	58	22
$CH_3COCO_2CH_3$[b]	0.045	71	20

[a] RSH = $HO_2CCH_2CH_2SH$. [b] Data taken from reference 23.

Results

Model System. Before we undertook the multistep synthesis of our cysteine protease inhibitors, we first wanted to investigate the degree to which the heteroatom influences the reactivity of the ketone in these compounds. We have thus measured the equilibrium constants for addition of water and thiol nucleophiles to simple 4-heterocyclohexanones. These nucleophilic additions serve as a model for reaction of the enzyme active site nucleophile with the inhibitors.

Table 1 shows equilibrium constants for addition of water and 3-mercaptopropionic acid to a variety of ketones. The equilibrium constants were determined using ^1H NMR spectroscopy according to the procedure of Burkey and Fahey.[18,23] Figure 1 shows NMR spectra of tetrahydropyran-4-one as an example of how these measurements were made. The bottom spectrum, taken in acetone-d_6, shows resonances that correspond to tetrahydropyranone. The middle spectrum, taken in D_2O, shows resonances for the both the ketone (a and b) and the hydrate (c and d). These two species are in slow exchange on the NMR time scale. Integration of the resonances can be used to determine the hydration equilibrium constant. The top spectrum shows a mixture of tetrahydropyranone and 3-mercaptopropionic acid in D_2O. We observe resonances for ketone, hydrate, hemithioketal (e–h), and free thiol (i and j). Equilibrium constants for several of the ketones listed in Table 1 have been measured previously under different reaction conditions.[18,24] Our equilibrium constants are in reasonable agreement with the

(14) (a) Hanzlik, R. P.; Jacober, S. P.; Zygmunt, J. *Biochim. Biophys. Acta* **1991**, *1073*, 33. (b) Berti, P. J.; Faerman, C. H.; Storer, A. C. *Biochemistry* **1991**, *30*, 1394.

(15) Bendall, M. R.; Cartwright, I. L.; Clart, P. I.; Lowe, G.; Nurse, D. *Eur. J. Biochem.* **1977**, *79*, 201.

(16) Geneste, P.; Durand, R.; Hugon, I.; Reminiac, C. *J. Org. Chem.* **1979**, *44*, 1971.

(17) Das, G.; Thornton, E. R. *J. Am. Chem. Soc.* **1993**, *115*, 1302.

(18) Burkey, T. J.; Fahey, R. C. *J. Org. Chem.* **1985**, *50*, 1304.

(19) (a) Allinger, N. L.; Tribgle, M. T.; Miller, M. A. *Tetrahedron* **1972**, *28*, 1173. (b) Gung, B. W.; Wolf, M. A.; Mareska, D. A.; Karipides, A. *J. Org. Chem.* **1994**, *59*, 4899.

(20) Transannular anomeric interactions have been used previously to explain reaction rates and axial selectivities for addition of nucleophiles to 4-heterocyclohexanones. It is possible that these types of interactions also stabilize the hemithioketal that results from nucleophilic addition of a thiol to these ketones. (a) Cieplak, A. S. *J. Am. Chem. Soc.* **1981**, *103*, 4540. (b) Cieplak, A. S. *J. Am. Chem. Soc.* **1989**, *111*, 8447 and references therein.

(21) (a) Imperiali, B.; Abeles, R. H. *Biochemistry* **1986**, *25*, 3760. (b) Brady, K.; Abeles, R. H. *Biochemistry* **1990**, *29*, 7608. (c) Govardhan, C. P.; Abeles, R. H. *Arch. Biochem. Biophys.* **1990**, *280*, 137.

(22) (a) Smith, R. A.; Copp, L. J.; Donnelly, S. L.; Spencer, R. W.; Krantz, A. *Biochemistry* **1988**, *27*, 6568. (b) Peptide monofluoromethyl ketones have been shown to be selective irreversible inhibitors of cysteine proteases: Rasnick, D. *Anal. Biochem.* **1985**, *149*, 461. (c) Rauber, P.; Angliker, H.; Walker, B.; Shaw, E. *Biochem. J.* **1986**, *239*, 633.

(23) Burkey, T. J.; Fahey, R. C. *J. Am. Chem. Soc.* **1983**, *105*, 868.

Scheme 1[a]

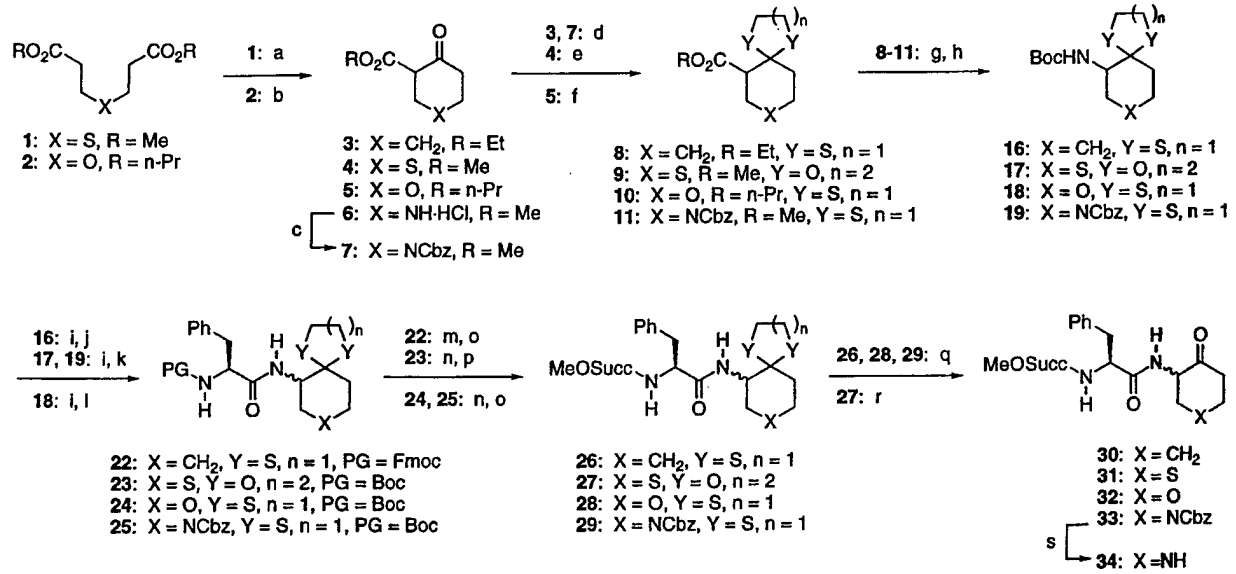

[a] (a) NaH, catalytic MeOH, 81%; (b) LDA, THF, −78 °C, 31%; (c) CbzCl, TEA, 95%; (d) ethanedithiol, TsOH, 94% from **3**, 74% from **7**; (e) 1,3-propanediol, TsOH, 77%; (f) ethanedithiol, BF_3·Et_2O, 43%; (g) NaOH, MeOH; (h) diphenylphosphoryl azide, benzene, followed by *t*-BuOK, THF, 60% from **8**, 37% from **9**, 44% from **10**, 71% from **11** (two step yields); (i) TFA, CH_2Cl_2; (j) FmocPhe-F, DIEA, 92% (two steps); (k) BocPhe-OH, EDC, HOBT, 84% from **17**, 81% from **19** (two step yields); (l) BocPhe-F, DIEA, 61% (two steps); (m) $N(CH_2CH_2NH_2)_3$, CH_2Cl_2; (n) TFA, CH_2Cl_2; (o) monomethyl succinate, EDC, HOBT, 70% from **22**, 70% from **24**, 89% from **25** (two step yields); (p) methyl(*N*-hydroxysuccinimidyl) succinate, DIEA, 77% (two steps); (q) NBS, H_2O, 80% from **26**, 66% from **28**, 68% from **29**; (r) acetone, TsOH, 79%; (s) H_2, 5% Pd/C, 79%.

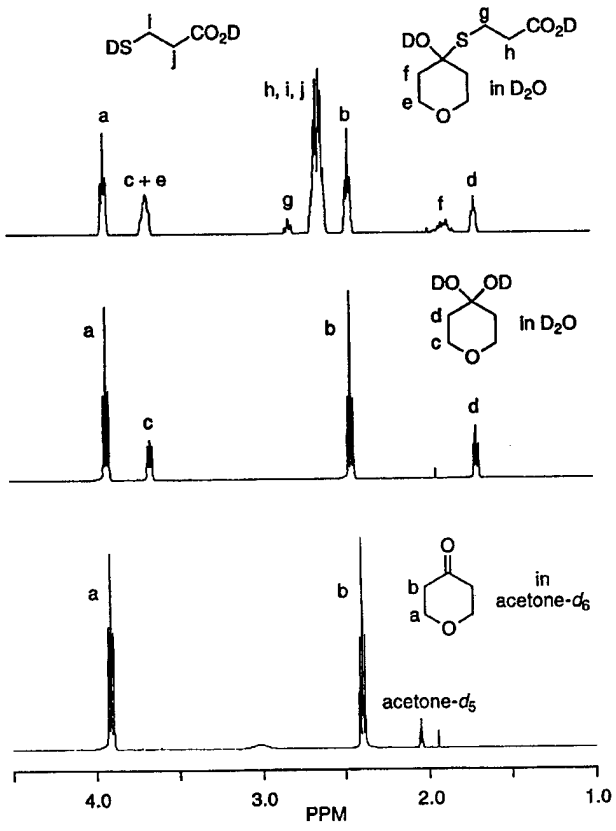

Figure 1. ^1H NMR spectra of the ketone, hydrate, and hemithioketal of tetrahydropyranone. The bottom spectrum shows the ketone in acetone-d_6 solution. The middle spectrum shows a mixture of ketone and hydrate in D_2O solution. The top spectrum shows a mixture of ketone, hydrate, hemithioketal, and free thiol in D_2O solution.

previously reported values. Equilibrium constants for acetone, pyruvic acid, and methyl pyruvate are taken from the literature.[23]

The hydration equilibrium constant for cyclohexanone is 35 times greater than that of acetone. In cyclohexanone, ring strain destabilizes the ketone and shifts the equilibrium by 2.1 kcal/mol in favor of hydrate when compared to acetone. Substituting electronegative functionality at the 4-position of the cyclohexanone ring leads to further destabilization of the ketone as a result of through-space electrostatic repulsion. For example, in the sulfone-containing molecule, the equilibrium is shifted by an additional 3.5 kcal/mol in favor of the hydrate. These results demonstrate that the electrostatic field effect, in combination with ring strain, can have a significant influence on the stability of hydrates. Similar trends are observed for the formation of hemithioketals.

The reaction between an enzyme and an inhibitor occurs in an aqueous environment. We must therefore consider that reaction between papain and the 4-heterocyclohexanone-based inhibitors will occur in competition with reaction between the inhibitor and water. This competition will lower the effective concentration of the inhibitor. We have calculated an *apparent* equilibrium constant for addition of thiol to ketone ($K_{RSH,app}$), first described by Jencks,[25] that accounts for the fact that the inhibitor will be present as a mixture of both ketone and hydrate in aqueous solution.

$$K_{RSH,app} = [\text{hemithioketal}]/[\text{ketone} + \text{hydrate}][\text{thiol}] = K_{RSH}/(1 + K_{H_2O}[H_2O]) \quad (1)$$

For molecules such as acetone that form a minimal amount of hydrate, the $K_{RSH,app}$ value is approximately equal to K_{RSH}. However, if a ketone forms a significant amount of hydrate, then $K_{RSH,app}$ is less than K_{RSH}. If the ketone, but not the hydrate form of these compounds, is the active inhibitory species, we would expect a correlation between the $K_{RSH,app}$ value of the parent ketone and the potency of the corresponding inhibitor.

Synthesis of Inhibitors. We have developed a generalized strategy for the synthesis of our papain inhibitors (Scheme 1). This strategy allows us to perform similar reactions in the

(24) (a) Wiberg, K. B.; Morgan, K. M.; Maltz, H. *J. Am. Chem. Soc.* **1994**, *116*, 11067. (b)Van Luppen, J. J.; Lepoivre, J. A.; Dommissee, R. A.; Alderweireldt, F. C. *Org. Magn. Reson.* **1979**, *12*, 399.

(25) Sanders, E. G.; Jencks, W. P. *J. Am. Chem. Soc.* **1968**, *90*, 6154.

preparation of each of the four target compounds. Dieckmann condensation of diesters **1** and **2** gives keto esters **4** and **5**. Compounds **3** and **6** are commercially available. The yield for cyclization of **2** is only 31%, presumably because of competing β-elimination. However, this represents a significant improvement over the previously reported synthesis of methyl tetrahydropyran-4-one-3-carboxylate, which proceeded in 8% yield.[26] The ketones in compounds **3**, **5**, and **7** are protected as thioketals. Since the oxidative conditions that are used for removal of this protecting group are not compatible with thioethers, compound **4** is protected as an oxygen ketal. The esters are hydrolyzed and the resulting carboxylic acids are treated with diphenylphosphoryl azide.[27] Curtius rearrangement followed by trapping of the isocyanates with *t*-BuOK gives carbamates **16**–**19**. The Boc protecting groups are removed with trifluoroacetic acid, and the resulting amines are coupled with an N-protected phenylalanine derivative.[28] After removing the phenylalanine protecting groups, the free amines are coupled to monomethyl succinate to give compounds **26**–**29**. The thioketal protecting groups in compounds **26**, **28**, and **29** are removed by treatment with *N*-bromosuccinimide,[29] and the diastereomers of inhibitors **30** and **32** are separated by HPLC. The Cbz protecting group in compound **33** is removed by catalytic hydrogenation to give inhibitor **34**, which is evaluated as a mixture of diastereomers. The diastereomers of **27** can be separated by flash chromatography, and each are then treated with acetone and *p*-toluenesulfonic acid to give the separate diastereomers of inhibitor **31**.

Racemization of Inhibitors. Papain is assayed in 100 mM phosphate buffer at pH 6.5. These conditions may catalyze the enolization of the ketone in our inhibitors and thus lead to their racemization. We have monitored this reaction using HPLC or ^{1}H NMR spectroscopy. The cyclohexanone-based inhibitor **30** was very stable under the assay conditions, showing less that 5% racemization after 24 h. Tetrahydropyranone **32** was somewhat less stable, with a half-time for racemization of 5.25 h. However, this reaction is slow enough so that over the time period of a typical enzyme assay, the compound racemizes less than 1%. We were unable to separate the diastereomers of piperidone inhibitor **34** or its precursor **33** by standard chromatographic techniques. However, the diastereomers of compound **35**, which has an acetyl group on its N-terminus rather than a methoxysuccinyl group, were readily separated by HPLC. We therefore chose to study racemization of compound **36** by ^{1}H NMR spectroscopy. Over the course of the 10 min required

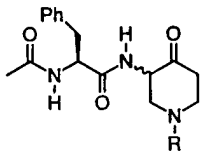

35 a and b: R = Cbz
36 a and b: R = H

to prepare the sample and acquire the spectrum, this compound was completely racemized. Therefore, we measured the inhibition constant for compound **34** as a mixture of diastereomers. We have not examined racemization of the tetrahydrothiopyranone-based inhibitor **31**, but observed reactivity trends and chemical intuition both suggest that it should have a racemization rate that falls between that of compounds **30** and **32**.

Inhibition Studies. The 4-heterocyclohexanone-based inhibitors **30**–**32** and **34** are all reversible competitive inhibitors

Table 2. Inhibition of Papain by 4-Heterocyclohexanone-Based Inhibitors

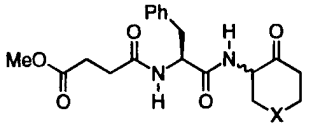

X	K_i (μM) more-potent diastereomer	K_i (μM) less-potent diastereomer
CH_2	78	3200
S	26	2400
O	11	3300
NH_2^+	121[a]	
Other Ketone-Based Inhibitors		
AcPhe-$NHCH_2COMe$		1550[b]
ZPhe-$NHCH_2COCO_2H$		7[c]
ZPhe-$NHCH_2COCO_2Me$		1[c]

[a] Assayed as a mixture of diastereomers. This compound racemizes under the assay conditions. [b] Data from ref 15. [c] Data from ref 11.

of papain (Table 2).[30] The enzyme shows a clear preference for one diastereomer of each inhibitor, although we have not determined the absolute configuration of the tighter binding diastereomer. Data for the acetone-, pyruvic acid-, and methyl pyruvate-based inhibitors are included in Table 2 for comparison. Although these three reference compounds do not have a methoxysuccinyl group on their N-terminus, our previous work has demonstrated that inhibitors with *N*-acetyl or *N*-Cbz blocking groups have inhibition constants that are within a factor of two of the *N*-methoxysuccinyl compounds.

The cyclohexanone-based inhibitor (X = CH_2) is 20 times more potent than the noncyclic acetone-based inhibitor. This is a reflection of the ring strain in cyclohexanone that destabilizes the ketone relative to the hemithioketal that is formed by reaction of the inhibitor with the active site nucleophile. Substituting electronegative functionality into the ring (X = S, O) leads to even better inhibitors. This trend in inhibition constants mirrors the differences that we observe for reaction of the parent ketones with water and thiol nucleophiles. The only compound that does not fit the trend is the piperidone-based inhibitor **34**. This compound is protonated under the assay conditions (pH 6.5), and its low potency is likely caused by the unfavorability of placing this positive charge into the enzyme active site.[9]

Discussion

Linear Free-Energy Relationship. We observe a correlation between the reactivity of 4-heterocyclohexanones and the electronic properties of the heteroatom in these molecules. This correlation requires an appropriate description of the magnitude of the through-space electrostatic repulsion between the heteroatom and the ketone. Swain and Lupton[31] have constructed a modified Hammett equation (eq 2) in which they describe the electronic characteristics of substituents in terms of two parameters; a field substituent constant F, and a resonance substituent constant R.

$$\log(K_x/K_H) = \rho(fF + rR) \qquad (2)$$

The terms f and r are empirical weighing factors that are specific for the particular reaction and set of reaction conditions,

(26) Dowd, P.; Choi, S.-C. *Tetrahedron* **1991**, *47*, 4847.
(27) Shioiri, T.; Ninomiya, K.; Yamada, S. *J. Am. Chem. Soc.* **1972**, *94*, 6203.
(28) (a) Carpino, L. A.; Sadat-Aalaee, D.; Chao, H. G.; DeSelms, R. H. *J. Am. Chem. Soc.* **1990**, *112*, 9651. (b) Carpino, L. A.; Mansour, E. M. E.; Sadat-Aalaee, D. *J. Org. Chem.* **1991**, *56*, 2611.
(29) Corey, E. J.; Erickson, B. W. *J. Org. Chem.* **1971**, *36*, 3553.
(30) Enzyme assays were performed according to the procedures of ref 11. None of these compounds showed evidence of slow-binding inhibition. Lineweaver–Burk plots are available in the Supporting Information.
(31) (a) Swain, C. G.; Lupton, E. C., Jr. *J. Am. Chem. Soc.* **1968**, *90*, 4328. (b) Swain, C. G.; Unger, S. H.; Rosenquist, N. R.; Swain, M. S. *J. Am. Chem. Soc.* **1983**, *105*, 492.

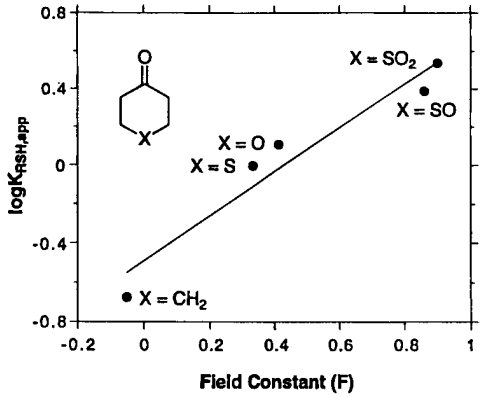

Figure 2. Correlation between the logarithm of the apparent equilibrium constant for addition of thiol to 4-heterocyclohexanones and the field substituent constant F (log $K_{RSH,app}$ = 1.1F − 0.5; correlation coefficient = 0.97).

while the F and R parameters are independent of the reaction. If the major interaction between the heteroatom and ketone is electrostatic, then the field substituent constant F should provide a good measure of this interaction.

The chemical systems that are used to define field substituent constants are designed so that the substituents are attached to the parent molecules through a single bond.[31] However, in 4-heterocyclohexanones the heteroatom is attached by two bonds. We have thus approximated the functionality at the 1-position of heterocyclohexan-4-ones by using the field constant for the substituents -CH_3, -SCH_3, -OCH_3, -$SOCH_3$, and -SO_2CH_3. Protonated piperidone has been omitted from our analysis because the F value for the corresponding substituent, -$NH_2CH_3^+$, has not been reported.

Figure 2 shows that there is a good correlation between the logarithm of the apparent equilibrium constants for addition of thiol to 4-heterocyclohexanones (log $K_{RSH,app}$) and the field substituent constants.[32] This correlation confirms that the interaction between the heteroatom and the ketone in 4-heterocyclohexanones is best described as a through-space electrostatic repulsion. Resonance effects, differences in ring strain, and transannular anomeric effects[20] have a relatively minor influence on the equilibria of the reversible addition of water and thiol nucleophiles to these ketones. The slope of the line in Figure 2 is 1.1. A similar plot for dissociation of 4-substituted benzoic acids has a slope of 0.49.[31] Comparison of these values suggests that addition of thiols to 4-heterocyclohexanones responds two times more strongly to the *field component* of the electronic effects exerted by substituents. The larger slope for the addition reaction is reasonable because the substituent and reaction center are closer together than they are in 4-substituted benzoic acids.

Correlation between Ketone Reactivity and Enzyme Inhibition. We have designed our cysteine protease inhibitors on the basis of the supposition that inhibitor potency is controlled by the stability of the hemithioketal that results from addition of the active site nucleophile to the inhibitor, although we have not proved the existence of this hemithioketal through structural studies. If this supposition is correct, we should observe a correlation between inhibition constants and the equilibrium constants for addition of thiol to the parent ketones. Because enzyme inhibition takes place in aqueous solvent, the most appropriate comparison is between inhibition constants and $K_{RSH,app}$ values.[33]

(32) A good correlation also exists between log K_{RSH} and F and between log K_{H_2O} and F. However, there is a poor correlation between log $K_{RSH,app}$ and the resonance substituent constant R (correlation coefficient = 0.41)

(33) For a similar analysis involving inhibitors of cathepsin B, see: ref 22a.

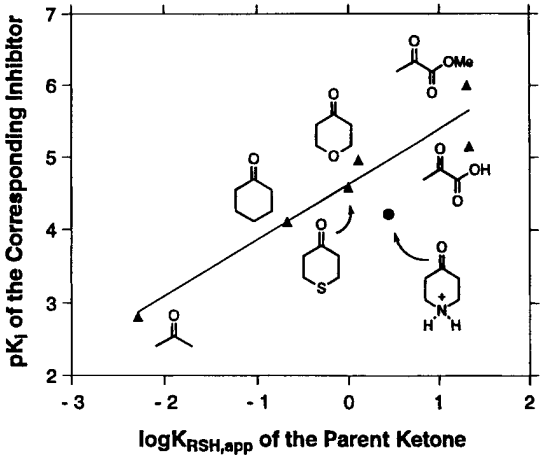

Figure 3. Correlation between inhibition constant (pK_i) of the ketone-based inhibitors and the logarithm of the apparent equilibrium constant for addition of thiol to the parent ketones (pK_i = 0.8 log $K_{RSH,app}$ + 4.6; correlation coefficient = 0.96).

The correlation shown in Figure 3 demonstrates that addition of 3-mercaptopropionic acid to simple ketones in aqueous solution is an appropriate model for addition of the enzyme active site cysteine residue to the corresponding ketone-based inhibitors. The apparent equilibrium constant for the model reaction provides a good prediction of inhibitor potency for this structurally homologous series of compounds. The plot of pK_i vs log $K_{RSH,app}$ has a slope of 0.8. This slope, which is less than unity, indicates that the enzymatic addition reaction responds less efficiently to the electrophilicity of the ketone than does the model system. The difference in reactivity is likely caused by the differences in steric, electronic, solvation, and orientational requirements of the enzymatic reaction compared to the reaction in solution.

We have omitted the piperidone-based inhibitor **34** from the linear regression in Figure 3 because the positive charge on this molecule perturbs its reactivity with the enzyme. As expected, this inhibitor does not fit well into a correlation that is based simply upon electrophilicity of the ketone in these molecules.

Conclusions. The results presented in this paper demonstrate that through-space electrostatic interactions can be useful and predictable design elements for construction of bioactive molecules. The physical-organic correlations point the way toward synthesis of more potent inhibitors. This goal can be achieved by choosing functionality that further increase the electrostatic repulsion between the heteroatom and the ketone in 4-heterocyclohexanones, such as a sulfoxide or sulfone. In addition, potency and specificity can be increased by functionalizing both the 3- and 5-positions of the heterocyclohexanone ring so that we extend noncovalent interactions of the inhibitor into the leaving group subsites. Future studies will be aimed toward proving formation of the hemithioketal intermediate using ^{13}C NMR spectroscopy in conjuction with an inhibitor that is labeled with ^{13}C at the ketone carbon.

Experimental Section

General Methods. NMR spectra were recorded on Brucker WM-250 or AM-400 instruments. Spectra were calibrated using TMS (δ = 0.00 ppm) for ^1H NMR and $CDCl_3$ (δ = 77.0) for ^{13}C NMR. IR spectra were recorded on a Perkin-Elmer 1700 series FT-IR spectrometer. Mass spectra were recorded on a Kratos MS 80 under electron impact (EI), chemical ionization (CI), or fast-atom bombardment (FAB) conditions. HPLC analyses were performed on a Rainin HPLC system with Rainin Microsorb silica or C18 columns and UV detection. Semipreparative HPLC was performed on the same system using a semipreparative column (21.4 × 250 mm).

Reactions were conducted under an atmosphere of dry nitrogen in oven-dried glassware. Anhydrous procedures were conducted using standard syringe and cannula transfer techniques. THF and toluene were distilled from sodium and benzophenone. Methylene chloride was distilled from CaH_2. Other solvents were of reagent grade and were stored over 4 Å molecular sieves. All other reagents were used as received. Organic solutions were dried with $MgSO_4$ unless otherwise noted. Solvent removal was performed by rotary evaporation at water aspirator pressure.

Experimental details of the synthesis of inhibitors **30**, **31**, and **34** are available in the Supporting Information.

Di-*n*-propyl 4-Oxa-1,7-heptanedioate 2. A solution of 3,3′-oxydipropionitrile (18.9 g, 152 mmol) and *p*-toluenesulfonic acid (*p*-TsOH) monohydrate (115.8 g, 608 mmol) in *n*-propanol (200 mL) was refluxed for 24 h. The solution was cooled and concentrated to approximately 150 mL. The resulting solution was partitioned between 350 mL of water and 350 mL of hexanes. The organic layer was separated and washed with saturated $NaHCO_3$ (200 mL), water (300 mL), and brine (150 mL). The solution was dried, filtered, and concentrated, and the crude material was purified by flash chromatography (1:3 EtOAc/hexanes) to yield **2** (21.2 g, 57%) as a colorless liquid. The product can also be purified by vacuum distillation (bp 158 °C, 6 mm) in somewhat lower yields (45%): R_f 0.66 (1:1 EtOAc/hexanes); ^{1}H NMR (400 MHz, $CDCl_3$) δ 0.94 (t, J = 7.4 Hz, 3H), 1.66 (dt, J = 7.0, 7.1 Hz, 2H), 2.57 (t, J = 6.1 Hz, 2H), 3.73 (t, J = 6.4 Hz, 2H), 4.04 (t, J = 6.7 Hz, 2H); ^{13}C NMR (100 MHz, $CDCl_3$) δ 10.3, 21.9, 35.0, 66.1, 66.4, 171.5; HRMS-FAB calcd for $C_{12}H_{22}O_5$ 246.1467, found 246.1467.

***n*-Propyl Tetrahydropyran-4-one-3-carboxylate 5.** To a solution of diispropylamine (4.65 g, 45.9 mmol) in THF (50 mL) at −78 °C was added *n*-butyllithium (4.38 mL of 10.0 M in hexanes). This solution was added via cannula to a solution of **2** (5.14 g, 20.9 mmol) in THF (300 mL) at −78 °C. The solution was stirred at −78 °C for 15 min, and then the reaction was quenched by the addition of 25 mL of H_2O. The solution was partitioned between 200 mL of 1 N HCl and 200 mL of hexanes. The resulting aqueous layer was extracted with EtOAc (150 mL), and the combined organic layers were washed with brine (300 mL). The solution was dried, filtered, and concentrated, and the crude material purified by flash chromatography (1:4 Et_2O/hexanes) to yield **5** (1.19 g, 31%) as a mixture of keto and enol tautomers: R_f = 0.54 (1:1 Et_2O/hexanes); ^{1}H NMR (400 MHz, $CDCl_3$) δ 0.95 (t, J = 6.3 Hz, 3H), 1.27−1.31 (m), 1.61−1.75 (m, 2H), 2.37−2.41 (m, 3H), 2.52−2.59 (m), 2.66−2.73 (m), 3.46−3.50 (m), 3.71−3.75 (m), 3.85 (t, J = 5.7 Hz, 2H), 3.98−4.10 (m), 4.12 (t, J = 6.6 Hz, 2H), 4.16−4.25 (m), 4.28 (t, J = 1.7 Hz, 2H), 11.85 (s, 1H); ^{13}C NMR (100 MHz, $CDCl_3$) δ 10.2, 21.9, 28.6, 41.8, 57.8, 63.9, 65.8, 66.3, 67.0, 68.1, 69.6, 97.4, 127.8, 129.7, 168.7, 170.1, 201.4; HRMS-EI (M^+) calcd for $C_9H_{14}O_4$ 186.0892, found 186.0894.

Tetrahydropyranone Thioketal 10. To a solution of **5** (1.26 g, 6.8 mmol) and 1,2-ethanedithiol (1.28 g, 13.6 mmol) in CH_2Cl_2 (20 mL) cooled in an ice bath was added BF_3·Et_2O (1.04 mL, 8.5 mmol). The solution was stirred at 0 °C for 4 h, and then it was washed with 10% aqueous NaOH solution, water, and brine (20 mL). The organic layer was dried, and concentrated, and the crude material was purified by flash chromatography (2:3 EtOAc/hexanes) to yield **10** (0.77 g, 43%) as a colorless oil: ^{1}H NMR (400 MHz, $CDCl_3$) δ 0.96 (t, J = 7.4 Hz, 3H), 1.63−1.73 (m, 2H), 1.93 (dm, J = 13.7 Hz, 1H), 2.84−2.88 (m, 1H), 2.91−2.92 (m, 1H), 3.24−3.32 (m, 4H), 3.64−3.69 (m, 1H), 3.90−3.93 (m, 2H), 4.08−4.14 (m, 3H); ^{13}C NMR (100 MHz, $CDCl_3$) δ 10.4, 21.9, 38.3, 39.1, 40.0, 54.8, 65.7, 66.5, 67.8, 69.5, 171.0; HRMS-EI (M^+) calcd for $C_{11}H_{18}O_3S_2$ 262.0697, found 262.0707.

Tetrahydropyranone Carboxylic Acid 14. To a solution of **10** (0.41 g, 1.58 mmol) in MeOH (10 mL) was added 1 N NaOH (10 mL). The solution was stirred at 30 °C for 50 h. The solution was then cooled and diluted with 0.2 N NaOH (10 mL). The solution was washed with 1:1 EtOAc/hexanes (10 mL), and the aqueous layer was separated and acidified with 1 N HCl. The acidic aqueous solution was extracted with EtOAc (2 × 40 mL). These organic extracts were washed with brine (50 mL), dried, and concentrated. The resulting solid was recrystallized from EtOAc/hexanes to yield **14** (0.22 g, 68%) as a white solid: ^{1}H NMR (400 MHz, $CDCl_3$) δ 1.98 (d, J = 13.8 Hz, 1H), 2.76 (m, 1H), 2.99 (t, J = 3.3 Hz, 1H), 3.29−3.35 (m, 4H), 3.68−3.74 (m, 1H), 3.88 (t, J = 4.3 Hz, 1H), 3.93 (t, J = 4.2 Hz, 1H), 3.99 (dd, J = 3.4, 12.2 Hz, 1H), 4.12 (dd, J = 3.4, 11.8 Hz, 1H); ^{13}C NMR (100 MHz, $CDCl_3$) δ 38.5, 39.2, 40.3, 54.2, 65.5, 67.8, 69.2; HRMS-EI (M^+) calcd for $C_8H_{12}O_3S_2$ 220.0228, found 220.0224.

Tetrahydropyranone Carbamate 18. A solution of **14** (0.22 g, 1.0 mmol), *N,N*-diisopropylethylamine (DIEA, 1.9 g, 1.50 mmol), and diphenylphosphoryl azide (DPPA, 0.28 g, 1.0 mmol) in benzene (10 mL) was refluxed overnight. Aliquots of the reaction mixture were monitored for disappearance of the acyl azide peak at 2168 cm^{-1} and appearance of the isocyanate peak at 2245 cm^{-1} by FT-IR. After the Curtius rearrangement was judged complete by IR, the solution was cooled in an ice bath and slowly added to an ice-cold solution of potassium *tert*-butoxide (0.34 g, 3.0 mmol) in THF (10 mL). The reaction was stirred for 15 min and then partitioned between 15 mL of 1 N HCl and 15 mL of EtOAc. The organic layer was separated and washed with 1 N NaOH and brine (15 mL). The solution was dried, filtered, and concentrated, and the crude material was purified by flash chromatography (1:4 EtOAc/hexanes) to yield **18** (0.19 g, 65%) as a white solid: ^{1}H NMR (400 MHz, $CDCl_3$) δ 1.45 (s, 9H), 2.21 (t, J = 4.5 Hz, 2H), 3.26−3.35 (m, 4H), 3.61−3.64 (m, 1H), 3.79−3.82 (m, 1H), 3.89−3.99 (m, 2H), 5.04 (brd, J = 7.7 Hz, 1H); ^{13}C NMR (100 MHz, $CDCl_3$) δ 27.5, 37.7, 37.9, 40.9, 54.2, 66.1, 70.0, 78.1, 154.4; HRMS-EI (M^+) calcd for $C_{12}H_{21}NO_3S_2$ 291.0963, found 291.0959.

Aminotetrahydropyranone·Trifluoroacetic Acid Salt 21. Trifluoroacetic acid (TFA, 3.0 mL) was added to a solution of **18** (0.18 g, 0.62 mmol) in CH_2Cl_2 (10 mL) that was cooled in an ice bath. The reaction was stirred at 0 °C for 1 h, concentrated, redissolved in CH_2Cl_2, and then concentrated again to remove excess TFA. The crude oil was then triturated with ether to yield **21** (0.18 g, 95%) as a white solid: ^{1}H NMR (400 MHz, $CDCl_3$) δ 2.14 (dt, J = 14.3, 5.6 Hz, 1H), 2.44 (dt, J = 14.1, 5.0 Hz, 1H), 3.32−3.47 (m, 5H), 3.70−3.76 (m, 3H), 4.04 (dd, J = 12.2, 3.0 Hz, 1H); ^{13}C NMR (100 MHz, $CDCl_3$) δ 39.9, 40.1, 41.1, 56.7, 68.1, 68.5, 68.6, 118.2 (q), 162.9 (q); HRMS-EI (M^+) calcd for $C_7H_{13}NOS_2$ 191.0439, found 191.0437.

Phenylalanyltetrahydropyranone 24. To a solution of **21** (250 mg, 0.82 mmol) and DIEA (529 mg, 4.1 mmol) in CH_2Cl_2 (10 mL) was added solid N-Boc-phenylalanyl fluoride[28] (240 mg, 0.90 mmol). The solution was stirred for 1 h and then washed with 1 N HCl, saturated $NaHCO_3$, and brine (10 mL). The solution was dried over Na_2CO_3 and concentrated, and the crude material was purified by flash chromatography (2:3 EtOAc/hexanes) to yield a mixture of diastereomers of **24** (218 mg, 61%) as a white solid: ^{1}H NMR (400 MHz, $CDCl_3$) δ 1.31 (s, 9H), 1.34 (s, 9H), 2.03−2.15 (m, 4H), 2.82 (brs, 1H), 2.94−3.16 (m, 13H), 3.46−3.51 (m, 2H), 3.57 (brm, 1H), 3.67−3.77 (m, 3H), 4.14 (brm, 1H), 4.19−4.27 (m, 2H), 4.37 (brm, 1H), 5.14 (brm, 1H), 5.31 (brm, 1H), 6.18 (brm, 1H), 6.58 (d, J = 9.0 Hz, 1H), 7.11−7.24 (m, 10H); ^{13}C NMR (100 MHz, $CDCl_3$) δ 27.8, 28.0, 37.7, 38.1, 38.77, 38.79, 38.84, 41.8, 52.8, 52.9, 53.0, 53.1, 55.4, 55.9, 66.79, 66.84, 69.4, 69.6, 69.7, 69.9, 79.8, 126.5, 126.6, 128.3, 128.4, 129.0, 129.2, 155.1, 170.6, 170.9; HRMS-FAB (M + Na^+) calcd for $C_{21}H_{30}N_2NaO_4S_2$ 461.1545, found 461.1544.

(Methoxysuccinyl)tetrahydropyranone 28. A solution of **24** (200 mg, 0.46 mmol) and TFA (3 mL) in CH_2Cl_2 (7 mL) was stirred at 25 °C for 1 h. This solution was concentrated, and the resulting material was triturated with ether to precipitate the TFA salt as a white solid. This solid was washed with ether, dried under vacuum, and then added to a solution of methyl succinate (61 mg, 0.46 mmol), 1-hydroxybenzotriazole (HOBT, 72 mg, 0.46 mmol), 1-(3-(dimethylamino)propyl)-3-ethylcarbodiimide hydrochloride (EDC, 114 mg, 0.60 mmol), and *N*-methylmorpholine (0.10 mL) in CH_2Cl_2 (5 mL). The reaction was stirred overnight at room temperature, and then it was washed with water, 1 M $KHSO_4$, saturated Na_2CO_3, and dried over Na_2CO_3. The dried solution was concentrated, and the crude material was purified by flash chromatography (7:3 EtOAc/hexanes) to yield a mixture of diastereomers of **28** (144 mg, 70%) as a white solid: ^{1}H NMR (400 MHz, $CDCl_3$) δ 2.11−2.14 (m, 4H), 2.45−2.50 (m, 2H), 2.52−2.54 (m, 2H), 2.57−2.64 (m, 4H), 2.97−3.13 (m, 5H), 3.19−3.26 (m, 9H), 3.53−3.62 (m, 3H), 3.65 (s, 3H), 3.67 (s, 3H), 3.76−3.86 (m, 3H), 4.17−4.22 (m, 1H), 4.26−4.31 (m, 1H), 4.66−4.71 (m, 1H), 4.77−4.82 (m, 2H), 6.25 (d, J = 6.3 Hz, 1H), 6.68 (d, J = 9.1 Hz, 1H), 6.77 (d, J = 8.0 Hz, 1H), 6.96 (d, J = 7.7 Hz, 1H), 7.21−7.30 (m, 10H); ^{13}C NMR (100 MHz, $CDCl_3$) δ 29.0, 29.1, 30.59, 30.61, 37.9, 38.2, 38.81, 38.88, 38.93, 41.9, 51.6, 53.0, 53.3, 54.3, 54.7, 66.9, 67.0, 69.48, 69.50, 69.7, 69.9, 126.6, 126.8, 128.4, 128.5, 129.1, 129.3, 136.5, 170.3,

170.7, 171.2, 171.4, 172.9, 173.0; HRMS-FAB (M + Na^+) calcd for $C_{21}H_{28}N_2NaO_5S_2$ 475.1338, found 475.1349.

Tetrahydropyranone Inhibitors 32a and 32b. A solution of *N*-bromosuccinimide (NBS, 440 mg, 2.47 mmol) in 80% aqueous MeCN (10 mL) was cooled in an ice bath. To this solution was added **28** (160 mg, 0.35 mmol) in MeCN (5 mL). The ice bath was removed, and the reaction mixture was stirred for 10 min. It was then partitioned between 1:1 CH_2Cl_2/EtOAc (25 mL) and saturated Na_2SO_3 (10 mL). The organic layer was separated, washed with saturated $NaHCO_3$ and brine, and dried over Na_2CO_3. The dried solution was concentrated, and the residue was redissolved in 1:1 MeCN/H_2O. This solution was filtered and extracted with 1:1 CH_2Cl_2/EtOAc. The resulting organic layer was dried and concentrated to yield a mixture of diastereomers of **32** (88 mg, 66%) as a white solid. The diastereomers were separated by HPLC (silica) with 3.5% 2-propanol in CH_2Cl_2 as the mobile phase. The retention times for diastereomers **32a** and **32b** were 13.1 and 14.1 min, respectively. For **32a**: ^{1}H NMR (400 MHz, $CDCl_3$) δ 2.45−248 (m, 3H), 2.59−2.74 (m, 3H), 2.93 (t, J = 9.9 Hz, 1H), 3.03 (m, 1H), 3.12−3.14 (m, 1H), 3.55 (t, J = 11.4 Hz, 1H), 3.67 (s, 3H), 4.29 (brm, 1H), 4.42 (brm, 1H), 4.61 (brm, 1H), 4.72 (brm, 1H), 6.28 (brm, 1H), 6.59 (brm, 1H), 7.17−7.31 (m, 5H); ^{13}C NMR (100 MHz, $CDCl_3$) δ 29.1, 30.9, 38.3, 42.2, 51.9, 54.4, 57.3, 68.8, 71.6, 127.1, 128.7, 129.2, 136.3, 170.7, 171.3, 173.4, 202.5; HRMS-FAB (M + Na^+) calcd for $C_{19}H_{24}N_2NaO_6$ 399.1532, found 399.1537. For **32b**: ^{1}H NMR (400 MHz, $CDCl_3$) δ 2.45−2.48 (m, 3H), 2.59−2.78 (m, 3H), 3.02−3.06 (m, 1H), 3.10−3.13 (m, 2H), 3.59 (t, J = 11.5 Hz, 1H), 3.67 (s, 3H), 4.27−4.32 (m, 1H), 4.54 (m, 2H), 4.73 (brm, 1H), 6.32 (brm, 1H), 6.66 (brm, 1H), 7.17−7.31 (m, 5H); ^{13}C NMR (100 MHz, $CDCl_3$) δ 29.1, 30.9, 38.2, 42.1, 51.8, 54.3, 57.5, 68.8, 71.8, 127.1, 128.7, 129.2, 136.1, 170.9, 171.3, 173.3, 202.2; HRMS-FAB (M + Na^+) calcd for $C_{19}H_{24}N_2NaO_6$ 399.1532, found 399.1521.

Measurement of K_{H_2O} and K_{RSH} by ^{1}H NMR Spectroscopy. These equilibrium constants were measured at 25 °C on a Brucker AM-400 NMR spectrometer according to the procedures of Burkey and Fahey.[18,23] Cyclohexanone, tetrahydropyran-4-one, tetrahydrothiopyran-4-one, and 4-piperidone hydrochloride were purchased from Aldrich Chemical Co. and used without further purification. NMR samples were prepared by dissolving the ketone (100 mM) in D_2O. For measurements of K_{RSH}, the concentration of 3-mercaptopropionic acid was 200 mM.

Racemization of Inhibitors. The racemization of the cyclohexanone inhibitors **30a** and **30b** was followed by RPHPLC using the conditions reported above for the separation of the two diastereomers. Each diastereomer was dissolved in 100 mM phosphate buffer at pH 6.5. Less than 5% racemization was detected after 24 h.

The racemization of the tetrahydropyranone inhibitors **32a** and **32b** was monitored using ^{1}H NMR spectroscopy by integration of the methyl ester signal at 3.47 ppm for **32a** and 3.45 ppm for **32b**. Each diastereomer was dissolved in 100 mM phosphate buffer at pH 6.5 that was prepared using D_2O. The observed first-order rate constant for racemization was measured to be $k_{obsd} = (2.2 \pm 0.5) \times 10^{-3}$ min^{-1}. This rate constant corresponds to a half-time for racemization of 5.25 h. Thus, over the time period of a typical enzyme assay, less than 1% of each diastereomer of the inhibitor will have racemized to the undesired diastereomer.

Racemization experiments for the piperidone-based inhibitor were performed using compounds **35a** and **35b**. These diastereomers were separated by HPLC with an eluent of 2% MeOH in CH_2Cl_2 (**35a** retention time 15.5 min; **35b** retention time 20.5 min). The Cbz protecting group in each diastereomer was removed using the procedure reported for the preparation of compound **34**, which yielded compounds **36a** and **36b**. ^{1}H NMR spectra demonstrated that these deprotections occurred with retention of stereochemistry. Diastereomer **36a** was split into two samples and each placed in an NMR tube. One sample was dissolved in 100 mM phosphate buffer (pH 6.5) that was prepared using D_2O. The ^{1}H NMR spectrum of this sample demonstrated that the compound was completely racemized within 10 min under these conditions. The second sample was dissolved in 1:1 acetone-d_6/D_2O. ^{1}H NMR of this sample showed relatively slow reaction, with complete racemization after approximately 22 h. Diastereomer **36b** gave similar results. For **36a**: ^{1}H NMR (400 MHz, $CDCl_3$) δ 1.98 (brs, 3H), 2.45−2.54 (brm, 3H), 3.06 (brs, 1H), 4.38−4.45 (brm, 2H), 4.75−4.82 (brm, 2H), 5.17 (brm, 2H), 6.34 (brs, 1H), 6.79 (brs, 1H), 7.18−7.38 (brm, 10H); ^{13}C NMR (100 MHz, $CDCl_3$) δ 23.2, 38.5, 40.4, 44.1, 48.7, 54.4, 56.6, 67.9, 127.1, 128.0, 128.2, 128.6, 128.7, 129.2, 136.2, 154.8, 170.0, 171.1, 202.88, 202.94; HRMS-FAB (M + Na^+) calcd for $C_{24}H_{27}N_3NaO_5$ 460.1849, found 460.1860. For **36b**: ^{1}H NMR (400 MHz, $CDCl_3$) δ 1.98 (brs, 3H), 2.44 (brm, 3H), 3.01 (brm, 3H), 4.46 (brs, 2H), 4.67−4.76 (brm, 2H), 5.18 (brm, 2H), 6.38 (brs, 1H), 6.68 (brs, 1H), 7.19−7.40 (brm, 10H); ^{13}C NMR (100 MHz, $CDCl_3$) δ 23.2, 38.7, 40.4, 44.2, 48.5, 54.5, 56.3, 67.9, 127.0, 128.0, 128.3, 128.6, 128.7, 129.3, 136.2, 136.4, 154.8, 170.2, 170.9, 203.2; HRMS-FAB (M + Na^+) calcd for $C_{24}H_{27}N_3NaO_5$ 460.1849, found 460.1849.

Papain Assays. Papain (recrystallized two times) and L-BAPNA (*N*α-benzoyl-L-arginine *p*-nitroanilide hydrochloride) were used as received from Sigma Chemical Co. Reaction progress was monitored with a Perkin-Elmer 8452A diode array UV-vis spectrometer. Papain was assayed at 25 °C in 100 mM phosphate buffer (pH 6.5) containing 5 mM EDTA and 5 mM cysteine. BAPNA and inhibitor stock solutions contained DMSO (10−100%), and all assay mixtures contained a final DMSO concentration of 10%. Papain stock solutions (0.5−1 mg/mL) were prepared in buffer (5×), and the enzyme was activated for 1 h before the assays were run. Initial rates were determined by monitoring the change in absorbance at 412 nm from 60 to 120 s after mixing. None of the inhibitors showed evidence of slow binding. The more potent diastereomer of each inhibitor was subjected to full kinetic analysis. For each inhibitor concentration examined (**30a** 0, 21, 53, 107, 160, 217 μM; **31a** 0, 2.7, 5.5, 27.4, 55, 110 μM; **32a** 0, 2, 25, 50, 75, 100 μM; **34a** 0, 13.9, 69.5, 139, 209, 417 μM) at least five substrate concentrations were used (**30a** 0.37, 0.53, 0.75, 1.5, 7.5 mM; **31a** 0.5, 0.66, 0.99, 2.0, 6.6 mM; **32a** 0.5, 0.65, 0.94, 1.7, 4.5, 8.0 mM; **34a** 0.5, 0.66, 0.99, 2.0, 6.6 mM) with at least two independent determinations at each concentration. K_m was measured to be 4.89 mM. The background hydrolysis rate was less than 1% of the slowest rate measure and thus ignored. K_i values were determined by nonlinear fit to the Michaelis−Menten equation for competitive inhibition using simple weighing. Competitive inhibition was confirmed by Lineweaver−Burk analysis using robust statistical weighing to the linear fit of $1/[V]$ vs $1/[S]$. For the less-potent diastereomer of each inhibitor, a single substrate concentration (**30a** 5.28 mM; **31a** 3.30 mM; **32a** 4.22 mM) was monitored at with least 4 different inhibitor concentration (**30a** 0, 130, 410, 830 μM; **31a** 0, 0.14, 0.29, 0.57, 1.14, 1.72 mM; **32a** 0, 0.1, 0.56, 1.1, 1.5, 1.9 mM). Competitive inhibition was assumed, and K_i was calculated using a Dixon analysis. Data analysis was performed with the commercial graphing package Grafit (Erithacus Software Ltd).

Acknowledgment. This research was supported by the American Cancer Society (grant IN-45-36), the American Chemical Society−Petroleum Research Fund (grant 30544-G4), the U.S. Army Medical Research and Materiel Command−Breast Cancer Research Initiative (Career Development Award to C.T.S., grant DAMD17-96-1-6328), and Brown University (Salomon Faculty Research Award). T.C.S. was supported by a Department of Education GAANN Fellowship and by the USAMRMC−Breast Cancer Research Initiative (Predoctoral Fellowship, grant DAMD17-96-1-6037). J.L.C. was supported by a GAANN Fellowship and by a University Fellowship from Brown University. We thank Professor David Cane for use of his UV−vis spectrometer.

Supporting Information Available: Lineweaver−Burk plots for the inhibition of papain by compounds **30**−**32** and **34**; ^{1}H and ^{13}C NMR characterization for compounds reported in the Experimental Section; experimental details of the synthesis of inhibitors **30**, **31**, and **34** (55 pages). See any current masthead page for ordering and Internet access instructions.

JA9641867

Demonstration by ^{13}C NMR Studies That Tetrahydropyranone-Based Inhibitors Bind to Cysteine Proteases by Reversible Formation of a Hemithioketal Adduct

Jeffrey L. Conroy and Christopher T. Seto*

Department of Chemistry, Brown University, Providence, Rhode Island 02912

Received October 3, 1997

Introduction

Cysteine proteases are important targets in medicinal chemistry.[1] Members of this class of proteolytic enzymes, such as the calpains[2] and cathepsins B and L,[1] are implicated in a variety of diseases including rheumatoid arthritis, muscular dystrophy, and cancer. In addition, a new family of cysteine proteases have recently been discovered that are related to interleukin-1β converting enzyme (ICE) and CED-3.[3] These new proteases share a specificity for substrates with aspartic acid at the P1 position and have been shown to play key roles in both the regulation and initiation of programmed cell death or apoptosis. Excessive apoptosis causes neural damage in both Alzheimer's and Huntington's diseases, while insufficient apoptosis occurs in many cancers and in autoimmune disorders such as AIDS. The implication of cysteine proteases in such a large number of disease states provides a strong motivation for developing potent and specific inhibitors of these enzymes. Such compounds may serve as both new therapeutic agents and as tools for investigating the role of cysteine proteases in disease processes.

We have recently described a new class of cysteine protease inhibitors that are based upon a 4-heterocyclohexanone nucleus (compounds **1**–**4**).[4] The electrophilic ketone group in these compounds is designed to react with the enzyme-active-site nucleophile to give a reversibly formed hemithioketal adduct. This adduct mimics the tetrahedral intermediate that is formed during enzyme-catalyzed peptide hydrolysis. The reactivity of this carbonyl is enhanced by ring strain and by through-space electrostatic repulsion from the heteroatom at the 4-position of the ring. There is a good correlation between the electrophilicity of this ketone moiety and the potency of the inhibitors against the enzyme papain.[4]

Our interpretation of inhibition studies with compounds **1**–**4** was based upon the assumption that a hemithioketal does indeed form between the inhibitors and the active-site cysteine residue. This assumption is reasonable on the basis of the well-established mechanism by which papain catalyzes cleavage of amide bonds[1] and comparison of 4-heterocyclohexanones with other inhibitors, such as peptide aldehydes, that are known to give this type of covalent adduct.[5,6] However, there are at least two other plausible explanations for the reactivity trends that we observed. First the hydrate of the ketone, and not the ketone itself, could be the active inhibitory species. Hydrates of active carbonyl compounds are good inhibitors of both aspartic proteases such as pepsin and renin and metalloproteases such as angiotensin-converting enzyme and carboxypeptidase A.[7] Second, the differences in inhibition could have been caused by formation of a specific hydrogen bond or electrostatic interaction between the enzyme and the polar heteroatom at the 4-position of the ring. The goal of our current work is to determine if the mechanism by which 4-heterocyclohexanones inhibit papain is through formation of a hemithioketal adduct. Our approach is to synthesize an inhibitor, tetrahydropyranone **10** (Scheme 1), that incorporates a ^{13}C label at the ketone carbon. Reaction of this labeled inhibitor with a stoichiometric amount of papain is monitored by ^{13}C NMR spectroscopy. These experiments allow us to observe directly formation of the hemithioketal adduct between enzyme and inhibitor. The results demonstrate that, like peptide aldehydes, 4-heterocyclohexanones are transition-state analogue inhibitors of cysteine proteases.[5,8]

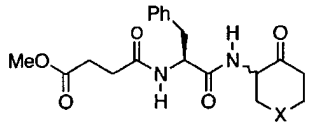

1: X = CH_2
2: X = S
3: X = O
4: X = NH_2^+

Results and Discussion

Synthesis of the Labeled Inhibitor. We have developed a synthesis of inhibitor **10** that places a single ^{13}C label specifically at the ketone carbon (Scheme 1). Reaction of bromoethyl ether **5** with $Et_4N^{13}CN$ gave dinitrile **6**.[9] The labeled reagent can be conveniently prepared from $K^{13}CN$ and Et_4NBF_4.[10] Alcoholysis of **6** followed by base-promoted cyclization of the resulting diester gave keto ester **7**. After protection of the ketone

(1) For a recent review of cysteine proteases and their inhibitors, see: Otto, H. H.; Schirmeister, T. *Chem. Rev.* **1997**, *97*, 133.

(2) Wang, K.; Yuen, P.-W. *Trends Pharmacol. Sci.* **1994**, *15*, 412.

(3) (a) Miller, D. K. *Ann. Rep. Med. Chem.* **1996**, *31*, 249. (b) Schwartz, L. M.; Milligan, C. E. *Trends Neurosci.* **1996**, *19*, 555. (c) Nicholson, D. W.; Ali, A.; Thornberry, N. A.; Vaillancourt, J. P.; Ding, C. K.; Gallant, M.; Gareau, Y.; Griffin, P. R.; Labelle, M.; Lazebnik, Y. A.; Munday, N. A.; Raju, S. M.; Smulson, M. E.; Yamin, T.-T.; Yu, V. L.; Miller, D. K. *Nature* **1995**, *376*, 37. (d) Nicholson, D. W. *Nature Biotech.* **1996**, *14*, 297.

(4) Conroy, J. L.; Sanders, T. C.; Seto, C. T. *J. Am. Chem. Soc.* **1997**, *119*, 4285.

(5) Gamcsik, M. P.; Malthouse, J. P. G.; Primrose, W. U.; Mackenzie, N. E.; Boyd, A. S. F.; Russell, R. A.; Scott, A. I. *J. Am. Chem. Soc.* **1983**, *105*, 6324.

(6) Recently, X-ray crystallography has been used to demonstrate formation of a hemithioketal adduct between a ketone-based inhibitor and the cysteine protease cathepsin K. Yamashita, D. S.; Smith, W. W.; Zhao, B.; Janson, C. A.; Tomaszek, T. A.; Bossard, M. J.; Levy, M. A.; Oh, H.-J.; Carr, T. J.; Thompson, S. K.; Ijames, C. F.; Carr, S. A.; McQueney, M.; D'Alessio, K. J.; Amegadzie, B. Y.; Hanning, C. R.; Abdel-Meguid, S.; DesJarlais, R. L.; Gleason, J. G.; Veber, D. F. *J. Am. Chem. Soc.* **1997**, *119*, 11351.

(7) (a) Gelb, M. H.; Svaren, J. P.; Abeles, R. H. *Biochemistry* **1985**, *24*, 1813. (b) Patel, D. V.; Rielly-Gauvin, K.; Ryono, D. E.; Free, C. A.; Smith, S. A.; Petrillo, E. W. *J. Med. Chem.* **1993**, *36*, 2431.

(8) For previous examples of this methodology, see: (a) Rich, D. H.; Bernatowicz, M. S.; Schmidt, P. G. *J. Am. Chem. Soc.* **1982**, *104*, 3535. (b) Moon, J. B.; Coleman, R. S.; Hanzlik, R. P. *J. Am. Chem. Soc.* **1986**, *108*, 1350. (c) Brisson, J. R.; Carey, P. R.; Storer, A. C. *J. Biol. Chem.* **1986**, *261*, 9087. (d) Liang, T. C.; Abeles, R. H. *Arch. Biochem. Biophys.* **1987**, *252*, 626. (e) Malthouse, J. P. G.; Mackenzie, N. E.; Boyd, A. S. F.; Scott, A. I. *J. Am. Chem. Soc.* **1983**, *105*, 1685.

(9) Simchen, G.; Kobler. H. *Synthesis* **1975**, 605.

(10) Kobler, H.; Munz, R.; Gasser, G. A.; Simchen, G. *Liebigs Ann. Chem.* **1978**, 1937.

S0022-3263(97)01834-3 CCC: $15.00
Published on Web 03/17/1998

Scheme 1[a]

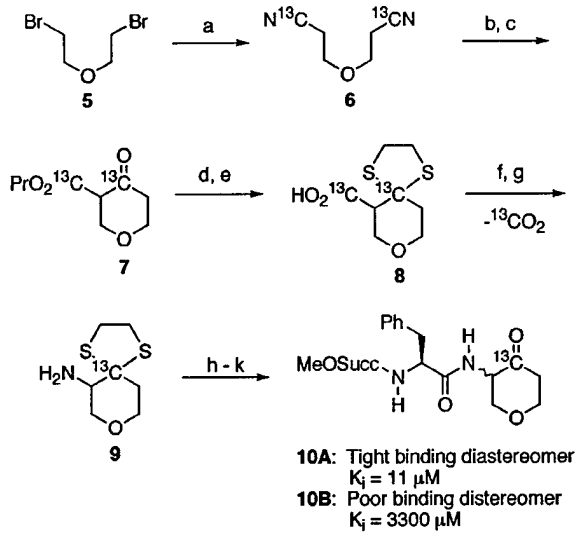

[a] Reagents: (a) $Et_4N^{13}CN$, 75%; (b) *n*-PrOH, *p*-TsOH; (c) LDA, THF, −78 °C; (d) ethanedithiol, BF_3·Et_2O; (e) NaOH, MeOH; (f) $(C_6H_5O)_2P(O)N_3$, C_6H_6, followed by *t*-BuOK, THF; (g) TFA, CH_2Cl_2; (h) BocPheOH, EDC, HOBT; (i) TFA, CH_2Cl_2; (j) monomethyl succinate, EDC, HOBT; (k) NBS, H_2O.

and saponification of the ester, compound **8** was treated with diphenyl phosphorazidate to induce a Curtius rearrangement. Trapping of the resulting isocyanate with *t*-BuOK yielded the corresponding Boc-protected amine. Removal of the Boc group with TFA resulted in loss of 1 equiv of $^{13}CO_2$ from the molecule to give amine **9**. This compound contained a single ^{13}C label at the desired position. The phenylalanine residue and methoxysuccinyl group were attached using standard peptide coupling procedures, and the diastereomers of **10** were separated using preparative HPLC.

Racemization of Inhibitors. Inhibitors that are based upon 4-heterocyclohexanones racemize at a significant rate in 100 mM phosphate buffer at pH 6.5, conditions used for kinetic assays of papain. For example, the tetrahydropyranone-based inhibitor racemizes with a half-life of 5.3 h under these conditions.[4] In our current studies, we have found that the rate of racemization is inversely correlated with buffer concentration. In the experiments described below, which use 10 mM phosphate at pH 6.5, inhibitor **10A** has a half-life for racemization of 192 h. The stability of the inhibitor under conditions that employ low buffer concentration have allowed us to acquire ^{13}C NMR spectra of the separated diastereomers of **10** in the presence of papain, without significant interference from racemization.

Enzyme Purification. Commercial preparations of papain are contaminated with a large amount of inactive enzyme. Papain used in this study was purified by affinity chromatography on a mercurial agarose column.[11] Enzyme purified in this manner is greater than 95% active as judged by titration of the active-site cysteine-25 thiolate with the reagent 2,2′-dipyridyl disulfide (DDS).[12]

^{13}C NMR Experiments. The two diastereomers of inhibitor **10** have very different inhibition constants

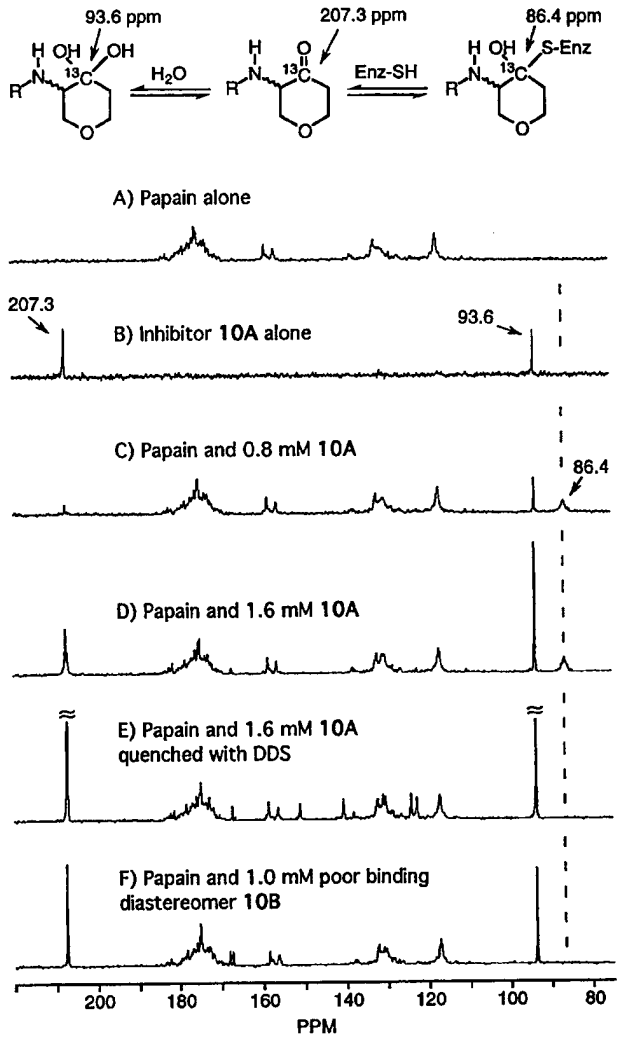

Figure 1. Partial ^{13}C NMR spectra of papain incubated with the ^{13}C-enriched inhibitor **10**. The concentration of enzyme in all spectra that contain papain is 0.9 mM.

against papain. The tight binding diastereomer **10A** has a K_i value of 11 μM, in contrast with the poor binding diastereomer **10B**, which has a K_i of 3300 μM. We have not determined the absolute configuration of these diastereomers. Figure 1 shows the ^{13}C NMR spectrum of each of these diastereomers in the presence of papain.

Figure 1A shows the ^{13}C NMR spectrum of papain alone. Figure 1B shows the spectrum of inhibitor **10A** alone. There are two major resonances in this spectrum. The resonance at 207.3 ppm corresponds to the ^{13}C-labeled ketone, and the resonance at 93.6 ppm corresponds to the hydrate. The similar intensities of these two resonances are consistent with the reported hydration equilibrium constant for tetrahydropyranone of 8.0×10^{-3} M^{-1}.[4] In $CDCl_3$ solution, inhibitor **10A** has a single major resonance for the ketone at 202.2 ppm. Figure 1C shows papain in the presence of slightly less than 1 equiv of **10A**. There are resonances for a small amount of both free ketone and hydrate. Importantly, a new resonance at 86.4 ppm appears that is not present in either Figure 1A or B. We assign this new resonance as the ^{13}C atom of a covalent hemithioketal adduct between the enzyme active-site nucleophile and the ketone of the inhibitor.

(11) Sluyterman, L. A.; Wijdenes, J. *Methods Enzymol.* **1974**, *34*, 544.
(12) Brocklehurst, K.; Little, G. *Biochem. J.* **1973**, *133*, 67.

Three lines of evidence support this structural assignment. First, the chemical shift of this peak clearly indicates that it corresponds to an sp^3-hybridized rather than an sp^2-hybridized carbon. This observation demonstrates that the new resonance cannot correspond to a simple noncovalent complex between the enzyme and the ketone form of the inhibitor. Second, the line width of this resonance, which is approximately 100 Hz, is fully consistent with an enzyme-bound species that is tumbling slowly on the NMR time scale.[13] Finally, reaction of inhibitor **10A** with the small molecule thiol, 3-thiopropionic acid, yields two diastereomeric hemithioketal adducts with resonances in the ^{13}C NMR spectrum at 82.6 and 83.7 ppm. These chemical shifts are similar to the 86.4 ppm that is found for the hemithioketal between **10A** and the enzyme-active-site cysteine residue.[14,15]

The resonances for free ketone and hydrate in Figure 1C are more pronounced than one would expect on the basis of the inhibition constant for compound **10A** and the enzyme and inhibitor concentrations in the sample. Using these values, we calculate that approximately 6% of the inhibitor should be in the free form. However, integration of the resonances suggests that the ratio of free inhibitor (ketone plus hydrate) to enzyme-bound inhibitor is approximately 1:2. Two factors are likely to contribute to this discrepancy. First, the sample may be contaminated with a small amount of the poor binding diastereomer **10B** due to incomplete separation of diastereomers during the HPLC purification. However, on the basis of the ^1H NMR spectrum of purified **10A**, we estimate that the sample was contaminated with not more than 5% of **10B** before the start of the experiment. A second factor, which we believe to be more important, is the differential saturation of the ^{13}C label in the free and enzyme-bound species. The ^{13}C label in the enzyme bound inhibitor will have a much longer correlation time and, likely, a longer relaxation time than the ^{13}C label in the free inhibitor. If the recycle time is shorter than either of these relaxation times, then the difference in the relaxation times will cause the integration for the enzyme-bound species to be smaller than expected on the basis of the true ratio of free to enzyme-bound inhibitor.

Addition of excess inhibitor to the enzyme (Figure 1D) simply results in an increase in the intensities of the resonances for free inhibitor. However, quenching the enzyme with DDS (Figure 1E), which forms a disulfide with the active-site cysteine residue and thus displaces the inhibitor from the active site, results in the disappearance of the resonance for hemithioketal. There is also a corresponding increase in the intensity of signals for free ketone and hydrate. These results show that inhibitor **10A** is bound at the enzyme active site through formation of a reversible covalent bond and that the inhibitor and papain are in equilibrium. The additional peaks in Figure 1E that appear between 120 and 160 ppm correspond to DDS and 2-thiopyridone.

Figure 1F shows 0.9 mM papain incubated with 1.0 mM of the poor binding diastereomer, **10B**. The absence of a broad resonance in the vicinity of 86.4 ppm shows that this diastereomer does not form a hemithioketal adduct. On the basis of the inhibition constant for compound **10B**, which is 3300 μM,[4] approximately 20% of the inhibitor should be bound to the enzyme at these concentrations.

It is noteworthy that the tight binding diastereomers of inhibitors **1**, **2**, and **3** have a range of inhibition constants against papain (78, 26, and 11 μM, respectively) and that these values correlate with both the electronic properties of the heteroatom in the 4-heterocyclohexanone ring and with the electrophilicity of the ketone moiety.[4] These data are consistent with a mechanism of inhibition that involves formation of a hemithioketal adduct. In addition, the NMR results shown above clearly demonstrate that the ^{13}C-labeled derivative of inhibitor **3** (compound **10A**) does indeed form such an adduct. We believe that these two observations, taken together, make it likely that the tight binding diastereomers of inhibitors **1** and **2** also form covalent adducts with the enzyme-active-site nucleophile.

In contrast, the poor-binding diastereomers of **1**–**3** all bind to papain with similar affinities (3.2, 2.4, and 3.3 mM, respectively), and there is no correlation between inhibition constants and ketone electrophilicity.[4] These observations, together with the fact that the poor binding diastereomer of ^{13}C-labeled **3** (compound **10B**) does not give a hemithioketal when incubated with papain, suggest that the poor-binding diastereomers of **1**–**3** all bind similarly in the active site and that none of these compounds form a reversible covalent bond with the active site cysteine residue.

In conclusion, we have demonstrated that the mechanism by which 4-heterocyclohexanone derivatives inhibit cysteine proteases involves nucleophilic attack by the active-site thiol on the reactive ketone. This attack results in reversible formation of a hemithioketal adduct that mimics the tetrahedral intermediate formed during enzyme-catalyzed hydrolysis of amide bonds. Future work will be aimed toward exploring the potential of 4-heterocyclohexanones as inhibitors for serine proteases and the hydrates of these compounds as inhibitors of metalloproteases and aspartic proteases.

Experimental Section

General Methods. NMR spectra were recorded on a Bruker AM-400 instrument. Spectra were calibrated using TMS (δ = 0.00 ppm) for ^1H NMR and $CDCl_3$ (δ = 77.0) or DMSO-d_6 (δ = 39.51) for ^{13}C NMR. Mass spectra were recorded on a Kratos MS 80 under electron impact (EI), chemical ionization (CI), or fast-atom bombardment (FAB) conditions. HPLC analyses were performed on a Rainin HPLC system with Rainin Microsorb silica or C18 columns and UV detection. Semipreparative HPLC was performed on the same system using a semipreparative column (21.4 × 250 mm). $K^{13}CN$ (99%) was obtained from Cambridge Isotope Laboratories. Details of the synthesis of unlabeled **10** from unlabeled **6** and experimental procedures for determining racemization rates have been reported previously.[4]

[Bis-^{13}CN]-3-oxa-1,5-pentanedinitrile (6). A solution of tetraethylammonium [^{13}C]cyanide (19.9 g, 126 mmol) in 60 mL of dry CH_2Cl_2 was cooled in an ice bath. To the solution was added 2-bromoethyl ether (13.97 g, 60 mmol) via syringe, and the reaction was stirred under an N_2 atmosphere and allowed to warm to room temperature overnight. The reaction mixture

(13) A line width of 88 Hz has been reported for the covalent complex between a peptide aldehyde inhibitor and papain (see ref 5).

(14) For comparison, reaction between papain and several ^{13}C-labeled nitrile-based inhibitors gave covalent thioimidate adducts with resonances in the ^{13}C NMR spectra in the range of 182.1–194.2 ppm. The thioimidate carbons of several model compounds are in the range of 193.0–198.5 ppm (see ref 8b–8d). Reaction between papain and a ^{13}C-labeled aldehyde-based inhibitor gave a hemithioacetal adduct with a chemical shift for the hemithioacetal carbon of 74.9 ppm. A model hemithioacetal had a chemical shift of 73.3 ppm (see ref 5).

(15) Addition of 3-thiopropionic acid to inhibitor **10B** also gives two diastereomeric hemithioketals with resonances in the ^{13}C NMR spectrum at 82.7 and 83.8 ppm.

was filtered through a plug of silica gel and eluted with ethyl acetate to remove the salts. The resulting solution was concentrated by rotary evaporation, and the crude product was purified by flash chromatography (1:1 EtOAc/hexanes) to yield compound **6** as a clear oil (5.72 g, 75%): ^{1}H NMR (400 MHz, $CDCl_3$) δ 2.66 (dt, J = 21.6, 6.2 Hz, 4H), 3.74 (dt, J = 6.3, 6.2 Hz, 4H); ^{13}C NMR (100 MHz, $CDCl_3$) δ 18.4 (d, J = 57.8 Hz), 65.4 (d, J = 3.1 Hz), 117.5 (s); HRMS-CI (M + H$^+$) calcd for $^{13}C_2{}^{12}C_4H_8N_2O$ 127.0782, found 127.0788.

Purification of Papain. Papain (twice crystallized) from Sigma was purified by affinity chromatography on an agarose–mercurial column according to the procedure of Sluyterman and Wijdenes.[11] Mercurial papain was eluted from the column using 10% DMSO, 0.5 mM $HgCl_2$, 1.0 mM EDTA, 100 mM KCl, and 50 mM NaOAc buffer at pH 5.0. The resulting solution of mercurial papain was concentrated using an Amicon Diaflow ultrafiltration apparatus with a YM-10 membrane. Mercurial papain can be stored at this stage in 0.5 mM $HgCl_2$ at a concentration of 3 mg/mL for over 1 month without loss of activity. Active papain was regenerated by washing the enzyme in the Amicon Diaflow apparatus with 1.0 mM cysteine, 1.0 mM EDTA, and 10 mM phosphate buffer at pH 6.5. The concentration of papain was determined by UV spectroscopy at 280 nm assuming an A_{280} of 25 absorbance units for a 1% solution and a molecular weight of 23, 000.[16] The activity of the enzyme preparations was determined by titrating the active-site cysteine nucleophile with 2,2′-dipyridyl disulfide according to the procedure of Brocklehurst and Little.[12] The samples were found to be greater than 95% active by this method.

^{13}C NMR Experiments. NMR samples of 2.0 mL were prepared in 10 mm NMR tubes. All samples contained 10 mM phosphate buffer at pH 6.5, 1 mM cysteine, 1 mM EDTA, and 5–10% DMSO-d_6. In addition, samples A–F (Figure 1) contained the following: (A) 0.9 mM papain; (B) inhibitor **10A**; (C) 0.9 mM papain and 0.8 mM **10A**; (D) 0.9 mM papain and 1.6 mM **10A**; (E) 0.9 mM papain, 1.6 mM **10A**, and 4.5 mM 2,2′-dipyridyl disulfide; and (F) 0.9 mM papain and 1.0 mM inhibitor **10B**. Inhibitor stock solutions were prepared in DMSO-d_6 to avoid racemization. Spectra were acquired on a Bruker AM-400 spectrometer operating at 100 MHz and were broad-band ^{1}H decoupled. A file size of 64K, a pulse width of 30°, and a receiver delay of 0.0 s was used to give a total acquisition time of 1.25 s. An exponential line broadening of 10 Hz was used during processing. Approximately 32, 000 scans were acquired for samples that contained protein.

(16) Glaser, A. N.; Smith, E. L. *J. Biol. Chem.* **1965**, *240*, 201.

Acknowledgment. This research was supported by the Petroleum Research Fund, administered by the American Chemical Society (Grant 30544-G4), the U.S. Army Medical Research and Materiel Command–Breast Cancer Research Initiative (Career Development Award to C.T.S., Grant DAMD17-96-1-6328), and Brown University (Salomon Faculty Research Award). J.L.C. was supported by a GAANN Fellowship from the Department of Education and by a University Fellowship from Brown University.

Supporting Information Available: ^{1}H and ^{13}C NMR spectra for compound **6** (2 pages). This material is contained in libraries on microfiche, immediately follows this article in the microfilm version of the journal, and can be ordered from the ACS; see any current masthead page for ordering information.

JO971834B

Pergamon

Tetrahedron Letters 39 (1998) 8253–8256

TETRAHEDRON LETTERS

Synthesis of Cyclohexanone-Based Cathepsin B Inhibitors that Interact with Both the S and S' Binding Sites

Jeffrey L. Conroy, Paul Abato, Mousumi Ghosh, Mariana I. Austermuhle, Michael R. Kiefer, and Christopher T. Seto[1]*

Department of Chemistry, Brown University
324 Brook St. Box H, Providence, Rhode Island 02912, U.S.A.

Received 30 June 1998; revised 27 July 1998; accepted 12 August 1998

Abstract: Solution and solid phase methods are described for the synthesis of inhibitors of the cysteine protease cathepsin B. These inhibitors are based on a cyclohexanone pharmacophore and are designed to interact with both the S and S' subsites of the enzyme active site.

The cysteine proteases cathepsin B, cathepsin K, and the ICE-like proteases are involved in disease processes that include metastasis of cancer,[2] bone resorption in osteoporosis,[3] and the control of programmed cell death.[4] These proteases are important targets for the development of inhibitors, both as therapeutic agents and as tools that can help to clarify the biological function of the enzymes.[5] We recently reported a new class transition-state analog inhibitors for cysteine proteases that are based upon a 4-heterocyclohexanone pharmacophore.[6] These inhibitors react with the enzyme active site nucleophile to give a reversibly formed hemithioketal adduct.[7] The 4-heterocyclohexanone nucleus was derivatized on one side of the reactive ketone so that the inhibitors made contacts with only the S subsites of the enzyme active site. However, inhibitors that extend interactions into both the S and S' subsites may have increased potency and specificity when compared to their singly-sided counterparts.[8] In this paper we describe solution and solid phase methods for synthesizing inhibitors of cathepsin B that are designed to interact with both the S and S' subsites. Development of a solid phase protocol for synthesis makes possible the construction of a combinatorial library of protease inhibitors based upon the cyclohexanone pharmacophore.

Compound **16** (Scheme 2) was designed as an inhibitor for cathepsin B using a combination of molecular modeling studies[9] and data from an X-ray crystal structure of the enzyme with an epoxysuccinyl inhibitor irreversibly bound to the active site nucleophile.[10] The ornithine side chain at the P2 position of **16** is designed to form a salt bridge with Glu 245 at the base of the S2 binding pocket of the enzyme. Proline is meant to fit into the shallow S2' binding site, with the free C-terminal carboxylate of the inhibitor forming hydrogen bonds with His 110 and His 111 of the protease. The structure of inhibitor **16** is intended to mimic the backbone of a natural peptide substrate. However, modeling studies suggested that this compound may be slightly too short to interact optimally with the two His residues. Therefore we have also synthesized compound **17**, which is one methylene unit longer than **16**, in order to account for this possibility.

0040-4039/98/$ - see front matter
PII: S0040-4039(98)01783-3

Synthesis of the cyclohexanone nucleus (Scheme 1) began with double deprotonation of ketoester **1**, followed by alkylation of the more reactive enolate with the appropriate bromoalkene to give compounds **2** and **3**.[11,12] Protection of the ketone with 1,3-propanediol and TMSCl,[13] followed by saponification of the ester gave carboxylic acids **6** and **7**. Reaction of the acids with diphenylphosphoryl azide in refluxing benzene induced the Curtius rearrangement.[14] The isocyanate product of these reactions was trapped with potassium *tert*-butoxide to yield the corresponding Boc protected amines. Finally, oxidative cleavage of the alkenes gave protected amino acids **8** and **9**. Analysis of the conformation of compound **7** by NMR studies using COSY and 1D-NOE experiments indicated that the carboxylic acid and butene substituents on the cyclohexanone ring were present in the thermodynamically favored *cis*-1,3 diequitorial orientation.

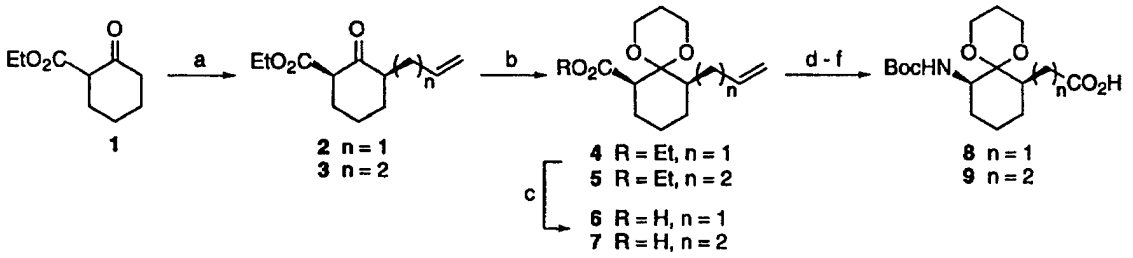

Reagents and Conditions: a) LDA (2 equiv.), 3-bromo-1-propene or 4-bromo-1-butene (1 equiv.), **2**: 64%, **3**: 60%; b) 1,3-propanediol, TMSCl, **4**: 70%, **5**: 62%; c) NaOH, MeOH, **6**: 58%, **7**: 80%; d) $(C_6H_5O)_2PON_3$, benzene, reflux; e) t-BuOK, THF; f) $KMnO_4$, $NaIO_4$, **8**: 70%, **9**: 59% (3 steps). One of two enantiomers is shown.

Scheme 1

The cyclohexanone nucleus was next coupled to proline methyl ester to give compounds **10** and **11** as mixtures of two diastereomers (Scheme 2). Removal of the Boc group followed by coupling to N-α-Fmoc-N-δ-Boc-Orn gave compounds **12** and **13**. The N-terminus was subsequently deprotected and capped with acetic anhydride to yield **14** and **15**. Finally the methyl ester was saponified, and the ketal and Boc protecting groups were removed by treatment with TFA in the presence of a small amount of water to yield inhibitors **16** and **17**.

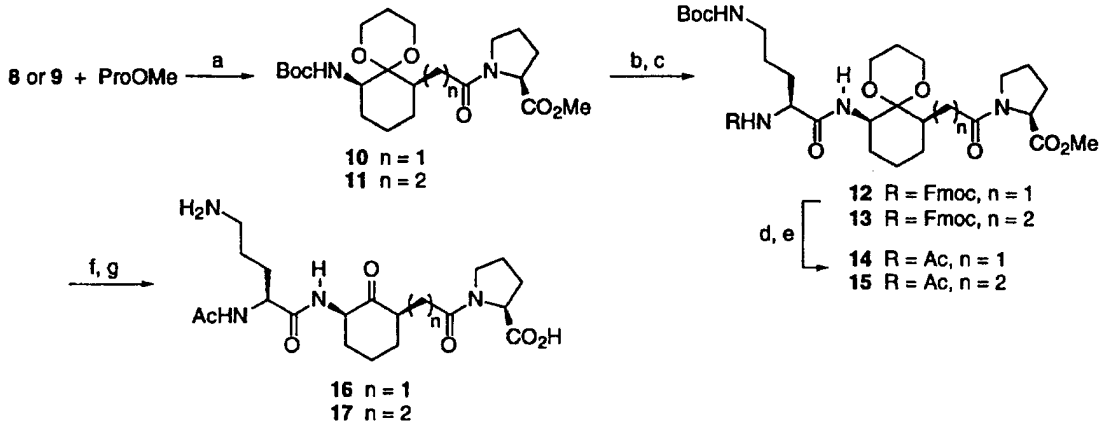

Reagents and Conditions: a) EDC, HOBt, **10**: 84%, **11**: 92%; b) TFA; c) N-α-Fmoc-N-δ-Boc-Orn, EDC, HOBt, **12**: 56%, **13**: 62% (2 steps); d) tris(2-aminoethyl)amine; e) Ac_2O, **14**: 51%, **15**: 71% (2 steps); f) LiOH; g) TFA, H_2O, **16**: 97%, **17**: 82% (2 steps). One of two diastereomers is shown.

Scheme 2

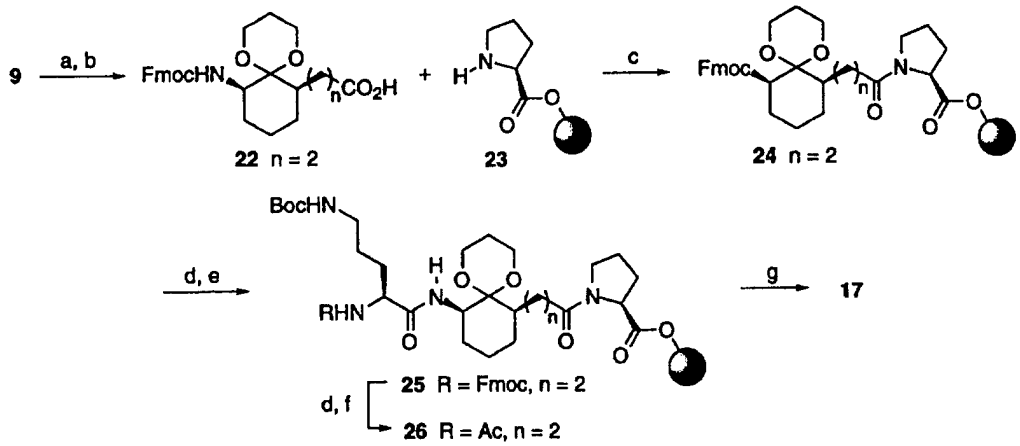

Reagents and Conditions: a) TFA; b) N-(9-fluorenylmethoxycarbonyloxy)succinimide; c) HBTU, DIEA; d) piperidine; e) N-α-Fmoc-N-δ-Boc-Orn, HBTU, DIEA; f) Ac_2O; g) TFA, H_2O. One of two diastereomers is shown.

Scheme 3

We have also developed a solid phase protocol for synthesizing these cyclohexanone-based protease inhibitors. The protocol, which is outlined in Scheme 3, is analogous to the Fmoc strategy for synthesizing peptides on a solid support. This synthesis required a derivative of the cyclohexanone pharmacophore that had a free C-terminal carboxylate, an Fmoc group on the N-terminus, and a protecting group on the ketone that could be removed under mild conditions. Compound **22** fulfilled these requirements. Solid phase synthesis of inhibitor **17** was performed on Wang resin that was preloaded with Fmoc-Pro. Standard coupling and Fmoc deprotection procedures were employed.[15] The N-terminus was capped with acetic anhydride, and TFA was used to cleave compound **26** from the solid support and to remove the Boc group. The ketal protecting group was removed by adding H_2O (30% v/v) to the cleavage cocktail and stirring the solution overnight at room temperature. The crude material was isolated by lyophilization and purified by reverse phase HPLC to yield inhibitor **17** that was identical to material obtained from the solution phase synthesis.

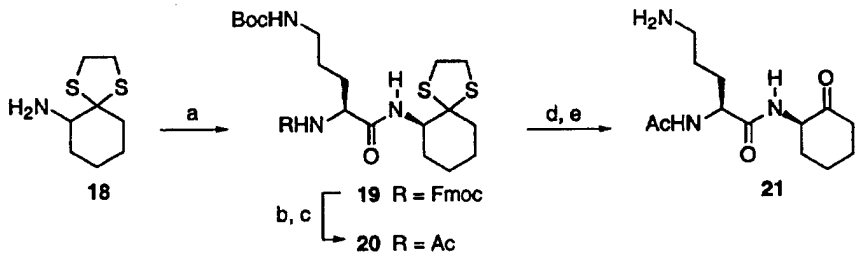

Reagents and Conditions: a) N-α-Fmoc-N-δ-Boc-Orn, EDC, HOBt, 80%; b) tris(2-aminoethyl)amine; c) Ac_2O, 99% (2 steps); d) N-bromosuccinimide, H_2O; e) TFA, 80% (2 steps). One of two diastereomers is shown.

Scheme 4

In order to determine how much the Pro residue in **16** and **17** contributes to the potency of the inhibitors, we have synthesized control compound **21** which lacks any binding interactions with the S' subsites of the enzyme. The synthesis of **21** (Scheme 4) began with amine **18**,[16] and was similar to the synthesis of the N-

terminal portion of inhibitors **16** and **17**. The only difference was that the ketone was carried through the synthesis as a thioketal, which was deprotected at the end of the sequence using N-bromosuccinimide and H_2O.[17]

The inhibitors were assayed against cathepsin B using the methylcoumarylamide substrate Z-Arg-Arg-NMec.[18] The hydrolysis reactions were monitored by fluorescence spectroscopy using excitation and emission wavelengths of 350 and 440 nm respectively. Control compound **21** is a poor inhibitor of cathepsin B with an inhibition constant of 24 mM. Compounds **16** and **17** have K_i values of 6.6 and 6.1 mM, respectively.[19] These results demonstrate that the potency of cyclohexanone-based inhibitors can be improved significantly by building in functionality that interact with the S' binding sites. Although our design efforts have not yet yielded inhibitors with high potency against cathepsin B, this work has set the stage for the solid phase synthesis of a combinatorial library of inhibitors that are constructed around the 4-heterocyclohexanone pharmacophore.

Acknowledgments: This research was supported by the NIH (Grant 1 R01 GM57327-01), the Petroleum Research Fund administered by the American Chemical Society (Grant 30544-G4), and the U.S. Army Medical Research and Materiel Command - Breast Cancer Research Initiative (Grant DAMD17-96-1-6161, Career Development Award to C.T.S.). J.L.C. and P.A. were supported by GAANN Fellowships from the Department of Education. J.L.C. was also supported by a University Fellowship from Brown University. M.I.A. was supported by a Brown University Undergraduate Teaching and Research Assistantship.

References and Notes:

1. E-mail: Christopher_Seto@Brown.edu; Fax: 401-863-2594.
2. (a) Liotta, L. A.; Steeg, P. S.; Stetler-Stevenson, J. G. *Cell* **1991**, *64*, 327. (b) Baricos, W. H.; Zhou, Y.; Mason, R. W.; Barrett, A. J. *Biochem. J.* **1988**, *252*, 301.
3. Yamashita, D. S.; Smith, W. W.; Zhao, B.; Janson, C. A.; Tomaszek, T. A.; Bossard, M. J.; Levy, M. A.; Oh, H.-J.; Carr, T. J.; Thompson, S. K.; Ijames, C. F.; Carr, S. A.; McQueney, M.; D'Alessio, K. J.; Amegadzie, B. Y.; Hanning, C. R.; Abdel-Meguid, S.; DesJarlais, R. L.; Gleason, J. G.; Veber, D. F. *J. Am. Chem. Soc.* **1997**, *119*, 11351 and references therein.
4. (a) Miller, D. K. *Ann. Rep. Med. Chem.* **1996**, *31*, 249. (b) Schwartz, L. M.; Milligan, C. E. *Trends Neurosci.* **1996**, *19*, 555. (c) Nicholson, D. W.; Ali, A.; Thornberry, N. A.; Vaillancourt, J. P.; Ding, C. K.; Gallant, M.; Gareau, Y.; Griffin, P. R.; Labelle, M.; Lazebnik, Y. A.; Munday, N. A.; Raju, S. M.; Smulson, M. E.; Yamin, T.-T.; Yu, V. L.; Miller, D. K. *Nature* **1995**, *376*, 37. (d) Nicholson, D. W. *Nature Biotech.* **14**, *297*, 1996.
5. For a recent review of cysteine proteases and their inhibitors, see Otto, H.-H.; Schirmeister, T. *Chem. Rev.* **1997**, *97*, 133.
6. Conroy, J. L.; Sanders, T. C.; Seto, C. T. *J. Am. Chem. Soc.* **1997**, *119*, 4285.
7. Conroy, J. L.; Seto, C. T. *J. Org. Chem.* **1998**, *63*, 2367.
8. For several examples of other reversible cysteine protease inhibitors that extend into both the S and S' binding sites see Hu, L.-Y.; Abeles, R. H. *Arch. Biochem. Biophys.* **1990**, *281*, 271, and reference 3.
9. Modeling studies were performed using QUANTA 4.0 molecular modeling software.
10. Turk, D.; Podobnik, M.; Popovic, T.; Katunuma, N.; Bode, W.; Huber, R.; Turk, V. *Biochemistry* **1995**, *34*, 4791.
11. Huckin, S. N.; Weiler, L. *J. Am. Chem. Soc.* **1974**, *96*, 1082.
12. All new compounds gave satisfactory analyses by ^{1}H NMR, ^{13}C NMR and high resolution MS.
13. Chan, T. H.; Brook, M. A.; Chaly, T. *Synthesis*, **1983**, 203.
14. Shioiri, T.; Ninomiya, K.; Yamada, S. *J. Am. Chem. Soc.* **1972**, *94*, 6203.
15. Fmoc-Pro-Wang resin with a loading of 0.75 mmol/g was purchased from Novabiochem (Product No. 04-12-2000). Three equivalents of carboxylic acid were used in each coupling reaction.
16. The synthesis of compound **18** has been reported in reference 6.
17. Cain, E. N.; Welling, L. L. *Tetrahedron Lett.* **1975**, 1353.
18. Barrett, A. J.; Kirschke, H. *Methods Enzymol.* **1981**, *80*, 535.
19. The error in the values of the inhibition constants is approximately ±20%.

of dimensions $0.28 \times 0.13 \times 0.07$ mm was used. A total of 6403 independent reflections were measured on a Siemens P4/PC diffractometer with graphite-monochromated $Cu_{K\alpha}$ radiation using ω scans. The structure was solved by the heavy atom (Patterson) method and all the major occupancy non-hydrogen atoms were refined anisotropically with absorption corrected (lamina [100]) data using full-matrix least-squares based on F^2 to give $R_1 = 0.071$, $wR_2 = 0.190$ for 5193 independent observed reflections ($|F_o| > 4\sigma(|F_o|)$, $2\theta \leq 120°$) and 443 parameters. Crystallographic data (excluding structure factors) for the structure reported in this paper have been deposited with the Cambridge Crystallographic Data Centre as supplementary publication no. CCDC-102341. Copies of the data can be obtained free of charge on application to CCDC, 12 Union Road, Cambridge CB2 1EZ, UK (fax: (+44) 1223-336-033; e-mail: deposit@ccdc.cam.ac.uk).

[9] An examination of contacts does not reveal any obvious reason for this difference in bond lengths. There is however an intermolecular contact between Cl(5) and its symmetry-related counterpart (3.51 Å).

[10] P. J. Bonasia, J. Arnold, *J. Organomet. Chem.* **1993**, *449*, 147; Ir–Te bond lengths in the range 2.626(1)–2.643(1) Å are observed in the cubane $[Ir_4(\mu\text{-}Te)_4(\eta\text{-}C_5Me_5)_4]$: S. Schulz, M. Andruh, T. Pape, T. Heinze, H. W. Roesky, L. Häming, A. Kuhn, R. Herbst-Irmer, *Organometallics*, **1994**, *13*, 4004.

Hydrolysis of Amides Catalyzed by 4-Heterocyclohexanones: Small Molecule Mimics of Serine Proteases**

Mousumi Ghosh, Jeffrey L. Conroy, and Christopher T. Seto*

One of the long-standing problems in bioorganic chemistry is the design of catalysts that hydrolyze amide bonds under mild conditions.[1, 2] Amides are stable species; the half-life for peptide hydrolysis under neutral conditions at 25 °C has been estimated to be seven years.[3] However, nature has been able to develop four different classes of proteases that are capable of sequence-specific hydrolysis of peptides with tremendous rate accelerations. Therefore, the design of artificial catalysts that begin to approach the activity and specificity of protein-based catalysts is a fascinating and challenging problem. Here we report that the cyclohexanone **1** and the 4-heterocyclohexanones **2**–**4** are efficient catalysts for the base-promoted hydrolysis of amides.

We have shown previously that 4-heterocyclohexanones can be used to synthesize inhibitors of cysteine proteases.[4] These compounds inhibit the protease by reaction of the

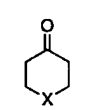

1: X = CH_2
2: X = NH
3: X = S
4: X = O

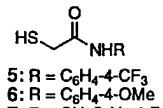

5: R = C_6H_4-4-CF_3
6: R = C_6H_4-4-OMe
7: R = $CH_2C_6H_4$-4-F

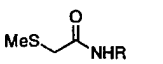

8: R = C_6H_4-4-CF_3

4-heterocyclohexanone carbonyl group with the active-site cysteine nucleophile of the enzyme with reversible formation of a hemithioacetal adduct.[5] In our current studies we are interested in developing catalysts of amide hydrolysis, and we reasoned that the amide substrates **5**–**7** could be anchored reversibly to a 4-heterocyclohexanone catalyst to form similar hemithioacetal adducts. Hydrolysis of the amide could then occur through a series of reactions that mimic the mechanism used by serine proteases to catalyze hydrolysis of peptides, as discussed below. These reactions serve as a model for hydrolysis of peptides specifically on the C-terminal side of cysteine residues.

We have monitored the hydrolysis of **5**–**7** catalyzed by 4-heterocyclohexanones by ^1H or ^{19}F NMR spectroscopy, or reverse-phase HPLC.[6] The reactions were performed under pseudo-first-order conditions, and they showed an exponential decrease in the substrate concentration as a function of time. Table 1 shows the observed rate constants for several reactions with a variety of substrates and catalysts. The most efficient catalysis that we have measured is shown in entry 5. In this reaction the hydrolysis of **5** is accelerated by more than four orders of magnitude relative to the background reaction when it is carried out in the presence of 600 mM tetrahydropyranone (THP, **4**).

Table 1. Observed rate constants for hydrolysis of amides catalyzed by 4-heterocyclohexanones.[a]

Entry	Catalyst	Substrate	k_{obs} [s^{-1}]	k_{rel}[b]
1	none	**5**	1.5×10^{-8}	
2	**1**	**5**	2.5×10^{-8}	2
3	**2**	**5**	5.9×10^{-8}	4
4	**3**[c]	**5**	3.7×10^{-8}	2
5	**4**	**5**	2.2×10^{-4}	14700
6	**4**	**6**	1.5×10^{-4}	10000
7	none	**6**	1.5×10^{-8}	
8	**4**	**7**	1.2×10^{-4}	3900
9	none	**7**	3.1×10^{-8}	
10	**4**[c]	**8**	1.0×10^{-7}	

[a] All reactions were performed at 25 °C with 20 mM substrate, 200 mM NaOD, and 600 mM catalyst (where present) D_2O/CD_3OD (4/1) unless otherwise specified. [b] Rate constant relative to the background reaction (no catalyst) with the same substrate. [c] Reaction was performed in D_2O/CD_3OD (1/1) because of low solubility of the catalyst or substrate in aqueous solution.

The efficiency of the hydrolysis reaction is highly dependent on the heteroatom in the 4-heterocyclohexanone catalyst (compare entries 2–5, Table 1). The reactivity of the carbonyl group in the catalyst is controlled by a through-space electrostatic repulsion between the dipoles of the ketone and the heteroatom. We have demonstrated previously that the equilibrium constant for addition of a thiol to 4-heterocyclo-

[*] Prof. Dr. C. T. Seto, M. Ghosh, J. L. Conroy
Department of Chemistry
Brown University
324 Brook Street, Box H, Providence, RI 02912 (USA)
Fax: (+1) 401-863-2594
E-mail: christopher_seto@brown.edu

[**] This work was supported by the U.S. Army Medical Research and Material Command (DAMD17-96-1-6161, Career Development Award to C.T.S.). J.L.C. was supported by a GAANN Fellowship from the U.S. Department of Education and a University Fellowship from Brown University.

Supporting information for this article is available on the WWW under http://www.wiley-vch.de/home/angewandte/ or from the author.

  1433-7851/99/3804-0514 $ 17.50+.50/0

hexanones is correlated with the strength of this electrostatic repulsion.[4] Thus THP, which has the strongest through-space interaction, is the most substrate bound and has the most effective catalyst at nonsaturating concentrations of substrate and catalyst.[7] In addition to simple binding of the substrate to the catalyst, this type of through-space electrostatic interaction can also exert other effects which significantly influence the rate of the hydrolysis reaction. For example, electrostatic interactions should alter the pK_a of the hemithioacetal hydroxyl group which is involved in catalysis. A combination of these effects causes THP to be a much better catalyst than the corresponding carbon, nitrogen, and sulfur analogues. It is interesting to note that benzaldehyde, acetophenone, and trifluoromethyl ketone derivatives are not effective catalysts for these hydrolysis reactions.

To investigate the mechanism of this reaction we have examined the kinetic order for hydrolysis of **5** catalyzed by THP by varying the NaOD and catalyst concentrations under pseudo-first order conditions (Figure 1). The observed rate

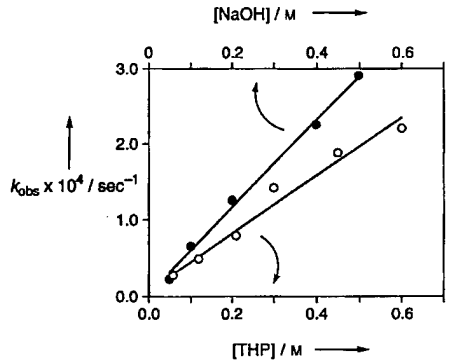

Figure 1. Hydrolysis of **5** catalyzed by tetrahydropyranone (THP, **4**) in D_2O/CD_3OD 4/1. ●: reactions with 20 mM substrate, 300 mM tetrahydropyranone, and NaOD in concentrations from 50 to 500 mM; slope = 5.72×10^{-3} M^{-1}s^{-1}. ○: reactions with 20 mM substrate, 200 mM NaOD, and THP in concentrations from 60 to 600 mM; slope = 3.77×10^{-3} M^{-1}s^{-1}.

constant increases linearly with the concentration of NaOD or THP. These results indicate that the rate expression for the hydrolysis reaction is defined by Equation (1).

$$\text{rate} = k_{hydr}[\text{substrate}][\text{catalyst}][\text{NaOH}] \quad (1)$$

We have used the slopes of the plots shown in Figure 1 to calculate the value of the third-order rate constant k_{hydr}. The experiments in which the catalyst concentration was varied (open circles) give a calculated rate constant of $k_{hydr} = 1.88 \times 10^{-3}$ M^{-2}s^{-1}, while the experiments in which the NaOD concentration was varied (closed circles) give $k_{hydr} = 1.91 \times 10^{-3}$ M^{-2}s^{-1}. The excellent agreement between these values provides further evidence that the rate expression formulated in Equation (1) is correct.

The observed rate constant for these reactions is a linear function of the catalyst concentration over the range of 60–600 mM THP (Figure 1). However, at concentrations at which the substrate is fully bound by catalyst, the rate constant should become independent of catalyst. These observations indicate that the association constant K_S for the binding of **5** to THP is less than 1.7 M^{-1}.[7]

To explore the scope of this reaction, we have measured the hydrolysis rates for the three substrates **5**–**7**. Interestingly, there is less than a twofold difference in the rate constants between **5**, which is an relatively activated substrate, and **7**, which is an example of an unactivated amide. These results indicate that THP can accelerate significantly the rate of hydrolysis of unactivated amides, and suggest that it may serve as a useful catalyst for the cleavage of peptide bonds.

Under strongly basic conditions, the rate of uncatalyzed amide hydrolysis typically shows a small dependence on the nature of the leaving group.[8] This observation can be rationalized because substituents on the leaving group have opposite effects on the rate of hydroxide addition to the amide carbonyl group and the rate of departure of the leaving group, which must be partially or fully protonated during this step. The small dependence of the rate of the catalyzed reaction on the nature of the leaving group suggests a similarity between the mechanisms of the catalyzed and uncatalyzed reactions.

Scheme 1 shows a plausible mechanism for the hydrolysis of amides catalyzed by 4-heterocyclohexanones. This mechanism mimics the series of reactions that occur during the

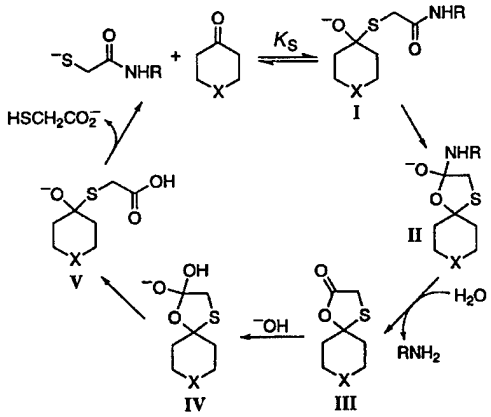

Scheme 1. Proposed mechanism for the hydrolysis of amides catalyzed by 4-heterocyclohexanones.

hydrolysis of peptides by serine proteases. Three important features of the enzymatic reaction are replicated in the proposed mechanism: 1) The substrate binds to the catalyst in a reaction that reaches equilibrium faster than amide hydrolysis. In Scheme 1 this entails nucleophilic attack by the substrate thiolate on the carbonyl group of the 4-heterocyclohexanone to yield hemithioacetal anion **I**. This strategy, which involves formation of a reversible covalent bond, provides a reliable method for anchoring the substrate to the catalyst in a well-defined geometry. 2) The substrate reacts with a catalyst nucleophile to generate an acyl-enzyme intermediate. In the small-molecule system, the anion in hemithioacetal **I** is positioned for nucleophilic attack on the amide carbonyl group through formation of a five-membered ring to give tetrahedral intermediate **II**. Breakdown of this tetrahedral intermediate releases the amine leaving group and

  1433-7851/99/3804-0515 $ 17.50+.50/0

generates acyl-catalyst intermediate **III**. Similar mechanisms have been observed in the neighboring group participation by carbonyl hydrates during the hydrolysis of carboxylate and phosphate esters. However these examples are stoichiometric reactions that are promoted by intramolecular carbonyl groups.[9–11] 3) Deacylation of the acyl-enzyme intermediate regenerates the catalysts. This process is mimicked by reaction of **III** with hydroxide to give tetrahedral intermediate **IV**, which then breaks down to yield hemithioacetal **V**. Dissociation of **V** releases the carboxylate anion and regenerates the 4-heterocyclohexanone catalyst.

We have performed two additional experiments to probe the validity of this proposed mechanism. First, we have synthesized control compound **8** in which the thiol group is blocked as the methyl thioether in order to determine if a thiol functionality in the substrate is necessary for catalysis. Comparison of entries 1 and 10 in Table 1 shows that the rate of hydrolysis of **8** in the presence of 600 mM catalyst is only sevenfold faster than the rate of hydrolysis of substrate **5** in the absence of catalyst. This comparison shows that a free thiol group in the substrate is required for catalysis. In addition, the results shows that the mechanism of the catalyzed reaction cannot involve simple intermolecular nucleophilic attack by the anion of the 4-heterocyclohexanone hydrate on the carbonyl of the amide substrate.

In a second experiment we have independently synthesized the acyl-catalyst intermediate **III** (Scheme 1) in which X = S, and we monitored its rate of hydrolysis under the reaction conditions. We find that this intermediate is hydrolyzed much faster than the amide substrates in any of the catalyzed reactions. These two observations are consistent with the mechanism proposed in Scheme 1, and they suggest that the rate-limiting step for the catalyzed reaction occurs before hydrolysis of intermediate **III**.

In conclusion, we have demonstrated that tetrahydropyranone (**4**) is an effective catalyst for the hydrolysis of amide substrates that contain an adjacent thiol functionality. The reaction displays two features that are most often associated with enzymatic systems. First, the substrate is bound to the catalyst through a preliminary equilibrium in order to decrease the entropic barrier to reaction. The catalysts employ reversible formation of a hemithioacetal to establish this equilibrium. We believe that formation of reversible covalent bonds of this type will prove to be a useful method for mediating the molecular recognition processes that are involved in catalysis and self-assembly. Reversible covalent bonds are complementary to the noncovalent interactions—such as hydrogen bonds, hydrophobic interactions, and electrostatic interactions—that are typically observed in biological recognition processes. A second similarity to enzymatic catalysis is that the reaction is catalyzed through the participation of neighboring groups. We are currently conducting experiments to characterize further the mechanism of the reaction, and also to explore the possibility of using 4-heterocyclohexanones to catalyze the cysteine-specific hydrolysis of peptides.

Received: August 17, 1998
Revised version: October 15, 1998 [Z12293IE]
German version: *Angew. Chem.* **1999**, *111*, 575–578

Keywords: amides · electrostatic interactions · enzyme mimetics · hydrolyses · synthetic proteases

[1] For amide hydrolysis promoted by metals, see a) J. T. Groves, L. A. Baron, *J. Am. Chem. Soc.* **1989**, *111*, 5442; b) A. W. Czarnik, K. Chen, S. P. Wathen, *Tetrahedron Lett.* **1992**, *33*, 6303; c) R. Breslow, A. Schepartz, *J. Am. Chem. Soc.* **1987**, *109*, 1814; d) N. N. Murthy, M. Mahroof-Tahir, K. D. Karlin, *J. Am. Chem. Soc.* **1993**, *115*, 10404; e) L. M. Sayre, K. V. Reddy, A. R. Jacobson, W. Tang, *Inorg. Chem.* **1992**, *31*, 937; f) T. J. Przystas, T. H. Fife, *J. Chem. Soc. Perkin Trans. 2* **1990**, 393; g) J. Chin, V. Jubian, K. Mrejen, *J. Chem. Soc. Chem. Commun.* **1990**, 1326; for examples of other types of catalysts, see h) J. W. Keillor, A. A. Neverov, R. S. Brown, *J. Am. Chem. Soc.* **1994**, *116*, 4669; i) J. Suh, I. M. Klotz, *J. Am. Chem. Soc.* **1984**, *106*, 2373.

[2] For catalytic hydrolysis of esters, see a) B. Zhang, R. Breslow, *J. Am. Chem. Soc.* **1997**, *119*, 1676; b) F. Diederich, G. Schurmann, I. Chao, *J. Org. Chem.* **1988**, *53*, 2744; c) F. M. Menger, L. G. Whitesell, *J. Am. Chem. Soc.* **1985**, *107*, 707; for a related transesterification reaction, see d) T. Sammakia, T. B. Hurley, *J. Am. Chem. Soc.* **1996**, *118*, 8967.

[3] D. H. Kahne, W. C. Still, *J. Am. Chem. Soc.* **1988**, *110*, 7529.

[4] J. L. Conroy, T. C. Sanders, C. T. Seto, *J. Am. Chem. Soc.* **1997**, *119*, 4285.

[5] J. L. Conroy, C. T. Seto, *J. Org. Chem.* **1998**, *63*, 2367.

[6] See the supporting information for representative examples.

[7] The apparent equilibrium constant for addition of 3-mercaptopropionic acid to tetrahydropyranone under neutral conditions in 100% D_2O is 1.3 M^{-1}; see reference [4] for details.

[8] a) M. L. Bender, R. J. Thomas, *J. Am. Chem. Soc.* **1961**, *83*, 4183; b) R. L. Schowen, H. Jayaraman, L. Kershner, *J. Am. Chem. Soc.* **1966**, *88*, 3373; c) L. D. Kershner, R. L. Schowen, *J. Am. Chem. Soc.* **1971**, *93*, 2014.

[9] See K. Bowden, *Chem. Soc. Rev.* **1995**, *24*, 431, and references therein.

[10] A similar mechanism has been proposed for the hydrolysis of sulfate esters catalyzed by human arylsulfatase A. This reaction involves participation by an aldehyde hydrate: G. Lukatela, N. Krauss, K. Theis, T. Selmer, V. Gieselmann, K. von Figura, W. Saenger, *Biochemistry* **1998**, *37*, 3654.

[11] For the hydrolysis of α-aminonitriles assisted by aldehydes and ketones, see M. Paventi, F. L. Chubb, J. T. Edwards, *Can. J. Chem.* **1987**, *65*, 2114, and references therein.

Highly Enantioselective Hydrogenation of Cyclic Enol Acetates Catalyzed by a Rh–PennPhos Complex**

Qiongzhong Jiang, Dengming Xiao, Zhaoguo Zhang, Ping Cao, and Xumu Zhang*

The growing demand for practical and effective chiral ligands and/or catalysts has fueled much recent progress in ligand design. Although benchmark ligands such as 2,2′-

[*] Prof. X. Zhang, Dr. Q. Jiang, D. Xiao, Dr. Z. Zhang, P. Cao
Department of Chemistry
The Pennsylvania State University
University Park, PA 16802 (USA)
Fax: (+1) 814-863-8403
E-mail: xumu@chem.psu.edu

[**] This work was supported by a Camille and Henry Dreyfus New Faculty Award and Teaching Scholar Award, an ONR Young Investigator Award, a DuPont Young Faculty Award, Catalytica Pharmaceuticals, and DuPont Agrochemical Products. We acknowledge a generous loan of precious metals from Johnson Matthey Inc. and a gift of chiral GC columns from Supelco. PennPhos = *P,P'*-1,2-phenylenebis(*endo*-2,5-dialkyl-7-phosphabicyclo[2.2.1]heptanes).

  1433-7851/99/3804-0516 $ 17.50+.50/0

4-Heterocyclohexanone-Based Inhibitors of the Serine Protease Plasmin

Tanya C. Sanders and Christopher T. Seto*

Department of Chemistry, Brown University, 324 Brook Street, Box H, Providence, Rhode Island 02912

Received March 11, 1999

Three inhibitors that are based upon a 4-heterocyclohexanone nucleus were synthesized and evaluated for activity against the serine protease plasmin. Inhibitors of plasmin have potential as cancer chemotherapeutic agents that act by blocking both angiogenesis and metastasis. Inhibitor **1** has moderate activity against plasmin but shows good selectivity for this enzyme compared to other serine proteases including trypsin, thrombin, and kallikrein. Inhibitor **2** shows both good activity and selectivity for plasmin. Inhibitor **3**, which does not incorporate an aminohexyl group that can interact with the S1 subsite, has poor activity. These results, along with previous work, demonstrate that the 4-heterocyclohexanone nucleus can effectively serve as the basis for designing inhibitors of both serine and cysteine proteases.

Introduction

Angiogenesis and metastasis are two processes that are central to the progression of cancer. As such, they have become important targets for the development of chemotherapeutic agents. Several recent reports in the literature have demonstrated that suppressing angiogenesis is an effective method for limiting the growth of primary tumors and producing dormancy in secondary metastases.[1,2] Both angiogenesis and metastasis require a proteolytic cascade that involves serine, cysteine, and metalloproteases. This proteolytic cascade degrades the basement membrane which surrounds blood vessels.[3] During angiogenesis the resulting lesion in the basement membrane allows epithelial cells to extend into the neighboring tissues and form new blood vessels. During metastasis cancer cells penetrate through the degraded basement membrane and extracellular matrix, become implanted in the underlying tissues, and subsequently form secondary tumors.[4] Compounds which inhibit enzymes in the proteolytic cascade may be useful for blocking these processes.

Plasmin is a serine protease that plays an important role in the proteolytic cascade. This protease acts directly by hydrolyzing components of the basement membrane such as fibrin, type IV collagen, fibronectin, and laminin and also acts indirectly by activating other enzymes in the cascade such as matrix metalloproteases.[3] Degradation of the basement membrane by plasmin is a multistep process. For example, during the first step in fibrin hydrolysis, plasminogen, which is the inactive precursor to plasmin, binds to fibrin via a lysine binding site. Next plasminogen is converted to active plasmin in a reaction that is catalyzed by urokinase plasminogen activator. Finally catalytic residues in the active site of plasmin, which is separate from the lysine binding site, hydrolyze fibrin via the mechanism that is common to serine proteases.[5] Most current pharmaceutical agents that are designed to inhibit plasmin are targeted to the lysine binding site.[6] These agents inhibit fibrinolysis by blocking the binding of plasminogen to fibrin, and thus halting production of new plasmin. α2-Antiplasmin, a natural plasmin inhibitor, is also targeted to the lysine binding site.[7] However these fibrinolysis inhibitors have no effect on the active site of the enzyme, which retains its catalytic activity. Thus plasmin that is already activated retains its catalytic activity even after treatment with inhibitors that are directed toward the lysine binding site. To overcome this problem, we are interested in developing inhibitors that are targeted to the active site of plasmin and are designed to shut down catalytic activity. In this paper we report the synthesis and evaluation of compounds **1**–**3** which are active site- directed inhibitors of plasmin. Compound **2** has both good activity and specificity against plasmin when compared to several other serine proteases.[8]

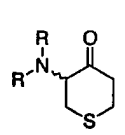

1 R = $(CH_2)_6NH_2$

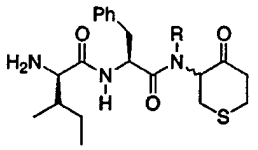

2 R = $(CH_2)_6NH_2$
3 R = H

Design of Inhibitors

We have recently reported a new class of inhibitors for cysteine proteases that are based upon a 4-heterocyclohexanone pharmacophore.[9] ^{13}C NMR studies using a ^{13}C-labeled inhibitor confirm that these molecules react with the enzyme to give a reversibly formed covalent hemithioketal adduct between the active site cysteine residue and the ketone of the inhibitor.[10] The key design feature in these molecules is the through-space electrostatic repulsion that occurs between the heteroatom and ketone functionalities in the 4-heterocyclohexanone pharmacophore. This repulsive interaction controls the electrophilicity of the ketone, which in turn controls the potency of the inhibitors.[9]

Because serine and cysteine proteases share a similar mechanism for hydrolyzing amide bonds, we expect that 4-heterocyclohexanones should be good inhibitors of both classes of enzymes. Reaction of the active site nucleophile of a serine protease with a 4-heterocyclohexanone-based inhibitor would give a reversibly formed hemiketal adduct. However, several reversible protease

10.1021/jm990110k CCC: $18.00
Published on Web 07/07/1999

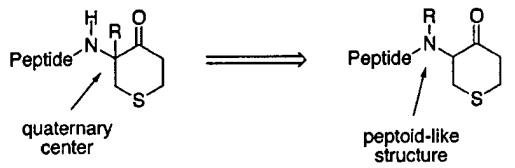

Figure 1. Shifting of the P1 side chain from the position α to the ketone to the exocyclic nitrogen to avoid formation of the quaternary center. R = $(CH_2)_6NH_2$.

inhibitors show activity against one class of enzyme and not the other. For example, trifluoromethyl ketones and boronic acids are good inhibitors of serine proteases[11] but not cysteine proteases.[12,13] Nitriles have the opposite specificity, while aldehydes and α-dicarbonyl compounds are good inhibitors of both classes of enzymes.[13] Thus one of our motivations for synthesizing compounds **1**–**3** was to determine if 4-heterocyclohexanones would prove to have activity against serine proteases, in addition to cysteine proteases as we have shown previously.[9]

Plasmin has a strong specificity for substrates with positively charged side chains in the P1 position. To accommodate this specificity we have included a lysine-like side chain in the structure of compounds **1** and **2**. However, attachment of this side chain in its "natural" peptide-like position would place it on the tetrahydrothiopyranone ring between the ketone and the exocyclic nitrogen (Figure 1). This placement would create a sterically demanding quaternary center α to the reactive ketone. Space-filling molecular models suggest that this quaternary center would sterically inhibit addition of an active site nucleophile to the ketone and thus decrease the potency of the inhibitor. To overcome this difficulty we have attached the P1 side chain to the amide nitrogen that is connected to the ring. This type of modification is well-precedented in peptoids.[14] To ensure that the lysine-like side chain of the inhibitor makes good contact with the aspartic acid at the base of the S1 binding site, we have increased the length of the aminoalkyl chain to six carbons. This chain length is based upon molecular modeling studies of inhibitor **2** bound in the active site of trypsin. The X-ray crystal structure of the active site of plasmin has not been solved; however, the active sites of plasmin and trypsin share significant homology.[15]

Compound **1** contains three functionalities that are designed to make specific contacts with the active site. The ketone will react with the active site nucleophile to give a hemiketal. In addition one of the aminoalkyl chains will bind in the S1 subsite, while the second aminoalkyl chain will extend along the main channel of the active site to make contacts with the S3 subsite. Okada and co-workers have shown that peptide-based substrates and inhibitors that contain a free N-terminus at the P3 position bind well to the enzyme.[16] In compound **2**, one of the aminoalkyl chains has been replaced by phenylalanine and D-isoleucine in order to include additional functionality that will interact with the S2 and S3 subsites.[16] The sulfur atom was incorporated into the cyclohexanone rings of the three inhibitors because the related tetrahydrothiopyranone-based inhibitor of the cysteine protease papain had good activity and its synthesis was relatively straightforward.[9] Compound **3**, which lacks an aminoalkyl functionality, was synthesized in order to determine how much the P1 side chain contributes to the affinity of the inhibitors for plasmin. We have also synthesized compound **22** (Scheme 4), which is similar in structure to **3** but lacks the electrophilic ketone functionality. This molecule provides a useful control for probing the mechanism of inhibition by inhibitors **1**–**3**.

Scheme 1[a]

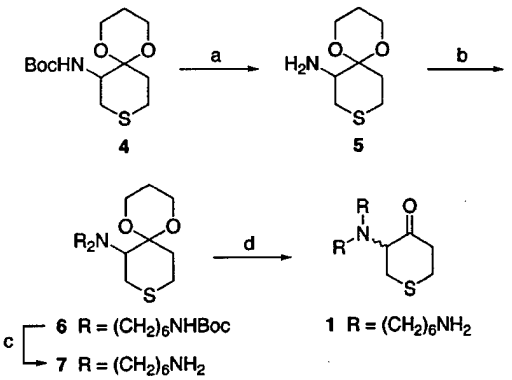

[a] Reagents and conditions: (a) TFA, 85%; (b) **10**, $NaBH(OAc)_3$, 22%; (c) TFA, H_2O, triisopropylsilane, thioanisole, 50%; (d) 6 N HCl, 99%.

Scheme 2[a]

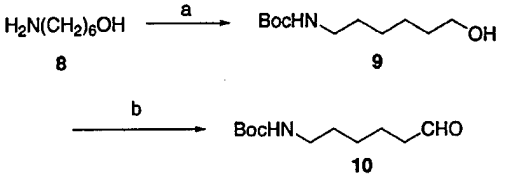

[a] Reagents and conditions: (a) $(Boc)_2O$, 88%; (b) pyridinium chlorochromate, 91%.

Scheme 3[a]

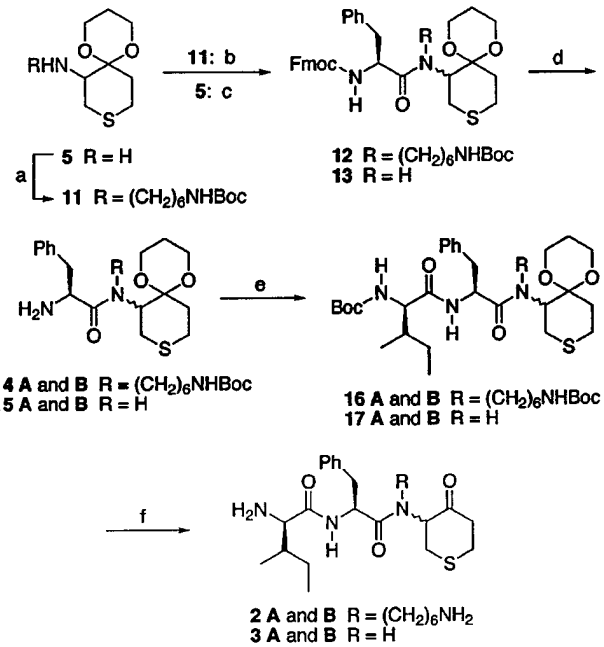

[a] Reagents and conditions: (a) **10**, $NaBH(OAc)_3$, dichloroethane, 50%; (b) Fmoc-Phe-F, DIEA, **12** (75%); (c) Fmoc-Phe, EDC, HOBT, **13** (36%); (d) piperidine, DMF, **14A** and **14B** (67%), **15A** and **15B** (81%); (e) Boc-D-Ile, EDC, HOBT, **16A** (78%), **16B** (63%), **17A** (88%), **17B** (86%); (f) TFA, H_2O, TIS, thioanisole, **2A** (50%), **2B** (9%), **3A** (34%), **3B** (82%). **A** and **B** represent two different diastereomers.

Scheme 4[a]

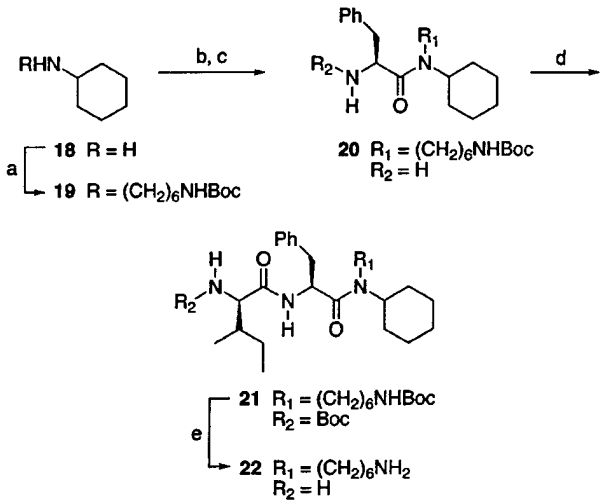

[a] Reagents and conditions: (a) **10**, $NaBH(OAc)_3$, dichloroethane, 25%; (b) Fmoc-Phe-F, DIEA; (c) piperidine, DMF, 66% (2 steps); (d) Boc-D-Ile, EDC, HOBT, 91%; (e) TFA, triisopropylsilane, ethanedithiol, 59%.

Chemistry

The synthesis of inhibitor **1**, which is outlined in Scheme 1, began with deprotection of the Boc-protected nitrogen in compound **4** with trifluoroacetic acid to give amine **5**. The synthesis of **4** has been reported previously.[9] Dialkylation of **5** by reductive amination with 2 equiv of aldehyde **10** gave the tertiary amine **6**. The Boc protecting groups were removed with TFA to give **7**, and the ketal was hydrolyzed using aqueous HCl to give inhibitor **1**. Aldehyde **10** was synthesized starting from 6-amino-1-hexanol (**8**) (Scheme 2). The amino group in **8** was first protected using $(Boc)_2O$ to give alcohol **9**, followed by oxidation of the alcohol using pyridinium chlorochromate.

The synthesis of inhibitors **2** and **3** began with reductive amination of **5** with 1 equiv of aldehyde **10** using sodium triacetoxyborohydride in dichloroethane to give secondary amine **11** (Scheme 3).[17] An alternate strategy for the preparation of **11** involving monoalkylation of **5** with the appropriate alkyl bromide gave a poor yield of the secondary amine. Amine **5** was coupled to Fmoc-Phe using a standard peptide coupling procedure that employed 1-(3-dimethylaminopropyl)-3-ethylcarbodiimide (EDC) and 1-hydroxybenzotriazole (HOBT). However, the more sterically hindered secondary amine **11** did not couple under these conditions and required reaction with the acid fluoride of Fmoc-Phe using methodology developed by Carpino.[18] These reactions gave compounds **12** and **13**, each as a mixture of two diastereomers. The Fmoc protecting groups in **12** and **13** were removed using piperidine in DMF to give amines **14** and **15**. The diastereomers of both compounds were separated at this stage using flash chromatography, and each of the diastereomers was carried separately through the remainder of the synthesis. The amines were next coupled to Boc-D-Ile using EDC and HOBT to give compounds **16** and **17**. Final removal of the Boc and ketal protecting groups in **16** and **17** was accomplished by treatment with trifluoroacetic acid and H_2O to give inhibitors **2** and **3**.

Table 1. Inhibition of Serine Proteases by Inhibitors **1**–**3** and **22**

	K_i (μM)			
compd[a]	plasmin	trypsin	thrombin	kallikrein
1	400 ± 35	1400 ± 110	>10000	>10000
2A	50 ± 5	1700 ± 1500	720 ± 550	630 ± 125
2B	130 ± 10			
3A	9000 ± 1000			
3B	16000 ± 1300			
22	520 ± 30			

[a] **A** and **B** represent two different diastereomers.

Control compound **22** was synthesized in a manner similar to that of inhibitor **2** (Scheme 4). Reductive alkylation of cyclohexylamine with aldehyde **10** gave secondary amine **19**. This material was coupled to Fmoc-Phe-F followed by removal of the Fmoc protecting group to give compound **20**. After a second coupling reaction with Boc-D-Ile, the Boc protecting groups were removed to give **22**.

Results and Discussion

Compound **1**, which incorporates two simple aminohexyl side chains, was assayed against four different serine proteases; plasmin, trypsin, thrombin, and kallikrein (Table 1). All of these proteases have a strong specificity for positively charged side chains such as lysine or arginine at the P1 position and thus provide a reasonable test of the specificity of the inhibitors for plasmin compared to other related enzymes. Compound **1** has modest activity against plasmin with an inhibition constant of 400 μM. It has greater than 25-fold selectivity for this protease when compared to thrombin and kallikrein and a 3-fold selectivity when compared to trypsin. The similar affinity of this inhibitor for plasmin and trypsin is reasonable based upon the sequence homology between the two enzymes.[15]

To increase both the potency and specificity of the inhibitors, we have replaced one of the aminohexyl chains in compound **1** with a D-Ile-L-Phe dipeptide to give inhibitors **2A** and **2B**. The free N-terminus of the D-Ile residue in these compounds positions a positive charge in the S3 enzyme subsite, which has been shown to be beneficial for binding.[16] In addition, the D-Ile and Phe side chains provide hydrophobic contacts with the S2 and S3 subsites. Compound **2A** is a good inhibitor of plasmin with an inhibition constant of 50 μM. By comparison it has significantly lower affinity for trypsin, thrombin, and kallikrein. The low activity of this inhibitor against trypsin is somewhat surprising given the reported similarity between the active sites of plasmin and trypsin.[16] Lineweaver–Burk analysis of **2A** against plasmin demonstrates that it is a reversible competitive inhibitor. This observation is consistent with a mechanism of inhibition that involves addition of the active site serine residue to the tetrahydrothiopyranone carbonyl group of the inhibitor to give a reversibly formed hemiketal. This mechanism has been demonstrated for related inhibitors of the cysteine protease papain.[10]

Compound **2B** has an affinity for plasmin that is 2–3 times lower than that of its diastereomer **2A**. In contrast, there is a 100-fold difference in the binding of

two diastereomers of analogous inhibitors for papain.[9] Papain has a relatively deep and narrow binding cleft[19] that discriminates strongly between two diastereomers that differ in stereochemistry at the position α to the reactive ketone. Based upon the similarities between plasmin and trypsin,[16] it is likely that plasmin has a binding cleft that is much more open and shallow when compared to papain. This sterically unrestrictive active site can accommodate both diastereomers of inhibitor **2**, and it is reasonable to expect that both diastereomers can find a conformation in the active site that allows reaction with the active site serine residue. Thus **2A** and **2B** can bind to plasmin with similar affinities.

We have synthesized compounds **3A** and **3B** in order to determine how much the aminohexyl side chain contributes to the potency of the inhibitors. These compounds are similar in structure to **2A** and **2B** but are missing the side chain which interacts with the S1 pocket in the enzyme active site. Since plasmin is specific for substrates that incorporate a lysine residue at P1, we expected that removing the aminohexyl group from the inhibitor should have a significant negative impact on its ability to bind. Compounds **3A** and **3B** have inhibition constants against plasmin of 9.0 and 16.0 mM, respectively. These values are 200–300 times higher than the inhibition constant for **2A**. This result confirms that the aminohexyl side chain, which mimics a lysine residue at the P1 position of the inhibitor, is critical for good recognition and affinity for the protease.

The design of these 4-heterocyclohexanone-based inhibitors depends on the supposition that the ketone of the inhibitors reacts in a reversible covalent fashion with the active site nucleophile. This mechanism has been confirmed for cysteine proteases[10] but remains unproven for serine proteases. Thus it is possible that compounds **1**–**3** are inhibiting plasmin through simple noncovalent interactions. To further explore the mechanism of inhibition, we have synthesized compound **22** (Scheme 4) which is missing the thioether and ketone functionalities that are present in inhibitor **2**. If the 4-heterocyclohexanones are interacting with the enzyme solely through noncovalent interactions such as salt bridges, hydrogen bonds, and hydrophobic interactions, control compound **22** should be a good mimic of inhibitor **2**, and the two molecules would be expected to have similar affinities for plasmin. However, if the ketone of inhibitor **2** is also reacting with the active site serine to give a reversibly formed covalent adduct, we would expect **22** to be a significantly weaker inhibitor. Table 1 shows that compound **22** has an inhibition constant against plasmin of 520 μM; a value that is 10-fold higher than that observed for inhibitor **2**. Although this result does not unambiguously prove the mechanism of inhibition, it is consistent with the reasonable mechanistic hypothesis that inhibitors **1**–**3** react with the active site serine to give a hemiketal adduct.

In conclusion, this work has shown that the 4-heterocyclohexanone nucleus can serve as the basis for designing good inhibitors of plasmin. In addition, our experiments highlight the versatility of the 4-heterocyclohexanone nucleus because we have now confirmed that it can be used to synthesize inhibitors of both serine and cysteine proteases. We have also demonstrated the feasibility of attaching P1 recognition elements to the inhibitors using the amide nitrogen in a strategy that is borrowed from peptoids.[14] Our future work will focus on extending the noncovalent interactions of these inhibitors into the leaving group subsites of plasmin in order to increase both their potency and specificity.

Experimental Section

General Methods. NMR spectra were recorded on a Bruker WM-250, Avance-300, or Avance-400 instrument. Spectra were calibrated using TMS ($\delta = 0.00$ ppm) for ^{1}H NMR and $CDCl_3$ ($\delta = 77.0$ ppm) or CD_3OD ($\delta = 49.0$ ppm) for ^{13}C NMR. IR spectra were recorded on a Perkin-Elmer 1700 series FT-IR spectrometer. Mass spectra were recorded on a Kratos MS 80 spectrometer under electron impact (EI), chemical ionization (CI), or fast-atom bombardment (FAB) conditions. HPLC analyses were performed on a Rainin HPLC system with Rainin Microsorb silica or C18 columns and UV detection. Semipreparative HPLC was performed on the same system using a semipreparative column (21.4 × 250 mm).

Reactions were conducted under an atmosphere of dry nitrogen in oven-dried glasswear. Anhydrous procedures were conducted using standard syringe and cannula transfer techniques. THF was distilled from sodium and benzophenone. Other solvents were of reagent grade and were stored over 4-Å molecular sieves. All other reagents were used as received. Organic solutions were dried over $MgSO_4$ unless otherwise noted. Solvent removal was performed by rotary evaporation at water aspirator pressure.

Primary Amine 5. A solution containing 9.5 mL of trifluoroacetic acid (TFA), 0.25 mL of triisopropylsilane (TIS), and 0.25 mL of thioanisole was added to the carbamate **4**[9] (4.8 g, 17 mmol) dissolved in 2 mL of CH_2Cl_2. After stirring at room temperature for 10 min the solvent was evaporated under reduced pressure. The crude product was purified by column chromatography (1:10:89 concentrated $NH_4OH/CH_3OH/CH_2Cl_2$) affording 2.8 g (15 mmol, 89%) of the primary amine **5**: ^{1}H NMR (300 MHz, MeOH-d_4) δ 1.44 (dm, $J = 13.5$ Hz, 1H), 1.65 (ddd, $J = 15.0, 11.6, 3.5$ Hz, 1H), 1.94–2.11 (m, 1H), 2.50 (dm, $J = 13.8$ Hz, 1H), 2.61 (ddd, $J = 13.1, 5.6, 1.8$ Hz, 1H), 2.73 (ddd, $J = 13.9, 11.4, 2.6$ Hz, 1H), 2.96 (dd, $J = 13.0, 11.2$ Hz, 1H), 3.21 (dm, $J = 14.4$ Hz, 1H), 3.30 (m, 1H), 3.89 (m, 2H), 4.10 (m, 2H); ^{13}C NMR (75 MHz, MeOH-d_4) δ 25.9, 26.4, 28.5, 31.1, 57.9, 60.9, 61.1, 96.5; HRMS-EI (M^+) calcd for $C_8H_{15}NO_2S$ 189.0824, found 189.0827.

Tertiary Amine 6. Amine **5** (0.15 g, 0.79 mmol) was dissolved in 5 mL of 1,2-dichloroethane (DCE) before the aldehyde **10** (0.38 g, 1.7 mmol) and sodium triacetoxyborohydride (0.23 g, 1.1 mmol) were added. After 6.5 h at room temperature the reaction was partitioned between saturated $NaHCO_3$ solution and EtOAc. The organic layer was dried over $MgSO_4$ and concentrated. The crude product was purified by flash chromatography (EtOAc) affording 0.10 g (0.18 mmol, 22%) of the tertiary amine **6**: ^{1}H NMR (400 MHz, MeOH-d_4) δ 1.24–1.35 (m, 37H), 1.96 (m, 1H), 2.28 (m, 1H), 2.51–2.63 (m, 3H), 2.78 (m, 3H), 2.93–3.00 (m, 5H), 3.23–3.27 (m, 2H), 3.75–4.02 (m, 4H); ^{13}C NMR (100 MHz, MeOH-d_4) δ 25.9, 26.5, 27.1, 27.9, 28.2, 28.8, 30.2, 31.1, 33.0, 41.4, 53.4, 59.6, 59.8, 68.2, 79.8, 100.8, 158.6; HRMS–FAB ($M + Na^+$) calcd for $C_{30}H_{57}N_3NaO_6S$ 610.3866, found 610.3882.

Ketal 7. Tertiary amine **6** (100 mg, 0.17 mmol) was dissolved in 1 mL of a solution containing 92.5% TFA, 2.5% TIS, 2.5% thioanisole, and 2.5% H_2O. The reaction was stirred at room temperature for 1 h before the TFA was removed under reduced pressure. The resultant material was dissolved in MeOH to which Et_2O was added until the solution turned cloudy. The ketal **7** (53 mg, 0.86 mmol, 50%) which settled out of the solution as an oily liquid was used without further purification: ^{1}H NMR (250 MHz, MeOH-d_4) δ1.46 (m, 9H), 1.66–1.85 (m, 10H), 2.07 (m, 1H), 2.49–2.54 (m, 1H), 2.79–3.01 (m, 7H), 3.25 (m, 2H), 3.45 (m, 1H), 3.59–3.64 (dd, $J =$ 12.0, 2.9 Hz, 1H), 3.93–4.28 (m, 5H); ^{13}C NMR (75 MHz, MeOH-d_4) δ 23.8, 25.9, 26.0, 26.5, 26.6, 27.4, 27.5, 27.8, 28.7, 28.8, 32.6, 40.9, 54.6, 55.6, 61.2, 61.4, 69.9, 98.3, 118 (q), 163.2 (q).

Alcohol 9. 6-Amino-1-hexanol (**8**) (2.0 g, 17 mmol) was dissolved in a 5:1 mixture of 1,4-dioxane/H_2O and cooled to 0 °C. Di-*tert*-butyl dicarbonate (7.5 g, 34 mmol) was added, and the reaction mixture was allowed to warm to room temperature and stirred for 12 h. The dioxane was evaporated under reduced pressure, and the remaining material was partitioned between EtOAc and saturated $NaHCO_3$ solution. The organic layer was washed with brine, dried over $MgSO_4$, and concentrated under reduced pressure. The crude product was purified by flash chromatography (4:1 EtOAc/hexanes) to afford alcohol **9** (3.2 g, 15 mmol, 88%): ^{1}H NMR (300 MHz, $CDCl_3$) δ 1.35–1.76 (m, 18H), 3.11 (q, J = 6.1 Hz, 2H), 3.64 (t, J = 6.3 Hz, 2H), 4.60 (bs, 1H); ^{13}C NMR (75 MHz, $CDCl_3$) δ 25.4, 26.4, 26.5, 28.4, 30.0, 32.6, 40.0, 62.4, 79.1, 156.2; HRMS-CI (M + H^+) calcd for $C_{11}H_{24}NO_3$ 218.1756, found 218.1760.

Aldehyde 10. The alcohol **9** (7.2 g, 33 mmol) was added to a CH_2Cl_2 solution (500 mL) containing 51 g of neutral alumina and pyridinium chlorochromate (11 g, 50 mmol). The reaction was allowed to stir at room temperature for 3 h and then was loaded directly onto a flash chromatography column. The product was eluted with 1:1 EtOAc/hexanes to afford 6.5 g (30 mmol, 91%) of the aldehyde **10**: IR 1704 cm^{-1} (CO); ^{1}H NMR (250 MHz, $CDCl_3$) δ 1.26–1.49 (m, 13H), 1.61 (pent, J = 7.2 Hz, 2H), 2.40 (t, J = 7.2 Hz, 2H), 3.08 (q, J = 6.6 Hz, 2H), 4.59 (bs, 1H), 9.76 (t, J = 1.7 Hz, 1H); ^{13}C NMR (100 MHz, $CDCl_3$) δ 22.5, 27.1, 29.2, 30.7, 41.4, 44.5, 79.8, 156.8, 203.0; HRMS-CI (M + H^+) calcd for $C_{10}H_{22}NO_2$ 216.1600, found 216.1600.

Secondary Amine 11. Aldehyde **10** (0.52 g, 2.4 mmol) was dissolved in 2 mL of DCE and added to a solution of primary amine **5** (0.51 g, 2.7 mmol) dissolved in 3 mL of DCE. After 10 min sodium triacetoxyborohydride (0.80 g, 3.8 mmol) was added, and the reaction was allowed to stir for an additional 3 h at room temperature. The reaction was then quenched with saturated $NaHCO_3$ solution and extracted with EtOAc. The organic layer was dried over $MgSO_4$ and concentrated under reduced pressure. The crude product was purified by flash chromatography (2:1:7 EtOAc/MeOH/Et_2O) providing the secondary amine **11** (0.53 g, 1.40 mmol, 50%): ^{1}H NMR (300 MHz, MeOH-d_4) δ 1.36–1.72 (m, 21H), 2.02 (m, 1H), 2.50 (dm, J = 13.7 Hz, 1H), 2.69 (ddd, J = 9.7, 9.7, 2.6 Hz, 1H), 2.76–2.89 (m, 4H), 3.00–3.07 (m, 4H), 3.87 (m, 2H), 4.02 (ddd, J = 11.9, 9.3, 2.5 Hz, 1H), 4.12 (ddd, J = 12.0, 12.0, 2.7 Hz, 4H); ^{13}C NMR (75 MHz, MeOH-d_4) δ 24.7, 25.2, 25.5, 25.9, 26.7, 28.2, 30.2, 40.4, 46.0, 60.0, 60.1, 62.8, 79.3, 96.1, 158.0; HRMS-FAB (M + Na^+) calcd for $C_{19}H_{36}N_2NaO_4S$ 411.2294, found 411.2306.

Fmoc Ketal 12. Fmoc-Phe-F[18] (0.34 g, 0.89 mmol) and diisopropylethylamine (DIEA; 0.10 mL, 0.60 mmol) were added to a solution of the secondary amine **11** (0.11 g, 0.30 mmol) dissolved in 15 mL of CH_2Cl_2. The reaction was heated at reflux for 5 h, then cooled, and washed with 10 mL of 1 N NaOH, 15 mL of 1 N HCl, and 15 mL of saturated $NaHCO_3$ solution. The organic layer was then dried over $MgSO_4$ and concentrated under reduced pressure. Flash chromatography (2:3 EtOAc/hexanes) of the resultant material afforded a mixture of two diastereomers of Fmoc ketal **12** (0.17 g, 0.22 mmol, 75%): ^{1}H NMR (300 MHz, $CDCl_3$) δ 1.02–2.07 (m, 21H), 2.28–2.45 (m, 1H), 2.56–5.09 (m, 18H), 5.39–5.90 (m, 1H), 7.20–7.83 (m, 13H); ^{13}C NMR (75 MHz, $CDCl_3$) δ 25.0, 26.5, 27.1, 27.3, 28.4, 28.7, 29.1, 30.1, 31.3, 40.5, 41.4, 44.9, 47.1, 47.3, 52.1, 52.4, 58.8, 59.0, 63.0, 66.6, 66.9, 97.1, 120.0, 125.1, 125.2, 126.5, 126.8, 127.0, 127.6, 128.3, 128.4, 128.5, 128.6, 129.4, 129.7, 136.4, 136.8, 141.3, 143.9, 144.0, 155.2, 156.0, 172.8; HRMS-FAB (M + Na^+) calcd for $C_{43}H_{55}N_3NaO_7S$ 780.3659, found 780.3663.

Fmoc Ketal 13. A DMF solution (75 mL) containing hydroxybenzotriazole (HOBT; 0.37 g, 2.8 mmol), *N*-(3-dimethylaminopropyl)-*N'*-ethylcarbodiimide hydrochloride (EDC; 0.69 g, 3.6 mmol), and Fmoc-phenylalanine (1.1 g, 2.8 mmol) was stirred at room temperature for 1 h. A solution of the primary amine **5** (0.52 g, 2.8 mmol) and 4-methylmorpholine (0.60 mL, 5.5 mmol) dissolved in 25 mL of DMF was then added to the reaction mixture. After 2 h the reaction mixture was partitioned between 100 mL of EtOAc and 100 mL of H_2O. The organic layer was washed with 100 mL of H_2O, 50 mL of saturated $KHSO_4$ solution, and 50 mL of saturated Na_2CO_3 solution, dried over $MgSO_4$, and concentrated under reduced pressure. Flash chromatography (1:1 EtOAc/hexanes) afforded a mixture of two diastereomers of Fmoc ketal **13** (0.56 g, 1.0 mmol, 36%): ^{1}H NMR (300 MHz, $CDCl_3$) δ 1.62–1.81 (m, 3H), 2.28–3.19 (m, 7H), 3.72–3.93 (m, 4H), 4.10–4.46 (m, 5H), 5.44 (m, 1H), 6.24–6.48 (m, 1H), 7.24–7.79 (m, 13H); ^{13}C NMR (75 MHz, $CDCl_3$) δ 25.0, 25.3, 25.4, 30.6, 30.7, 32.0, 32.2, 39.2, 39.5, 47.6, 56.6, 56.9, 59.4, 59.5, 59.6, 67.5, 96.3, 96.4, 120.4, 125.47, 125.54, 127.3, 127.5, 128.1, 129.0, 129.1, 129.8, 129.9, 136.8, 137.0, 141.7, 144.2, 156.2, 170.4, 170.6; HRMS–FAB (M + Na^+) calcd for $C_{32}H_{34}N_2NaO_5S$ 581.2086, found 581.2099.

Amino Ketals 14A and 14B. A DMF solution (35 mL) of Fmoc ketal **12** (1.75 g, 2.3 mmol) and piperidine (1.4 mL, 14 mmol) was stirred at room temperature for 1 h. The solvent was evaporated under reduced pressure, and the crude material was purified by flash chromatography (98:2 CH_2Cl_2/MeOH) to give the two separate diastereomers of the amino ketals **14A** (0.43 g, 0.50 mmol) and **14B** (0.41 g, 0.76 mmol) with a combined yield of 67%. **14A**: ^{1}H NMR (300 MHz, $CDCl_3$) δ 1.08 (m, 1H), 1.09–1.34 (m, 7H), 1.36–1.52 (m, 14H), 1.68–1.73 (m, 4H), 1.84–1.97 (m, 1H), 2.36 (dq, J = 13.5, 1.8 Hz, 1H), 2.65–2.82 (m, 2H), 2.91–3.02 (m, 2H), 3.09–3.19 (m, 4H), 3.44–3.59 (m, 1H), 3.63 (dd, J = 11.4, 3.3 Hz, 1H), 3.71–3.91 (m, 4H), 4.02 (dt, J = 11.9, 2.4 Hz, 1H), 4.10 (dd, J = 10.0, 5.7 Hz, 1H), 4.60 (bm, 1H), 7.19–7.39 (m, 5H); ^{13}C NMR (75 MHz, $CDCl_3$) δ 27.6, 29.2, 29.8, 30.3, 31.2, 31.9, 32.8, 34.1, 45.4, 47.5, 55.5, 61.6, 62.0, 65.2, 100.1, 129.1, 131.2, 132.2, 140.6, 180.0; HRMS-ESI (M + H^+) calcd for $C_{28}H_{46}N_3O_5S$ 536.3158, found 536.3163. **14B**: ^{1}H NMR (300 MHz, $CDCl_3$) δ 1.25–1.67 (m, 27H), 1.96–2.02 (m, 2H), 2.43–2.51 (m, 2H), 2.67 (dd, J = 13.6, 9.3 Hz, 1H), 2.79–2.83 (m, 1H), 3.11–3.30 (m, 6H), 3.36–3.52 (m, 2H), 3.69–4.05 (m, 6H), 4.27 (dd, J = 11.2, 2.9 Hz, 1H), 4.61 (bs, 1H), 7.20–7.34 (m, 5H); ^{13}C NMR (75 MHz, $CDCl_3$) δ 24.0, 24.1, 24.3, 25.6, 25.8, 26.1, 26.4, 27.5, 27.7, 28.0, 28.3, 29.3, 30.2, 30.7, 30.9, 39.8, 41.5, 42.0, 43.6, 43.8, 52.6, 52.9, 57.9, 58.0, 58.1, 58.3, 62.3, 78.2, 78.3, 96.7, 97.2, 125.5, 125.9, 127.6, 127.7, 128.6, 128.7, 137.6, 138.6, 155.2, 155.5, 175.0, 175.8; HRMS-ESI (M + H^+) calcd for $C_{28}H_{46}N_3O_5S$ 536.3158, found 536.3140.

Amino Ketals 15A and 15B. A solution of piperidine (0.6 mL, 6.0 mmol) and Fmoc ketal **13** (0.56 g, 1.0 mmol) in 5 mL of DMF was allowed to stir at room temperature for 5 h. The reaction mixture was then partitioned between 50 mL of EtOAc and 50 mL of H_2O. The organic layer was washed with H_2O, dried over $MgSO_4$, and concentrated. The crude material was purified by flash chromatography (2:98 MeOH/CH_2Cl_2) to afford the two separate diastereomers of the amino ketals **15A** (0.17 g, 0.50 mmol) and **15B** (0.11 g, 0.32 mmol) with a combined yield of 81%. **15A**: ^{1}H NMR (300 MHz, $CDCl_3$) δ 1.26 (s, 2H), 1.47 (m, 2H), 1.68 (m, 1H), 2.30 (bm, 1H), 2.50 (m, 2H), 2.73 (dd, J = 13.7, 9.2 Hz, 5H), 2.93 (m, 1H), 3.26 (dd, J = 13.7, 3.9 Hz, 1H), 3.67 (dd, J = 9.2, 4.0 Hz, 1H), 3.81 (m, 1H), 3.93 (m, 2H), 4.14 (m, 1H), 4.66 (bm, 1H), 7.23–7.34 (m, 5H), 8.01 (d, J = 8.6 Hz, 1H); ^{13}C NMR (75 MHz, $CDCl_3$) δ 25.9, 26.7, 31.3, 32.7, 42.6, 57.6, 60.5, 60.8, 97.9, 128.2, 129.9, 131.0, 134.3, 139.2, 176.8; HRMS–FAB (M + H^+) calcd for $C_{17}H_{25}N_2O_3S$ 337.1586, found 337.1579. **15B**: ^{1}H NMR (300 MHz, $CDCl_3$) δ 1.53–1.72 (m, 4H), 2.29 (bs, 1H), 2.52 (m, 2H), 2.76 (dd, J = 13.7, 9.1 Hz, 2H), 2.96 (dd, J = 10.8, 2.1 Hz, 1H), 3.26 (dd, J = 13.7, 4.5 Hz, 1H), 3.64 (dd, J = 9.1, 4.6 Hz, 1H), 3.82 (m, 1H), 3.94 (m, 2H), 3.96 (m, 1H), 4.70 (bm, 1H), 7.22–7.35 (m, 5H), 7.90 (d, J = 9.2 Hz, 1H); ^{13}C NMR (75 MHz, $CDCl_3$) δ 25.9, 26.6, 31.2, 32.7, 42.8, 57.9, 60.5, 60.7, 97.8, 128.1, 130.0, 130.9, 139.4, 176.8; HRMS–FAB (M + H^+) calcd for $C_{17}H_{25}N_2O_3S$ 337.1586, found 337.1592.

Boc Ketal 16A. A DMF solution (10 mL) containing HOBT (103 mg, 0.76 mmol), EDC (192 mg, 1.0 mmol), and Boc-D-Ile (172 mg, 0.76 mmol) was stirred at room temperature for 20 h. A solution of the amino ketal **14A** (0.41 g, 0.76 mmol) and 4-methylmorpholine (0.17 mL, 1.5 mmol) dissolved in 10 mL of DMF was then added to the reaction mixture. After 4 h the reaction mixture was partitioned between EtOAc and H_2O. The

organic layer was washed with H_2O, dried over $MgSO_4$, and concentrated under reduced pressure. Flash chromatography (4:1 EtOAc/hexanes) afforded the Boc ketal **16A** (0.44 g, 0.59 mmol, 78%). This compound appears in the NMR spectra as a mixture of two conformational isomers: ^{1}H NMR (300 MHz, $CDCl_3$) δ 0.75–0.99 (m, 6H), 1.06–1.36 (m, 34H), 2.27–2.32 (m, 1H), 2.62 (t, J = 13.1 Hz, 1H), 2.75 (t, J = 12.3 Hz, 1H), 2.87 (t, J = 11.5 Hz, 1H), 2.97–3.17 (m, 5H), 3.46–4.03 (m, 6H), 4.56 (m, 0.5H), 4.97–5.30 (m, 1.5H), 6.90 (d, J = 7.1 Hz, 1H), 7.17–7.31 (m, 5H); ^{13}C NMR (100 MHz, $CDCl_3$) δ 11.9, 15.6, 15.77, 15.83, 25.0, 25.2, 25.3, 26.3, 26.8, 27.4, 27.5, 28.6, 28.7, 29.4, 30.4, 31.4, 37.8, 38.2, 40.4, 40.8, 41.2, 41.3, 45.3, 51.2, 51.3, 59.2, 63.3, 79.3, 79.9, 97.3, 98.3, 127.1, 128.7, 129.0, 129.7, 130.0, 130.1, 136.6, 137.0, 155.9, 170.3, 170.4, 173.0, 192.2, 201.5; HRMS–FAB (M + Na^+) calcd for $C_{39}H_{64}N_4NaO_8S$ 771.4166, found 771.4334 for a mixture of diastereomers **16A** and **16B**.

Boc Ketal 16B. Compound **16B** was prepared from **14B** (270 mg, 0.51 mmol), HOBT (68 mg, 0.51 mmol), EDC (130 mg, 0.67 mmol), Boc-D-Ile (120 mg, 0.51 mmol), and 4-methylmorpholine (0.11 mL, 1.0 mmol) in 20 mL of DMF using the method described for the synthesis of **16A**. The crude material was purified by HPLC (1.5% MeOH/CH_2Cl_2 over 45 min) to afford **16B** (240 mg, 0.32 mmol, 63%). This compound appears in the NMR spectra as a mixture of two conformational isomers: ^{1}H NMR (300 MHz, $CDCl_3$) δ 0.67–1.07 (m, 6H), 1.32–1.48 (m, 26H), 1.62–1.79 (m, 2H), 1.91–2.03 (m, 2H), 2.44 (m, 1.5H), 2.76–3.49 (m, 8H), 3.66 (m, 0.5H), 3.80–4.05 (m, 4H), 4.57 (m, 1H), 4.92–5.29 (m, 3H), 6.48 (m, 0.5H), 6.65 (m, 0.5H), 7.18–7.30 (m, 5H); ^{13}C NMR (100 MHz, $CDCl_3$) δ 11.9, 12.1, 15.6, 15.8, 24.8, 24.9, 25.0, 25.36, 25.41, 26.5, 26.9, 27.4, 28.4, 28.7, 28.8, 28.9, 29.2, 30.1, 31.3, 31.6, 37.7, 38.2, 38.5, 40.6, 40.9, 44.8, 45.2, 50.7, 51.1, 53.8, 59.1, 59.2, 59.3, 59.4, 59.5, 63.0, 77. 7, 79.4, 80.0, 97.9, 98.2, 126.8, 127.4, 128.6, 128.9, 129.8, 129.9, 137.0, 138.0, 155.9, 171.1, 173.1; HRMS–FAB (M + Na^+) calcd for $C_{39}H_{64}N_4NaO_8S$ 771.4166, found 771.4334 for a mixture of diastereomers **16A** and **16B**.

Boc Ketal 17A. Compound **17A** was prepared from compound **15A** (110 mg, 0.32 mmol), HOBT (43 mg, 0.32 mmol), EDC (80 mg, 0.42 mmol), Boc-D-Ile (74 mg, 0.32 mmol), and 4-methylmorpholine (0.070 mL, 0.64 mmol) in 15 mL of DMF by the method described for the synthesis of **16A**. The crude material was purified by flash chromatography (4:1 EtOAc/hexanes) to afford **17A** (156 mg, 0.28 mmol, 88%): ^{1}H NMR (300 MHz, $CDCl_3$) δ 0.80–0.95 (m, 7H), 1.24–1.44 (m, 10H), 1.60–1.81 (m, 6H), 2.46–2.59 (m, 3H), 2.82–3.13 (m, 3H), 3.76–4.01 (m, 5H), 4.44 (m, 1H), 4.73 (q, J = 6.9 Hz, 1H), 5.01 (m, 1H), 6.58 (m, 2H), 7.19–7.32 (m, 5H); ^{13}C NMR (100 MHz, $CDCl_3$) δ 11.9, 15.8, 24.9, 25.4, 28.7, 30.6, 31.9, 37.8, 38.6, 54.8, 59.6, 80.4, 96.3, 127.3, 129.0, 129.8, 136.8, 156.0, 170.4, 171.8; HRMS–FAB (M + H^+) calcd for $C_{28}H_{44}N_3O_6S$ 550.2951, found 550.2961.

Boc Ketal 17B. Compound **17B** was prepared from compound **15B** (106 mg, 0.32 mmol), HOBT (43 mg, 0.32 mmol), EDC (78 mg, 0.41 mmol), Boc-D-Ile (73 mg, 0.32 mmol), and 4-methylmorpholine (0.070 mL, 0.64 mmol) in 15 mL of DMF by the method described for the synthesis of **16A**. The crude material was purified by flash chromatography (4:1 EtOAc/hexanes) to give compound **17B** (148 mg, 0.27 mmol, 86%): ^{1}H NMR (300 MHz, $CDCl_3$) δ 0.81–1.02 (m, 7H), 1.23–1.80 (m, 16H), 2.27–2.74 (m, 4H), 2.95–3.18 (m, 2H), 3.70–3.99 (m, 5H), 4.38 (s, 1H), 4.67 (q, J = 8.2 Hz, 1H), 5.11 (m, 1H), 6.41 (m, 1H), 6.81 (d, J = 7.5 Hz, 1H), 7.20–7.31 (m, 5H); ^{13}C NMR (100 MHz, $CDCl_3$) δ 12.0, 15.8, 24.9, 25.3, 28.7, 30.5, 32.0, 38.1, 38.8, 55.2, 59.5, 59.6, 80.3, 96.3, 127.4, 129.1, 129.7, 137.0, 156.0, 170.1, 171.7; HRMS–FAB (M + H^+) calcd for $C_{28}H_{44}N_3O_6S$ 550.2951, found 550.2953.

Inhibitor 1. Ketal **7** (53 mg, 0.09 mmol) was dissolved in a solution of 5 mL of MeOH and 10 mL of 6 N HCl. The reaction was heated at reflux for 1 h before the solvent was removed under reduced pressure. The crude material was dissolved in a small amount of MeOH to which Et_2O was added until the solution turned cloudy. The Et_2O was pipetted off and the oily residue further purified by RPHPLC (H_2O with 0.1% TFA) to afford 53 mg (0.09 mmol, 99%) of inhibitor **1**: ^{1}H NMR (300 MHz, MeOH-d_4) δ 1.31 (m, 10H), 1.67–1.83 (m, 10H), 2.92–3.04 (m, 9H), 3.14 (m, 1H), 4.61 (dd, J = 11.6, 5.3 Hz, 1H); ^{13}C NMR (75 MHz, MeOH-d_4) δ 24.9, 25.9, 26.06, 26.12, 26.3, 27.3, 28.1, 29.0, 39.5, 44.5, 53.0, 53.2, 69.9, 201.9.

Inhibitor 2A. The Boc ketal **16A** (100 mg, 0.14 mmol) was dissolved in 1 mL of a solution containing 92.5% TFA, 2.5% TIS, 2.5% thioanisole, and 2.5% H_2O. After 18 h the TFA was removed under reduced pressure. The crude mixture was purified by reverse-phase HPLC (0–50% MeCN/H_2O over 45 min) affording 49 mg (0.068 mmol, 50%) of the inhibitor **2A**: ^{1}H NMR (300 MHz, MeOH-d_4) δ 0.83–0.97 (m, 7H), 1.31–1.41 (m, 7H), 1.71–1.79 (m, 4H), 2.79–2.99 (m, 7H), 3.05–3.21 (m, 2H), 3.39–3.48 (m, 2H), 3.69 (d, J = 5.5 Hz, 1H), 4.10 (dd, J = 11.1, 5.9 Hz, 1H), 5.12 (dd, J = 9.3, 5.8 Hz, 1H), 7.26–7.38 (m, 5H); ^{13}C NMR (75 MHz, MeOH-d_4) δ 12.0, 15.3, 25.4, 27.5, 27.6, 27.9, 28.0, 28.8, 28.9, 30.7, 32.3, 34.6, 38.1, 39.8, 41.0, 45.2, 50.8, 52.1, 52.8, 53.7, 54.2, 59.4, 61.3, 67.8, 128.7, 130.2, 130.3, 130.8, 131.1, 138.0, 138.2, 163.4, 169.5, 172.7, 190.3, 204.6; HRMS–FAB (M + H^+) calcd for $C_{26}H_{43}N_4O_3S$ 491.3056, found 491.3067.

Inhibitor 2B. Inhibitor **2B** was prepared from compound **16B** (240 mg, 0.32 mmol) and 1 mL of the TFA solution specified in the synthesis of **2A**. The crude product was purified by RPHPLC (0–50% MeCN/H_2O over 45 min) to afford inhibitor **2B** (21 mg, 0.030 mmol, 9%): ^{1}H NMR (300 MHz, MeOH-d_4) δ 0.52–0.82 (m, 7H), 1.06–1.12 (m, 1H), 1.19–1.36 (m, 5H), 1.49–1.64 (m, 5H), 2.64–2.85 (m, 6H), 2.91–2.98 (m, 1H), 3.08 (dd, J = 14.5, 4.6 Hz, 1H), 4.93 (dd, J = 10.2, 4.6 Hz, 1H), 7.00–7.24 (m, 5H); ^{13}C NMR (75 MHz, MeOH-d_4) δ 12.1, 15.2, 25.4, 27.6, 28.9, 31.0, 32.6, 38.2, 39.1, 41.0, 45.3, 50.8, 52.9, 59.4, 68.1, 128.6, 130.1, 130.5, 130.7, 138.5, 169.6, 173.1, 204.0; HRMS-ESI (M + H^+) calcd for $C_{26}H_{43}N_4O_3S$ 491.3056, found 491.3065.

Inhibitor 3A. Compound **17A** (53 mg, 0.10 mmol) was dissolved in 1 mL of a solution containing 92.5% TFA, 2.5% TIS, 2.5% H_2O, and 2.5% thioanisole. After 1 h the TFA was removed under reduced pressure. The crude mixture was purified by flash chromatography (10:89:1 MeOH/CH_2Cl_2/concentrated NH_4OH) before the final purification was performed using RPHPLC (0–100% MeCN/H_2O over 45 min) affording the inhibitor **3A** (17 mg, 0.03 mmol, 34%). In MeOH-d_4 solution, the inhibitor is visible as an approximate 1:1 mixture of hemiketal and ketone: ^{1}H NMR (400 MHz, MeOH-d_4) δ 0.70–0.78 (m, 7H), 1.15 (m, 1H), 1.65 (m, 1H), 1.83 (m, 0.5H), 1.99 (m, 0.5H), 2.17 (m, 0.5H), 2.38 (m, 0.5H), 2.59–3.00 (m, 5H), 3.13 (ddd, J = 13.2, 5.6, 2.8 Hz, 0.5H), 3.28 (m, 0.5H), 3.67 (m, 1H), 4.13 (m, 0.5H), 4.72 (dd, J = 11.6, 4.8 Hz, 0.5H), 4.82 (dd, J = 11.2, 7.2 Hz, 0.5H), 7.23–7.35 (m, 5H); ^{13}C NMR (100 MHz, MeOH-d_4) δ 10.7, 13.6, 24.0, 24.7, 25.0, 25.1, 30.45, 30.49, 34.7, 35.2, 36.7, 37.8, 38.0, 44.4, 64.99, 55.02, 58.00, 58.03, 59.8, 95.5, 96.2, 115.5 (q, J = 284 Hz), 160.3 (q, J = 34 Hz), 168.3, 168.4, 172.4, 172.68, 172.71, 204.4; HRMS–FAB (M + Na^+) calcd for $C_{20}H_{29}N_3NaO_3S$ 414.1827, found 414.1823.

Inhibitor 3B. Inhibitor **3B** was prepared from compound **17B** (60 mg, 0.11 mmol) and 1 mL of the TFA solution specified in the synthesis of **3A**. The crude product was purified by RPHPLC (0–100% MeCN/H_2O over 45 min) to afford inhibitor **3B** (45 mg, 0.090 mmol, 82%). In MeOH-d_4 solution, the inhibitor is visible as an approximate 1:1 mixture of hemiketal and ketone: ^{1}H NMR (400 MHz, MeOH-d_4) δ 0.58–1.05 (m, 7H), 1.16–1.40 (m, 1H), 1.65–1.81 (m, 1H), 1.94–2.14 (m, 1H), 2.39–3.05 (m, 6H), 3.15–3.23 (m, 1H), 3.69 (d, J = 5.2 Hz, 1H), 4.05–4.11 (m, 0.5H), 4.67 (dd, J = 11.5, 5.3 Hz, 0.5H), 4.73 (dd, J = 10.1, 5.8 Hz, 0.5H), 4.84 (dd, J = 10.2, 5.2 Hz, 0.5H), 7.22–7.32 (m, 5H); ^{13}C NMR (75 MHz, MeOH-d_4) δ 14.2, 14.3, 27.7, 27.8, 28.5, 33.8, 34.0, 38.1, 38.8, 40.30, 40.33, 41.4, 41.7, 48.0, 58.5, 59.0, 61.5, 61.7, 63.6, 99.2, 130.6, 130.7, 132.2, 132.8, 140.6, 140.8, 172.0, 172.4, 175.6, 176.1, 207.9; HRMS–FAB (M + Na^+) calcd for $C_{20}H_{29}N_3NaO_3S$ 414.1827, found 414.1834.

Secondary Amine 19. Compound **19** was prepared from **18** (3.8 mL, 33.5 mmol), compound **10** (6.6 g, 30.5 mmol), and

sodium triacetoxyborohydride (3.7 g, 17.5 mmol) in 20 mL of DCE using the method described for the synthesis of **11**. The crude material was purified by flash chromatography (2:1:7 EtOAc/MeOH/Et_2O) to afford the secondary amine **19** (1.3 g, 4.4 mmol, 25%): ^{1}H NMR (300 MHz, $CDCl_3$) δ 0.96–1.47 (m, 23H), 1.57–1.73 (m, 3H), 1.84 (m, 2H), 2.32–2.42 (m, 1H), 2.58 (t, J = 7.1 Hz, 2H), 3.07 (q, J = 6.5 Hz, 2H), 4.60 (bs, 1H); ^{13}C NMR (75 MHz, $CDCl_3$) δ 25.5, 26.6, 27.1, 27.5, 28.5, 30.4, 30.8, 34.0, 40.7, 47.3, 57.3, 79.3, 156.4; HRMS–FAB (M + Na^+) calcd for $C_{17}H_{34}N_2NaO_2$ 321.2518, found 321.2522.

Primary Amine 20. A solution of Fmoc-Phe-F (5 g, 13.2 mmol), DIEA (2.3 mL, 13.2 mmol), and the secondary amine **19** (1.3 g, 4.4 mmol) in 100 mL of CH_2Cl_2 was heated at reflux for 18 h. The mixture was then diluted with 100 mL of EtOAc and washed with 100 mL each of 1 N NaOH, 1 N HCl, and saturated $NaHCO_3$ solution. The resultant organic layer was dried over $MgSO_4$ and concentrated. The crude material was purified by flash chromatography (1:1 EtOAc/hexanes) which provided a mixture of Fmoc-Phe and the expected coupling product. The mixture was dissolved in 85 mL of DMF, and piperidine (2.2 mL, 22 mmol) was added. After 15 min the solution was partitioned between 150 mL of EtOAc and 150 mL of H_2O. The organic layer was dried over $MgSO_4$ and concentrated. The crude material was purified by flash chromatography (2% MeOH/CH_2Cl_2) to afford the primary amine **20** as a mixture of two conformational isomers that interconvert slowly on the NMR time scale (1.3 g, 2.9 mmol, 66%): ^{1}H NMR (300 MHz, $CDCl_3$) δ 1.02–1.74 (m, 27H), 2.65–3.34 (m, 6H), 3.67 (t, J = 7.0 Hz, 0.5H), 3.89 (t, J = 7.0 Hz, 0.5H), 4.22 (m, 0.5H), 4.67 (m, 0.5H), 7.16–7.33 (m, 5H); ^{13}C NMR (75 MHz, $CDCl_3$) δ 25.6, 25.9, 26.3, 26.4, 26.7, 26.8, 27.4, 28.8, 29.7, 30.4, 30.9, 31.2, 31.7, 32.1, 32.6, 42.7, 43.9, 53.3, 54.2, 54.4, 57.1, 127.0, 128.8, 128.9, 129.1, 129.7, 138.3, 156.4, 174.5; HRMS–FAB (M + Na^+) calcd for $C_{26}H_{43}N_3NaO_3$ 468.3202, found 468.3216.

Boc Dipeptide 21. Compound **21** was prepared from **20** (1.3 g, 2.9 mmol), HOBT (0.39 g, 2.9 mmol), EDC (0.73 g, 3.8 mmol), Boc-D-Ile (0.68 g, 2.9 mmol), and 4-methylmorpholine (0.66 g, 6 mmol) in 75 mL of DMF using the method described for the synthesis of **16A**. The crude material was purified by flash chromatography (4:1 EtOAc/hexanes) to afford Boc dipeptide **21** (1.7 g, 2.6 mmol, 91%): ^{1}H NMR (300 MHz, $CDCl_3$) δ 0.76–0.82 (m, 7H), 0.94–1.77 (m, 36H), 2.60–3.29 (m, 6H), 4.00–4.12 (m, 2H), 4.69–5.53 (m, 3H), 7.07–7.28 (m, 5H); ^{13}C NMR (75 MHz, $CDCl_3$) δ 11.9, 15.8, 24.87, 24.94, 25.5, 26.0, 26.1, 26.8, 27.3, 28.7, 28.79, 28.81, 30.3, 31.0, 31.4, 40.4, 40.5, 42.7, 50.5, 54.6, 57.4, 59.5, 79.8, 127.2, 128.8, 129.8, 129.9, 136.8, 137.0, 155.9, 170.7, 171.0, 171.3; HRMS–FAB (M + Na^+) calcd for $C_{37}H_{62}N_4NaO_6$ 681.4567, found 681.4550.

Amine 22. The Boc dipeptide **21** (180 mg, 0.27 mmol) was dissolved in 1 mL of CH_2Cl_2 before 1 mL of a solution containing 95% TFA, 2.5% TIS, and 2.5% ethanedithiol was added. After 30 min the solvent was removed under vacuum. The crude product was purified by flash chromatography (10:89:1 MeOH/CH_2Cl_2/concentrated aqueous NH_4OH) to afford amine **22** (0.11 g, 0.16 mmol, 59%): ^{1}H NMR (300 MHz, $CDCl_3$) δ 0.83–0.92 (m, 6H), 1.00–1.20 (m, 3H), 1.33–1.87 (m, 19H), 2.89–3.12 (m, 5H), 3.24–3.34 (m, 3H), 3.38 (m, 0.5H), 3.68 (dd, J = 8.3, 5.7 Hz, 1H), 3.94–4.18 (m, 1H), 5.15 (t, J = 7.7 Hz, 1H), 7.23–7.35 (m, 5H); ^{13}C NMR (75 MHz, $CDCl_3$) δ 10.67, 10.69, 13.9, 14.0, 24.1, 25.2, 25.5, 25.8, 25.9, 26.0, 26.1, 26.2, 26.4, 26.8, 27.4, 27.5, 29.1, 30.6, 31.0, 31.2, 31.5, 37.0, 38.4, 38.9, 39.58, 39.63, 42.5, 43.9, 51.3, 52.2, 55.5, 58.0, 116.0 (q, J = 293 Hz), 127.1, 127.22, 127.24, 128.6, 128.7, 128.8, 129.4, 129.5, 129.6, 136.8, 137.0, 162.1 (q, J = 34 Hz), 168.6, 168.7, 171.6, 171.9; HRMS–FAB (M + Na^+) calcd for $C_{27}H_{46}N_4NaO_2$ 481.3519, found 481.3523.

Enzyme Assays. The amidolytic activity of plasmin, thrombin, kallikrein, and trypsin was determined using chromogenic substrates D-Val-Leu-Lys-pNA, H-D-Phe-Pip-Arg-pNA, H-D-Pro-Phe-Arg-pNA, and H-D-Phe-Pip-Arg-pNA, respectively.[20] Enzymes and substrates were used as received from Sigma-Aldrich or Chromogenix (distributor: DiaPharma Group, Inc.) without further purification. Reaction progress was monitored on a Perkin-Elmer 8452A diode array UV–vis spectrometer. All enzymes were assayed at 25 °C in 50 mM sodium phosphate buffer (pH 7.4) with or without inhibitor. Due to solubility, inhibitors **2** and **3** were assayed in a solution with a final concentration of 10% DMSO. Initial rates were determined by monitoring the change in absorbance at 404 nm from 60 to 120 s after mixing. None of the inhibitors showed evidence of slow binding behavior. Inhibitor **2A** was subjected to full kinetic analysis against plasmin. For each inhibitor concentration examined (**2A**: 0, 8.6, 43, 86, 170, 260 μM) five substrate concentrations were used (75, 150, 300, 600, 1200 μM) with at least two independent determinations at each concentration. K_i values were determined by nonlinear fit to the Michaelis–Menten equation for competitive inhibition using simple weighing. Competitive inhibition was confirmed by Lineweaver–Burk analysis using simple statistical weighing to the linear fit of $1/v$ vs $1/[S]$. For the less potent compounds (**1, 2B, 3A, 3B**) a substrate concentration of 300 μM was monitored with six different inhibitor concentrations (**1**: 0, 110, 210, 430, 860, 1700 μM; **2B**: 0, 110, 230, 460, 690, 920 μM; **3A**: 0, 0.8, 1.6, 2.4, 3.1, 3.9 mM; **3B**: 0, 0.9, 1.8, 2.7, 3.6, 4.5 mM). For inhibitor **2A** assayed against thrombin (Thr), kallikrein (Kal), and trypsin (Try), a single substrate concentration (Thr: 50 μM; Kal: 100 μM; Try: 50 μM) was monitored with six different inhibitor concentrations (Thr: 0, 26, 53, 79, 110, 160 μM; Kal: 0, 48, 96, 144, 190, 240 μM; Try: 0, 26, 53, 79, 110, 160 μM). Competitive inhibition was assumed, and K_i values were calculated using a Dixon analysis. Data analysis was performed with the commercial graphing package Grafit (Erithacus Software Ltd.). K_m values for the substrates were determined both with and without 10% DMSO (without DMSO: plasmin 220 μM, Thr 10 μM, Kal 117 μM, Try 42 μM; with DMSO: plasmin 370 μM, Thr 22 μM, Kal 63 μM, Try 50 μM).

Acknowledgment. This research was supported by the NIH (Grant 1 R01 GM57327-01), the Petroleum Research Fund administered by the American Chemical Society (Grant 30544-G4), and the U.S. Army Medical Research and Materiel Command–Breast Cancer Research Initiative (Grant DAMD17-96-1-6161; Career Development Award to C.T.S.). T.C.S. was supported by a Predoctoral Fellowship from the U.S. Army Medical Research and Materiel Command–Breast Cancer Research Initiative (Grant DAMD17-96-1-6037).

References

(1) Cao, Y.; O'Reilly, M. S.; Marshall, B.; Flynn, E.; Ji, R.; Folkman, J. Expression of Angiostatin cDNA in Murine Fibrosarcoma Suppresses Primary Tumor Growth and Produces Long-Term Dormancy of Metastases. *J. Clin. Invest.* **1998**, *101*, 1055.

(2) Wu, Z.; O'Reilly, M. S.; Folkman, J.; Shing, Y. Suppression of Tumor Growth With Recombinant Murine Angiostatin. *Biochem. Biophys. Res. Commun.* **1997**, *236*, 651.

(3) Pepper, J. S.; Montesano, R.; Mandriots, S. J.; Orci, L.; Vassalli, J. Angiogenesis: A Paradigm for Balanced Extracellular Proteolysis During Cell Migration and Morphogenesis. *Enzyme Protein* **1996**, *49*, 138.

(4) Liotta, L. A. Cancer Cell Invasion and Metastasis. *Sci. Am.* **1992**, *February*, 54.

(5) Sherry, S. *Fibrinolysis, Thrombosis, and Hemostasis*; Lea & Febiger: Philadelphia, PA, 1992; Chapter 1.

(6) Okada, Y.; Tsuda, Y.; Teno, N.; Wanaka, K.; Bohgaki, M.; Hijikata-Okunomiya, A.; Naito, T.; Okamoto, S. Synthesis of Active Center-Directed Peptide Inhibitors of Plasmin. *Chem. Pharm. Bull.* **1988**, *36*, 1289.

(7) Ganu, V. S.; Shaw, E. Improved Synthetic Inactivators of Plasmin. *Thromb. Res.* **1987**, *45*, 1.

(8) For other active site-directed inhibitors of plasmin, see: Teno, N.; Wanaka, K.; Okada, Y.; Taguchi, H.; Okamoto, U.; Hijikata-Okunomiya, A.; Okamoto, S. Development of Active Center-Directed Plasmin and Plasma Kallikrein Inhibitors and Studies on the Structure-Inhibitory Activity Relationship. *Chem. Pharm. Bull.* **1993**, *41*, 1079. Wanaka, K.; Okamoto, S.; Horie, N.; Hijikata-Okunomiya, A.; Okamoto, U.; Naito, T.; Ohno, N.; Bohgaki, M.; Tsuda, Y.; Okada, Y. Use of an Active Center-

Directed Plasmin Inhibitor Elucidates the Multiplicity of Plasmin Actions. *Thromb. Res.* **1996**, *82*, 79. Tamura, S. Y.; Goldman, E. A.; Brunck, T. K.; Ripka, W. C.; Semple, J. E. Rational Design, Synthesis, and Serine Protease Inhibitory Activity of a Novel P_1-Argininal Derivative Featuring a Conformationally Constrained P_2–P_3 Bicyclic Lactam Moiety. *Bioorg. Med. Chem. Lett.* **1997**, *7*, 331; and refs 6 and 16.

(9) Conroy, J. L.; Sanders, T. C.; Seto, C. T. Using the Electrostatic Field Effect to Design a New Class of Inhibitors for Cysteine Proteases. *J. Am. Chem. Soc.* **1997**, *119*, 4285.

(10) Conroy, J. L.; Seto, C. T. Demonstration by ^{13}C NMR Studies that Tetrahydropyranone–Based Inhibitors Bind to Cysteine Proteases by Reversible Formation of a Hemithioketal Adduct. *J. Org. Chem.* **1998**, *63*, 2367.

(11) Brady, K.; Abeles, R. H. Inhibition of Chymotrypsin by Peptidyl Trifluoromethyl Ketones: Determinants of Slow-Binding Kinetics. *Biochemistry* **1990**, *29*, 7608.

(12) Smith, R. A.; Copp, L. J.; Donnelly, S. L.; Spencer, R. W.; Krantz, A. Inhibition of Cathepsin B by Peptidyl Aldehydes and Ketones: Slow-Binding Behavior of a Trifluoromethyl Ketone. *Biochemistry* **1988**, *27*, 6568.

(13) Otto, H.-H.; Schirmeister, T. Cysteine Proteases and Their Inhibitors. *Chem. Rev.* **1997**, *97*, 133.

(14) Simon, R. J.; Kania, R. S.; Zuchermann, R. N.; Huebner, V. D.; Jewell, D. A.; Banville, S.; Ng, S.; Wang, L.; Rosenberg, S. Peptoids: A Modular Approach to Drug Discovery. *Proc. Natl. Acad. Sci. U.S.A.* **1992**, *89*, 9367.

(15) Matsuzaki, T.; Sasaki, C.; Umeyama, H. A Predicted Tertiary Structure of a Thrombin Inhibitor-Trypsin Complex Explains the Mechanisms of the Selective Inhibition of Thrombin, Factor Xa, Plasmin, and Trypsin. *J. Biochem.* **1988**, *103*, 537.

(16) Teno, N.; Wanaka, K.; Okada, Y.; Tsuda, Y.; Okamoto, U.; Hijikata-Okunomiya, A.; Naito, T.; Okamoto, S. Development of Active Center-Directed Inhibitors Against Plasmin. *Chem. Pharm. Bull.* **1991**, *39*, 2340.

(17) Abdel-Magid, A. F.; Carson, K. G.; Harris, B. D.; Maryanoff, C. A.; Shah, R. D. Reductive Amination of Aldehydes and Ketones with Sodium Triacetoxyborohydride. Studies in Direct and Indirect Reductive Amination Procedures. *J. Org. Chem.* **1996**, *61*, 3849.

(18) Carpino, L. A.; Sadat-Aalace, D.; Chao, H. G.; DeSelms, R. H. ((9-Fluorenylmethyl)oxy)carbonyl (Fmoc) Amino Acid Fluorides. Convenient New Peptide Coupling Reagents Applicable to the Fmoc/*tert*-Butyl Strategy for Solution and Solid-Phase Synthesis. *J. Am. Chem. Soc.* **1990**, *112*, 9651.

(19) Kamphuis, I. G.; Kalk, K. H.; Swarte, M. B. A.; Drenth, J. Structure of Papain Refined at 1.65 Å Resolution. *J. Mol. Biol.* **1984**, *179*, 233.

(20) Hitomi, Y.; Ikari, N.; Fujii, S. Inhibitory Effect of a New Synthetic Protease Inhibitor (FUT-175) on the Coagulation System. *Haemostasis* **1985**, *15*, 164.

JM990110K

Combinatorial Library of Serine and Cysteine Protease Inhibitors That Interact with Both the S and S′ Binding Sites

Paul Abato, Jeffrey L. Conroy, and Christopher T. Seto*

Department of Chemistry, Brown University, 324 Brook Street, Box H, Providence, Rhode Island 02912

Received June 1, 1999

A combinatorial library of 400 inhibitors has been synthesized and screened against several serine and cysteine proteases including plasmin, cathepsin B, and papain. The inhibitors are based upon a cyclohexanone nucleus and are designed to probe binding interactions in the S2 and S2′ binding sites. This methodology has led to the discovery of inhibitor **15A**, which incorporates Trp at both the P2 and P2′ positions and has an inhibition constant against plasmin of 5 μM. Data from screening of the library shows that plasmin has a strong specificity for Trp at the S2 subsite and prefers to bind hydrophobic and aromatic amino acids such as Ile, Phe, Trp, and Tyr at the S2′ subsite. In contrast, the S2′ subsites of cathepsin B and papain do not show a strong preference for any particular amino acid.

Introduction

Combinatorial chemistry has emerged as a powerful method for generating lead compounds for drug discovery and for optimizing the biological activity of those leads.[1] This technique has been used to develop new ligands for a variety of biological targets including proteases, kinases, various receptors, and antibodies, among others. Proteases are particularly interesting targets because they are involved with a wide variety of important diseases that include AIDS, cancer, and malaria. Many of the libraries that have been generated for screening against proteases incorporate a chemical functionality that mimics the tetrahedral intermediate that occurs during enzyme-catalyzed peptide hydrolysis. For example, phosphonic acids have been screened against the metalloprotease thermolysin,[2] and statine,[3] (hydroxyethyl)amine,[4] and diamino diol[5] isosteres have been used to synthesize libraries against the aspartic protease HIV protease. In addition, a peptide aldehyde library has been targeted against the cysteine protease interleukin-1β converting enzyme.[6]

We have recently designed a new class of inhibitors for serine and cysteine proteases that are based upon a 4-heterocyclohexanone pharmacophore.[7,8] These inhibitors react with the enzyme active site nucleophile to generate a reversibly formed hemiketal or hemithioketal adduct that also mimics the tetrahedral intermediate.[9] One attractive feature of the 4-heterocyclohexanone-based inhibitors is that they can be derivatized in two directions, allowing them to make contacts with both the S and S′ subsites.[10–12] Thus, the 4-heterocyclohexanone pharmacophore, with its bidirectional nature, can easily be incorporated into a combinatorial synthesis of inhibitors. In this paper we describe the synthesis and screening of a 400-membered library of inhibitors that are based upon a cyclohexanone nucleus (Figure 1). The X_{aa} position in compound **1** is designed to fit into the S2 specificity pocket, the Y_{aa} position will fit into the S2′ site, and the carbonyl moiety of the cyclohexanone ring is designed to react with the active site nucleophile to give a reversibly formed covalent adduct.

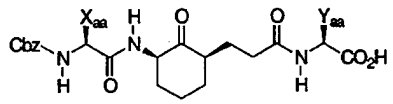

1

Figure 1. General structure of the compounds that are present in the 400-member combinatorial library of inhibitors. X_{aa} and Y_{aa} are each one of 20 different amino acids.

This work has three objectives. First, we demonstrate that the cyclohexanone nucleus can be a useful platform for developing protease inhibitors that interact with both the S and S′ binding sites using combinatorial chemistry. Second, the library is screened against several medicinally relevant serine and cysteine proteases in order to discover potential leads. Third, we explore the S2′ specificity of these proteases. For many of these enzymes the specificity of this site has not been well defined.

Results and Discussion

Design and Synthesis of the Library. Before we began constructing the library, we needed to devise an efficient synthesis of a building block such as compound **4** (Scheme 1). This molecule incorporates the cyclohexanone nucleus, is amenable to solid-phase peptide synthesis, and carries the ketone functionality in a suitably protected form. We have reported previously that compound **2** can be converted to **4** by oxidative cleavage of the double bond and replacement of the Boc protecting group with Fmoc.[10] However, we have found that on larger scale, reaction of the amino acid with Fmoc chloride or Fmoc *N*-hydroxysuccinimide ester under a variety of conditions gave relatively low and inconsistent yields of **4**. This problem can be circumvented by switching the protecting groups first and then oxidizing the alkene to the acid as shown in Scheme 1. Compound **4** is a mixture of two diastereomers, each of which has the substituents on the cyclohexanone ring in the 2,6-*cis* configuration.[10]

We have chosen the "split synthesis" strategy, first described by Furka,[13] for constructing the library and

10.1021/jm990272g CCC: $18.00
Published on Web 09/03/1999

Scheme 1[a]

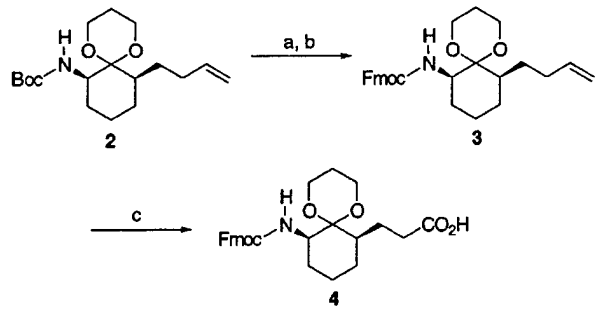

[a] Reagents: (a) TFA, CH_2Cl_2; (b) FmocCl, DIEA; (c) $NaIO_4$, $KMnO_4$, $NaHCO_3$. One of two enantiomers is shown.

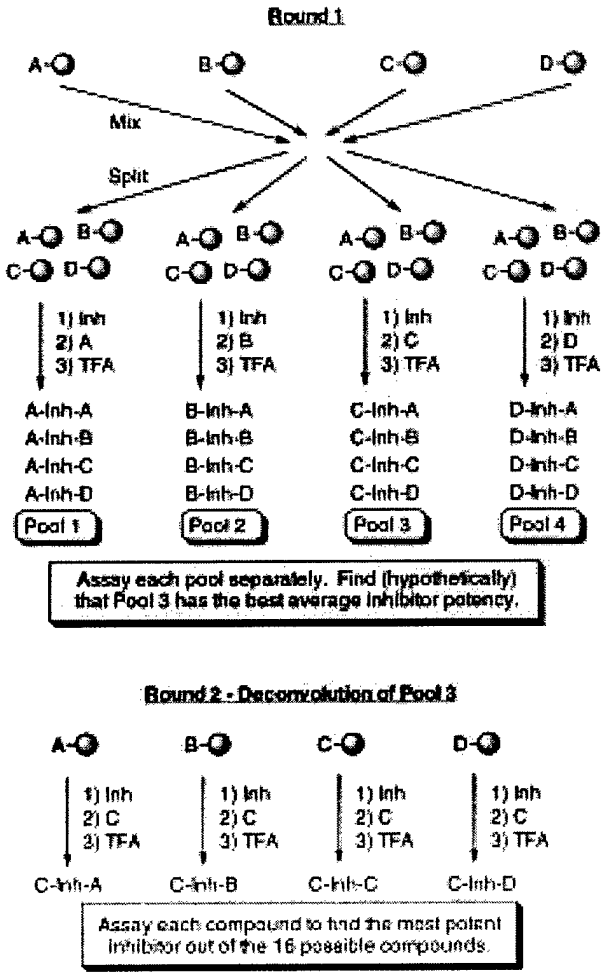

Figure 2. Schematic diagram of the deconvolution strategy used in the synthesis and screening of the combinatorial library of protease inhibitors. **A**–**D** correspond to four different amino acids. In the actual library 20 amino acids were used, but the figure has been limited to 4 amino acids for the sake of clarity. Inh represents the cyclohexanone pharmacophore, and TFA is F_3CCO_2H.

the iterative deconvolution strategy, developed by Houghten, for assaying its biological activity.[14] These techniques, as applied to the cyclohexanone-based inhibitor library, are outlined in Figure 2. Synthesis of the library began with 20 batches of peptide synthesis resin, each with a different amino acid attached. The resin was mixed and then split into 20 pools that contained a mixture of all 20 amino acids. The inhibitor

Scheme 2[a]

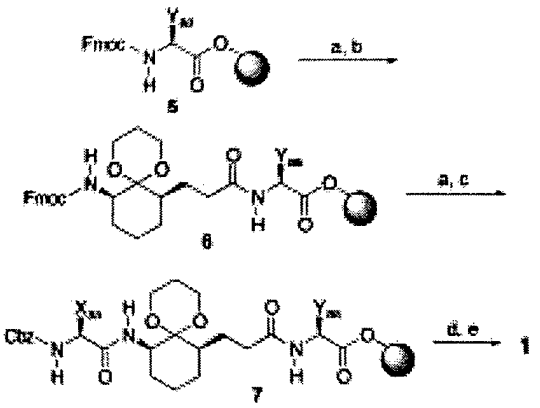

[a] Reagents: (a) piperidine, DMF; (b) **4**, HBTU, DIEA; (c) Cbz-X_{aa}-OH, HBTU, DIEA; (d) TFA; (e) TFA, H_2O. One of two diastereomers is shown.

core was attached to all of the pools, followed by a second amino acid, each pool receiving a different amino acid. Finally, the inhibitors were cleaved from the beads, and the protecting groups were removed. This resulted in 20 pools of inhibitors, each containing 20 different compounds. The inhibitors in an individual pool all have the same amino acid on their N-terminus, but a mixture of the 20 different amino acids on the C-terminus. The pools were assayed for inhibitory activity, and one or several of the pools which showed the highest activity were for chosen for deconvolution.

The second round of synthesis again began with 20 pools of resin, each with a different amino acid attached. These were coupled to the inhibitor core; then every compound was coupled to the N-terminal amino acid that corresponded to the pool from the first round of synthesis that was chosen for deconvolution. After cleavage from the solid support and removal of the protecting groups, these pools were assayed to determine which amino acid was optimal for the C-terminal side of the inhibitor. Although the iterative deconvolution strategy does not always result in identification of the best inhibitor in the library,[1e] it is a straightforward and reliable method for determining the structure of molecules that have high activity compared to the other members of the library.

The details of the solid-phase synthesis are shown in Scheme 2. Resin was purchased preloaded with the Fmoc-protected amino acids. The N-terminus was deprotected with piperidine and then coupled to inhibitor core **4** using HBTU to give **6**. Piperidine deprotection followed by coupling to an N-Cbz amino acid gave compound **7**. The side chains of the amino acids were then deprotected using TFA, which also released the inhibitors from the solid support. Finally, the ketal protecting group was removed by adding H_2O to the cleavage cocktail from the previous reaction and allowing the solution to stand at room temperature overnight. Using this same chemistry, we have reported previously the solid-phase synthesis of an N-acetylated inhibitor that contained Orn and Pro at the X_{aa} and Y_{aa} positions, respectively.[10] This inhibitor was fully characterized, and the overall yield of the isolated and HPLC-purified compound was 50%.

Eighteen of the 20 common amino acids were incorporated into the library. Cysteine and methionine were

omitted to avoid problems associated with sulfur oxidation, and they were replaced with hydroxyproline (Hyp) and ornithine (Orn).

Assay of the Library. The initial library of inhibitors was assayed against five proteases: cathepsin B, plasmin, urokinase, kallikrein, and papain. The first four of these enzymes have all been implicated in the progression of cancer.[15] These enzymes promote the processes of angiogenesis and metastasis, either directly by degrading components of the basement membrane which surround blood vessels or indirectly by activating other proteases which in turn attack the basement membrane.[16] Compounds which inhibit these proteases may have potential as anticancer chemotherapeutic agents.[17] Papain was chosen as a control protease since it is well-established that this enzyme prefers aromatic amino acids such as phenylalanine at the P2 position.[18] Thus we expected that in the screening of the initial library against papain, the pools which incorporated aromatic amino acids at the X_{aa} position would show good activity against this protease.

Figure 3 shows the results of the solution-phase assays of the library against plasmin, cathepsin B, and papain. The assays were performed using *p*-nitroanilide substrates and were monitored by UV spectroscopy. A single concentration of the inhibitors was used, and the runs were performed in duplicate or triplicate. The concentration of each individual inhibitor in these assays was 50 μM, giving a total inhibitor concentration for all 20 inhibitors in each pool of 1 mM. The inhibitors in several of the pools were not soluble at this concentration, so the assays were performed in more dilute solution as noted in the captions to Figures 3, 5, and 6.

For papain the three best pools of inhibitors incorporate Phe, Trp, and Tyr at the X_{aa} position as expected, based upon the known specificity of the S2 subsite of this protease.[18] We infer from these results that for papain, the inhibitors are binding in the active site in the anticipated manner with X_{aa} in the S2 subsite.

Cathepsin B displays relatively small differences in activity between the various pools, with most showing between 10% and 30% inhibition. Ile and Leu are the only pools that show significantly better activity. These data are consistent with information from previous inhibition studies, which suggest that cathepsin B prefers hydrophobic amino acids such as Leu, Ile, and Phe at the P2 position.[16]

Unlike papain and cathepsin B, plasmin shows very high selectivity for one particular pool within the library. This pool contains Trp at the X_{aa} position. Thus plasmin prefers the extended aromatic side chain of Trp at the P2 position to the exclusion of all other amino acids, including those with smaller aromatic groups such as Phe and Tyr and those with simple hydrophobic side chains such as Ile and Leu. The X-ray crystal structure of the active site portion of plasmin has not been reported. However it will be interesting to see, once the structure has been solved, if this selectivity is caused by specific aromatic stacking interactions between the inhibitor and aromatic side chains in the S2 subsite. Alternately, S2 could comprise a simple hydrophobic pocket that has good shape complementarity to extended aromatic rings, or there may be a specific

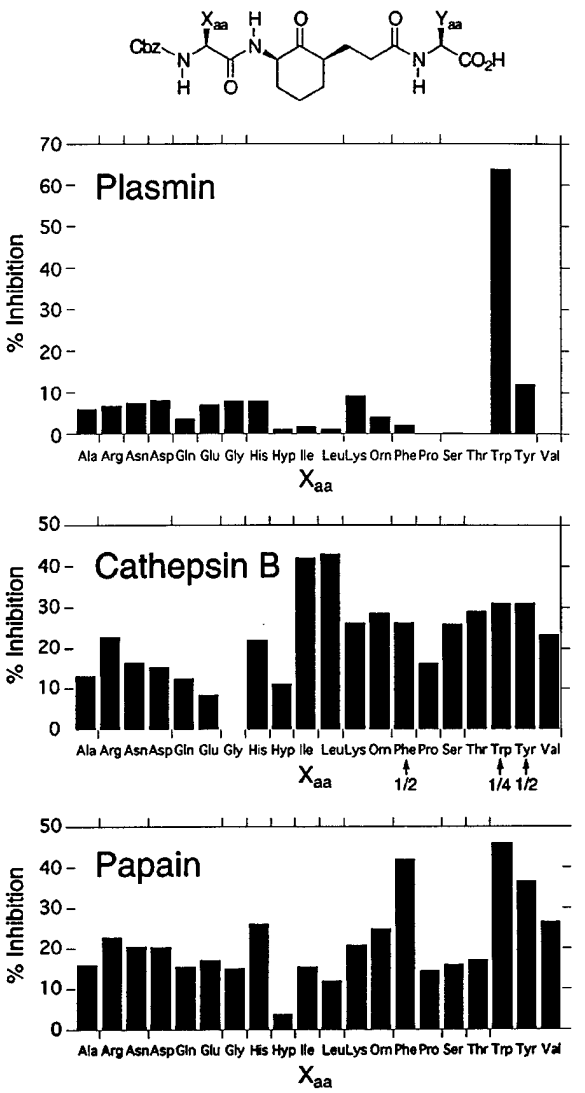

Figure 3. Assay of 20 pools of 20 compounds each against plasmin, cathepsin B, and papain. Each pool contains compounds in which the X_{aa} position is defined by the amino acids on the *x*-axes of the graphs, and Y_{aa} is a mixture of all 20 amino acids. The error in these measurements is approximately ±5%. For cathepsin B the pools in which X_{aa} = Phe and Tyr were assayed at 1/2 concentration and for X_{aa} = Trp at 1/4 concentration, compared to the other pools in the library due to low solubility of the inhibitors in the assay solution.

hydrogen-bonding interaction that occurs with the N-H functionality of Trp.

We have also assayed the inhibitor library against urokinase and kallikrein. With these two proteases only low levels of inhibition were observed, and the variations between the pools were similar to the approximate ±5% error in the assays (data not shown). There are several possible explanations for this lack of inhibition. First, the structure or conformation of the inhibitors in the library may not be sterically compatible with the active sites of kallikrein and urokinase. Second, the inhibitors may bind to the enzyme through weak noncovalent interactions but not react with the active site nucleophile to give the reversibly formed covalent adduct. In the 4-heterocyclohexanone series of inhibitors, such compounds have inhibition constants in the millimolar range against papain. Thus inhibitors of this type are

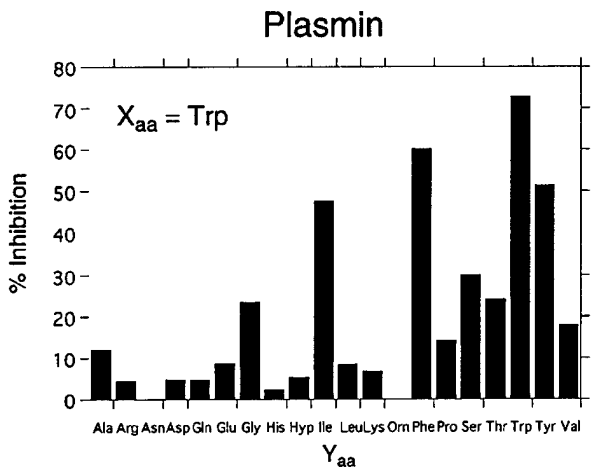

Figure 4. Assay of the Trp deconvolution against plasmin. Each bar represents the assay of one compound which has Trp at the X_{aa} position and an amino acid at the Y_{aa} position that is indicated by the *x*-axis of the graph.

not likely to give significant activity under our assay conditions.[7,9]

On the basis of the results of the initial assays, we chose several pools for deconvolution. For plasmin, only the Trp pool was worth exploring further. For cathepsin B, we chose to deconvolute the Ile pool and the three pools that had aromatic amino acids at the X_{aa} position, Phe, Trp, and Tyr. The later three pools had activities comparable to that of several other pools in the library, but they were assayed at lower concentrations and thus should contain better inhibitors on average when compared to the other pools. For papain, the Phe and Trp pools showed the best activity and were thus chosen for deconvolution.

The results from the assays of the deconvolutions are shown in Figures 4–6. Plasmin (Figure 4) clearly prefers hydrophobic amino acids at the Y_{aa} position of these inhibitors, with Ile, Phe, Trp, and Tyr showing significantly higher activities than the other compounds in the deconvolution. Of the three enzymes, plasmin again shows the largest variation in activity among the 20 pools of the library.

Cathepsin B displays limited variations in activity among the four different deconvolutions, as shown in Figure 5. In general, we observe that this protease has a small preference for amino acids such as Arg, Gln, His, Ile, Leu, Phe, and Trp at the Y_{aa} position of the inhibitors. In addition, the inhibitors with Gly, Hyp, and Ser at this position all have low activity.

One of the assumptions that we make in using the iterative deconvolution strategy is that binding interactions at one part of the inhibitor do not significantly perturb binding at another part. If this assumption were strictly true, then binding of the inhibitors to the S2 and S2′ subsites should be completely decoupled from one other, with the result that all four of the deconvolutions in Figure 5 would have identical binding profiles and differ only in magnitude. For cathepsin B, this does not appear to be the case. However, on the basis of the combined data from the four deconvolutions, we conclude that this protease has a limited preference for hydrophobic amino acids at the S2′ subsite. When a binding site has low specificity as we observed for the

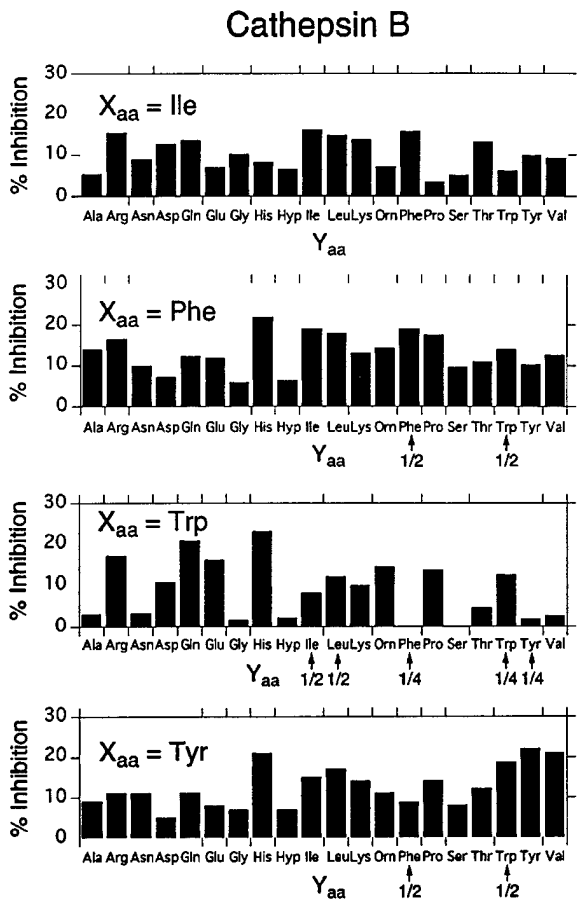

Figure 5. Assay of the Ile, Tyr, and Phe deconvolutions against cathepsin B. Several of the assays were performed at 1/2 or 1/4 concentration as noted on the *x*-axes.

S2′ site of cathepsin B, the specificity of the site only becomes visible by comparing the results of multiple deconvolutions and is not easily apparent from a single deconvolution.

For papain, hydrophobic amino acids including Ile, Leu, Phe, Trp, and Tyr are preferred at the Y_{aa} position of the inhibitors. In addition, when X_{aa} = Trp, residues such as Glu, Pro, and Val at the Y_{aa} position have good activity. For this protease, comparison of the deconvolutions shown in Figure 6 indicates that the specificity patterns at the Y_{aa} positions for the two sets of inhibitors have some similarity. This similarity suggests that binding interactions at the P2′ position are not significantly perturbed by differences that may occur when Phe or Trp is present at P2.

Resynthesis and Evaluation of Inhibitors 15–18. After evaluating all of the data from the assays of the combinatorial library, we have chosen to resynthesize four of the inhibitors (**15–18**, Scheme 3) using solution-phase methods and to examine the biological activity of these compounds in greater detail. The four inhibitors were selected based upon a combination of their activity against the individual proteases and the presence of overlapping activity among the three enzymes. The solution-phase synthesis of inhibitors **15–18**, shown in Scheme 3, follows closely the solid-phase synthesis that was used to construct the library. The only significant differences in the solution-phase chemistry were that Boc protecting groups were used for

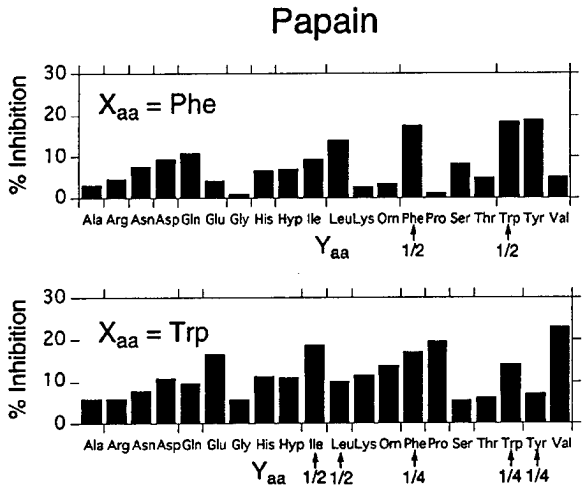

Figure 6. Assay of the Phe and Trp deconvolutions against papain. Several of the assays were performed at 1/2 or 1/4 concentration as noted on the *x*-axes.

Scheme 3[a]

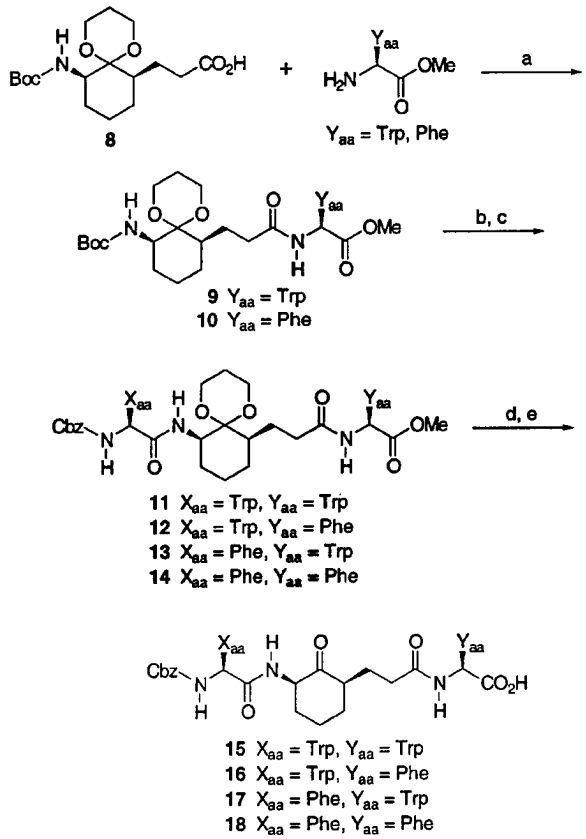

[a] Reagents: (a) HBTU, DIEA; (b) TFA; (c) Cbz-X_{aa}-OH where X_{aa} = Trp and Phe, HBTU, DIEA; (d) LiOH; (e) TFA, H_2O. One of two diastereomers is shown.

amines and the C-termini of the inhibitors were protected as methyl esters. The esters were removed using basic hydrolysis near the end of the synthesis.

Compounds **15–18** were assayed against plasmin, cathepsin B, and papain, and the resulting inhibition data are shown in Table 1. Compound **18** has low activity against cathepsin B, with a K_i value of 1.1 mM. This result is expected based upon the low activity of the compound during the library screening (Figure 5).

Table 1. Inhibition of Proteases by Inhibitors **15–18**

			K_i (μM)		
compd[a]	X_{aa}	Y_{aa}	plasmin	papain	cathepsin B
15A	Trp	Trp	5 ± 0.6	380[b] ± 60	
15B			10 ± 2		
16A	Trp	Phe	100 ± 20	250[b] ± 80	
16B			150 ± 25		
17[b]	Phe	Trp	420 ± 40	490 ± 70	
18[b]	Phe	Phe	3000 ± 1000	870 ± 90	1100 ± 200

[a] **A** and **B** represent two different diastereomers. [b] Assayed as a mixture of two diastereomers.

Compounds **15–18** all have moderate activity against papain with inhibition constants that range from 250 to 870 μM. These values are also consistent with the assays of the library against papain (Figure 6).

Compounds **17** and **18**, both of which have Phe at the X_{aa} position, are expected to be weak inhibitors of plasmin as indicated by the low activity of the X_{aa} = Phe pool against this protease (Figure 3). Analysis of the inhibitors that have been resynthesized by solution-phase methods gives inhibition constants of 420 and 3000 μM, respectively, for these two compounds. In contrast inhibitors **15** and **16**, which have Trp at the X_{aa} position, should have good activity against plasmin as indicated by the data in Figure 4. We have used HPLC to separate the two diastereomers of each of these compounds, although we have not determined their absolute configurations. Compounds **16A,B** have K_i values of 100 and 150 μM, while compounds **15A,B** have values of 5 and 10 μM, respectively. These results demonstrate that we have been able to generate an inhibitor with good activity against plasmin, such as **15A**, by synthesizing a combinatorial library of inhibitors around a cyclohexanone nucleus that take advantage of binding interactions in both the S2 and S2′ subsites.

We have recently reported the synthesis and evaluation of a "rationally designed" inhibitor of plasmin that is based upon a tetrahydrothiopyranone ring system.[19] This inhibitor incorporates an aminoalkyl side chain at the P1 position that is designed to interact with an aspartic acid residue at the base of the S1 subsite. Plasmin is specific for substrates that have a positively charged amino acid at the P1 position, and interactions with the S1 subsite are critical for recognition and binding of both substrates and inhibitors.[20] In the tetrahydrothiopyranone-based inhibitors, we have found that if the aminoalkyl side chain at the P1 position is removed, there is a 200–300-fold decrease in potency.[19] In light of these observations, it is interesting to note that compound **15A** has significant affinity for plasmin with an inhibition constant of 5 μM, although it does not incorporate a positively charged P1-like side chain.

Using the combinatorial library described in this paper, we have discovered **15A** as a potential lead compound for developing high-affinity inhibitors of plasmin. Two modifications to the structure of **15A** are likely to increase its potency. First, we can incorporate an aminoalkyl side chain that is positioned to bind in the S1 subsite. The amide nitrogen at the 2-position of the cyclohexanone ring should be an appropriate place to attach such functionality.[19] Second, we can substitute the methylene group at the 4-position of the cyclohexanone ring with an electronegative functionality such

as S, O, or SO_2. This electronegative functionality will increase the electrophilicity of the ketone by inducing an unfavorable through-space electrostatic repulsion between the electronegative group and the dipole of the ketone.[7] We have demonstrated previously that there is a good correlation between ketone electrophilicity and inhibition constants in 4-heterocyclohexanone-based inhibitors.[7]

Conclusions

In this paper we have described the construction and screening of a combinatorial library of protease inhibitors that extend into both the S and S′ specificity sites. Using this method we have found an inhibitor that has significant affinity for the serine protease plasmin. In addition, this work has shown that combinatorial chemistry is an efficient method for probing the specificity of the S2′ subsite. Currently there is little information available concerning the binding specificity of this position for many proteases.

Our data have shown that for plasmin, the S2′ subsite prefers to bind hydrophobic and especially aromatic amino acids. Furthermore, binding of such hydrophobic residues in this site significantly increases the affinity of the inhibitor for the enzyme. On the other hand, the S2′ subsites of cathepsin B and papain do not appear to have strong preferences for any particular amino acid, and binding in this position leads to only incremental increases in affinity. Concerning the S2 subsites, the data that we have presented are consistent with the known specificity of cathepsin B and papain, which prefer hydrophobic amino acids at this position.[18] For plasmin, it has been believed that Phe binds well in the S2 subsite. However our results show that Trp, with its larger aromatic surface and potential for hydrogen bonding, provides up to an 80-fold increase in affinity when compared to Phe. Clearly, combinatorial chemistry has provided useful information concerning the binding interactions at the S2 and S2′ subsites of several proteases. A similar approach should be equally amenable to exploring the specificities of the other leaving group subsites and for incorporating nonpeptidic functionality into the inhibitors.

Experimental Section

General Methods. NMR spectra were recorded on Bruker Avance-300 or Avance-400 instruments. Spectra were calibrated using TMS (δ = 0.00 ppm) for ^{1}H NMR. Mass spectra were recorded on a Kratos MS 80 under fast-atom bombardment (FAB) conditions or were performed using electrospray ionization at the Harvard University Chemistry Department Mass Spectrometry Facility. HPLC analyses were performed on a Rainin HPLC system with Rainin Microsorb silica or C18 columns and UV detection. Semipreparative HPLC was performed on the same system using semipreparative columns (21.4 × 250 mm). UV spectra were recorded on a Perkin-Elmer 8452A diode array UV−vis spectrophotometer.

Reactions were conducted under an atmosphere of dry nitrogen in oven-dried glassware. Anhydrous procedures were conducted using standard syringe and cannula transfer techniques. THF and toluene were distilled from sodium and benzophenone. Piperidine was distilled from KOH. Other solvents were of reagent grade and were stored over 4 Å molecular sieves. All other reagents were used as received. Organic solutions were dried over $MgSO_4$ unless otherwise noted. Solvent removal was performed by rotary evaporation at water aspirator pressure. Wang resins that were prederivatized with Fmoc amino acids were purchased from Calbiochem-Novabiochem Corp. Amino acids and their side chain protecting groups were used as follows: Ala, Arg(PMC), Asn(Trt), Asp(*t*-Bu), Gln(Trt), Glu(*t*-Bu), Gly, His(Trt), Hyp(*t*-Bu), Ile, Leu, Lys(Boc), Orn(Boc), Phe, Pro, Ser(*t*-Bu), Thr(*t*-Bu), Trp(Boc), Tyr(*t*-Bu), and Val.

Synthesis of the Library. Dry Wang resin that was prederivatized with the 20 Fmoc amino acids (0.2 mmol each) was combined in a flask and shaken with 125 mL of methylene chloride. The solvent was removed; the beads were dried under vacuum and then split into 20 even batches. The beads were placed into 20 1- × 10-cm Econo-Columns (Biorad) which served as synthesis vessels. The columns were fitted with Teflon stopcocks and connected to a 24-port vacuum manifold (Burdick and Jackson) that was used to drain solvents and reagents from the columns. The resin in each column was swelled in DMF; then the Fmoc protecting groups were removed by treatment with 2 mL of a 1:1 solution of DMF and piperidine for 10 min. After washing with 5 × 5 mL of DMF, a positive Kaiser test indicated the presence of free amines on the resin.

Coupling of Compound 4. To couple compound **4** to the resin, a stock solution was prepared that contained compound **4** (5.6 g, 12 mmol, 3 equiv), HBTU (4.54 g, 12 mmol, 3 equiv), diisopropylethylamine (DIEA; 2.76 mL, 16 mmol, 4 equiv), and DMF solvent in a total volume of 40 mL. Aliquots (2 mL) of this stock solution were added to each of the synthesis vessels and the reactions were gently agitated for 1.5 h. A negative Kaiser test indicated that the reaction had gone to completion. The resin was washed with 5 × 5 mL of DMF; then any unreacted amino groups were capped by treating the resin for 10 min with 2 mL of a freshly prepared stock solution that contained acetic anhydride (1.5 mL, 20 mmol, 5 equiv), DIEA (2.76 mL, 16 mmol, 4 equiv), and DMF in a total volume of 40 mL. After capping, the resin was then washed with 5 × 5 mL of DMF, and the N-terminal Fmoc group was deprotected as described above.

Coupling of the Second Amino Acid. To couple the second amino acid to the resin, the 20 synthesis vessels were treated with 3 equiv of an N-Cbz amino acid, each vessel receiving a different amino acid. The reactions also contained 3 equiv of HBTU and 4 equiv of DIEA in 2 mL of DMF and were agitated for 1.5 h. After the reactions were complete as judged by a negative Kaiser test, the resin was washed with 5 × 5 mL of DMF, 5 × 10 mL of methylene chloride, and 5 × 10 mL of MeOH, and dried under vacuum overnight.

Cleavage from the Resin and Removal of Protecting Groups. The inhibitors were cleaved from the resin and the protecting groups on the amino acid side chains were removed by treating each batch of resin with 3 mL of cleavage cocktail for 2 h. The cleavage cocktail contained 95% TFA, 2.5% water, and 2.5% triisopropylsilane. The solutions were filtered to remove the resin, and the beads were washed with 3 × 1 mL of fresh TFA. The ketal protecting groups on the cyclohexanone rings were removed by adding 3 mL of water to the TFA solutions from the previous reactions and agitating the solutions for 30 h at room temperature. After the initial addition of water to the TFA solutions, the reactions became cloudy. However, after several hours at room temperature, the reactions became homogeneous. After the reactions were complete, the TFA and water were removed and the residual material was dried at 0.02 mmHg for 48 h. The 20 batches of inhibitors were each dissolved in 1 mL of DMSO, filtered, and stored in a freezer at −48 °C. If a total yield of 50% is assumed for the synthesis, then each inhibitor stock solution contained 20 different compounds, with a concentration of 5 mM for each individual compound in the mixtures.

Deconvolution Syntheses. The solid-phase syntheses of the various deconvolutions were performed using a similar procedure as described above. The only changes that were made were that the mix and split step at the beginning was omitted and the syntheses were performed on a 0.04-mmol scale per inhibitor.

Papain Assays. Papain (EC 3.4.22.2; purchased from Sigma) was assayed using L-BAPNA as the substrate, and the reaction progress was monitored by UV spectroscopy.[11a] Initial rates were determined by monitoring the formation of *p*-nitroaniline at 412 nm from 30 to 120 s after mixing. Assay solutions contained 1.5 mM substrate, 5 mM EDTA, 5 mM cysteine, 50 mM sodium phosphate at pH 7.5, and 15% DMSO. Assays of the initial library, which constituted 20 pools of inhibitors with 20 compounds per pool, also contained a total inhibitor concentration of 1 mM (50 μM of each individual inhibitor) and were performed in triplicate. Assays of the deconvolutions contained an inhibitor concentration of 200 μM. Assays of compounds **15**–**18** contained 1.7 mM substrate and inhibitor concentrations that ranged from 2 to 500 μM. K_i values were calculated using a Dixon analysis. Data analysis was performed with the commercial graphing package Grafit (Erithacus Software Ltd.). The K_m value under these conditions was measure to be 6.8 mM. In the absence of DMSO, the K_m value has been reported as 3.2 mM in 100 mM phosphate buffer at pH 7.5.[21]

Cathepsin B Assays. Cathepsin B (EC 3.4.22.1; purchased from Sigma) was assayed using L-BAPNA as the substrate.[22] Assay solutions contained 1.5 mM substrate, 1.5 mM EDTA, 3 mM DTT, 50 mM sodium phosphate buffer at pH 7.4, and 15% DMSO. Assays of compounds **15**–**18** contained 0.7 mM substrate. All other conditions were the same as indicated for the assays of papain. The K_m value under these conditions was measure to be 3.3 mM. The K_m value in the absence of DMSO and in sodium acetate buffer at pH 5.1 is reported to be 1.3 mM.[22]

Plasmin Assays. Plasmin (EC 3.4.21.7; purchased from Sigma) was assayed using D-Val-Leu-Lys-*p*-nitroanilide as substrate.[23] Assay solutions contained 250 μM substrate, 50 mM sodium phosphate buffer at pH 7.4, and 10% DMSO. Assays of compounds **15**–**18** contained 180 μM substrate. All other conditions were the same as indicated for the assays of papain. The K_m value under these conditions was measure to be 180 μM. The K_m value in the absence of DMSO and in Tris-HCl buffer at pH 8.3 is reported to be 270 μM.[24]

Fmoc Alkene 3. To a solution of **2**[10] (9.9 g, 30.5 mmol) in CH_2Cl_2 (75 mL) was added TFA (25 mL) at 0 °C. The solution was warmed to room temperature, stirred for 1 h, and concentrated to remove the TFA. The resulting oil was redissolved in 20 mL of CH_2Cl_2 and washed with saturated Na_2CO_3 and brine (200 mL). The solution was dried over Na_2CO_3 and filtered, and then DIEA (6 mL) and FmocCl (7.89 g, 30.5 mmol) were added. This solution was stirred for 3 h, then washed with 1 N HCl, saturated Na_2CO_3, and brine, and dried. The solution was then reduced to approximately 20 mL, diluted with hexanes (200 mL), and placed in a refrigerator overnight to allow crystallization. White crystals of **3** (9.22 g, 67%) were isolated by vacuum filtration and dried in vacuo: ^{1}H NMR (400 MHz, $CDCl_3$) δ 1.26–1.30 (m, 1H), 1.42–1.62 (br m, 7H), 1.62–1.90 (br m, 3H), 1.93–2.02 (m, 1H), 2.14–2.23 (m, 1H), 3.85–3.90 (m, 4H), 4.25–4.44 (m, 3H), 4.97–5.07 (m, 2H), 5.15 (br s, 1H), 5.78–5.88 (m, 1H), 7.31 (t, J = 7.4 Hz, 2H), 7.39 (t, J = 7.4 Hz, 2H), 7.62 (t, J = 6.8 Hz, 2H), 7.76 (d, J = 7.5 Hz, 2H); ^{13}C NMR (100 MHz, $CDCl_3$) δ 14.1, 18.8, 22.6, 25.1, 28.8, 31.6, 31.8, 47.3, 58.8, 59.0, 66.5, 99.1, 114.8, 119.9, 125.1, 127.0, 127.6, 138.7, 141.3, 156.4; HRMS-FAB (M + Na^+) calcd for $C_{28}H_{33}NNaO_4$ 470.2307, found 470.2322.

Fmoc Carboxylic Acid 4. To compound **3** (0.46 g, 1.1 mmol) were added 25 mL of 7:3 acetone/H_2O, $NaIO_4$ (1.1 g, 5.2 mmol), $KMnO_4$ (32 mg, 0.20 mmol), and $NaHCO_3$ (0.10 g, 1.0 mmol) and the reaction was stirred at room temperature for 7 h. The reaction was diluted with EtOAc (150 mL) and washed with 100 mL of 1 N HCl and 100 mL of brine, and the organic layer was dried over $MgSO_4$. The crude material was purified by flash chromatography (3:2 EtOAc/hexanes) to yield compound **4** (308 mg, 0.66 mmol, 63%): ^{1}H NMR (300 MHz, $CDCl_3$) δ 1.43–1.71 (m, 10H), 2.07–2.12 (m, 3H), 2.35–2.53 (m, 2H), 3.91 (br s, 4H), 4.14–4.30 (m, 2H), 4.37–4.48 (m, 2H), 5.17 (br s, 1H), 7.31 (t, J = 7.4 Hz, 2H), 7.41 (t, J = 7.4 Hz, 2H), 7.62 (m, 2H), 7.78 (d, J = 7.5 Hz, 2H); ^{13}C NMR (100 MHz, $CDCl_3$) δ 18.8, 22.0, 25.0, 28.4, 32.1, 47.3, 59.0, 66.7, 98.8, 119.9, 125.1, 127.0 127.6, 141.3, 144.0, 156.5, 179.0; HRMS-FAB (M + Na^+) calcd for $C_{27}H_{31}NNaO_6$ 488.2049, found 488.2041.

Tryptophan Methyl Ester 9. To carboxylic acid **8** (250 mg, 0.73 mmol) were added H-Trp-OMe (250 mg, 0.87 mmol), HBTU (398 mg, 0.88 mmol), and 2 mL of DMF, followed by DIEA (0.40 mL, 1.75 mmol). The reaction was stirred for 3 h at room temperature, then diluted with 50 mL of EtOAc. The organic layer was washed with 35 mL of 1 N $KHSO_4$, 35 mL of saturated $NaHCO_3$, and 35 mL of brine and dried over $MgSO_4$. The resulting solution was concentrated by rotary evaporation, and the residual material was purified by flash chromatography (EtOAc) to yield methyl ester **9** (400 mg, 0.68 mmol, 74%): ^{1}H NMR (300 MHz, MeOH-d_4) δ 1.30–1.75 (m, 19H), 1.76–2.00 (m, 1H), 2.05–2.10 (m, 2H), 2.15–2.40 (m, 2H), 3.12–3.21 (m, 1H), 3.62–3.70 (m, 3H), 3.72–3.95 (m, 4H), 4.72–4.79 (m, 1H), 6.89–7.21 (m, 3H), 7.35 (d, J = 8.0 Hz, 1H), 7.53–7.56 (d, J = 7.5 Hz, 1H); ^{13}C NMR (75 MHz, MeOH-d_4) δ 18.9, 25.2, 27.4, 29.7, 33.8, 51.7, 53.7, 58.9, 79.1, 99.2, 109.8, 111.4, 118.1, 118.8, 121.4, 123.5, 127.6, 137.1, 157.2, 173.2, 175.2, 209.2; HRMS-ESI (M + Na^+) calcd for $C_{29}H_{41}N_3NaO_7$ 566.2840, found 566.2858.

Phenylalanine Methyl Ester 10. To carboxylic acid **8** (500 mg, 1.46 mmol) were added H-Phe-OMe (312 mg, 1.75 mmol), HBTU (796 mg, 1.75 mmol), and 4 mL of DMF, followed by DIEA (0.8 mL, 3.5 mmol). The procedure was identical to that used for the preparation of compound **9**. The crude material was purified by flash chromatography (2:3 hexanes/EtOAc) to yield compound **10** (1.10 g, 2.14 mmol, 74%): ^{1}H NMR (300 MHz, DMSO-d_6) δ 1.20–2.83 (m, 19H), 1.77–2.00 (m, 2H), 2.01–2.34 (m, 2H), 2.93–3.02 (m, 1H), 3.22–3.14 (m, 1H), 3.55–3.71 (m, 3H), 3.74–3.86 (m, 4H), 4.66–4.74 (m, 1H), 7.22–7.33 (m, 5H); ^{13}C NMR (75 MHz, MeOH-d_4) δ 19.0, 25.3, 27.8, 28.7, 33.8, 37.4, 51.8, 54.2, 59.0, 17.2, 99.2, 126.9, 128.5, 129.2, 137.2, 157.1, 172.7, 175.3; HRMS-ESI (M + Na^+) calcd for $C_{41}H_{48}N_4NaO_8$ 527.2732, found 527.2751.

Trp-X-Trp Ester 11. To compound **9** (370 mg, 0.68 mmol) was added a solution of CH_2Cl_2 (11.5 mL), TFA (4.5 mL), and triisopropylsilane (0.38 mL). The reaction was stirred at room temperature for 1 h; then the solvents were removed under vacuum. The crude amine was dissolved in 2 mL of DMF, and DIEA (~0.5 mL) was added to neutralize the residual TFA and to raise the pH to 8 (as measured with moist pH paper). Cbz-Trp-OH (276 mg, 0.816 mmol), HBTU (309 mg, 0.816 mmol), and DIEA (0.28 mL, 1.6 mmol) were added to the flask and the reaction was allowed to stir for 2 h at room temperature. The workup was identical to the procedure used in the preparation of compound **9**. The crude material was purified by flash chromatography (1:5 hexanes/EtOAc) to yield **11** (0.40 g, 0.52 mmol, 76%): ^{1}H NMR (300 MHz, MeOH-d_4) δ 0.94 (t, J = 6.9 Hz, 1H), 1.12–1.65 (m, 10H), 1.75–1.90 (m, 2H), 2.10–2.14 (m, 1H), 2.20–2.29 (m, 1H), 3.11–3.20 (m, 3H), 3.28–3.30 (m, 1H), 3.50–3.70 (m, 6H), 4.50–4.58 (m, 1H), 4.75–4.85 (m, 1H), 4.98–5.08 (m, 2H), 7.01–7.35 (m, 13H), 7.51–7.61 (m, 2H); ^{13}C NMR (75 MHz, MeOH-d_4) δ 13.5, 18.3, 18.7, 19.9, 24.9, 25.2, 27.4, 28.3, 29.1, 33.7, 51.9, 53.7, 56.4, 58.9, 60.5, 66.6, 99.8, 109.8, 111.0, 118.1, 118.4, 118.8, 121.4, 121.5, 127.7, 128.5, 137.2, 157.1, 172.9, 173.2, 173.5, 175.2; HRMS-FAB (M + H^+) calcd for $C_{43}H_{50}N_5O_8$ 764.3659, found 764.3647.

Trp-X-Phe Ester 12. Compound **10** (387 mg, 0.54 mmol) was deprotected and coupled to Cbz-Trp-OH using a procedure that was similar to that used for the preparation of compound **11**. The crude material was purified by flash chromatography (1:5 hexanes/EtOAc) to give compound **12** (255 mg, 0.391 mmol, 73%): ^{1}H NMR (300 MHz, MeOH-d_4) δ 0.82–0.91 (t, J = 6.3 Hz, 1H), 1.21–1.60 (m, 10H), 1.90–1.96 (m, 1H), 1.97–2.03 (m, 1H), 2.05–2.30 (m, 2H), 2.90–2.99 (m, 1H), 3.07–3.30 (m, 3H), 3.60–3.85 (m, 6H), 4.53 (t, J = 7.3 Hz, 1H), 4.66–4.72 (m, 1H), 5.01–5.12 (m, 2H), 7.00–7.35 (m, 14H), 7.63 (d, J = 7.7 Hz, 1H); ^{13}C NMR (75 MHz, MeOH-d_4) δ 13.5, 18.8, 19.8, 25.3, 28.3, 33.7, 37.3, 51.8, 54.2, 59.0, 60.5, 66.6, 98.8, 110.0, 111.3, 118.4, 118.5, 121.4, 123.7, 126.9, 127.7, 128.5,

129.3, 137.1, 137.4, 172.0, 172.7, 175.3; HRMS-ESI ($M + Na^+$) calcd for $C_{41}H_{48}N_4NaO_8$ 747.4932, found 747.4967.

Phe-X-Trp Ester 13. Compound **9** (450 mg, 0.83 mmol) was deprotected and coupled to Cbz-Phe-OH (297 mg, 1.0 mmol) using a procedure that was similar to that used for the preparation of compound **11**. The crude material was purified by flash chromatography (1:4 hexanes/EtOAc) to yield **13** (280 mg, 0.38 mmol, 46%): ^{1}H NMR (300 MHz, DMSO-d_6) δ 1.15–1.55 (m, 10H), 1.63–1.66 (m, 1H), 1.70–1.90 (m, 1H), 1.96–2.00 (m, 2H), 2.14–2.22 (m, 1H), 2.70–2.78 (m, 1H), 2.90–3.19 (m, 3H), 3.40 (s, 3H), 3.56–3.60 (m, 4H), 3.74 (m, 3H), 4.32–4.40 (m, 1H), 4.47–4.55 (m, 1H), 4.93–4.97 (m, 2H), 6.97–7.02 (t, J = 7.3 Hz, 1H), 7.05–7.10 (t, J = 7.9 Hz, 1H), 7.15–7.35 (m, 10H), 7.46–7.52 (m, 2H), 8.23–8.28 (m, 1H), 10.9 (s, 1H); ^{13}C NMR (75 MHz, MeOH-d_4) δ 15.8, 20.3, 22.4, 26.4, 28.7, 35.0, 39.3, 53.4, 54.8, 57.7, 60.0, 61.4, 66.8, 100.0, 111.3, 113.1, 119.7, 120.1, 122.6, 125.2, 127.8, 128.7, 129.1, 129.4, 129.6, 129.7, 129.9, 130.0, 130.9, 137.8, 138.7, 139.9, 157.5, 172.9, 174.3; HRMS-ESI ($M + Na^+$) calcd for $C_{41}H_{48}N_4NaO_8$ 747.3367, found 747.3386.

Phe-X-Phe Ester 14. Compound **10** (302 mg, 0.60 mmol) was deprotected and coupled to Cbz-Phe-OH (244 mg, 0.82 mmol) using a procedure that was similar to that used for the preparation of compound **11**. The crude material was purified by flash chromatography (1:4 hexanes/EtOAc) to yield **14** (267 mg, 0.39 mmol, 65%): ^{1}H NMR (300 MHz, MeOH-d_4) δ 0.86–0.95 (m, 1H), 1.20–1.55 (m, 11H), 1.82–1.90 (m, 1H), 2.03–2.30 (m, 2H), 2.82–3.02 (m, 2H), 3.14–3.22 (m, 2H), 3.68–3.85 (m, 6H), 4.44–4.49 (q, J = 5.1 Hz, 1H), 4.67–4.70 (m, 1H), 5.04 (s, 2H), 7.21–7.32 (m, 13H), 7.51 (d, J = 8.3 Hz, 1H), 8.30 (d, J = 7.6 Hz, 1H); ^{13}C NMR (75 MHz, MeOH-d_4) δ 13.5, 18.8, 24.6, 25.3, 33.7, 38.2, 51.7, 54.2, 56.9, 59.0, 59.1, 60.6, 66.6, 99.0, 126.7, 126.8, 126.9, 127.7, 128.0, 128.4, 128.5, 129.2, 129.3, 129.4, 137.2, 137.6, 157.1, 172.8, 175.2, 175.3; HRMS-ESI ($M + Na^+$) calcd for $C_{39}H_{47}N_3NaO_8$ 708.3259, found 708.3251.

Inhibitor 15. Compound **11** (0.39 g, 0.511 mmol) was dissolved in 20 mL of MeOH. To this solution was added a solution of LiOH (80 mg, 3.3 mmol) dissolved in 5 mL of water, and the reaction was stirred for 12 h at room temperature. The basic solution was neutralized with 1 N HCl to pH 7, and the solvents were removed under vacuum at 25 °C. The crude carboxylic acid was dissolved in 8 mL of TFA and 3 mL of water and the solution was stirred for an additional 12 h at room temperature. The solvents were again removed under vacuum at 25 °C and the crude material was purified by flash chromatography (7% MeOH in CH_2Cl_2). Diastereomers **15A,B** were separated by preparative HPLC on a silica column (96.5% CH_2Cl_2, 3.4% MeOH, 0.1% TFA). The compound had a low solubility in this solvent system, so the crude material was suspended in solvent and filtered to remove the product that did not dissolve, and the portion that remained in solution was purified by HPLC. This procedure gave **15A** (6 mg, 0.009 mmol, 2%) and **15B** (2 mg, 0.003 mmol, 1%). The large majority of the material was left in crude form and not purified. **15A**: ^{1}H NMR (300 MHz, DMSO-d_6) δ 1.25–1.75 (m, 2H), 1.81–2.05 (m, 3H), 2.13–2.45 (m, 4H), 3.06–3.23 (m, 2H), 3.34–3.42 (m, 2H), 4.42–4.65 (m, 3H), 5.03–5.13 (m, 2H), 7.10–7.56 (m, 12H), 7.68 (d, J = 7.6 Hz, 1H), 7.81 (d, J = 7.8 Hz, 1H), 8.17–8.31 (m, 1H), 10.97 (s, 1H); ^{13}C NMR (75 MHz, DMSO-d_4) δ 24.1, 25.4, 27.9, 28.8, 33.2, 34.7, 49.0, 53.5, 56.3, 58.2, 65.4, 111.1, 112.2, 119.0, 121.7, 124.3, 124.7, 128.3, 129.2, 136.9, 137.9, 156.6, 172.4, 172.8, 209.1. **15B**: ^{1}H NMR (300 MHz, DMSO-d_6) δ 0.92–1.22 (m, 1H), 1.20–1.29 (m, 3H), 1.52–1.60 (m, 2H), 1.63–1.70 (m, 1H) 1.91–2.07 (m, 4H), 2.25–2.34 (m, 1H) 2.74–3.08 (m, 4H), 4.22–4.39 (m, 6H), 4.84 (s, 2H), 6.83–7.31 (m, 11H), 7.42 (d, J = 7.6 Hz, 1H), 7.52 (d, J = 7.7 Hz, 1H), 7.92 (d, J = 7.4 Hz, 1H), 7.98 (d, J = 8.0 Hz, 1H), 10.70 (s, 2H); ^{13}C NMR (75 MHz, DMSO-d_4) δ 24.1, 25.5, 27.9, 28.9, 33.3, 34.8, 35.5, 46.9, 48.2, 49.1, 53.7, 56.4, 58.2, 66.1, 110.9, 112.2, 119.0, 119.4, 121.6, 124.4, 124.7, 128.0, 128.2, 128.5, 129.1, 136.9, 137.9, 156.6, 172.3, 172.9, 174.5, 194.4, 209.0; HRMS-ESI ($M + Na^+$) calcd for $C_{39}H_{41}N_5NaO_7$ 714.2900, found 714.2883 for the mixture of diastereomers **15A,B**.

Inhibitor 16. Compound **12** (291 mg, 0.40 mmol) was deprotected using the procedure outlined for the preparation of inhibitor **15**. The diastereomers were separated using preparative reverse-phase HPLC (40% MeCN, 60% H_2O, 0.1% TFA) to give **16A** (25 mg, 0.04 mmol, 10%) and **16B** (25 mg, 0.04 mmol, 10%). Similar to inhibitor **15**, inhibitor **16** was not very soluble in the solvent used during the purification so that a majority of the material was left in crude form and was not purified. **16A**: ^{1}H NMR (300 MHz, DMSO-d_6) δ 1.15–1.20 (m, 1H), 1.25–1.35 (m, 1H), 1.36–1.60 (m, 1H), 1.65–1.90 (m, 3H), 1.97–2.13 (m, 3H), 2.13–2.25 (m, 1H), 2.35–2.40 (m, 1H), 2.80–2.96 (m, 2H), 3.05–3.21 (m, 2H), 3.34 (s, 3H), 4.32–4.50 (m, 3H), 4.95 (s, 2H), 6.95–7.47 (m, 12H), 7.64–7.67 (d, J = 7.4 Hz, 1H), 8.05 (d, J = 7.1 Hz, 1H), 8.14 (d, J = 8.0 Hz, 1H), 10.82 (s, 1H); ^{13}C NMR (75 MHz, DMSO-d_6) δ 24.1, 25.5, 28.9, 33.3, 34.9, 35.6, 49.0, 54.2, 56.4, 58.2, 66.0, 111.0, 112.1, 119.0, 119.4, 121.7, 124.7, 127.3, 127.8, 128.2, 128.5, 129.0, 129.2, 130.0, 136.8, 138.0, 138.7, 156.6, 172.2, 172.8, 174.1, 209.0. **16B**: ^{1}H NMR (300 MHz, DMSO-d_6) δ 1.10–1.21 (m, 1H), 1.25–1.34 (m, 2H), 1.65–1.80 (m, 3H), 1.91–2.11 (m, 4H), 2.25–2.35 (m, 1H), 2.80–2.97 (m, 2H), 3.05–3.12 (m, 2H), 3.30 (s, 3H), 4.29–4.42 (m, 3H), 4.89–4.99 (m, 2H), 6.95–7.42 (m, 12H), 7.67 (d, J = 7.5 Hz, 1H), 8.05 (d, J = 7.4 Hz, 1H), 8.16 (d, J = 8.2 Hz, 1H), 10.82 (s, 1H), 12.61 (s, 1H); ^{13}C NMR (75 MHz, DMSO-d_6) δ 24.2, 25.5, 28.9, 33.2, 34.6, 25.3, 37.5, 48.9, 54.1, 56.4, 58.1, 66.0, 111.1, 112.1, 119.0, 119.4, 121.7, 124.7, 127.2, 128.3, 128.5, 129.0, 129.9, 136.9, 137.8, 138.7, 156.7, 172.4, 172.9, 174.1, 209.1; HRMS-ESI ($M + Na^+$) calcd for $C_{37}H_{40}N_4NaO_7$ 675.2792, found 675.2784 for the mixture of diastereomers **16A,B**.

Inhibitor 17. Compound **13** (240 mg, 0.33 mmol) was deprotected using the procedure outlined for the preparation of inhibitor **15**. The purification was accomplished using preparative reverse-phase HPLC (40% MeCN, 60% H_2O, 0.1% TFA) to yield **17** (99 mg, 0.15 mmol, 45%): ^{1}H NMR (300 MHz, DMSO-d_6) δ 1.10–1.20 (m, 1H), 1.25–1.35 (m, 2H), 1.67–1.72 (m, 2H), 1.80–1.87 (m, 2H), 2.00–2.15 (m, 4H), 2.35–2.38 (m, 2H), 2.72–2.79 (m, 2H), 2.94–3.01 (m, 2H), 3.14 (d, J = 4.6 Hz, 1H), 3.18–3.20 (m, 1H), 4.35–4.49 (m, 2H), 4.95 (s, 1H), 6.95–7.35 (m, 11H), 7.50–7.55 (m, 2H), 8.10 (q, J = 3.4 Hz, 1H), 8.82 (s, 1H); ^{13}C NMR (75 MHz, DMSO-d_6) δ 23.1, 24.1, 25.5, 27.9, 33.3, 34.7, 35.3, 35.6, 49.1, 53.7, 57.0, 58.2, 66.0, 110.9, 112.2, 119.0, 121.8, 124.3, 127.1, 128.1, 128.2, 128.8, 129.1, 130.1, 136.9, 137.9, 138.8, 139.1, 156.6, 156.7, 171.8, 172.2, 172.9, 174.4, 207.3, 209.1; HRMS-ESI ($M + Na^+$) calcd for $C_{37}H_{40}N_4NaO_7$ 675.2792, found 675.2797.

Inhibitor 18. Compound **14** (271 mg, 0.40 mmol) was deprotected using the procedure outlined for the preparation of inhibitor **15**. The purification was accomplished using preparative reverse-phase HPLC (40% MeCN, 60% H_2O, 0.1% TFA) to yield **18** (100 mg, 0.15 mmol, 39%): ^{1}H NMR (300 MHz, DMSO-d_6) δ 1.65–1.80 (m, 3H), 2.00–2.10 (m, 3H), 2.35–2.42 (m, 3H), 2.95–3.10 (m, 2H), 4.30–4.44 (m, 2H), 4.95 (s, 2H), 7.20–7.30 (m, 13H), 7.56 (d, J = 8.3 Hz, 1H), 8.03–8.16 (m, 1H), 12.40 (s, 1H); ^{13}C NMR (75 MHz, DMSO-d_6) δ 24.2, 25.5, 33.3, 33.4, 33.7, 34.9, 35.7, 38.6, 49.0, 54.1, 57.0, 58.1, 66.0, 71.0, 127.1, 127.2, 128.2, 128.4, 129.0, 130.1, 137.9, 138.7, 138.9, 139.1, 156.7, 164.2, 171.8, 172.1, 172.7, 209.0; HRMS-ESI ($M + Na^+$) calcd for $C_{35}H_{39}N_3NaO_8$ 636.2684, found 636.2654.

Acknowledgment. This research was supported by the NIH (Grant 1 R01 GM57327-01), the Petroleum Research Fund administered by the American Chemical Society (Grant 30544-G4), and the U.S. Army Medical Research and Materiel Command – Breast Cancer Research Initiative (Grant DAMD17-96-1-6161, Career Development Award to C.T.S.). J.L.C. and P.A. were supported by GAANN Fellowships from the Department of Education. J.L.C. was also supported by a University

Fellowship from Brown University. We thank Dr. Andrew Tyler of the Harvard University Chemistry Department Mass Spectrometry Facility for providing several of the mass spectra. This facility is supported by grants from the NSF (CHE-9020045) and the NIH (SIO-RR06716).

Supporting Information Available: HPLC characterization for compounds **15**–**18**. This material is available free of charge via the Internet at http://pubs.cas.org.

References

(1) For several recent reviews, see: (a) Lowe, G. Combinatorial Chemistry. *Chem. Soc. Rev.* **1995**, *24*, 309. (b) Ellman, J. A. Design, Synthesis, and Evaluation of Small-Molecule Libraries. *Acc. Chem. Res.* **1996**, *29*, 132. (c) Gordon, E. M.; Gallop, M. A.; Patel, D. V. Strategy and Tactics in Combinatorial Organic Synthesis. Applications to Drug Discovery. *Acc. Chem. Res.* **1996**, *29*, 144. (d) Balkenhohl, F.; von dem Bussche-Hunnefeld, C.; Lansky, A.; Zechel, C. Combinatorial Synthesis of Small Organic Molecules. *Angew. Chem., Int. Ed. Engl.* **1996**, *35*, 2288. (e) Thompson, L. A.; Ellman, J. A. Synthesis and Applications of Small Molecule Libraries. *Chem. Rev.* **1996**, *96*, 555.

(2) Campbell, D. A.; Bermak, J. C.; Burkoth, T. S.; Patel, D. V. A Transition State Analogue Inhibitor Combinatorial Library. *J. Am. Chem. Soc.* **1995**, *117*, 5381.

(3) Owens, R. A.; Gesellchen, P. D.; Houchins, B. J.; Dimarchi, R. D. The Rapid Identification of HIV Protease Inhibitors Through the Synthesis and Screening of Defined Peptide Mixtures. *Biochem. Biophys. Res. Commun.* **1991**, *181*, 402.

(4) Kick, E. K.; Ellman. J. A. Expedient Method for the Solid-Phase Synthesis of Aspartic Acid Protease Inhibitors Directed toward the Generation of Libraries. *J. Med. Chem.* **1995**, *38*, 1427.

(5) Wang, J. T.; Li, S.; Wideburg, N.; Krafft, G. A.; Kempf, D. J. Synthetic Chemical Diversity: Solid-Phase Synthesis of Librarries of C2 Symmetric Inhibitors of HIV Protease Containing Diamino Diol and Diamino Alcohol Cores. *J. Med. Chem.* **1995**, *38*, 2995.

(6) Rano, T. A.; Timkey, T.; Peterson, E. P.; Rotonda, J.; Nicholson, D. W.; Beckeer, J. W.; Chapman, K. T.; Thornberry, N. A. A Combinatorial Approach Defines Specificities of Members of the Caspase Family and Granzyme B. Functional Relationships Established for Key Mediators of Apoptosis. *Chem. Biol.* **1997**, *4*, 149.

(7) Conroy, J. L.; Sanders, T. C.; Seto, C. T. Using the Electrostatic Field Effect to Design a New Class of Inhibitors for Cysteine Proteases. *J. Am. Chem. Soc.* **1997**, *119*, 4285.

(8) For reviews of serine and cysteine protease inhibitors, see: (a) Mehdi, S. Synthetic and Naturally Occurring Protease Inhibitors Containing an Electrophilic Carbonyl Group. *Bioorg. Chem.* **1993**, *21*, 349. (b) Wells, G. J.; Bihovsky, R. Calpain Inhibitors as Potential Treatment for Stroke and Other Neurodegenerative Diseases: Recent Trends and Developments. *Exp. Opin. Ther. Pat.* **1998**, *8*, 1707.

(9) Conroy, J. L.; Seto, C. T. Demonstration by ^{13}C NMR Studies that Tetrahydropyranone-Based Inhibitors Bind to Cysteine Proteases by Reversible Formation of a Hemithioketal Adduct. *J. Org. Chem.* **1998**, *63*, 2367.

(10) Conroy, J. L.; Abato, P.; Ghosh, M.; Austermuhle, M. I.; Kiefer, M. R.; Seto, C. T. Synthesis of Cyclohexanone-Based Cathepsin B Inhibitors that Interact with Both the S and S′ Binding Sites. *Tetrahedron Lett.* **1998**, *39*, 8253.

(11) For other reversible inhibitors of serine and cysteine proteases that can make contacts with both the S and S′ subsites, see: (a) Hu, L.-Y.; Abeles, R. H. Inhibition of Cathepsin B and Papain by Peptidyl α-Keto Esters, α-Keto Amides, α-Diketones, and α–Keto Acids. *Arch. Biochem. Biophys.* **1990**, *281*, 271. (b) Imperiali, B.; Abeles, R. H. Extended Binding Inhibitors of Chymotrypsin that Interact with Leaving Group Subsites S1′–S3′. *Biochemistry* **1987**, *26*, 4474. (c) Yamashita, D. S.; Smith, W. W.; Zhao, B.; Janson, C. A.; Tomaszek, T. A.; Bossard, M. J.; Levy, M. A.; Oh, H.-J.; Carr, T. J.; Thompson, S. K.; Ijames, C. F.; Carr, S. A.; McQueney, M.; D'Alessio, K. J.; Amegadzie, B. Y.; Hanning, C. R.; Abdel-Meguid, S.; DesJarlais, R. L.; Gleason, J. G.; Veber, D. F. Structure and Design of Potent and Selective Cathepsin K Inhibitors. *J. Am. Chem. Soc.* **1997**, *119*, 11351.

(12) For several other examples of serine and cysteine protease inhibitors, see: (a) Dragovich, P. S.; Prins, T. J.; Zhou, R.; Fuhrman, S. A.; Patick, A. K.; Matthews, D. A.; Ford, C. E.; Meador, J. W., III; Ferre, R. A.; Worland, S. T. Structure-Based Design, Synthesis, and Biological Evaluation of Irreversible Human Rhinovirus 3C Protease Inhibitors. 3. Structure–Activity Studies of Ketomethylene-Containing Peptidomimetics. *J. Med. Chem.* **1999**, *42*, 1203. (b) Roush, W. R.; Gwaltney, S. L., II; Cheng, J.; Scheidt, K. A.; McKerrow, J. H.; Hansell, E. Vinyl Sulfonate Esters and Vinyl Sulfonamides: Potent, Irreversible Inhibitors of Cysteine Proteases. *J. Am. Chem. Soc.* **1998**, *120*, 10994. (c) Liu, S.; Hanzlik, R. P. Structure–Activity Relationships for Inhibition of Papain by Peptide Michael Acceptors. *J. Med. Chem.* **1992**, *35*, 1067. (d) Harbeson, S. L.; Abelleira, S. M.; Akiyama, A.; Barrett, R., III; Carroll, R. M.; Straub, J. A.; Tkacz, J. N.; Wu, C.; Musso, G. F. Stereospecific Synthesis of Peptidyl α-Keto Amides as Inhibitors of Calpain. *J. Med. Chem.* **1994**, *37*, 2918. (e) Bromme, D.; Klaus, J. L.; Okamoto, K.; Rasnick, D.; Palmer, J. T. Peptidyl Vinyl Sulfones: A New Class of Potent and Selective Cysteine Protease Inhibitors. S2P2 Specificity of Human Cathepsin O2 in Comparison With Cathepsins S and L. *Biochem. J.* **1996**, *315*, 85. (f) Palmer, J. T.; Rasnick, D.; Klaus, J. L.; Bromme, D. Vinyl Sulfones as Mechanism-Based Cysteine Protease Inhibitors. *J. Med. Chem.* **1995**, *38*, 3193. (g) Chatterjee, S.; Gu, Z.-Q.; Dunn, D.; Tao, M.; Josef, K.; Tripathy, R.; Bihovsky, R.; Senadhi, S. E.; O'Kane, T. M.; McKenna, B. A.; Mallya, S.; Ator, M. A.; Bozyczko-Coyne, D.; Siman, R.; Mallamo, J. P. D-Amino Acid Containing, High-Affinity Inhibitors of Recombinant Human Calpain I. *J. Med. Chem.* **1998**, *41*, 2663. (h) Angelastro, M. R.; Mehdi, S.; Burkhart, J. P.; Peet, N. P.; Bey, P. α-Diketone and α-Keto Ester Derivatives of N–Protected Amino Acids and Peptides as Novel Inhibitors of Cysteine and Serine Proteinases. *J. Med. Chem.* **1990**, *33*, 11.

(13) (a) Sebestyen, F.; Dibo, G.; Kovacs, A.; Furka, A. Chemical Synthesis of Peptide Libraries. *Bioorg. Med. Chem. Lett.* **1993**, *3*, 413. (b) Furka, A.; Sebestyen, F.; Asgedom, M.; Dibo, G. General Method for Rapid Synthesis of Multicomponent Peptide Mixtures. *Int. J. Pept. Protein Res.* **1991**, *37*, 487.

(14) Dooley, C. T.; Chung, N. N.; Wilkes, B. C.; Schiller, P. W.; Bidlack, J. M.; Pasternak, G. W.; Houghten, R. A. An All D-Amino Acid Opioid Peptide with Central Analgesic Activity from a Combinatorial Library. *Science* **1994**, *266*, 2019.

(15) (a) Yamaguchi, N.; Chung, S.; Shiroeda, O.; Koyama, K.; Imanishi, J. Characterization of a Cathepsin L-Like Enzyme Secreted from Human Pancreatic Cancer Cell Line HPC–YP. *Cancer Res.* **1990**, *50*, 658. (b) Liotta, L. A.; Steeg, P. S.; Stetler-Stevenson, J. G. Cancer Metastasis and Angiogenesis: An Imbalance of Positive and Negative Regulation. *Cell* **1991**, *64*, 327. (c) Baricos, W. H.; Zhou, Y.; Mason, R. W.; Barrett, A. J. Human Kidney Cathepsins B and L. Characterization and Potential Role in Degradation of Glomerular Basement Membrane. *Biochem. J.* **1988**, *252*, 301.

(16) Pepper, J. S.; Montesano, R.; Mandriots, S. J.; Orci, L.; Vassalli, J. Angiogenesis: A Paradigm for Balanced Extracellular Proteolysis During Cell Migration and Morphogenesis. *Enzyme Protein* **1996**, *49*, 138.

(17) (a) Zou, Z.; Anisowicz, A.; Hendrix, M. J. C.; Thor, A.; Neveu, M.; Sheng, S.; Rafidi, K.; Seftor, E.; Sager, R. Maspin, a Serpin with Tumor-Suppressing Activity in Human Mammary Epithelial Cells. *Science* **1994**, *263*, 526. (b) Kimura, T.; Fuchimoto, S.; Iwagaki, H.; Hizuta, A.; Orita, K. Inhibitory Effect of Nafamostat Mesilate in Metastasis into the Livers of Mice and on Invasion of the Extracellular Matrix by Cancer Cells. *J. Int. Med. Res.* **1992**, *20*, 343.

(18) Otto, H.-H.; Schirmeister, T. Cysteine Proteases and Their Inhibitors. *Chem. Rev.* **1997**, *97*, 133.

(19) Sanders, C. T.; Seto, C. T. 4-Heterocyclohexanone-Based Inhibitors of the Serine Protease Plasmin. *J. Med. Chem.* **1999**, *42*, 2969–2976.

(20) Teno, N.; Wanaka, K.; Okada, Y.; Tsuda, Y.; Okamoto, U.; Hijikata-Okunomiya, A.; Naito, T.; Okamoto, S. Development of Active Center-Directed Inhibitors Against Plasmin. *Chem. Pharm. Bull.* **1991**, *39*, 2340.

(21) Mole, J. E.; Horton, H. R. Kinetics of Papain-Catalyzed Hydrolysis of α-N-Benzoyl-L-arginine-*p*-nitroanilide. *Biochemistry* **1973**, *12*, 816.

(22) Bajkowski, A. S.; Frankfater, A. Specific Spectrophotometric Assays for Cathepsin B_1. *Anal. Biochem.* **1975**, *68*, 119.

(23) Hitomi, Y.; Ikari, N.; Fujii, S. Inhibitory Effect of a New Synthetic Protease Inhibitor (FUT-175) on the Coagulation System. *Haemostasis* **1985**, *15*, 164.

(24) Ohno, K.; Kosaki, G.; Kambayashi, J.; Imaoka, S.; Hirata, F. FOY: [Ethyl *p*-(6-guanidinohexanoyloxy)benzoate] Methanesulfonate as a Serine Proteinase Inhibitor. I. Inhibition of Thrombin and Factor X_a In Vitro. *Thrombosis Res.* **1980**, *19*, 579.

JM990272G

ORGANIC LETTERS

1999
Vol. 1, No. 12
1945–1948

Inhibition of Phosphatase Activity by Positively-Charged Cyclodextrins

Mousumi Ghosh, Tanya C. Sanders, Rui Zhang, and Christopher T. Seto*

Department of Chemistry, Brown University, 324 Brook Street, Box H, Providence, Rhode Island 02912
christopher_seto@brown.edu

Received September 27, 1999

ABSTRACT

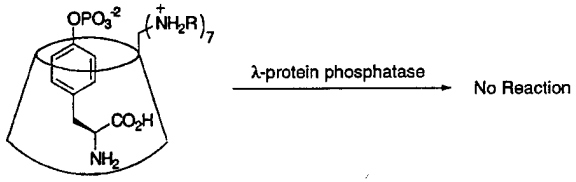

Aminocyclodextrins are known to bind phosphate esters such as phosphotyrosine and *p*-nitrophenyl phosphate. This paper describes the inhibition of phosphate ester hydrolysis, as catalyzed by λ-protein phosphatase and acid phosphatase, that is caused by such binding interactions. ROESY studies provide structural information about the cyclodextrin–aryl phosphate complexes. In addition, these experiments are used to generate approximations of the rates of dissociation of the noncovalent complexes.

Cyclodextrins are one of the most important classes of molecules in the field of molecular recognition. They have gained widespread use in such diverse areas as biomimetic catalysis and chromatography and as drug carriers.[1] Aminocyclodextrins are cyclodextrins in which one or several of the primary hydroxyl groups at the 6-position of the sugar units have been replaced by amines. In 1979 Boger and Knowles demonstrated that such molecules bind to benzyl phosphate through a combination of electrostatic and hydrophobic interactions.[2] Since then a number of investigators have examined the binding properties of aminocyclodextrins with a variety of phosphate esters including nucleotide mono- and triphosphates,[3,4] *p*-nitrophenyl phosphate and other 4-substituted phenyl phosphates,[4,5] phosphotyrosine,[6] and cyclic phosphate esters.[7] In this paper we demonstrate that aminocyclodextrins, because they are able to bind to phosphotyrosine and other aryl phosphate esters with significant affinity, can inhibit the hydrolysis of these phosphate ester guests catalyzed by λ-protein phosphatase and acid phosphatase.[8] The development of new phosphatase inhibitors is of current interest because of the important role that phosphatases play in intracellular signal transduction.[9] In addition, we use ^{1}H and ^{31}P NMR spectroscopy to examine intermolecular interactions between aminocyclodextrin hosts and phosphotyrosine guests and show that these experiments provide information about the kinetics of dissociation of the aminocyclodextrin–phosphotyrosine complexes.

The structures of the modified cyclodextrin hosts and the aryl phosphate guests used in this study are shown in Figure 1. Compounds **1**β and **2**α are derived from β- and α-cyclodextrin, respectively, and the syntheses of these molecules have been described previously by Darcy[4] and Thatcher.[10] The primary hydroxyl groups at the 6-positions of the sugar

(1) For a recent series of comprehensive reviews on all aspects of cyclodextrin chemistry, see: *Chem. Rev.* **1998**, *98*, No. 5.
(2) (a) Boger, J.; Knowles, J. R. *J. Am. Chem. Soc.* **1979**, *101*, 7631. (b) Boger, J.; Brenner, D. G.; Knowles, J. R. *J. Am. Chem. Soc.* **1979**, *101*, 7630.
(3) (a) Eliseev, A. V.; Schneider, H.-J. *Angew. Chem., Int. Ed. Engl.* **1993**, *32*, 1331. (b) Eliseev, A. V.; Schneider, H.-J. *J. Am. Chem. Soc.* **1994**, *116*, 6081.
(4) (a) Schwinte, P.; Darcy, R.; O'Keeffe, F. *J. Chem. Soc., Perkin Trans. 2* **1998**, 805. (b) Ahern, C.; Darcy, R.; O'Keeffe, F.; Schwinte, P. *J. Incl. Phenom. Mol. Recognit. Chem.* **1996**, *25*, 43.
(5) Vizitiu, D.; Thatcher, G. R. J. *J. Org. Chem.* **1999**, *64*, 6235.
(6) Cotner, E. S.; Smith, P. J. *J. Org. Chem.* **1998**, *63*, 1737.
(7) Breslow, R.; Schmuck, C. *J. Am. Chem. Soc.* **1996**, *118*, 6601.
(8) For a demonstration that aminocyclodextrins can inhibit neurite growth by binding to glycosaminoglycan sulfates, see: Borrajo, A. M. P.; Gorin, B. I.; Dostaler, S. M.; Riopelle, R. J.; Thatcher, G. R. J. *Bioorg. Med. Chem. Lett.* **1997**, *7*, 1185.
(9) Burke, T. R.; Zhang, Z.-Y. *Biopolymers* **1998**, *47*, 225.
(10) Vizitiu, D.; Walkinshaw, C. S.; Borin, B. I.; Thatcher, G. R. J. *J. Org. Chem.* **1997**, *62*, 8760.

10.1021/ol990301h CCC: $18.00
Published on Web 11/06/1999

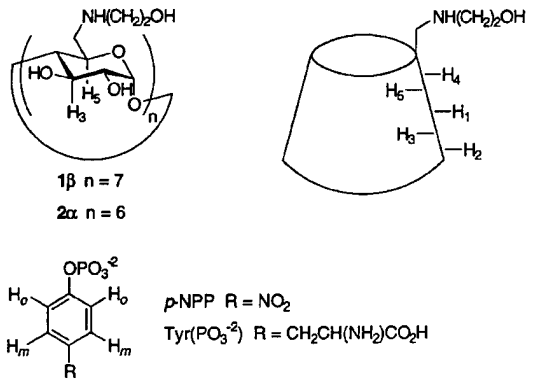

Figure 1. Structures of positively charged cyclodextrin hosts and aryl phosphate guests. The schematic diagram on the right shows the positions of the protons in the interior and exterior of the cyclodextrin cavity. The proton labels correspond to the annotated resonances in the ROESY spectra shown in Figure 3.

units have been replaced with 2-hydroxyethylamino groups. Several of these groups are protonated at pH 7, and they provide a positively charged binding site along one rim of the cyclodextrin cavity that forms electrostatic interactions with negatively charged guests. Two aryl phosphates were used as guests: *p*-nitrophenyl phosphate (*p*-NPP) and phosphotyrosine ($Tyr(PO_3^{-2})$).

The inhibition of λ-protein phosphatase and acid phosphatase by cyclodextrin **1β** was monitored using a UV assay to follow dephosphorylation of the aryl phosphate substrates. The data were analyzed using the reaction scheme shown in eq 1, where CD is cyclodextrin **1β**, S is the substrate, E is the enzyme, and P is the product. This reaction scheme is simply the Michaelis–Menten formalism that has been modified to incorporate a preliminary equilibrium between free substrate and the cyclodextrin–substrate complex (CD·S).

$$CD{\cdot}S \overset{K_d}{\rightleftharpoons} CD + S + E \overset{K_M}{\rightleftharpoons} E{\cdot}S \xrightarrow{k_{cat}} E + P \qquad (1)$$

The rate of the enzyme-catalyzed reaction is given by eqs 2–4, where S_{app} is the concentration of free substrate, S_0 is the total substrate concentration, CD_0 is the total cyclodextrin concentration, and K_d is the dissociation constant of the CD·S complex.

$$\text{rate} = V_{max}S_{app}/(K_M + S_{app}) \qquad (2)$$

$$S_{app} = S_0 - CD{\cdot}S \qquad (3)$$

$$CD{\cdot}S = \frac{CD_0}{2} + \frac{(S_0 + K_d)}{2}\left[1 - \left(\frac{CD_0{}^2 - 2CD_0(S_0 - K_d)}{(S_0 + K_d)^2} + 1\right)^{1/2}\right] \qquad (4)$$

Equation 4 can be derived from a simple 1:1 binding isotherm between CD and S.[11] The rate expression shown in eq 2 is based upon the assumption that the enzyme is able to hydrolyze only the free substrate and cannot react with substrate that is complexed with the cyclodextrin. This assumption is reasonable because in the complex the phosphate ester is completely surrounded by the cyclodextrin and binding to the enzyme is precluded by both steric and electrostatic repulsion. The initial rates of the enzyme-catalyzed reactions were determined using a single substrate concentration and a range of cyclodextrin concentrations.[12] The data were fitted to eqs 2–4 using a nonlinear curve fitting procedure, which gave estimates of K_d. An example of one set of data, along with the corresponding curve fit, is shown in Figure 2. K_M values for the substrates were determined separately using standard methods. Table 1 shows the association constants for the cyclodextrin–aryl phosphate complexes that were extracted from the kinetic data.

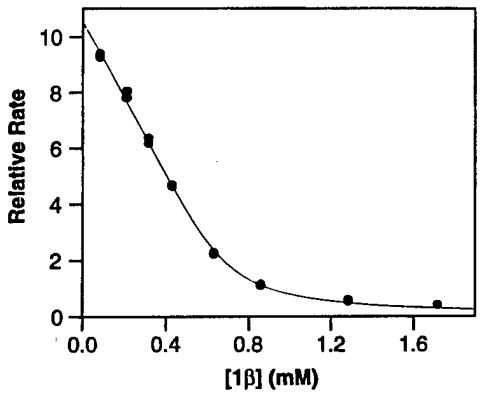

Figure 2. Inhibition of acid phosphatase by cyclodextrin **1β** in 100 mM Tris pH 7.0. The substrate, *p*-NPP, was present at a concentration of 0.64 mM. The curve corresponds to the best fit of the data to eq 2.

Table 1. Association Constants of Cyclodextrin **1β** with Aryl Phosphates As Measured by Inhibition of Phosphatase Activity and by ^1H NMR Experiments

			K_{assoc} (M^{-1})	
Substrate	Enzyme[a]	Buffer[b]	Enzyme Kinetics	NMR Method
p-NPP	AP	100 mM Tris	37,000 ± 8,000	
p-NPP	λ-PP	100 mM Tris	13,000 ± 3,000	
p-NPP		100 mM Tris		60,000 ± 15,000[c]
p-NPP	AP	10 mM HPO_4^{-2}	1,400 ± 300	
p-NPP		10 mM HPO_4^{-2}		2,200 ± 400[c]
$Tyr(PO_3^{-2})$	AP	100 mM Tris	23,000 ± 5,000	
$Tyr(PO_3^{-2})$	λ-PP	100 mM Tris	19,000 ±4,000	
$Tyr(PO_3^{-2})$		100 mM Tris		130,000 ± 25,000[d]

[a] AP is acid phosphatase and λ-PP is λ-protein phosphatase. [b] Assays with AP and λ-PP were performed at pH 7.0 and 7.8, respectively. λ-PP was not stable at pH 7.0. [c] Measured by ^1H NMR titration. [d] Measured by ^1H NMR dilution.

We have also measured association constants by NMR spectroscopy for the sake of comparison (Table 1). The complex between 1β and *p*-NPP was in fast exchange on the NMR time scale and showed only one set of resonances for the aryl phosphate protons. Thus, ^{1}H NMR titrations were used to determine association constants.[11] In contrast, the complex between 1β and Tyr(PO_3^{-2}) was in slow exchange on the NMR time scale and displayed well-resolved signals for the free and bound aryl phosphate. In this case the relative integration of the aromatic protons of free and bound Tyr(PO_3^{-2}), along with the known concentrations of Tyr(PO_3^{-2}) and the cyclodextrin, were used to determine the association constant.

Comparison of the association constants derived from enzyme kinetics and from the NMR experiments shows that, for the 1β–*p*-NPP complex with acid phosphatase in either Tris or phosphate buffers, there is reasonable agreement between values measured using the two different techniques. The association constants measured in 100 mM Tris buffer are significantly higher than those measured in phosphate buffer. In Tris-HCl buffer, the chloride anion does not strongly complex with the positively charged cyclodextrin and therefore does not compete significantly with *p*-NPP for binding to 1β. In contrast, the phosphate buffer binds relatively tightly to the cyclodextrin and must be displaced before *p*-NPP can bind.[13] This competition by the buffer lowers the observed association constant.

For the 1β–*p*-NPP complex with λ-protein phosphatase and the 1β–Tyr(PO_3^{-2}) complex with either enzyme, the association constants measured using the enzyme kinetics method are significantly lower than the values measured using NMR spectroscopy. Two factors lower the sensitivity of the enzyme kinetics method and limit our ability to measure large association constants using this technique. First, the concentration of the substrate in these assays must be similar to the K_M value so that significant rates are achieved in the absence of inhibitor. Second, the difference in extinction coefficients between Tyr(PO_3^{-2}) and Tyr is relatively small. In addition, the assays with λ-protein phosphatase were performed at pH 7.8, while the assays with acid phosphatase and the NMR measurements were performed at pH 7.0. The higher pH decreases the protonation state of the cyclodextrin and lowers the electrostatic attraction between host and guest.[14] Despite the limitations of the kinetic method, the results presented here demonstrate that positively charged cyclodextrins, because they sequester phosphate ester guests, can effectively inhibit hydrolysis of the phosphate ester linkage as catalyzed by phosphatase enzymes.

We have acquired ROESY spectra of several of the cyclodextrin–aryl phosphate complexes (Figure 3). These

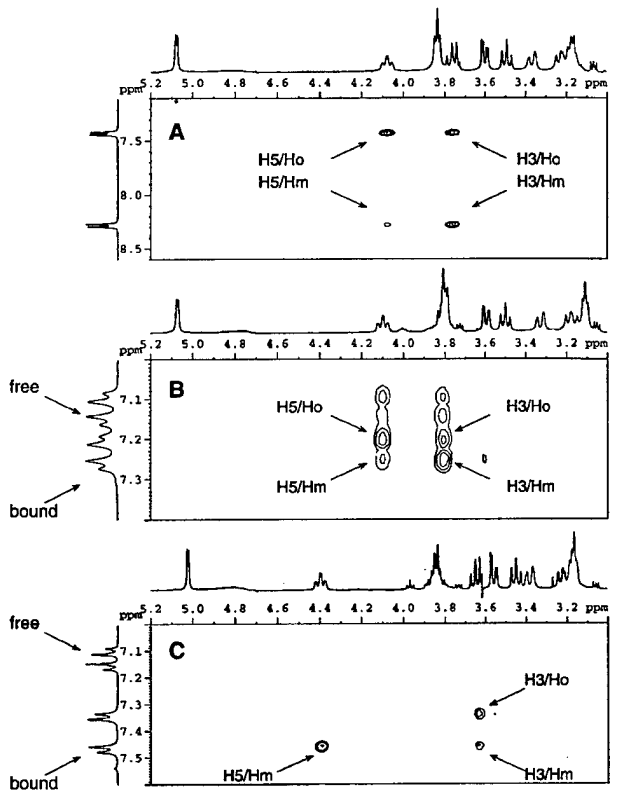

Figure 3. ROESY spectrum showing intermolecular NOEs between protons on the interior of the cyclodextrin cavity and the *ortho* and *meta* protons of *p*-NPP and Tyr(PO_3^{-2}). Spectrum A: 1β + *p*-NPP. Spectrum B: 1β + Tyr(PO_3^{-2}). Spectrum C: 2α + Tyr(PO_3^{-2}).

spectra not only give information about the structure and conformation of the noncovalent complexes[15] but they also provide insights into the kinetics of their dissociation. Spectrum A (Figure 3) shows the complex between cyclodextrin 1β and *p*-NPP. Exchange between free and bound *p*-NPP is fast on the NMR time scale, and thus only one set of resonances is observed for the aromatic protons of *p*-NPP. The ROESY spectrum shows strong intermolecular NOE cross-peaks between the *ortho* protons of *p*-NPP and both the H3 and H5 protons on the interior wall of the cyclodextrin cavity (see Figure 1 for the positions of the protons). In addition, there is a strong cross-peak between the *meta* protons of *p*-NPP and H3 and a weaker cross-peak between the *meta* protons and H5 of the cyclodextrin.[16] These NOEs are consistent with a binding conformation in which the phosphate interacts with the ammonium groups of the cyclodextrin and the aromatic ring is positioned inside the cyclodextrin cavity. The *ortho* protons are relatively deep in the cavity and are proximal to both H3 and H5, while the

(11) Wilcox, C. S.; Cowart, M. D. *Tetrahedron Lett.* **1986**, *27*, 5563.

(12) Addition of unmodified α- or β-cyclodextrin to the enzyme-catalyzed reactions has no effect on the reaction rate.

(13) A related positively charged cyclodextrin has been shown to bind inorganic phosphate with an association constant of 3.7×10^3 M^{-1}. See ref 3b.

(14) The association constant for the complex between cyclodextrin 1β and Tyr(PO_3^{-2}) measured by ^{1}H NMR spectroscopy in 100 mM Tris buffer at pH 7.8 is 10 000 ± 2000 M^{-1}.

(15) Schneider, H.-J.; Hacket, F.; Rudiger, V.; Ikeda, H. *Chem. Rev.* **1998**, *98*, 1755.

(16) The assignments of the resonances in the NMR spectra were performed using COSY spectra of the aryl phosphate–cyclodextrin complexes.

meta protons occupy a more shallow position and interact strongly only with H3. From the limiting chemical shift values of the aromatic protons in the free and bound forms, along with the observation that this acquisition, which was recorded at 25 °C, is well above the coalescence point, we estimate that the dissociation rate constant for this complex is much greater than 150 s^{-1}.[17]

Spectrum B shows the complex between cyclodextrin **1**β and Tyr(PO_3^{-2}). Unlike the complex between **1**β and *p*-NPP, this complex is in slow exchange on the NMR time scale so that separate resonances are observed for free and bound Tyr(PO_3^{-2}). The ROESY spectrum shows cross-peaks between the aromatic protons of both free and bound Tyr(PO_3^{-2}) and H3 and H5 of the cyclodextrin. We expect only bound Tyr(PO_3^{-2}), and not free Tyr(PO_3^{-2}), to have NOE interactions with the cyclodextrin. However, the exchange rate between free and bound Tyr(PO_3^{-2}) is fast compared to the 350 ms spinlock time used in the ROESY experiments. During the spinlock period, bound Tyr(PO_3^{-2}) molecules that experience NOEs with the cyclodextrin can dissociate to the unbound form. Therefore, the spectrum shows cross-peaks with both the free and bound forms, even though the NOE interactions occur only between bound Tyr(PO_3^{-2}) and the cyclodextrin. Since this complex shows slow exchange on the NMR time scale, but ROESY cross-peaks for both the free and bound forms using a 350 ms spinlock time, we estimate that the dissociation rate constant for this complex must fall in the range between 3 and 75 s^{-1}.[18] ^{31}P 2D exchange spectroscopy (EXSY) can be used to more accurately determine exchange rates.[19] Using this method we have found that the dissociation rate constant for the complex between **1**β and Tyr(PO_3^{-2}) is 7 $\pm$ 1 s^{-1}, a value that is consistent with the estimate derived from the ROESY experiments.

For the complex between Tyr(PO_3^{-2}) and cyclodextrin **2**α (spectrum C), exchange between free and bound Tyr(PO_3^{-2}) is again slow on the NMR time scale. However, in this case the exchange rate is slow compared to the 350 ms spinlock time used in the ROESY experiments. As a result we observe NOE cross-peaks between the aromatic protons of only the bound form, and not the free form, of Tyr(PO_3^{-2}) and H3 and H5 of **2**α. These results demonstrate that only bound Tyr(PO_3^{-2}) molecules are in close proximity to the cyclodextrin as we expect and put an upper limit on the dissociation rate constant for this complex of 3 s^{-1}. Slow dissociation of Tyr(PO_3^{-2}) from **2**α when compared to **1**β is likely caused by the narrower, more restrictive cavity of the α-cyclodextrin derivative. The association constant of this complex in 100 mM Tris buffer is 30 000 $\pm$ 4500 M^{-1}.[20]

The pattern of NOE intensities that we observed in the **2**α–Tyr(PO_3^{-2}) complex is different than the pattern that appears in the complex with **1**β. With the α-cyclodextrin derivative, there are strong interactions between H3 of the cyclodextrin and both the *ortho* and *meta* protons of the aryl phosphate. However, there is a strong interaction between H5 and the *meta* protons, while the interaction between H5 and the *ortho* protons is absent. These observations are consistent with a binding conformation in which the Tyr(PO_3^{-2}) molecule is positioned "upside down" in the cyclodextrin cavity with the phosphate group oriented away from the ammonium groups. This conformation is somewhat surprising since it precludes a strong electrostatic interaction between the negatively charged phosphate group and the positively charged rim of the cyclodextrin. On the other hand, this conformation allows electrostatic interactions to form with the carboxylate group of Tyr(PO_3^{-2}).

The experiments presented in this paper demonstrate that the binding interactions between positively charged cyclodextrin hosts and aryl phosphate guests inhibit the hydrolysis of the guest molecules catalyzed by phosphatase enzymes. The ROESY studies show that the aryl phosphates bind in the interior of the cyclodextrin cavity and also provide limits on the dissociation rates of the aryl phosphate–cyclodextrin complexes. These limits can be confirmed using ^{31}P 2D exchange spectroscopy. We are currently investigating in greater depth the kinetics and thermodynamics of these types of binding interactions.

Acknowledgment. This research was supported by the U.S. Army Medical Research and Materiel Command–Breast Cancer Research Initiative through a Career Development Award to C.T.S. (Grant DAMD17-96-1-6161) and a Predoctoral Fellowship to T.C.S. (Grant DAMD17-96-1-6037).

OL990301H

(17) Sandstrom, J. *Dynamic NMR Spectroscopy*; Academic Press: New York, 1982.

(18) The upper limit for the exchange rate is derived from the difference in chemical shift values for free Tyr(PO_3^{-2}) and Tyr(PO_3^{-2}) that is fully bound to cyclodextrin **1**β, along with the fact that this acquisition which was recorded at room temperature is well below the coalescence point. See also ref 17.

(19) Hartzell, C. J.; Mente, S. R.; Eastman, N. I.; Beckett, J. L. *J. Phys. Chem.* **1993**, *97*, 4887.

(20) Reference 5 provides some related coalescence temperature data for similar aminocyclodextrin–aryl phosphate complexes.

The Effects of Buffers on the Thermodynamics and Kinetics of Binding between Positively-Charged Cyclodextrins and Phosphate Ester Guests

Mousumi Ghosh, Rui Zhang, Ronald G. Lawler, and Christopher T. Seto*

Department of Chemistry, Brown University, 324 Brook Street, Box H, Providence, Rhode Island 02912

Received October 15, 1999

Cyclodextrin derivatives in which the primary hydroxyl groups at the 6-positions of the sugar units have been replaced with 2-hydroxethylamino groups are known to bind phosphate esters with significant affinity. Association between the host and guest is mediated by a combination of hydrophobic and electrostatic interactions. Association constants for two cyclodextrin hosts with three phosphate ester guests are measured in a variety of buffer solutions, and it is found that the buffer has a large impact on the electrostatic component of the binding interaction. Negatively charged buffers such as phosphate and ADA (*N*-(2-acetamido)iminodiacetic acid) compete with the phosphate ester guests for binding to the positively charged cyclodextrins. This competition lowers the effective association constant between host and guest. Positively charged buffers such as Tris-HCl do not strongly compete and are thus more conducive to binding. The kinetics of dissociation of the host–guest complexes were measured in several buffers using ^{31}P EXSY experiments. These measurements demonstrate that negatively charged buffers decrease the equilibrium constant by lowering the rate of association of these complexes but in most cases do not effect the dissociation rates.

Introduction

In aqueous solution, cyclodextrins bind hydrophobic molecules in the interior of their cavities. The synthesis of modified cyclodextrins has expanded their recognition properties to include noncovalent binding motifs beyond simple hydrophobic interactions.[1] For example, the binding properties of a large number of modified cyclodextrins have been investigated that incorporate hydrogen bonding, electrostatic, and metal binding interactions.[2] Aminocyclodextrins (AminoCDs) are cyclodextrin derivatives that incorporate amino-containing functionality in place of the primary hydroxyl groups at the 6-positions of the sugar units. Such aminoCDs were first demonstrated to bind to phosphate esters such as benzyl phosphate through a combination of hydrophobic and electrostatic interactions by Knowles and Boger in 1979.[3] Since that time, a variety of aminoCDs have been developed that recognize phosphate esters,[4,5] including several with biological significance such as nucleotide mono- and triphosphates[6,7] and phosphotyrosine.[8] We have recently demonstrated that the binding interactions between phosphotyrosine and aminoCDs can be used to inhibit hydrolysis of the phosphate ester linkage in phosphotyrosine catalyzed by phosphatase enzymes.[9] Additionally, the investigations of Thatcher and co-workers have shown that aminoCDs bind to glycosaminoglycan sulfates and inhibit growth of neurites.[10] In vitro biological studies of this type typically require the use of solutions that contain buffers, and buffers are likely to mediate the strength of the electrostatic binding interactions between aminoCDs and negatively charged guest molecules. Therefore, the goal of the present study is to clarify the role that buffer structure and concentration plays in determining both the thermodynamics and kinetics of association between aminoCD hosts and phosphate ester guests. From a broader perspective, these studies provide a model system to study the effects of buffers on binding interactions, including small molecule–protein and protein–protein interactions, that occur in aqueous solution and that are mediated by electrostatic forces.

Results and Discussion

Cyclodextrin Hosts and Phosphate Ester Guests. Figure 1 shows the structures of compounds 1β and 2α, the two aminoCD hosts that are used in this study. The syntheses of these compounds has been reported by Darcy[7] and Thatcher,[11] respectively. Three aryl phosphates were used as guests; *p*-nitrophenyl phosphate (*p*-NPP), phosphotyrosine (Tyr(PO_3^{2-})), and *N*-acetyl-phosphotyrosine methyl ester (AcTyr(PO_3^{2-})OMe). The latter

(1) For a recent series of comprehensive reviews on all aspects of cyclodextrin chemistry, see: *Chem. Rev.* **1998**, *98*(5).

(2) For several recent examples of modified cyclodextrins binding to amino acids, see: (a) Bonomo, R. P.; Pedotti, S.; Vecchio, G.; Rizzarelli, E. *Inorg. Chem.* **1996**, *35*, 6873. (b) Liu, Y.; Zhang, Y.-M.; Qi, A.-D.; Chen, R.-T.; Yamamoto, K.; Wada, T.; Inoue, Y. *J. Org. Chem.* **1997**, *62*, 1826. (c) Liu, Y.; Zhang, Y.-M.; Qi, A.-D.; Chen, R.-T.; Yamamoto, K.; Wada, T.; Inoue, Y. *J. Org. Chem.* **1998**, *63*, 10085.

(3) (a) Boger, J.; Knowles, J. R. *J. Am. Chem. Soc.* **1979**, *101*, 7631. (b) Boger, J.; Brenner, D. G.; Knowles, J. R. *J. Am. Chem. Soc.* **1979**, *101*, 7630.

(4) Vizitiu, D.; Thatcher, G. R. J. *J. Org. Chem.* **1999**, *64*, 6235.

(5) Breslow, R.; Schmuck, C. *J. Am. Chem. Soc.* **1996**, *118*, 6601.

(6) (a) Eliseev, A. V.; Schneider, H.-J. *Angew. Chem., Int. Ed. Engl.* **1993**, *32*, 1331. (b) Eliseev, A. V.; Schneider, H.-J. *J. Am. Chem. Soc.* **1994**, *116*, 6081.

(7) (a) Schwinte, P.; Darcy, R.; O'Keeffe, F. *J. Chem. Soc., Perkin Trans. 2* **1998**, 805. (b) Ahern, C.; Darcy, R.; O'Keeffe, F.; Schwinte, P. *J. Incl. Phenom. Mol Recog. Chem.* **1996**, *25*, 43.

(8) Cotner, E. S.; Smith, P. J. *J. Org. Chem.* **1998**, *63*, 1737.

(9) Ghosh, M.; Sanders, T. C.; Zhang, R.; Seto, C. T. *Org. Lett.* **1999**, *1*, 1945.

(10) Borrajo, A. M. P.; Gorin, B. I.; Dostaler, S. M.; Riopelle, R. J.; Thatcher, G. R. J. *Bioorg. Med. Chem. Lett.* **1997**, *7*, 1185.

(11) Vizitiu, D.; Walkinshaw, C. S.; Borin, B. I.; Thatcher, G. R. J. *J. Org. Chem.* **1997**, *62*, 8760.

10.1021/jo991616d CCC: $19.00
Published on Web 01/14/2000

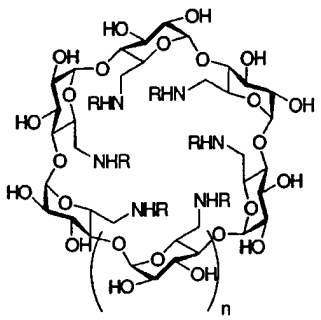

1β n = 2, R = $(CH_2)_2OH$
2α n = 1, R = $(CH_2)_2OH$

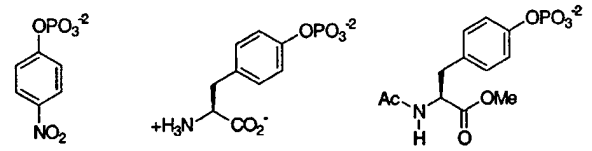

p-NPP Tyr(PO_3^{-2}) AcTyr(PO_3^{-2})OMe

Figure 1. Structures of positively charged cyclodextrin hosts and aryl phosphate guests.

Scheme 1[a]

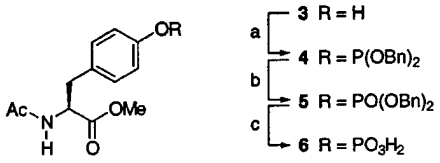

[a] Reagents and conditions: (a) $(BnO)_2PNEt_2$, tetrazole; (b) *m*-CPBA, 0 °C; (c) 5% Pd/C, H_2, MeOH.

compound was included in the study to determine if blocking the charged ammonium carboxylate portion of phosphotyrosine causes enhanced affinity to the cyclodextrin hosts. The synthesis of AcTyr(PO_3^{2-})OMe (**6**) is outlined in Scheme 1. *N*-Acetyltyrosine methyl ester was phosphorylated with dibenzyl-*N*,*N*-diethylphosphoramidite to give phosphite **4**. This compound was oxidized with *m*-CPBA to give the corresponding phosphate triester **5**. Finally, removal of the benzyl protecting groups with hydrogen and Pd/C gave the desired phosphate monoester **6**.

Measurement of Association Constants by NMR Spectroscopy. A variety of experimental methods have been used to measure association constants of cyclodextrins with guest molecules. These include UV and CD spectroscopies, calorimetry, potentiometric titration, and NMR spectroscopy. Potentiometric titration is one of the most common methods for investigating the binding interactions between positively charged cyclodextrins and phosphate esters.[6,7] This technique is useful because it provides information about both association constants and pK_a's of ionizable groups. However, potentiometric titration measurements must be performed in the absence of buffer, and buffers are typically required when investigating in vitro biological activity. Thus, association constants measured using this method may not accurately predict what will occur in biological systems.

Several reports show that nucleotide phosphates bind to positively charged cyclodextrins with significant affinity ($K_a \sim 10^4-10^5$ M^{-1}). These values were measured using potentiometric titration in nonbuffered aqueous NaCl solution.[6,7] Knowles has reported that benzyl phosphate binds to a positively charged cyclodextrin in triethanolamine buffer with similar affinity ($K_a \sim 3.2 \times 10^4$ M^{-1}).[3] In contrast, Breslow and Smith have shown that binding of aryl phosphates to positively charged cyclodextrins in *phosphate buffer* is somewhat weaker ($K_a \sim 10^2-10^3$ M^{-1}).[5,8] The 2- to 3-order of magnitude difference between these reported binding constants may simply reflect the differences in structures between the various cyclodextrin hosts and phosphate ester guests used in the studies. However, since electrostatic interactions are important in determining the strength of binding in all of these systems, it is also possible that the aqueous environment, specifically the buffer, plays a significant role in determining the association constants. Negatively charged buffers may have reasonable affinities for the positively charged cyclodextrins and effectively compete with a phosphate ester guest for binding with the cyclodextrin. This competition would have the effect of lowering the observed binding constant between host and guest.

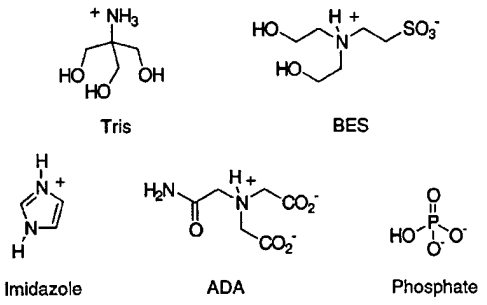

Tris BES

Imidazole ADA Phosphate

Figure 2. Structures of buffers.

To investigate this issue, we have measured the association constants of cyclodextrins 1β and 2α with three aryl phosphates in five different buffer systems in order to clarify the role that buffer structure and concentration plays in determining the magnitude of the binding interactions. Association constants were measured using NMR spectroscopy because this method is compatible with a variety of aqueous solutions. The structures of the buffers used in this study are shown in Figure 2. These buffers encompass a range of functional groups, sizes, and charge states that vary from −2 for phosphate at pH 7 to +1 for imidazole and Tris.

Three NMR methods were used to measure the association constants: ^1H NMR titrations and ^1H and ^{31}P NMR dilution experiments. We chose a particular experiment for a given complex based upon two considerations; signal dispersion of the aromatic protons of the guest and the rate of exchange between the free and bound guest. In general, complexes with *p*-NPP as the guest were in fast exchange on the NMR time scale, while complexes with Tyr(PO_3^{2-}) and AcTyr(PO_3^{2-})OMe were in the slow exchange regime. For complexes that displayed good signal dispersion and that were in fast exchange on the NMR time scale, the ^1H NMR titration method was used. In these experiments, the chemical shift of the aryl phosphate protons were monitored as a function of added cyclodextrin. Data were analyzed using a nonlinear curve fitting procedure to an equation, reported by Wilcox, that is based upon a simple 1:1 binding isotherm.[12] An

Table 1. Association Constants for Cyclodextrins 1β and 2α with Aryl Phosphates in a Variety of Buffers[a]

		K_{assoc} (M^{-1})						
CD	guest	Tris	imidazole	D_2O, NaCl	BES	ADA	10 mM HPO_4^{-2}	100 mM HPO_4^{-2}
1β	*p*-NPP	60 000[b] ± 15 000	210 000[b] ± 60 000	65 000[b] ± 13 000	34 000[b] ± 8000	2700[b] ± 600	2200[b] ±400	410[b] ± 80
1β	$Tyr(PO_3^{2-})$	130 000[c] ± 25 000			16 000[c] ±3000	1500[d] ± 300		710[d] ± 140
1β	$AcTyr(PO_3^{2-})OMe$	610 000[c] ± 120 000		430 000[c] ± 90 000				
2α	*p*-NPP	30 000[b] ± 6000		70 000[b] ± 10 000				370[d] ± 80
2α	$Tyr(PO_3^{2-})$	42 000[c] ± 8000						
2α	$AcTyr(PO_3^{2-})OMe$	150 000[c] ± 30 000		33 000[c] ± 6000				

[a] Buffer concentrations are 100 mM unless noted otherwise. The pH of all solutions was 7.0. [b] Measured by ^1H NMR titration experiments. [c] Measured ^1H NMR dilution experiments. [d] Measured by ^{31}P NMR dilution experiments.

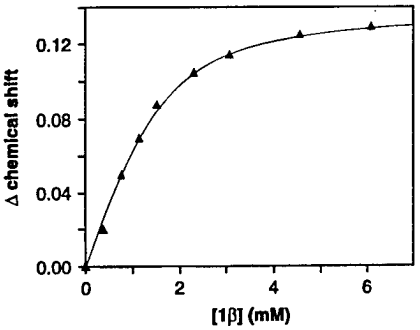

Figure 3. Titration of *p*-NPP (1.5 mM) with cyclodextrin 1β in 100 mM ADA buffer as monitored by ^1H NMR spectroscopy. The curve corresponds to the best fit of the data to a simple 1:1 binding isotherm.

example of one data set, along with the curve fit, is shown in Figure 3.

Complexes that were in slow exchange on the NMR time scale showed well-resolved signals for the free and bound guest. Integration of these resonances gave a measure of the relative concentrations of free and bound aryl phosphate. In these cases, an NMR sample containing aryl phosphate and a slight excess of cyclodextrin was prepared. The solution was diluted with buffer in several steps, and the ^1H NMR spectrum was monitored until it showed approximately a 1:1 mixture of free and bound aryl phosphate. At this point, the signals were integrated and the binding constant calculated on the basis of the known concentrations of aryl phosphate and cyclodextrin.

For several of the complexes in this study, the ^1H NMR spectra were not useful for measuring association constants because either exchange was intermediate on the NMR time scale and resonances were broad or the protons of the aryl phosphate were overlapping. In these cases, the ^{31}P NMR spectra showed well-resolved resonances for free and bound aryl phosphate. Thus, ^{31}P NMR dilution experiments were used to measure association constants. In all cases, there was a significant chemical shift difference between free and bound aryl phosphate in the ^{31}P spectrum, reflecting the large difference in environment experienced by the phosphate group in the free and bound forms. Relaxation rates (T_1) were measured for several of the free and complexed aryl phosphates to ensure that the relaxation delays used in the ^1H and ^{31}P NMR spectra were long enough to allow for accurate integration of resonances.

(12) Wilcox, C. S.; Cowart, M. D. *Tetrahedron Lett.* **1986**, *27*, 5563.

Association constants for the two cyclodextrin hosts with the three aryl phosphate guests in a variety of buffers are shown in Table 1. From these data, it is apparent that buffers have a dramatic impact on the value of the measured association constants. Differences of 3−4 orders of magnitude are observed on the basis of the structure and concentration of the buffer. The weakest binding constants were measured in 100 mM phosphate. Phosphate can associate with the ammonium groups of the cyclodextrin[13] and must be displaced before the aryl phosphate guest can bind. Part of the free energy that is gained from binding the aryl phosphate to the cyclodextrin is offset by the loss of binding interactions between the buffer and the cyclodextrin. This has the effect of lowering the observed binding constant. Lowering the phosphate concentration from 100 to 10 mM increases the association constant of *p*-NPP with 1β by a factor of 5 because there is less competition from the buffer. Measurements in 100 mM ADA buffer, which has one negative charge compared to phosphate with two negative charges, gives higher association constants. This result indicates that ADA is bound less tightly by the cyclodextrin than is phosphate.

A zwitterionic, but overall neutral, buffer such as BES does not compete as strongly for the cyclodextrin host. The sulfonate anion of BES is significantly stabilized by the intramolecular ammonium ion and gains only a small amount of additional stabilization by complexing with the cyclodextrin. Therefore, association constants measured in this buffer are significantly higher than those measured in ADA and phosphate buffers. In D_2O/NaCl solution that has been pH adjusted to 7.0, the association constants for *p*-NPP and $AcTyr(PO_3^{2-})OMe$ with 1β are in the range of 10^4-10^5 M^{-1}. These values are similar to those reported for binding of nucleotide phosphates to positively charged cyclodextrins as measured by potentiometric titration under similar conditions.[6,7] Association constants measured in buffers that bear a positive charge such as Tris and imidazole are of similar orders of magnitude. These solutions allow optimal interactions between the aryl phosphates and positively charged cyclodextrins, with the chloride counterion of the buffers providing little competition to the binding event.

Figure 4 shows a plot of the free energy of association for the various cyclodextrin−aryl phosphate combinations as a function of the buffer. From this pictorial represen-

(13) Schneider has reported that the binding constant between an aminoCD and inorganic phosphate is 3.7×10^3 M^{-1}. See ref 6.

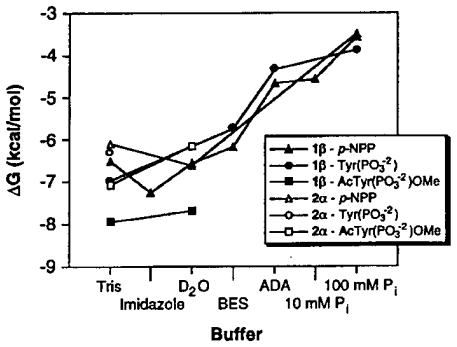

Figure 4. Free energy for the binding interaction between the cyclodextrin hosts and the aryl phosphate guests as a function of buffer structure.

tation of the binding data it becomes apparent that the two cyclodextrin hosts bind the three aryl phosphate guests with similar affinity in any particular buffer system. The only exception is the complex between 1β and AcTyr(PO_3^{2-})OMe, which has an association constant that is significantly higher than the other complexes. The difference in affinity between the complexes of 1β with Tyr(PO_3^{2-}) and AcTyr(PO_3^{2-})OMe suggests that the later compound makes better hydrophobic contacts with the cyclodextrin host. In addition, molecular models suggest that there is a good steric compatibility between AcTyr(PO_3^{2-})OMe and cyclodextrin 1β, while the cavity of 2α is too narrow for an optimal fit.

The binding data presented here demonstrate that negatively charged buffers weaken the association between aryl phosphate guests and positively charged cyclodextrin hosts by competing with the guest for the available binding sites. If these cyclodextrin derivatives are used to influence the activity of biological macromolecules in vitro, positively charged buffers should be used in order to maximize binding interactions between negatively charged guests and the aminoCD hosts.

Measurement of Dissociation Rates by Exchange Spectroscopy. The equilibrium constants discussed in the previous section provide insights into how buffers affect the thermodynamics of aryl phosphates binding to cyclodextrins. We are also interested in how buffers influence the kinetics of such binding events. In previous work we have used ROESY experiments to make rough estimates of the dissociation rate constants of several of the complexes.[9] To determine these rate constants more precisely, we have measured them using ^{31}P 2D exchange spectroscopy (EXSY). These experiments were performed on the complex between Tyr(PO_3^{-2}) and cyclodextrin 1β in a variety of buffers in order to examine the relationship between dissociation rate and buffer structure.

The EXSY experiment uses the same pulse sequence as a NOESY experiment, and cross-peaks of opposite sign are observed for NOEs and exchange. For the complex between Tyr(PO_3^{2-}) and 1β, we observe separate resonances for free and bound Tyr(PO_3^{2-}) in the ^{31}P NMR spectrum, and no cross-peaks can occur for NOE interactions. If the mixing time used in the experiment is short compared to the rate of exchange between free and bound Tyr(PO_3^{2-}), then no cross-peak is observed between these species. However, if the mixing time is of the same order of magnitude or longer than the exchange rate, then a cross-peak will be observed. The volume of the cross-peak is proportional to the amount of exchange that has occurred during the mixing time and, thus, can be used to calculate the exchange rate. One EXSY spectrum is shown in Figure 5 as an example, and a summary of the exchange data is given in Table 2.

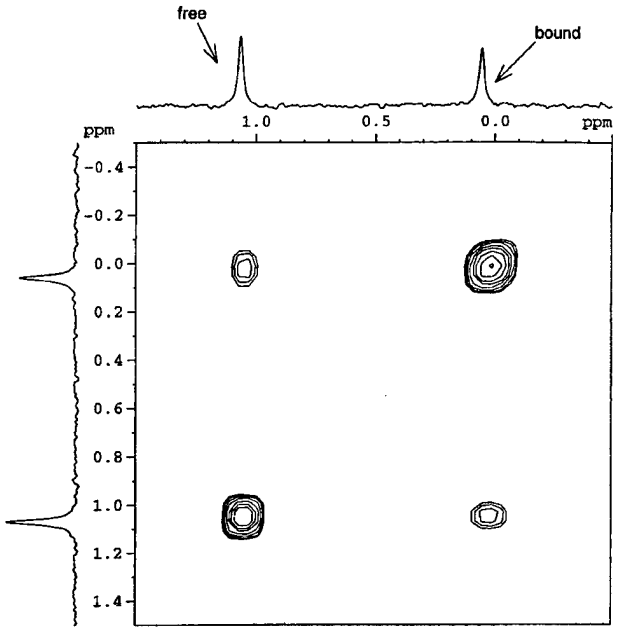

Figure 5. ^{31}P EXSY spectrum of the complex between cyclodextrin 1β and Tyr(PO_3^{-2}) in 100 mM ADA buffer at pH 7.0. The mixing time in this experiment was 50 ms.

Table 2. Rate Constants, k_{off}, for Dissociation of Complexes between Positively-Charged Cyclodextrins and Tyr(PO_3^{2-}) Determined by ^{31}P EXSY Experiments (T = 25 °C)

CD	buffer	k_{off} (s^{-1})	k_{on}[a] ($M^{-1}s^{-1}$)
1β	100 mM phosphate	45 ± 5	32 000
1β	100 mM ADA	7 ± 1	10 500
1β	100 mM BES	7 ± 1	110 000
1β	100 mM Tris	7 ± 1	910 000
2α	100 mM Tris	$2 \times 10^{-3} \pm 0.4 \times 10^{-3}$ [b]	84

[a] k_{on} values are inferred based upon the measured k_{off} and K_{assoc} values shown this table and Table 1. [b] This value is extrapolated from measurements that were performed at higher temperatures (see text).

When ADA, BES, and Tris are used as buffers, the dissociation rate constants are 7 s^{-1}, despite the fact that the binding constants in these buffers range from 1500 M^{-1} for ADA to 130 000 M^{-1} for Tris. The fact that these off-rates are idential shows that the buffer does not participate during the rate-limiting step for dissociation. Thus, the dissociation rate constant of 7 s^{-1} simply represents the rate at which phosphotyrosine dissociates from the cyclodextrin in aqueous solution. This slow step is then followed by a second fast step that involves binding of the buffer to the empty cyclodextrin. In contrast, the buffer is critical for determining the rate that Tyr(PO_3^{2-}) associates with the cyclodextrin. Association rate constants (k_{on}) are provided in Table 2 and have been calculated on the basis of the measured K_{assoc} and k_{off} values. These data are consistent with an interpretation in which the cyclodextrin, in the absence of Tyr(PO_3^{2-}), binds to buffers that incorporate a negatively charged functional group. In order for Tyr(PO_3^{2-}) to bind, the buffer must first dissociate, and it is this dissociation reaction that controls the overall rate at which Tyr(PO_3^{2-})

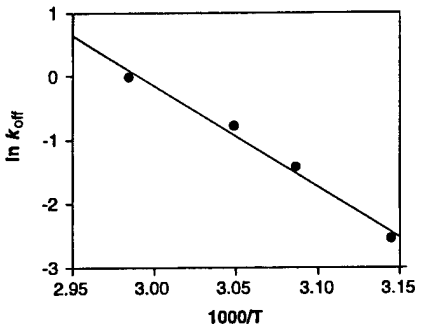

Figure 6. Arrenhius plot for dissociation of the complex between cyclodextrin 2α and Tyr(PO_3^{-2}) in 100 mM Tris buffer at pH 7.0. The *y*-intercept gives the preexponential factor ($A = 1.4 \times 10^{22}$ s^{-1}) and the slope gives E_a/R. The activation energy for this dissociation reaction is 34 kcal/mol. The rate constants for dissociation at the four temperatures are k = 0.064 s^{-1} (45 °C), 0.22 s^{-1} (51 °C), 0.42 s^{-1} (55 °C), and 0.98 s^{-1} (62 °C).

binds to the cyclodextrin. After the buffer dissociates from the cyclodextrin, the Tyr(PO_3^{2-}) can bind to the empty cavity in a faster second step. Tris, which is positively charged and has chloride as the counterion, is not likely to complex strongly with the cyclodextrin and provides the fastest association rate between Tyr(PO_3^{2-}) and the cyclodextrin. BES, which is neutral overall but possesses a negatively charged sulfonate group, slows the association rate by almost 1 order of magnitude. The association rate is slowest in ADA buffer, which has an overall negative charge and is likely to bind well to the cyclodextrin.

In phosphate buffer, the dissociation rate constant is six to seven times faster than what is observed in ADA, BES, and Tris buffers. The higher off-rate suggests that phosphate, unlike the other buffers, is playing an active role in facilitating dissociation of Tyr(PO_3^{2-}) from 1β. We suggest two possible interpretations of this result. First, phosphate may actively catalyze displacement of the Tyr(PO_3^{2-}) from the cyclodextrin by stabilizing the transition state for dissociation through formation of electrostatic interactions with the ammonium groups of the cyclodextrin. A second possibility is that the ground state of the complex actually involves a ternary aggregate between Tyr(PO_3^{2-}), 1β, and inorganic phosphate. Electrostatic interactions between inorganic phosphate and the cyclodextrin would weaken the interactions with Tyr(PO_3^{2-}) and thus decrease the amount of energy necessary for dissociation.

The dissociation rate constant for the complex between Tyr(PO_3^{2-}) and the α-cyclodextrin derivative 2α is too small to measure at room temperature using the ^{31}P EXSY experiment. The phosphorus nuclei relax completely to the ground state before any exchange takes place, and therefore, no cross-peaks are observed in the EXSY spectrum no matter how long the mixing time that is used. To circumvent this problem, we have measured the dissociation rate constant at several different temperatures above 25 °C in a range in which the rate can be measured conveniently by EXSY spectroscopy. Extrapolation of the rate constant back to room temperature gives the value for this complex shown in Table 2. Figure 6 shows an Arrenhius plot of the exchange data at four different temperatures, and these data can be used to calculate thermodynamic parameters for the transition-state of the dissociation reaction. The calculated values are $\Delta G^{\ddagger} = 21$ kcal/mol, $\Delta H^{\ddagger} = 33$ kcal/mol, and $\Delta S^{\ddagger} = 41$ eu ($T\Delta S^{\ddagger} = 12$ kcal/mol at 25 °C). The reaction is entropically favored as is expected for a dissociation process, and the enthalpy change on going to the transition-state is surprisingly high for a reaction that involves only noncovalent interactions. There is likely to be significant error in the entropy calculation because the temperature range covered by these experiments is fairly small.

The dissociation rate constant for the Tyr(PO_3^{2-})–2α complex is 3 orders of magnitude smaller than the complex with 1β, and the calculated rate constant for association is also small. The interior diameter of the cavity in α-cyclodextrin is significantly narrower than that of β-cyclodextrin, and presents a sterically constrained hydrophobic pocket through which the phosphate group of Tyr(PO_3^{2-}) must pass in order for association or dissociation to occur. In the case of 1β, the cavity is large enough to allow the phosphate group, perhaps in the solvated form, to pass through it during these processes. This lowers the energy of the transition state for exchange. However, in the case of 2α the tight confines of the cavity do not easily allow Tyr(PO_3^{2-}), in the free or solvated form, to pass through it during exchange. Therefore, there is a large energy barrier for both association and dissociation. This interpretation is supported by molecular models of the two complexes.[14]

Conclusions

The structure and concentration of buffers play a major role in controlling both the thermodynamics and kinetics of binding interactions of aminoCDs 1β and 2α with aryl phosphate guest molecules. Negatively charged buffers compete with the aryl phosphate guest for the positively charged binding site of the cyclodextrin, and this competition lowers the effective binding constant. Based upon these results, we conclude that positively charged buffers such as Tris and imidazole should be used when studying the influence of these cyclodextrins on biological systems. The ^{31}P EXSY experiments show that, with the exception of phosphate, buffers exert a major influence on the association rates of aryl phosphates with cyclodextrins, but have no effect on the dissociation rates.

One of the disadvantages of the aminoCDs in their present form is that they show low selectivity and will thus bind to many sterically compatible phosphate esters. To make the aminoCDs more useful for biological studies, we are modifying their structure to make them more specific for particular phosphotyrosine-containing sequences and structures within peptides and proteins. Such modifications include addition of a second CD unit that is designed to bind to the side chain of a nearby hydrophobic residue, and functionalization of the aminoCDs with Lewis acidic groups such as activated carbonyl compounds or boronic acids that are designed to interact with the side chains of proximal nucleophilic amino acids.

Experimental Section

General Methods. Reactions were conducted under an atmosphere of dry nitrogen in oven-dried glassware. Anhy-

(14) Thatcher and co-workers have recently reported that the coalescence temperature for free 4-isopropylphenyl phosphate and 4-isopropylphenyl phosphate that is bound to an aminoCD is approximately 100 °C. These authors also attribute the large barrier to exchange to the passage of the phosphate group through the hydrophobic cavity of the CD. See ref 4.

drous procedures were conducted using standard syringe and cannula transfer techniques. THF was distilled from sodium and benzophenone. Other solvents were of reagent grade and were stored over 4 Å molecular sieves. All other reagents were used as received. Organic solutions were dried over $MgSO_4$ unless otherwise noted. Solvent removal was performed by rotary evaporation at water aspirator pressure.

***N*-Acetyl-L-tyrosine Dibenzyl Phosphate Methyl Ester 5.** 1*H*-Tetrazole (1.68 g, 23.5 mmol), *N*-acetyl-L-tyrosine methyl ester (2.0 g, 7.8 mmol), and dibenzyl *N,N*-diethylphosphoramidite (4.7 mL, 15.6 mmol) were combined in 8 mL of dry THF, and the solution was stirred at 25 °C for 1 h. The mixture was then cooled to −40 °C in a dry ice−acetone bath, and a solution of 77% *m*-CPBA (2.6 g, 11.6 mmol) dissolved in 20 mL of methylene chloride was added via syringe. After the addition was complete, the reaction was warmed to 25 °C and stirred for 30 min, then 10 mL of a 10% aqueous solution of $NaHSO_3$ was added and the reaction was stirred for an additional 10 min. The mixture was extracted with ether, and the organic layer was washed twice with 10% aqueous $NaHSO_3$, twice with 5% aqueous $NaHCO_3$, and once with brine and dried over $MgSO_4$. The solvent was removed by rotary evaporation, and the product was purified by flash chromatography (1:9 hexanes/ethyl acetate) to give 1.9 g (3.9 mmol, 50%) of *N*-acetyl-L-tyrosine dibenzyl phosphate methyl ester: ^{1}H NMR (300 MHz, $CDCl_3$) δ 1.94 (s, 3H), 3.02−3.08 (m, 2H), 3.67 (s, 3H), 4.82 (dd, J = 14.6, 6.3 Hz, 1H), 5.10 (d, J = 8.3 Hz, 4H), 6.43 (d, J = 7.7 Hz, 1H), 7.03 (d, J = 8.6 Hz, 2H), 7.07 (d, J = 8.6 Hz, 2H), 7.31 (s, 10H); ^{13}C NMR (75 MHz, $CDCl_3$) δ 22.7, 36.8, 52.1, 69.5 (d, J = 5.6 Hz), 119.8 (d, J = 4.7 Hz), 127.8, 128.3, 128.4, 130.3, 132.8, 135.1 (d, J = 7.1 Hz), 149.4 (d, J = 7.1 Hz), 169.7, 171.8; HRMS-FAB (M + H$^+$) calcd for $C_{26}H_{29}NO_7P$ 498.1680, found 498.1692.

***N*-Acetyl-L-tyrosinephosphate Methyl Ester 6.** To a solution of **5** (0.77 g, 1.4 mmol) in 2 mL of MeOH was added a catalytic amount of 5% Pd/C, and hydrogen gas was bubbled into the reaction mixture. The reaction was stirred for 3 h at 25 °C under an atmosphere of hydrogen. The catalyst was removed by filtration, and the solvent was removed by rotary evaporation to give 421 mg (1.27 mmol, 91%) of compound **6** as a clear oil: ^{1}H NMR (300 MHz, MeOH-d_4) δ 1.93 (s, 3H), 2.95 (dd, J = 13.6, 9.3 Hz, 2H), 3.14 (dd, J = 13.6, 5.7 Hz, 1H), 3.69 (s, 3H), 4.65 (dd, J = 9.3, 5.7 Hz, 1H), 7.15 (d, J = 8.6 Hz, 2H), 7.21 (d, J = 8.6 Hz, 2H); ^{13}C NMR (75 MHz, MeOH-d_4) δ 21.2, 36.6, 51.6, 54.3, 120.3 (d, J = 4.7 Hz), 130.3, 133.6, 150.7 (d, J = 6.2 Hz), 172.2, 172.4; HRMS-FAB (M + Na$^+$) calcd for $C_{12}H_{16}NNaO_7P$ 340.0561, found 340.0562.

^{1}H NMR Titration Experiments. For the ^{1}H NMR titration experiments, the conditions that were used during each titration are provided in the following format: Complex: buffer, cyclodextrin concentration or range of concentrations used, aryl phosphate concentration or range of concentrations used, identity of the proton or protons that were monitored during the titration experiment. 1β−*p*-NPP: 100 mM Tris, 0−0.25 mM, 0.05 mM, aromatic protons of the aryl phosphate. 1β−*p*-NPP: 100 mM imidazole, 0.05 mM, 0−0.20 mM, H4 of the cyclodextrin. 1β−*p*-NPP: D_2O/NaCl, 0−0.38 mM, 0.1 mM, aromatic protons of the aryl phosphate. 1β−*p*-NPP: 100 mM BES, 0−1.0 mM, 0.21 mM, aromatic protons of the aryl phosphate. 1β−*p*-NPP: 100 mM ADA, 0−6.1 mM, 1.5 mM, aromatic protons of the aryl phosphate. 1β−*p*-NPP: 10 mM phosphate, 0−4.4 mM, 0.74 mM, aromatic protons of the aryl phosphate. 1β−*p*-NPP: 100 mM phosphate, 0−10 mM, 1.0 mM, aromatic protons of the aryl phosphate. 2α−*p*-NPP: 100 mM Tris, 0.05 mM, 0−0.25 mM, H4 of the cyclodextrin. 2α−*p*-NPP: D_2O/NaCl, 0.1 mM, 0−0.63 mM, H4 of the cyclodextrin.

^{1}H NMR Dilution Experiments. For the ^{1}H NMR dilution experiments, the conditions that were used during each experiment are provided in the following format: Complex: buffer, final cyclodextrin concentration, final aryl phosphate concentration, identity of the proton or protons that were monitored during the dilution experiment. 1β−AcTyr(PO_3^{-2})-OMe: 100 mM Tris, 0.027 mM, 0.025 mM, *N*-Ac protons of the aryl phosphate. 1β−Tyr(PO_3^{-2}): 100 mM Tris, 0.019 mM, 0.018 mM, aromatic protons of the aryl phosphate. 1β−Tyr(PO_3^{-2}): 100 mM BES, 0.14 mM, 0.087 mM, aromatic protons of the aryl phosphate. 1β−AcTyr(PO_3^{-2})OMe: D_2O/NaCl, 0.026 mM, 0.022 mM, *N*-Ac protons of the aryl phosphate. 2α−Tyr(PO_3^{-2}): 100 mM Tris, 0.093 mM, 0.067 mM, aromatic protons of the aryl phosphate. 2α−AcTyr(PO_3^{-2})OMe: 100 mM Tris, 0.063 mM, 0.050 mM, *N*-Ac protons of the aryl phosphate. 2α−AcTyr(PO_3^{-2})OMe: D_2O/NaCl, 0.055 mM, 0.050 mM, *N*-Ac protons of the aryl phosphate.

^{31}P NMR Dilution Experiments. For the ^{31}P NMR dilution experiments, the conditions that were used during each experiment are provided in the following format: Complex: buffer, final cyclodextrin concentration, final aryl phosphate concentration. In all of these experiments, the resonance of the phosphate group of the aryl phosphate was monitored. 1β−Tyr(PO_3^{-2}): 100 mM ADA, 1.40 mM, 1.12 mM. 1β−Tyr(PO_3^{-2}): 100 mM phosphate, 2.9 mM, 2.6 mM. 2α−*p*-NPP: 100 mM phosphate, 8.0 mM, 4.5 mM.

^{31}P 2D Exchange Spectroscopy Experiments. The phase-sensitive 2D ^{31}P−^{31}P EXSY spectra were recorded at 27 °C at 161.9 MHz on a Bruker AMX 400 spectrometer equipped with an SGI computer, using a 5 mm QNP probe. The 2D EXSY maps were obtained from the basic NOESY pulse sequence that involves three 90° pulses with time-proportional phase increments and 16-order phase cycling. Sixteen scans were accumulated for each of the 128 t_1 increments, zero filled to 512 W in the F_1 dimension and using 512 W in the F_2 dimension with no zero filling, a 2 s relaxation delay and a spectral window of 3221 Hz. Preliminary experiments with longer relaxation delays did not reveal any significant change in the relative integrals of the resonances, indicating essentially full relaxation within the recycling delay. The free induction delay was multiplied by a sine bell function with $\phi = \pi/2$. The 2D spectra were phase and baseline corrected in both dimensions and diagonal and cross-peak volumes were determined using the standard Bruker Avance software. The rate constants were evaluated using the method of Harzell and co-workers.[15]

For cases in which the T_1 values of the free and bound aryl phosphate were much less than the exchange rate constant ($k_{ex} \equiv k_{off}$), the effects of longitudinal cross relaxation rates were ignored. For cases in which the T_1 values were of the same order of magnitude as the exchange rate constant, the k_{ex} value was corrected for the effects of longitudinal cross relaxation using the method described by Macura and Ernst.[16] The equation relating the values of k_{ex} to the ratios of the areas of bound diagonal to cross-peaks, I_{ii}/I_{ij}, for the case of equal concentration of free and bound species, is shown below and is taken from ref 16.

$$I_{ii}/I_{ij} = 1/2(R_c/k_{ex})[(1 + e^{-Rc\tau m})/(1 - e^{-Rc\tau m})] - {}^1/_2(\Delta R/k_{ex})$$

In this equation, $\Delta R = R_{(bound)} - R_{(free)} = 1/T_{1(bound)} - 1/T_{1(free)}$, and $R_c = [\Delta R^2 + 4k_{ex}^2]^{1/2}$. The value of k_{ex} was obtained using a computer program to solve in an iterative fashion for I_{ii}/I_{ij}, starting from a given value of k_{ex} and the observed values of T_1 for each temperature. Iterations were continued until the calculated I_{ii}/I_{ij} ratio agreed to better than 1% with the experimentally observed value. Data for the complex between cyclodextrin 2α and Tyr(PO_3^{2-}) in 100 mM Tris buffer at four different temperatures are as follows, where $k_{ex,uncorr}$ corresponds to the experimentally observed values and $k_{ex,corr}$ are the values that have been corrected for the effects of longitudinal cross relaxation. 45 °C: $k_{ex,uncorr}$ = 0.078 s^{-1}, $k_{ex,corr}$ = 0.064 s^{-1}; 51 °C: $k_{ex,uncorr}$ = 0.239 s^{-1}, $k_{ex,corr}$ = 0.217 s^{-1}; 55 °C: $k_{ex,uncorr}$ = 0.457 s^{-1}, $k_{ex,corr}$ = 0.415 s^{-1}; 62 °C: $k_{ex,uncorr}$ = 1.09 s^{-1}, $k_{ex,corr}$ = 0.980 s^{-1}.

T_1 Measurements. Phosphorus T_1 relaxation times were measured using a ^{31}P inversion recovery sequence with increasing delays between the 180° inversion pulse and the

(15) Hartzell, C. J.; Mente, S. R.; Eastman, N. I.; Beckett, J. L. *J. Phys. Chem.* **1993**, *97*, 4887.

(16) Macura, S.; Ernst, R. R. *Mol. Phys.* **1980**, *41*, 95, eq 23.

90° observe pulse. The intensities of the peaks were plotted against the delay times, and the T_1 values were calculated using standard Bruker software. To measure the T_1 value of the phosphate group in a cyclodextrin–aryl phosphate complex, a solution of the complex was prepared in which greater than 99% of the aryl phosphate was present in the complexed form. **1**β–Tyr(PO_3^{2-}): T_1 = 1.01 s (100 mM phosphate, 25 °C); Tyr(PO_3^{2-}): T_1 = 6.29 s (100 mM phosphate, 25 °C); **2**α–Tyr(PO_3^{2-}): T_1 = 1.89 s (100 mM Tris, 62 °C); **2**α–Tyr(PO_3^{2-}): T_1 = 1.33 s (100 mM Tris, 45 °C); Tyr(PO_3^{2-}): T_1 = 6.88 s (100 mM Tris, 62 °C); Tyr(PO_3^{2-}): T_1 = 5.23 s (100 mM Tris, 45 °C).

Acknowledgment. This research was supported by the U.S. Army Medical Research and Material Command–Breast Cancer Research Initiative through a Career Development Award to C.T.S. (Grant No. DAMD17-96-1-6161).

Supporting Information Available: Copies of ^1H and ^{13}C NMR spectra for compounds **5** and **6**. This material is available free of charge via the Internet at http://pubs.acs.org.

JO991616D

THE JOURNAL OF BIOLOGICAL CHEMISTRY
Vol. 275, No. 29, Issue of July 21, pp. 22452–22460, 2000
Printed in U.S.A.

Biotinylation of Substituted Cysteines in the Nicotinic Acetylcholine Receptor Reveals Distinct Binding Modes for α-Bungarotoxin and Erabutoxin a*

Received for publication, February 15, 2000, and in revised form, April 27, 2000
Published, JBC Papers in Press, April 28, 2000, DOI 10.1074/jbc.M001283200

Armin Spura‡§, Ryan U. Riel‡, Neal D. Freedman‡, Shantanu Agrawal‡, Christopher Seto¶, and Edward Hawrot‡‖

From the ‡Department of Molecular Pharmacology, Physiology, and Biotechnology, Division of Biology and Medicine, and the ¶Department of Chemistry, Brown University, Providence, Rhode Island 02912

Although previous results indicate that α-subunit residues Trp[187], Val[188], Phe[189], Tyr[190], and Pro[194] of the mouse nicotinic acetylcholine receptor are solvent-accessible and are in a position to contribute to the α-bungarotoxin (α-Bgtx) binding site (Spura, A., Russin, T. S., Freedman, N. D., Grant, M., McLaughlin, J. T., and Hawrot, E. (1999) *Biochemistry* 38, 4912–4921), little is known about the accessibility of other residues within this region. By determining second-order rate constants for the reaction of cysteine mutants at α184–α197 with the thiol-specific biotin derivative (+)-biotinyl-3-maleimidopropionamidyl-3,6-dioxaoctanediamine, we now show that only very subtle differences in reactivity (~10-fold) are detectable, arguing that the entire region is solvent-exposed. Importantly, biotinylation in the presence of saturating concentrations of the long neurotoxin α-Bgtx is significantly retarded for positions αW187C, αF189C, and reduced wild-type receptors (αCys[192] and αCys[193]), further emphasizing their major contribution to the α-Bgtx binding site. Interestingly, although biotinylation of position αV188C is not affected by the presence of α-Bgtx, erabutoxin a, which is a member of the short neurotoxin family, inhibits biotinylation at position αV188C, but not at αW187C or αF189C. Taken together, these results indicate that short and long neurotoxins establish interactions with distinct amino acids on the nicotinic acetylcholine receptor.

The nicotinic acetylcholine receptor (AChR)[1] is the major prototype for neurotransmitter-gated ion channels and is found at high concentrations in the postsynaptic membranes of muscle cells, where it mediates the rapid propagation of electrical signals at the neuromuscular junction. It is a pentameric protein composed of four subunit types in a molar ratio $2\alpha:\beta:\gamma:\delta$ (see Ref. 1 for review).

An important first step in assessing the structure and function of such ion channels at a molecular level is to determine their transmembrane topology. To address this issue, a variety of techniques have been developed (see Ref. 2 for review). The most commonly used methods are the epitope protection assay (3–5), in which an epitope that is recognized by a specific antibody is fused to the protein of interest, and *N*-linked glycosylation tagging, wherein *N*-linked glycosylation sites can be engineered into the protein under investigation and glycosylation can then be evaluated (6–8).

The above methods, however, are only useful to assess overall topology of membrane proteins. For the nAChR, there is general consensus on the overall topology, although final proof will have to await high resolution structural data; each subunit possesses a large, extracellular amino-terminal domain, which is followed by four transmembrane-spanning regions and a short extracellular carboxyl terminus (9). In contrast, the key structural issue of whether individual residues are solvent-exposed has not been resolved. To address this issue, Gallivan *et al.* (10) have recently employed the *in vivo* nonsense suppression technique to incorporate derivatives of the unnatural amino acid biocytin into the nAChR heterologously expressed in *Xenopus* oocytes. By evaluating the binding of ^{125}I-streptavidin to biotinylated receptors, they studied the surface exposure of individual residues comprising the main immunogenic region (spanning positions 67–76; Ref. 11) and showed that position α70 was highly exposed.

In the current study, we have used the substituted cysteine accessibility method (12, 13) to systematically map the accessibility of individual residues between positions 184 and 197 of the α-subunit, the main determinant for agonist and competitive antagonist binding to the nAChR (14–16). To achieve this, we have introduced cysteine residues into the nAChR and labeled them with thiol-reactive, water-soluble biotin derivatives. Subsequently, we precipitated biotinylated receptors with immobilized streptavidin and probed the immunoprecipitates by Western blotting. Previous studies of oocyte-expressed Cys substitution mutations of α-subunit residues 181–197 (17) indicate that the majority of these substitutions are well tolerated and lead to minimal perturbations in receptor function.

Here, we show that positions 184–197 are all amenable to biotinylation, suggesting that the entire region is surface-exposed. In addition, modifications with the uncharged biotin derivative occur with similar rates for all of these residues. Moreover, we demonstrate that preincubation with the competitive antagonist α-Bgtx, a long-chain α-neurotoxin, selectively

* This work was supported by Research Grant GM32629 (to E. H.) from the National Institutes of Health. The costs of publication of this article were defrayed in part by the payment of page charges. This article must therefore be hereby marked "*advertisement*" in accordance with 18 U.S.C. Section 1734 solely to indicate this fact.

§ This work was done in partial fulfillment of the requirements for a Ph.D. degree from Brown University.

‖ To whom correspondence should be addressed. Tel.: 401-863-1034; Fax: 401-863-1595; E-mail: edward_hawrot@brown.edu.

[1] The abbreviations used are: AChR, acetylcholine receptor; ACh, acetylcholine; nAChR, nicotinic acetylcholine receptor; BrACh, bromoacetylcholine; Bgtx, bungarotoxin; DTT, dithiothreitol; Ea, erabutoxin a; MTSEA-biotin, *N*-biotinylaminoethyl methanethiolsulfonate; MTSEDE-biotin, *N*-methanethiolsulfonyl-*N*′-biotinyl-2,2′-(ethylenedioxy)bis (ethylamine), MTSET, [2-(trimethylammonium)ethyl-]methanethiolsulfonate; *Nmm*I, *Naja mossambica mossambica* I; PEO-biotin;(+)-biotinyl-3-maleimidopropionamidyl-3,6-dioxaoctanediamine; DMF, dimethylformamide; mAb, monoclonal antibody; Boc, butoxycarbonyl; RIPA, radioimmune precipitation buffer.

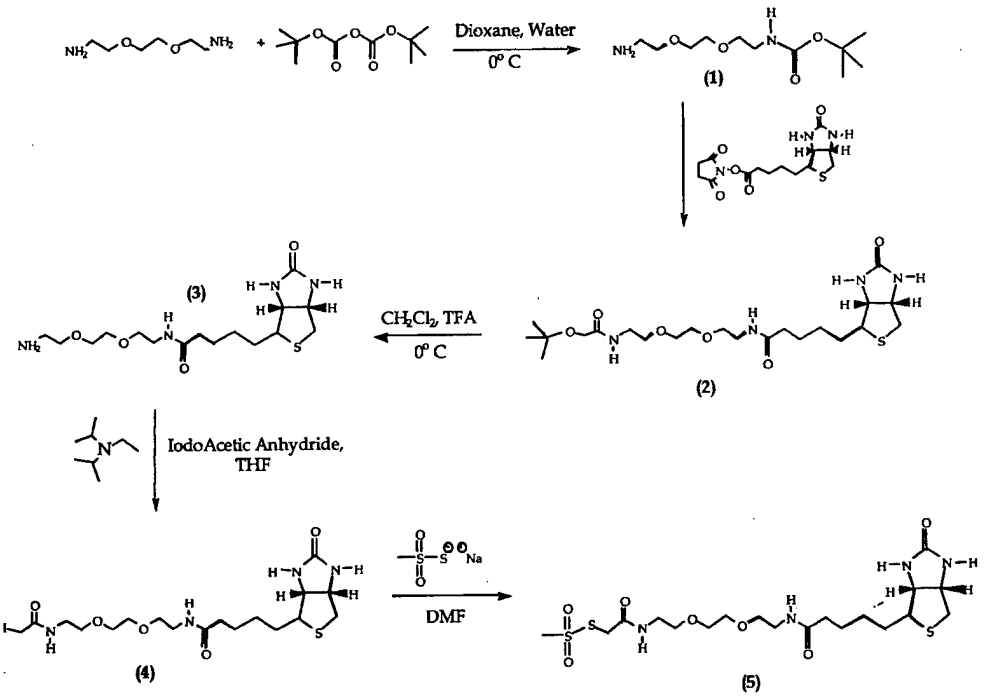

FIG. 1. **Synthesis scheme for MTSEDE-biotin.**

blocks biotinylation of positions 187, 189, and cysteines 192 and 193 in reduced wild-type receptors, demonstrating the importance of these residues in the binding of α-Bgtx and further supporting results we obtained previously (16). In contrast, preincubation with Ea, a short-chain α-neurotoxin, yields a different footprint, preventing only position 188 and reduced wild-type receptors from biotinylation. Thus, our findings strongly argue that long- and short-chain α-neurotoxins interact selectively with different positions when blocking agonist binding on the nAChR.

MATERIALS AND METHODS

Reagents

MTSEA-biotin was from Toronto Research. PEO-biotin and streptavidin-agarose beads were from Pierce, mAb 35 from Research Biochemicals International, and Protein G-agarose beads from Santa Cruz Biotechnology.

Mutagenesis

We used a cytomegalovirus-based expression vector (GWI, British Biotechnology, Oxford, United Kingdom) to express the cDNAs for the α-, β-, γ-, and δ-subunits of the mouse muscle nicotinic AChR. Mutations were introduced using the Quikchange mutagenesis kit (Stratagene, La Jolla, CA) following the manufacturer's specifications. Mutations were confirmed by diagnostic restriction enzyme digests and bidirectional sequencing of the entire insert following a DyeDeoxy terminator protocol (Perkin-Elmer).

Transfections and Cell Lines

These have been described previously (16).

Synthesis of N-Methanethiolsulfonyl-N'-biotinyl-2,2'-(ethylenedioxy)bis(ethylamine) (MTSEDE-biotin)

MTSEDE-biotin belongs to a class of compound generally known as alkyl alkanethiolsulfonates. It was synthesized as follows (Fig. 1).

Step 1: N-Boc-2,2'-(ethylenedioxy)bis(ethylamine) Derivative (18)—2,2'-(Ethylenedioxy)bis(ethylamine) (38 g, 257 mmol) was dissolved in 40 ml of deionized water and 40 ml of dioxane. While this solution was stirring, di-*tert*-butyl dicarbonate (8 g, 36.7 mmol) dissolved in 80 ml of dioxane was added dropwise. Formation of the bis-Boc-protected product was discouraged by performing the dropwise addition at 0 °C. The reaction was warmed to room temperature and stirred for 6 h. The solvents were removed by rotary evaporation, and the product was dissolved in ethyl acetate and washed with saturated $NaHCO_3$. The organic layers were dried over sodium carbonate, gravity-filtered, and rotary-evaporated to remove ethyl acetate. Flash chromatography using a 20% MeOH, 1% NH_4OH, CH_2Cl_2 solvent system gave a 66% yield (6 g, 2.4 mmol) of a yellowish oil.

Step 2: N-Boc-N'-biotinyl-2,2'-(ethylenedioxy)bis(ethylamine) Derivative (18)—The mono-Boc-protected diamine (0.38 g, 0.15 mmol) was dissolved in 8 ml of methanol. To this solution was added diisopropylethylamine (1.2 g, 0.9 mmol) and biotin *N*-hydroxysuccinimide ester (0.78 g, 0.2 mmol). The flask was stirred at room temperature for 4 h, concentrated by rotary evaporation, and redissolved in 50 ml of ethyl acetate. This solution was washed once with 10 ml HCl, once with 10 ml of $NaHCO_3$, and once with brine. The organic layer was dried over magnesium sulfate, gravity-filtered through celite, and rotary-evaporated. Flash chromatography with an 8% $MeOH/CH_2Cl_2$ solvent system gives a 69% yield (0.5 g, 0.1 mmol) of a white solid.

Step 3: N'-Biotinyl-2,2'-(ethylenedioxy)bis(ethylamine) Derivative (19)—The Boc-protected biotin diamine (0.5 g, 0.1 mmol) was dissolved in 4.9 ml of trifluoroacetic acid and stirred at room temperature for 20 min. The reaction flask was rotary-evaporated to remove trifluoroacetic acid, producing a brownish oil. This oil was dissolved in a few drops of deionized water and placed under vacuum to remove any remaining trifluoroacetic acid. Thin layer chromatography (15% $MeOH/CH_2Cl_2$) showed the product spot very close to the base line, suggesting that it contained the extremely polar free amine.

Step 4: N-Iodoacetyl-N'-biotinyl-2,2'-(ethylenedioxy)bis(ethylamine) Product—The biotin diamine (0.06 g, 0.02 mmol) was dissolved in 2 ml of tetrahydrofuran and stirred at room temperature. To this solution, iodoacetic anhydride (0.17 g, 0.05 mmol) and diisopropylethylamine (0.12 g, 0.1 mmol) were added. The reaction was allowed to proceed for 1 h, after which the flask was rotary evaporated to remove the tetrahydrofuran and placed under vacuum. Flash chromatography was performed using 10% $MeOH/CH_2Cl_2$ as the eluent, giving an 88% yield of an off-white solid (0.06 g, 0.01 mmol).

Step 5: N-Methanethiolsulfonyl-N'-biotinyl-2,2'-(ethylenedioxy)bis(ethylamine)—The iodobiotin diamine (0.75 g, 1.4 mmol) was taken up in 10 ml of dimethylformamide (DMF). To this solution was added sodium methanethiolsulfonate (0.37 g, 0.003 mmol), and the reaction was allowed to stir at room temperature for 2 h. The flask was placed under high vacuum to remove the DMF, and the product was flash-chromatographed using a 15% $MeOH/CH_2Cl_2$ solvent system. An 88% yield (0.64 g) of a yellowish oil was isolated. NMR spectra for MTSEDE-biotin and its intermediates were determined to confirm the purity of the product (data not shown) and are available upon request.

Step 6: Biotin N-Hydroxysuccinimide Ester (20)—Biotin (5.5 g, 22.6

mmol) was dissolved in 70 ml of DMF. To this solution was added *N*-hydroxysuccinimide (3.12 g, 27.1 mmol) and diisopropyl carbodiimide (3.42 g, 27 mmol). The reaction was stirred at 90 °C overnight, after which rotary evaporation was used to remove DMF, giving a yellowish solid. Ethyl ether (150 ml) was added to the crude product to dissolve impurities, after which the crude solid was suction filtered. This off-white solid had a melting point range of 177–182 °C. The crude product was recrystallized in isopropanol and suction-filtered to give an 84.5% yield of a white solid (6.5 g, 19 mmol). The melting point of this solid was 200–202 °C.

Step 7: Sodium Methanethiolsulfonate (21)—Sodium hydrosulfide was dried over P_2O_5 for 3 days. This dried sodium hydrosulfide (11 g, 20 mmol) was then dissolved in 150 ml of absolute ethanol. Methanesulfonyl chloride (11.4 g, 9.9 mmol) was added dropwise to this solution as it stirred at room temperature and under a nitrogen atmosphere. After all of the methanesulfonyl chloride had been added, the reaction was allowed to stir for another 2 h, under nitrogen. As nitrogen gas was bubbled through the reaction, it was forced through a drying tube and then bubbled through 2000 ml of bleach in order to neutralize the developing hydrogen sulfide gas. After 2 h, the reaction flask was heated to 65–70 °C for 1 h. The flask was allowed to cool, and then 100 ml of absolute ethanol were added before leaving the flask under nitrogen overnight. After this time, the solution was gravity-filtered to remove NaCl and then rotary-evaporated to remove ethanol. Recrystallization was performed with warm ethanol to yield a white solid with a melting point of 271.5 °C. The yield was 3.8 g (2.88 mmol).

Step 8: Iodoacetic Anhydride—Iodoacetic acid (20 g, 107 mmol) was dissolved in 290 ml of ethyl acetate. Diisopropyl carbodiimide (6.8 g, 54 mmol) was added to this solution, and the reaction was stirred at room temperature for 1 h under nitrogen. IR spectroscopy showed that the reaction had gone to completion by the formation of two strong, sharp peaks at 1793.7 and 1735.6 cm^{-1} and the disappearance of a strong, broad peak at 3401.5 cm^{-1} (COOH peak). Ethyl acetate was removed by rotary evaporation, yielding a ruby red oil of iodoacetic anhydride.

Covalent Cysteine Modification with Biotin Reagents and Preincubations with α-Bgtx or Erabutoxin a

Two days after transfection, cells were harvested by gentle agitation in phosphate-buffered saline containing 5 mM Na_2-EDTA (~0.5–1 × 10^7 cells obtained from one 75-cm^2 tissue culture flask). After a brief centrifugation at ~600 × *g*, the cells were resuspended in high potassium Ringer's solution (22), pooled, divided into 300-μl aliquots, and incubated for the specified times with 5–500 μM MTSEDE-biotin or PEO-biotin. For MTSEA-biotin, the reagent was dissolved in Me_2SO instead of water before being added to the cells at 500 μM. For each biotin reagent, we added an excess of BrACh (1.5 mM) to terminate the reaction. The unbound biotin was removed by pelleting the cells (2 min at 20 °C), and resuspending the pellet in 0.5 ml of high potassium Ringer's. This wash was repeated three times in total. For preincubations with α-Bgtx or Ea, the cells were incubated for 2 h at room temperature with 10 μM amounts of the respective toxin to allow for a saturation of binding sites. PEO-biotin was then added directly into the tubes for the times indicated. Typically, HEK-293 cells transiently transfected with wild-type AChR subunits yielded 50–100 fmol of biotinylated surface receptor/cm^2 of confluent cells.

Precipitation with Streptavidin-Agarose Beads

After treatment with PEO-biotin, cells were lysed in 450 μl of ice-cold RIPA solution (1% Nonidet P-40, 0.5% sodium deoxycholate, 0.1% SDS) with added proteinase inhibitors (10 μg/ml aprotinin, 200 μM phenylmethylsulfonyl fluoride, and 100 μM benzamide) and incubated on ice for 15 min. The lysate was centrifuged at 14,000 × *g* for 15 min, and the supernatant was precipitated with 50 μg of streptavidin-agarose beads (Pierce) at 4 °C overnight. Under these conditions, we found that the maximal amount of biotinylated receptor was precipitated, as the addition of larger volumes of beads did not lead to an increase in detectable α-subunit. The precipitated samples were washed three times with 500 μl of RIPA solution (4,000 × *g*, 2 min, 4 °C). Typically, lysed cells containing ~1 mg of total protein were precipitated and the equivalent of ~200 fmol of toxin binding sites was retrieved and loaded onto SDS-polyacrylamide gels.

Surface Labeling with mAb 35 and Immunoprecipitation

To determine receptor surface expression, intact cells containing ~1 mg of total protein were incubated with 5 μg of monoclonal anti-nAChR mAb 35 (11, 23) in a final volume of 500 μl of Ringer's solution for 90 min on ice. Subsequently, unbound antibody was removed by washing as above, cells were lysed with 450 μl of RIPA solution as above, and receptors were precipitated overnight using 50 μl of Protein G-agarose. The precipitated samples were washed three times with 500 μl of RIPA solution (4,000 × *g*, 2 min, 4 °C). The conditions chosen are saturating, as neither the addition of larger amounts of Protein G-agarose or mAb 35 nor the prolonged exposure with mAb 35 lead to an increased precipitation of α-subunit.

SDS-Polyacrylamide Gel Electrophoresis and Western Blot Analysis

Biotinylated receptor-streptavidin-agarose bead complexes (or Protein G-receptor complexes in the case of mAb 35-treated samples) were brought to a final concentration of 4% SDS, 0.002% bromphenol blue, 0.12 M Tris-HCl, pH 6.8, and 10% glycerol. Prior to loading, DTT and β-mercaptoethanol were added to a final concentration of 500 mM each. Samples were heated to 95 °C for 3 min before being loaded onto a 10% SDS-polyacrylamide gel (24). The gels were transferred onto polyvinylidene difluoride membranes and blocked with phosphate-buffered saline containing 0.1% Tween and 3% bovine serum albumin (Sigma). Primary antibody incubations were performed in the same buffer using a 1:500 dilution of antibody 43.37 (120 μg/ml stock) (25). Blots were then incubated with anti-mouse IgG horseradish peroxidase-conjugated secondary antibody (working dilution 1:2500; Transduction Laboratories). Proteins were visualized using the enhanced chemiluminescence detection method (ECL Plus, Amersham Pharmacia Biotech).

Calculation of the Rates of Receptor Biotinylations

Visualized receptor bands were quantitated by densitometry using the software ImageJ (National Institutes of Health, Bethesda, MD). A calibration curve relating band intensities to femtomoles of ACh binding sites was established for mutant and wild-type receptors by running known concentrations of *Torpedo* membranes on a gel, followed by Western blotting, ECL exposure, and densitometry quantitation. These defined amounts of *Torpedo* membranes were run alongside with the biotinylated receptors and subjected to identical experimental conditions. Using these calibration curves, intensities of biotinylated receptor bands were then converted from pixel values to femtomoles of ACh binding sites for each time point. Rate constants for the biotinylation of AChR were then determined using a second-order rate equation (26). In cases where α-Bgtx or Ea led to a substantial inhibition (>10-fold), second-order reaction rates were estimated by comparing the maximal amounts of biotinylation in the absence or presence of the toxins for three PEO-biotin concentrations (5, 50, and 500 μM).

RESULTS

In previous studies, we demonstrated that a cysteine can be substituted for all of the individual amino acids between positions 184 and 197 of the mouse muscle-type α-subunit without dramatic effect on receptor functionality (<6-fold changes in the EC_{50}) as measured by ACh responsiveness in *Xenopus* oocytes (17). Moreover, we showed that within this region, residues Trp^{187}, Val^{188}, Phe^{189}, Tyr^{190}, and Pro^{194} are solvent-accessible and are in a position to contribute to the α-Bgtx binding site. In order to explore further the topology of the bracketing region extending from 184 to 197, we have now modified the appropriate Cys-substituted mutants with thiol-specific biotin derivatives following their expression in HEK-293 cells, permitting a more detailed analysis of the accessibility of these Cys-substituted residues.

PEO- and MTSEDE-biotin Specifically Modify Cysteines 192/193 in Reduced Wild-type nAChR—Initially, we wanted to determine whether alkyl methane thiosulfonate derivatives of biotin could be used to specifically modify surface-exposed cysteines in the nAChR. Previously, we and others showed that smaller alkyl methane thiosulfonate derivatives and bromoacetylcholine, an alkylammonium compound containing an α-haloacyl ester moiety, react covalently and specifically with Cys^{192} and Cys^{193} of the nAChR following their selective reduction with 1 mM DTT (16, 17, 27–29). As shown in Fig. 2, when cells expressing the wild-type nAChR were selectively reduced at positions 192 and 193 with 1 mM DTT and then treated with 500 μM of MTSEDE-biotin (Fig. 2*A*, *lane 4*), we detected a band corresponding to the α-subunit of the nAChR.

As these studies were under way, a similar biotin derivative (PEO-biotin) became commercially available. When we applied this reagent to reduced wild-type receptors, we obtained results comparable to those for MTSEDE-biotin (Fig. 2*B*, *lane 4*). Importantly, this band was not present when unreduced nAChR was exposed to MTSEDE-biotin (Fig. 2*A*, *lane 3*) or PEO-biotin (Fig. 2*B*, *lane 3*).

Biotinylation was blocked by preincubation with either 1.5 mM BrACh or 1.5 mM MTSET for both MTSEDE- and PEO-biotin, confirming its specificity (Fig. 3*B*, *lane 3*; Fig. 5*A*). In contrast, exposure of cells to the more hydrophobic MTSEA-biotin leads to considerable nonspecific labeling, as we detected α-subunit labeling that was equally pronounced both before and after reduction with DTT. These results suggest that this reagent is capable of penetrating the lipid bilayer to a large degree and may have access to the internal cysteines at position αCys^{222} (in presumed transmembrane segment M1) and αCys^{418} (M4) (compare Fig. 2*A*, *lanes 6* and *7*). In addition, we observed that MTSEA-mediated biotinylation of reduced wild-type and mutant receptors cannot be blocked by 1.5 mM BrACh (data not shown), further pointing to its reactivity with an internal cysteine. For PEO- and MTSEDE-biotin, we detected nonspecific labeling of native unreduced receptors only when concentrations were raised to 1.5 mM and above (data not shown). The weak signal we obtained in the presence of DTT alone may suggest nonspecific absorption of the receptor to the streptavidin beads that are used for precipitation, although the result presented here was somewhat exceptional, and we generally did not observe a signal in the presence of DTT alone (Fig. 2*A*, *lane 2*). Additionally, labeling of surface-expressed α-subunit by incubation of intact cells with the mouse monoclonal nAChR antibody, mAb 35 (11) (directed against region α67–76), followed by immunoprecipitation enabled us to the detect an α-band of an intensity comparable to that for the biotinylated wild-type receptor, indicating that at least a large fraction of the surface population of wild-type nAChRs can be biotinylated (Fig. 2*A*, *lane 5*). However, it should be noted that a direct comparison of the signal intensities is not 100% accurate. Although we have optimized conditions such that maximal amounts of both mAb 35-labeled and biotinylated receptor are precipitated, it remains possible that the recovery of receptor eluted from the beads is different for the two methods. Nevertheless, we could use mAb 35 to test surface expression of all the cysteine mutants from position α184C to α197C, and we detected no noticeable difference in cell-surface expression levels among these mutants (Fig. 3*A*).

Rate of Biotinylation of Reduced Wild-type nAChR and Retardation in the Presence of α-Bgtx—In an effort to quantitate the reactivity of reduced wild-type and mutant nAChRs with PEO-biotin, we exposed nAChRs to 5 μM PEO-biotin for various incubation times (Fig. 4*A*). Second-order reaction rates were

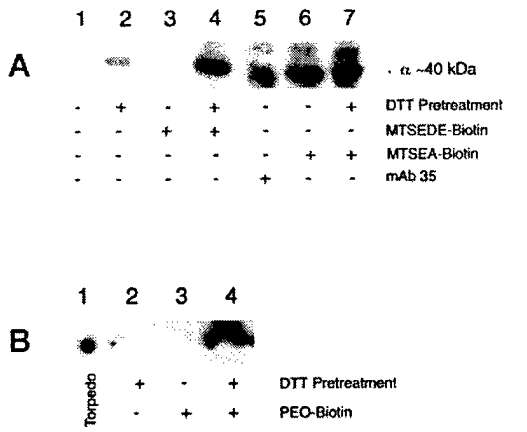

FIG. 2. **Reactivity of wild-type nAChR toward various thiol-specific biotins.** HEK-293 cells were transfected with α wild-type cDNA and the three other (β, γ, δ) AChR subunit cDNAs, harvested after 2 days of incubation, and treated with various thiol-specific biotin derivatives for 10 min at 20 °C. Streptavidin or Protein G precipitation (in the case of mAb 35), electrophoresis, Western blotting, and visualization of the α-subunit were performed as described under "Materials and Methods." The concentration for all biotin reagents was 500 μM. Incubations for the individual lanes are as follows. *A*, *lane 1*, no DTT, no biotin; *lane 2*, 1 mM DTT (20 min, 20 °C); *lane 3*, MTSEDE-biotin; *lane 4*, 1 mM DTT (20 min, 20 °C), followed by three washes, followed by MTSEDE-biotin; *lane 5*, mAb 35 (see "Materials and Methods" for details); *lane 6*, MTSEA-biotin; *lane 7*, 1 mM DTT, followed by three washes, followed by MTSEA-biotin. *B*, *lane 1*, *Torpedo* membranes (100 fmol of α-Bgtx binding sites); *lane 2*, 1 mM DTT; *lane 3*, PEO-biotin; *lane 4*, 1 mM DTT, followed by three washes, followed by PEO-biotin. Samples shown in *panels A* and *B* were run on separate gels. For each gel analysis, however, equivalent amounts of cell surface receptors (~200 fmol of toxin binding sites) were reacted with the respective biotin modifiers.

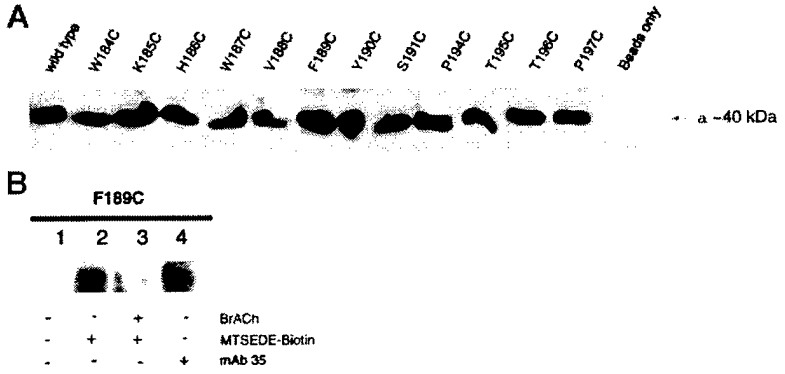

FIG. 3. **Surface expression of mutants α184C–α197C.** cDNAs encoding for wild-type or the respective mutant α-subunits were transfected together with wild-type β-, γ-, and δ-subunits into HEK-293 cells, which were harvested after 2 days of incubation, and treated with mAb 35 (*A*) or MTSEDE-biotin (*B*). Protein G and streptavidin precipitations, electrophoresis, Western blotting, and visualization of the α-subunit were performed as described under "Materials and Methods." *A*, surface expression of mutant α-subunit-containing nAChR in comparison to expression of wild-type receptor. For all the samples, equal amounts of receptor (~200 fmol in toxin binding sites) were exposed to mAb 35 as described under "Materials and Methods." For the *lane* denoted "*Beads only*," cells transfected with wild-type receptor were used, lysed without prior mAb 35 treatment, and precipitated overnight with Protein G-agarose beads. *B*, biotinylation of mutant αF189C with MTSEDE-biotin can be blocked by BrACh pretreatment. For *lanes 2* and *3*, the incubation with 500 μM MTSEDE-biotin was performed for 10 min at 20 °C, and terminated by the addition of 1.5 mM BrACh. For *lane 3*, 1.5 mM BrACh was first added for 10 min at 20 °C, followed by three washes. Then, MTSEDE-biotin was added. *Lane 1*, no reagent added; *lane 2*, MTSEDE-biotin only; *lane 3*, BrACh and MTSEDE-biotin; *lane 4*, mAb 35 only (as in *A*). For all the samples, equal amounts of receptor (~200 fmol in toxin binding sites) were modified and loaded into each lane.

TABLE I

Second-order reaction rates of mutant α-subunits with PEO-biotin

Wild-type or the respective mutant α-subunits encoding cDNAs were transfected together with wild-type β-, γ-, and δ-subunits into HEK-293 cells, which were harvested after 2 days of incubation, and treated with PEO-biotin. Streptavidin precipitation, electrophoresis, Western blotting and visualization of the α-subunit and calculation of second-order reaction rates were performed as described under "Materials and Methods." Second-order reaction rate constants in the absence (k) and presence of α-Bgtx (k_{Bgtx}) were determined using 50 μM PEO-biotin for all of the mutants, except for mutant αW187C (500 μM) and reduced wild-type receptors (5 μM). Positions 192 and 193 form a vicinal disulfide bond in the wild-type receptor and are not listed separately, since they are indistinguishable and become modified in PEO-biotin-exposed reduced wild-type receptors. In cases where α-Bgtx led to a blockade of the second-order reaction rate with PEO-biotin, only estimates of the maximal rates of biotinylation in the presence of α-Bgtx could be calculated, due to nonspecific labeling at high concentrations of PEO-biotin. The reduction in the rate of reactivity was estimated by comparing the intensities obtained for 10-min incubations with 5, 50, and 500 μM biotin in the presence and absence of the α-Bgtx.

Mutant	Second-order reaction rate k	Ratio k/k_{Bgtx}
	$M^{-1} s^{-1}$	
αD71C	39.5 ± 5.1	0.98 ± 0.03
Reduced wild-type (α192/193)	103.6 ± 3.4	>100
αW184C	41.3 ± 3.9	0.89 ± 0.08
αK185C	23.5 ± 3.1	1.1 ± 0.05
αH186C	28.3 ± 3.5	0.91 ± 0.09
αW187C	10.8 ± 0.9	>10
αV188C	101.9 ± 12.8	1.34 ± 0.07
αF189C	93.7 ± 9.6	>100
αY190C	55.6 ± 13.3	0.86 ± 0.07
αS191C	37.1 ± 1.9	0.88 ± 0.05
αP194C	21.1 ± 3.2	1.36 ± 0.09
αT195C	36.8 ± 4.4	0.98 ± 0.05
αT196C	59.3 ± 3.3	0.96 ± 0.06
αP197C	47.6 ± 9.4	1.21 ± 0.11

calculated as described under "Materials and Methods." For reduced wild receptors, we obtained a rate constant of 103.6 $M^{-1} s^{-1}$ (Table I). Comparable results were obtained with MTSEDE-biotin (data not shown). However, since the MTS compound was more light-sensitive and degraded rapidly at room temperature, we focused the remainder of our studies exclusively on the effects mediated by PEO-biotin.

When 10 μM α-Bgtx was added to cells and allowed to equilibrate for 2 h, the reactivity of reduced wild-type receptors toward PEO-biotin was substantially slowed (>100-fold). Using 5 and 50 μM PEO-biotin, we could not detect any biotinylation of the α-subunit, and even after incubation with 500 μM PEO-biotin, we obtained only a weak signal (~10% of the maximum intensity; Fig. 4*B*). A precise determination of the second-order rate constant in the presence of α-Bgtx was not possible, since PEO concentrations of 1.5 mM and above would have to be used, and under these conditions, there was considerable background stemming from the presumed modification of an internal cysteine or other unidentified sites.

Rate of the Biotinylation of Mutant αV188C nAChR Is Unaffected by the Presence of α-Bgtx—Previous results showed that mutant αV188K leads to a ~680-fold decrease in affinity for a short α-neurotoxin, *Nmm*I, although the effect of this mutation was much less pronounced in affecting α-Bgtx binding (15, 30, 31). In addition, modification of αV188C with 1.5 mM BrACh or MTSET leads to a ~50% reduction in the number of α-Bgtx binding sites (16). On the other hand, a mutation introducing a negative charge at this position (αV188D) merely produced a ~10-fold decrease in *Nmm*I binding. To more closely examine the role of this position in α-Bgtx binding, we determined second-order reaction rates for αV188C with 50 μM PEO-biotin in the presence (Fig. 5*B*) and absence of α-Bgtx (Fig. 5*A*). In the absence of α-Bgtx, we obtained a rate of 102 $M^{-1} s^{-1}$, whereas

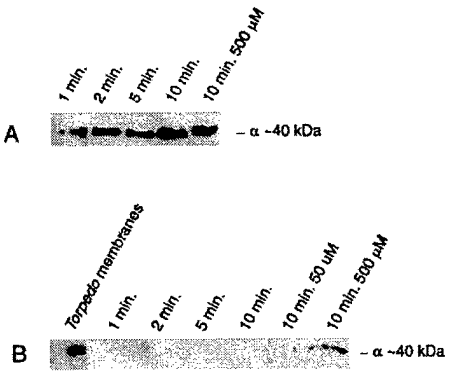

FIG. 4. **Reactivity of reduced wild-type receptors with PEO-biotin and inhibition of biotinylation in the presence of α-Bgtx.** Wild-type α-subunit encoding cDNAs were transfected together with wild-type β-, γ-, and δ-subunits into HEK-293 cells, which were harvested after 2 days of incubation, and treated with PEO-biotin. The PEO-biotin concentration for all time points was 5 μM, unless otherwise indicated in the figure. Streptavidin precipitation, electrophoresis, Western blotting, and visualization of the α-subunit were performed as described under "Materials and Methods." *A*, time course of biotinylation in the absence of α-Bgtx. Biotinylation was terminated by the addition of the thiol-specific BrACh (1.5 mM) at the indicated time points. *B*, biotinylation in the presence of 10 μM α-Bgtx. Harvested cells were first incubated with 10 μM α-Bgtx for 2 h, and PEO-biotin was then added directly. In *lane 1*, *Torpedo* membranes (100 fmol of toxin binding sites) were loaded as a standard reference. For all samples in *A* and *B*, transfected cells were pooled prior to modification, and equal amounts of receptor (~200 fmol of toxin binding sites) were modified and loaded onto each lane.

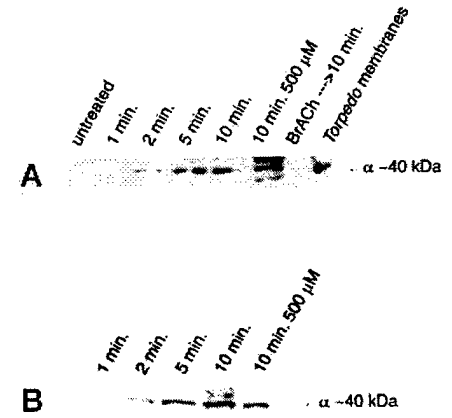

FIG. 5. **Reactivity of mutant αV188C with PEO-biotin in the presence or absence of α-Bgtx.** The αV188C mutant α-subunit encoding cDNA was transfected together with wild-type β-, γ-, and δ-subunits into HEK-293 cells, which were harvested after 2 days of incubation, and treated with PEO-biotin. The PEO-biotin concentration for all time points was 50 μM, unless otherwise stated in the figure. Streptavidin precipitation, electrophoresis, Western blotting, and visualization of the α-subunit were performed as described under "Materials and Methods." *A*, biotinylation in the absence of α-Bgtx. Biotinylation was terminated by the addition of the thiol-specific BrACh (1.5 mM) at the indicated time points. *Torpedo* membranes (100 fmol in toxin binding sites) were loaded as a standard reference. For BrACh preincubation, the sample was exposed to 1.5 mM BrACh for 10 min at 20 °C, followed by three washes, prior to the addition of PEO-biotin. *B*, biotinylation in the presence of 10 μM α-Bgtx. Harvested cells were first incubated with 10 μM α-Bgtx for 2 h, and PEO-biotin was then added directly. For all samples in *A* and *B*, equal amounts of receptor (~200 fmol of toxin binding sites) were modified and loaded onto each lane.

incubation in the presence of α-Bgtx resulted in only a slightly diminished rate of 77 $M^{-1} s^{-1}$. Therefore, we found no indication that α-Bgtx binding to the α-subunit protected this Cys-substituted residue from biotinylation. Interestingly, a comparison between Figs. 4 and 5 shows that the signal intensity for

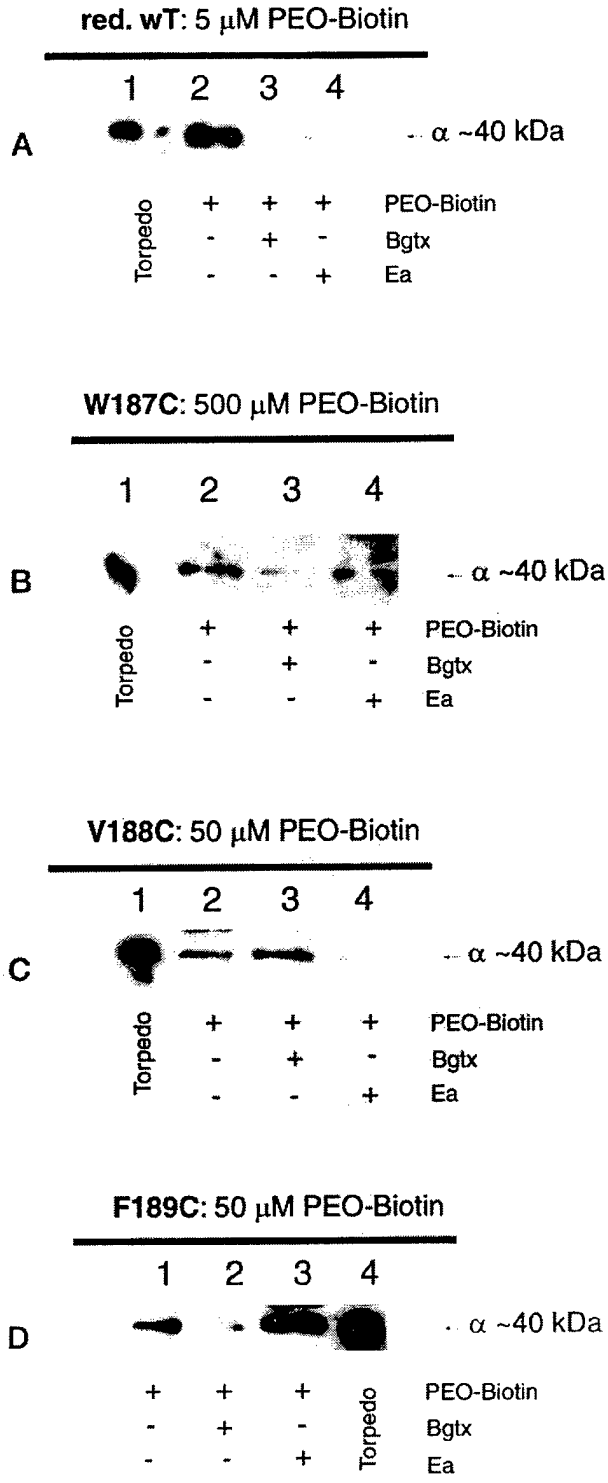

FIG. 6. **Protection of PEO-biotin-mediated modification of reduced wild-type nAChR and mutants αW187C, αV188C, and αF189C in the presence of α-Bgtx or Ea.** Wild-type or the respective mutant α-subunits encoding cDNAs were transfected together with wild-type β-, γ-, and δ-subunits into HEK-293 cells, which were harvested after 2 days of incubation, and treated with PEO-biotin at the concentrations indicated. Streptavidin precipitation, electrophoresis, Western blotting, and visualization of the α-subunit were performed as described under "Materials and Methods." *A*, protection of the biotinylation of reduced wild-type receptors by α-Bgtx and Ea. Wild-type receptor was reduced with 1 mM DTT (20 min, 20 °C). All biotinylations were done with 5 μM PEO-biotin for 10 min at 20 °C. For *lanes 3* and *4*, 10 μM α-Bgtx or Ea, respectively, were added for 2 h prior to PEO-biotin addition. *Lane 1*, *Torpedo* membranes (200 fmol in toxin binding sites); *lane 2*, PEO-biotin only; *lane 3*, α-Bgtx and PEO-biotin; *lane 4*, Ea and PEO-biotin. For *lanes 2–4*, equal amounts of receptor (~200 fmol in toxin binding sites) were reacted and loaded. *B*, protection of the biotinylation of mutant αW187C by α-Bgtx and Ea. For all the lanes shown, biotinylations were performed with 500 μM PEO-biotin for 10 min at 20 °C. *Lane 1*, *Torpedo* membranes (200 fmol in toxin binding sites); *lane 2*, PEO-biotin only; *lane 3*, α-Bgtx (10 μM) and PEO-biotin; *lane 4*, Ea (10 μM) and PEO-biotin. For *lanes 2–4*, equal amounts of receptor (~100 fmol in toxin binding sites) were reacted and loaded. *C*, protection of the biotinylation of mutant αV188C by α-Bgtx and Ea. For all the lanes shown, biotinylations were performed with 50 μM PEO-biotin for 10 min at 20 °C. *Lane 1*, *Torpedo* membranes (200 fmol in toxin binding sites); *lane 2*, PEO-biotin only; *lane 3*, α-Bgtx (10 μM) and PEO-biotin; *lane 4*, Ea (10 μM) and PEO-biotin. For *lanes 2–4*, equal amounts of receptor (~100 fmol in toxin binding sites) were reacted and loaded. *D*, protection of the biotinylation of mutant αF189C by α-Bgtx and Ea. All biotinylations were performed with 50 μM PEO-biotin for 10 min at 20 °C. *Lane 1*, PEO-biotin only; *lane 2*, α-Bgtx (10 μM) and PEO-biotin; *lane 3*, Ea (10 μM) and PEO-biotin; *lane 4*, *Torpedo* membranes (200 fmol in toxin binding sites). For *lanes 1–3*, equal amounts of receptor (~100 fmol in toxin binding sites) were reacted and loaded.

the biotinylation of mutant αV188C is less than that for reduced wild-type receptors, despite the fact that their reaction rates are comparable (Table I). Most likely, two factors contribute to this observation. First, reduced wild-type receptors contain two modifiable free thiol groups ($\alpha Cys^{192/193}$), *i.e.* although the reaction rate is comparable to that for αV188C, the signal intensity will be twice as high for any given time point. Additionally, it is possible that, for αV188C, only a portion of the receptor population contributes to the signal, whereas the rest is either refractory to biotinylation or to the subsequent sterically constrained reaction with streptavidin beads. This view is strengthened by the fact that preincubation with α-Bgtx enhances the yield of biotinylated receptor approximately 2-fold (Fig. 6*C*).

Evidence That All Amino Acid Residues within Region α184 to α197 Are Solvent-exposed—Although positions αW187C, αV188C, αF189C, αY190C, and αP194C were modifiable with BrACh and their modification resulted in a substantial blockade in α-Bgtx binding (16), the surface disposition of the other residues spanning region α184 to α197 is not well understood. Specifically, it was previously impossible to distinguish whether cysteine-substituted residues 184–186, 191, and 195–197 were modified following the application of thiol-specific reagents. By systematically examining the reactivity of these residues with PEO-biotin, we now show that all of these residues are surface-exposed and accessible to biotinylation to a similar degree. Their second-order reaction rate constants fell within the range of ~10 to ~100 M^{-1} s^{-1} (αW187C: 10.8 M^{-1} s^{-1}; αV188C: 101.9 M^{-1} s^{-1}; Table I).

Table I also lists the second-order reaction rate for positions αD71C and αW184C to αP197C in the presence of saturating concentrations of α-Bgtx. Importantly, the reaction rate for the biotinylation of αD71C is unaffected in the presence of α-Bgtx, confirming its location outside of the α-Bgtx binding site (11). Apart from reduced wild-type receptors, only residues αW187C (at least a 10-fold reduction) and F189C (at least a 100-fold reduction) exhibit a substantial reduction in the reaction rate in the presence of α-Bgtx. It should be noted that an accurate determination of reaction rates for these mutants in the presence of α-Bgtx was not possible. This would have required using concentrations of PEO-biotin in excess of 1.5 mM, a concentration that leads to the modification of other sites in addition to the engineered cysteine. Due to its reduced reactivity with PEO-biotin even in the absence of α-Bgtx, this is especially true for mutant αW187C.

Effects of Erabutoxin a Co-incubation on the Reactivity of Residues αW184C to αP197C with PEO-biotin—Previous studies suggested contradicting roles for positions αTrp^{187}, αVal^{188},

TABLE II

Comparison of the inhibition of substituted cysteine biotinylation by α-Bgtx and erabutoxin a

Wild-type or the respective mutant α-subunits encoding cDNAs were transfected together with wild-type β-, γ-, and δ-subunits into HEK-293 cells, which were harvested after 2 days of incubation, and treated with PEO-biotin. Only region α187 to α193 is shown, since there was no difference in the observed effects for α-Bgtx and Ea for the other mutants examined. Results for positions α192 and α193 were obtained with reduced wild-type receptor, which contains two free thiols at these positions. The symbol "+" in the table denotes a greater than 10-fold reduction in the second-order reaction rate constant k in the presence of either α-Bgtx or Ea. The symbol "−" is used to represent a change of less than 2-fold in the reaction rate (for α-Bgtx), or a <50% reduction in the maximum amount of labeling in the presence of Ea. For reasons described in the text and Table I, rates for the biotinylation of mutants αW187C, αF189C, and $\alpha Cys^{192/193}$ in the presence of α-Bgtx are estimates of the maximum rate and could not be determined accurately from the data. This is also the case for the biotinylation of positions αV188C and $\alpha Cys^{192/193}$ in the presence of Ea.

	Position						
	Trp^{187}	Val^{188}	Phe^{189}	Tyr^{190}	Ser^{191}	Cys^{192}	Cys^{193}
α-Bgtx	+	−	+	−	−	+	+
Erabutoxin a	−	+	−	−	−	+	+

and αPhe^{189} in the binding of α-neurotoxins. For example, using a double mutant cycle analysis of the short-chain α-neurotoxin *Nmm*I with nAChRs, Ackermann *et al.* (31) found no indication for the involvement of αTrp^{187} and αPhe^{189} in toxin binding. On the other hand, our previous work suggests that all three positions (187–189) contribute to the binding of the long-chain α-neurotoxin α-Bgtx. To characterize further the precise roles of these residues, we expanded our biotinylation studies to investigate the effect of a short α-neurotoxin. In this assay, Erabutoxin a (10 μM) was added to HEK-293 cells transfected with αW187C, αV188C, and αF189C 2 h prior to PEO-biotin addition.

Fig. 6 shows the profile of α-neurotoxin (α-Bgtx or Ea) protection from biotinylation for reduced wild-type, αW187C, αV188C, and αF189C mutant receptors. Biotinylation of reduced wild-type receptors is blocked by approximately 90% with Ea and completely with α-Bgtx (Fig. 6*A*, *lanes 2–4*) when 5 μM PEO-biotin is added for 10 min. In contrast, Ea does not protect positions αW187C and αF189C from biotinylation (Fig. 6, *B* (*lanes 2* and *4*) and *D* (*lanes 1* and *3*), respectively). α-Bgtx, on the other hand, clearly blocks biotinylation at these positions (Fig. 6, *B* (*lane 3*) and *D* (*lane 2*)). Similarly, Ea completely abrogates biotinylation of mutant αV188C (Fig. 6*C*, *lanes 2* and *4*), whereas α-Bgtx has little effect (Fig. 6*C*, *lane 3*). It should be noted that different PEO-biotin concentrations were used to account for the different reaction rates of the various mutants. However, we repeated these experiments for reduced wild-type nAChRs with 50 and 500 μM PEO-biotin and for αV188C and αF189C with 500 μM and obtained comparable results (data not shown).

For all other positions, the effects of Ea and α-Bgtx on PEO biotinylation of engineered cysteines seem to be comparable; none of the other positions shows a substantial blockade of biotinylation, as is summarized in Table II. Again, as stated above (and in the legend for Tables I and II), accurate determinations of second-order rate constants for the biotinylation in the presence of Ea were not possible for positions αW187C, αV188C, and reduced wild-type receptors. Furthermore, in those cases where Ea did not appear to protect against biotinylation, precise reaction rates were not calculated. Instead, the reduction of the rate was estimated by comparing the intensities obtained for 10-min incubations with 5, 50, and 500 μM PEO-biotin in the presence and absence of Ea.

DISCUSSION

Our primary aim was to define in more detail the topology and solvent accessibility of residues 184–197 in the α-subunit of the mouse muscle nicotinic acetylcholine receptor. To achieve this, we engineered individual cysteine substitutions and modified the introduced cysteine side chains with water-soluble, thiol-reactive derivatives of biotin. A similar approach has been used, for example, by Grunewald and co-workers (32) to determine the topology of the astroglial glutamate transporter GLT-1. Likewise, the solvent-accessible structure of the γ-aminobutyric acid A receptor has been investigated with a combined cysteine mutagenesis/biotinylation procedure (33).

Thiol-reactive Biotin Derivatives That Are Hydrophilic Are More Selective in Modifying External Cysteines—The success and accuracy of cysteine modifications with thiol-reactive biotin derivatives strongly depends on the hydrophilicity of the reagent. As can be seen in Fig. 1 (*A* and *B*), the relatively hydrophobic modifier MTSEA-biotin reacts strongly with wild-type nAChR. In these receptors, there are intrinsic cysteine disulfide pairs at positions 128 and 142 as well as at positions 192 and 193, but no free thiols in the extracellular domain, and thus there should be no reactivity with thiol reagents. The observed labeling is most likely explained by MTSEA-biotin entering the lipid bilayer and reacting with the solvent inaccessible unpaired αCys^{222} and/or αCys^{418}. This is further supported by the fact that preincubation with 1.5 mM BrACh does not protect against biotinylation of reduced wild-type and mutant receptors when MTSEA-biotin is used (data not shown). In sharp contrast, the more hydrophilic, water-soluble derivatives, MTSEDE-biotin and PEO-biotin, do not react with wild-type nAChR unless the disulfide bond at positions 192/193 is selectively reduced with 1 mM DTT (27, 28), indicating that these reagents are not membrane-permeable. With the hydrophilic reagents, biotinylation was blocked completely using either 1.5 mM BrACh or MTSET (see Fig. 3*B* for MTSEDE-biotin and Fig. 5*A* for PEO-biotin). As BrACh and MTSET are charged derivatives, their block of biotinylation confirms the specificity of the reaction and supports the conclusion that biotinylation with MTSEDE-biotin or PEO-biotin is restricted to the solvent-accessible surface of the nAChR in our studies using intact cells. Either biotin conjugate would have been useful in the present study, although we decided to concentrate on PEO-biotin, as MTSEDE-biotin was more light-sensitive and degraded more rapidly at room temperature. Nonetheless, MTSEDE-biotin would offer advantages in cases where the introduction of a reversible disulfide bond is desired.

All Amino Acid Residues between Positions α184 and α197 Are Solvent-exposed—Table I summarizes the second-order reaction rates for the individual Cys substitutions of amino acid residues between positions α184 and α197. Their second-order reaction rate constants fall within the range of ~10 to ~100 M^{-1} s^{-1} (αW187C: 10.8 M^{-1} s^{-1}; αV188C: 101.9 M^{-1} s^{-1}). As even the least reactive of these positions, αW187C, clearly contributes to the α-Bgtx binding site and is modifiable by the charged reagent BrACh (16), we conclude that second-order reaction rates for modification with PEO-biotin that are as low as 10 M^{-1} s^{-1} are consistent with solvent accessibility. We further conclude, therefore, that all of the residues within the region tested are surface-exposed. Minor perturbations in reactivity occur, in general, over a 10-fold range and are likely to be due to variations in the chemical and steric environment surrounding the individual positions (34). Additionally, favorable electrostatic and steric interactions may enhance biotinylation. As an additional reference point, we included an analysis of mutant αD71C. It is well established that Asp^{71} forms one of the main determinants in the epitope recognized by

antibodies directed against the main immunogenic region (11) and therefore should be surface-accessible. Indeed, the second-order reaction rate (39.5 M^{-1} s^{-1}) is also in the range obtained with the 184–197 series of Cys substitutions. Similarly, a comparable reaction rate constant (~200 M^{-1} s^{-1}) has been reported for the reaction of an *N*-ethylmaleimide derivative with β-mercaptoethanol in phosphate buffer (35).

Further, the second-order reaction rate with PEO-biotin seems to be identical for the two α-subunits of the nAChR, regardless of position of the introduced cysteine mutation. Using a linear regression fitting routine, we calculated a curve with a very good fit to the data ($R > 0.98$ for all the mutants investigated; data not shown) assuming a single class of binding sites.

Our conclusions on the solvent accessibility of the 184–197 region are in line with a number of recently published studies. Structural predictions derived from the NMR studies of a receptor-peptide fragment bound to α-Bgtx (36) suggest that residues 187–190 are likely to be surface-accessible in the native receptor. The conclusions concerning surface accessibility of α-subunit residues 187–190 are also consistent with studies of the Bgtx-resistant nAChRs found in cobra and mongoose muscle and of HEK-expressed mouse muscle nAChRs containing glycosylation signals found in the cobra and mongoose AChR (23, 37). The surface accessibility of αVal^{188} was demonstrated by McLaughlin *et al.* (17) and is also supported by recent studies of Ackermann *et al.* (30, 31). A recent double mutant cycle analysis concludes that position αPro^{197} interacts with *Nmm*I residues Arg^{33} and Lys^{27} and must therefore be surface-exposed. In addition, our study demonstrates for the first time that positions corresponding to αTrp^{184}, αLys^{185}, αSer^{191}, αThr^{195}, and αThr^{196} are on the solvent-accessible surface of the receptor.

α-Bgtx Protects Mutants αW187C, αF189C, and Reduced Wild-type Receptors, but Not Mutant αV188C, from Biotinylation with PEO-biotin—In the present study, we provide evidence that positions α71, α184, α185, α191, α195, α196, and α197 do not form part of a stable α-Bgtx binding site, as the presence of bound α-Bgtx does not have a significant effect on the second-order reaction rate for PEO-biotin (Table I). One reservation concerning the interpretation of the Cys substitution studies is that the substitution itself may locally distort the structure. Thus, negative results of the protection experiments may not be as conclusive as positive results. Furthermore, it is possible, depending on the local geometry, that an introduced cysteine is both in some proximity to bound Bgtx and in a position where Bgtx does not occlude the site from biotinylation.

Interestingly, the biotinylation of mutants αV188C and αY190C is not affected by the presence of α-Bgtx, even though the tethering of a methylammonium moiety to these residues leads to a blockade of α-Bgtx binding (16). These results allow us to refine our understanding of the interaction between α-Bgtx and positions 188 and 190, as they suggest that these positions, at least when substituted with cysteine side chains, do not interact directly and stably with α-Bgtx (Fig. 3 and Table I). Nevertheless, there is good evidence that these positions are within 8 Å of the toxin binding site. The introduction of an alkylammonium moiety, through the action of either BrACh or MTSET, leads to a significant perturbation of the receptor-toxin interaction (16). With both BrACh and MTSET, a covalently attached adduct of cysteine is formed that would fit into a cylinder 8 Å long and 6 Å in diameter (38). Furthermore, the results presented here are compatible with NMR structural studies of the complex formed between the dodecapeptide α185–196 and α-Bgtx (36). The NMR analysis revealed intermolecular nuclear Overhauser effect cross-peaks between one γ-methyl group of αVal^{188} and the two γ-methyl groups of Bgtx residue Val^{39}, thus placing these latter methyl protons at a distance of ~4–5 Å from that of αVal^{188}. Although this distance constraint certainly places Val^{188} in the proximity of Bgtx residue Val^{39} in this complex, there was no further indication of a more intimate or extensive contact between these hydrophobic side chains. In contrast, α-Bgtx clearly blocks the biotinylation of residues αW187C and αF189C, and thereby provides independent support that these residues are critical for a stable receptor-toxin interaction (16, 37, 39). Furthermore, the biotinylation of positions 192 and 193 in reduced wild-type receptors is also inhibited by α-Bgtx and underlines the importance of these residues for α-Bgtx binding. Nevertheless, the modification of these cysteines and of αW187C and αF189C with non-methylammonium-containing modifiers does not affect α-Bgtx binding significantly (16), suggesting additional complexity in Bgtx binding. In addition, it should be emphasized that the saturation binding assay used in these modification studies would not have detected decreases of α-Bgtx binding affinity <50-fold (16). Theoretically, it is also possible that the presence of α-Bgtx leads to the complete abrogation of biotinylation on only one of the two α-subunits, whereas the other site remains unaffected. If this were the case, we would expect to see a 2-fold reduction of the maximum intensity of the biotinylation signal. Our results argue against such a scenario, since the maximum intensity of the signal is largely unaltered for all of the investigated mutants.

It is somewhat surprising that the "footprint" of α-Bgtx protection from biotinylation is not larger. Previous studies have suggested that the Bgtx-receptor contact site would involve multiple points and a large portion of the toxin surface (40, 41). Our results suggest that the number of strong contacts may be fewer than expected. In addition, any additional contacts may be flexible enough to allow sufficient structural fluctuation to permit access to the reactive derivatives over the time course of the reaction incubation. Alternatively, some of the residues in this region may interact with Bgtx and the biotinylation reagents via non-overlapping surfaces.

Short and Long Chain Neurotoxins Establish Distinct Contact Points with the nAChR—Ackermann *et al.* (31) have argued that the short neurotoxin *Nmm*I interacts with αVal^{188}, whereas their results do not implicate positions αTrp^{187} and αPhe^{189} in *Nmm*I binding. The results presented here (Fig. 6, Table II) seem to reconcile the *Nmm*I studies with our previous results, suggesting an important role of αPhe^{189} in αBgtx binding (16, 39). Second-order reaction rates for the biotinylation of positions αW187C and αF189C are inhibited at least 10-fold by bound α-Bgtx, whereas αV188C is not affected. In contrast, Ea, a short neurotoxin very similar to *Nmm*I, leads to a >10-fold protection of position αV188C, but does not alter biotinylation at positions αW187C and αF189C. This suggests that α-Bgtx and Ea interact with distinct amino acids on the nAChR.

A Model for the Bgtx-mediated Blockade of Receptor Biotinylation—The model we propose here for the mechanism of α-Bgtx-mediated blockade of biotinylation is based on the mode of interaction between fasciculin and acetylcholine esterase (42–47). In this model, α-Bgtx, which carries a large net positive charge (+4; see Refs. 48 and 49) could bind to a site near a gorge leading to the agonist binding site and could obstruct PEO-biotin access to substituted cysteines (or ACh access to its binding site), which, in our experiments, would be reflected by a decrease in the second-order reaction rate of biotinylation. It is unlikely, however, that α-Bgtx blocks the putative gorge entirely, as only some of the residues implicated in ACh binding can be protected from biotinylation by concomitant α-Bgtx

incubation (αW187C, αF189C, and αCys[192/193]), whereas other residues that are thought to be crucial for the receptor-ACh interaction (*e.g.* αY190C; Ref. 16), are not affected. Rather, our results argue that the gorge would be only partially blocked by α-Bgtx, and that the remaining cavity is large enough to accommodate the entry of PEO-biotin (29 Å in fully extended length and 5.6 Å in width at the biotin ring). Finally, it is interesting that, between positions α186 and α190, biotinylation of only every other residue is inhibited by α-Bgtx binding. Therefore, our results are consistent with NMR studies arguing that residues α186–190 are in an extended β-sheet orientation (36). In addition, these results suggest that α-Bgtx may establish contact with one of the two faces of the β-sheet, whereas the other face remains accessible to PEO-biotin.

REFERENCES

1. Karlin, A., and Akabas, M. H. (1995) *Neuron* **15,** 1231–1244
2. White, S. H. (ed.) (1994) *Membrane Structure: Methods in Physiology*, Oxford University Press Inc., New York
3. Bennett, J. A., and Dingledine, R. (1995) *Neuron* **14,** 373–384
4. Anand, R., Bason, L., Saedi, M. S., Gerzanich, V., Peng, X., and Lindstrom, J. (1993) *Biochemistry* **32,** 9975–9984
5. Chavez, R. A., and Hall, Z. W. (1992) *J. Cell Biol.* **116,** 385–393
6. Pedemonte, C. H., Sachs, G., and Kaplan, J. H. (1990) *Proc. Natl. Acad. Sci. U. S. A.* **87,** 9789–9793
7. Olivares, L., Aragon, C., Gimenez, C., and Zafra, F. (1997) *J. Biol. Chem.* **272,** 1211–1217
8. Bennett, E. R., and Kanner, B. I. (1997) *J. Biol. Chem.* **272,** 1203–1210
9. Unwin, N. (1993) *Cell* **72,** 31–41
10. Gallivan, J. P., Lester, H. A., and Dougherty, D. A. (1997) *Chem. Biol.* **4,** 739–749
11. Saedi, M., Anand, R., Conroy, W., and Lindstrom, J. (1990) *FEBS Lett.* **267,** 55–59
12. Akabas, M. H., Stauffer, D. A., Xu, M., and Karlin, A. (1992) *Science* **258,** 307–310
13. Stauffer, D. A., and Karlin, A. (1994) *Biochemistry* **33,** 6840–6849
14. Sine, S. M. (1997) *J. Biol. Chem.* **272,** 23521–23527
15. Machold, J., Weise, C., Utkin, Y., Tsetlin, V., and Hucho, F. (1995) *Eur. J. Biochem.* **234,** 427–430
16. Spura, A., Russin T. S., Freedman N. D., Grant M., McLaughlin J. T., and Hawrot, E. (1999) *Biochemistry* **38,** 4912–4921
17. McLaughlin, J. T., Hawrot, E., and Yellen, G. (1995) *Biochem. J.* **310,** 765–769
18. Sigal, G., Mammen, M., Dahmann, G., and Whitesides, G. (1996) *J. Am. Chem. Soc.* **118,** 3789–3800
19. Becker, J. M., Wilchek, M., and Katchalski, E. (1971) *Proc. Natl. Acad. Sci. U. S. A.* **68,** 2604–2607
20. Currier, S. F., and Mautner, H. G. (1977) *Biochemistry* **16,** 1944–1948
21. Bruice, T., and Kenyon, G. (1982) *J. Protein Chem.* **1,** 47–58
22. Sine, S., and Taylor, P. (1981) *J. Biol. Chem.* **256,** 6692–6699
23. Kreienkamp, H.-J., Sine, S. M., Maeda, R. K., and Taylor, P. (1994) *J. Biol. Chem.* **269,** 8108–8114
24. Laemmli, U. K. (1970) *Nature* **227,** 680–685
25. Chase, B. A., Holliday, J., Reese, J. H., Chun, L. L., and Hawrot, E. (1987) *Neuroscience* **3,** 959–976
26. Sine, S., and Taylor, P. (1978) *J. Biol. Chem.* **254,** 3315–3325
27. Damle, V. N., McLaughlin, M., and Karlin, A. (1978) *Biochem. Biophys. Res. Commun.* **84,** 845–851
28. De Souza-Otero, A., and Hamilton, S. L. (1984) *Biochemistry* **23,** 2321–2328
29. Criado, M., Sarin, V., Fox, J. L., and Lindstrom, J. (1986) *Biochemistry* **25,** 2839–2846
30. Ackermann, E. J., and Taylor, P. (1997) *Biochemistry* **36,** 12836–12844
31. Ackermann, E. J., Ang, E. T.-H., Kanter, J. R., Tsigelny, I., and Taylor, P. (1998) *J. Biol. Chem.* **273,** 10958–10965
32. Grunewald, M., Bendahan, A., and Kanner, B. I. (1998) *Neuron* **21,** 623–632
33. Boileau, A. J., Evers, A. R., Davis, A. F., and Czajkowski, C. (1999) *J. Neurosci.* **19,** 4847–4854
34. Pascual, J. M., and Karlin, A. (1998) *J. Gen. Physiol.* **111,** 717–739
35. Schelte, P., Boeckler, C., Frisch, B., and Schuber, F. (2000) *Bioconjugate Chem.* **11,** 118–123
36. Basus, V., Song, G., and Hawrot, E. (1993) *Biochemistry* **32,** 12290–12298
37. Keller, S. H., Kreienkamp, H.-J., Kawanishi, C, and Taylor, P. (1995) *J. Biol. Chem.* **270,** 4165–4171
38. Zhang, H., and Karlin, A. (1997) *Biochemistry* **36,** 15
39. Levandoski, M. M., Lin, Y., Moise, L., McLaughlin, J. T., Cooper, E., and Hawrot, E. (1999) *J. Biol. Chem.* **274,** 26113–26119
40. Tremeau, O., Lemaire, C., Drevet, P., Pinkasfeld, S., Ducancel, F., Boulain, J. C., and Menez, A. (1995) *J. Biol. Chem.* **270,** 9362–9369
41. Love, R. A., and Stroud, R. M. (1986) *Protein Eng.* **1,** 37–46
42. Harel, M., and Sussman, J. L. (1993) *Proc. Natl. Acad. Sci. U. S. A.* **90,** 9031–9035
43. Miyazawa, A., Fujiyoshi, Y., Stowell, M., and Unwin, N. (1999) *J. Mol. Biol.* **288,** 765–786
44. Cerveòansky, C., Engstrom, A., and Karlsson, E. (1994) *Biochim. Biophys. Acta* **1199,** 1–5
45. Sussman, J. L., and Silman, I. (1991) *Science* **253,** 872–879
46. Bourne, Y., Taylor, P., and Marchot, P. (1995) *Cell* **83,** 503–512
47. Harel, M., Kleywegt, G. J., Ravelli, R. B. G., Silman, I., and Sussman, J. L. (1995) *Structure* **3,** 1355–1366
48. Lentz, T., and Wilson, P. (1988) *Int. Rev. Neurobiol.* **29,** 117–160
49. Rosenthal, J. A., Levandoski, M. M., Chang, B., Potts, J. F., Shi, Q. L., and Hawrot, E. (1999) *Biochemistry* **38,** 7847–55

Bibliography of Publications

1. "Using the Electrostatic Field Effect to Design a New Class of Inhibitors for Cysteine Proteases" Conroy, J. L; Sanders, T. C.; Seto*, C. T. *J. Am. Chem. Soc.* **1997**, *119*, 4285.
2. "^{13}C NMR Studies Demonstrate that Tetrahydropyranone-Based Inhibitors Bind to Cysteine Proteases by Reversible Formation of a Hemithioketal Adduct" Conroy, J. L.; Seto*, C. T., *J. Org. Chem.* **1998**, *63*, 2367.
3. "Synthesis of Cyclohexanone-Based Cathepsin B Inhibitors that Interact with Both the S and S' Binding Sites" Conroy, J. L.; Abato, P.; Ghosh, M.; Austermuhle, M. I.; Kiefer, M. R.; Seto*, C. T. *Tetrahedron Lett.* **1998**, *39*, 8253 - 8256.
4. "Hydrolysis of Amides Catalyzed by 4-Heterocyclohexanones: Small Molecule Mimics of Serine Proteases" Ghosh, M.; Conroy, J. L.; Seto*, C. T. *Angew. Chemie. Int. Ed. Engl.* **1999**, *38*, 514 - 516.
5. "4-Heterocyclohexanone-Based Inhibitors of the Serine Protease Plasmin" Sanders, T. C.; Seto*, C. T. *J. Med. Chem.* **1999**, *42*, 2969.
6. "A Combinatorial Library of Serine and Cysteine Protease Inhibitors that Interact with Both the S and S' Binding Sites" Abato, P.; Conroy, J. L.; Seto*, C. T. *J. Med. Chem.* **1999**, *42*, 4001.
7. "Inhibition of Phosphatase Activity by Positively-Charged Cyclodextrins" Ghosh, M.; Sanders, C. T.; Zhang, R.; Seto*, C. T. *Org. Lett.* **1999**, *1*, 1945..
8. "The Effects of Buffers on the Thermodynamics and Kinetics of Binding Between Positively-Charged Cyclodextrins and Phosphate Ester Guests" Ghosh, M.; Zhang, R.; Lawler, R. G.; Seto*, C. T. *J. Org. Chem.* **2000**, *65*, 735.
9. "Biotinylation of Substituted Cysteines in the Nicotinic Acetylcholine Receptor Reveals Distinct Binding Modes for α-Bungarotoxin and Erabutoxin a" Spura, A.; Riel, R. U.; Freedman, N. D.; Agrawal, S.; Seto, C. T.; Hawrot, E.* *J. Biol. Chem.* **2000**, *275*, 22452.

List of Personnel Receiving Pay from the Research Effort

Christopher T. Seto
Associate Professor
Department of Chemistry
Brown University
324 Brook St. Box H
Providence, RI 02912